Chemical and Molecular Analysis of Libyan Desert Plants used in Camel Feed

A thesis presented by

Samar Abolgasem Ben Zaed

For the degree of Doctor of Philosophy

of

University of Strathclyde

November 2016

Strathclyde Institute of Pharmacy and Biomedical Sciences

(SIPBS)

Glasgow, UK

Declaration

This thesis is the result of the author's original research. It has been composed by the author and has not been previously submitted for examination which has led to the award of a degree.

The copyright of this thesis belongs to the author under the terms of the United Kingdom copyright Acts as qualified by University of Strathclyde Regulation 3.49. Due acknowledgement must always be made of the use of any material contained in, or derived from, this thesis.

Signed:

Date:

By the name of Allah

Dedicated to my husband

****

Acknowledgments

First and foremost, I would like to express my gratitude to Allah (SWT) for blessing me and giving me strength to complete this study.

I would like to express my sincere gratitude and appreciation to my Supervisors: Prof. Alexander Gray, Dr. Valerie Ferro and Dr. Rothwelle Tate for their inspiration, moral support and encouragement, during the entire period of this research and also for their guidance, and patience during this project, perseverance which paved a successful way for my work.

My sincere thanks also goes to Prof. John Igoli for his valuable time, knowledge and support. I would also like to thank Fatma Habib (Kuwait University) who suggested the idea of this project and my lab members for their support and encouragement during the project work.

My acknowledgements also go to the Ministry of Higher Education in Libya for awarding me the scholarship and providing me with the opportunity to study abroad to undertake my PhD degree in the United Kingdom.

Finally, I would like to express my deepest gratitude to all members of my family in particular my parents for their prayers and strong encouragement of my academic endeavours over the years. Thanks to my sisters and brothers for supporting me at all times.

Abstract

Camels form an integral part of everyday life of Bedouins and other communities living in arid/desert zones. There is evidence that these communities use camel milk and urine for therapeutic purposes. The aim of this study was to determine the chemical composition of *Rhanterium epapposum, Astragalus spinosus, Tamarix aphylla* and *Citrullus colocynthus* -desert plants used commonly in camel fodder, which may be a source of therapeutically active compounds that could be transferred to camel body fluids.

Plants were investigated phytochemically and a range of compounds, including phenolic compounds containing sulphur, were elucidated; one of which appears to be novel. In addition, flavonoids, isoflavonoid derivatives, cucurbitacin, and cucurbitacin glycosides were isolated from these plants.

Isolated compounds produced in adequate quantities were screened *in vitro* for cytotoxic activity against human cancer cell lines: A375 (malignant melanoma), PANC-1 (pancreatic carcinoma), A2780 (ovarian carcinoma), ZR-75-1 (breast carcinoma), LNCaP (prostate carcinoma), and HeLa (cervical cancer) and a non-cancer (PNT2) cell line using an AlamarBlue® assay.

In parallel, this study also attempted to examine miRNAs present in the plants, camel milk and urine, which might have a therapeutic role via the dietary xenomir hypothesis which suggests plant-derived small nucleic acids can be passed through the food chain to humans and potentially regulate human gene expression.

In conclusion, compounds were identified for the first time from camel fodder, some of which had anti-cancer activity. In addition, to phytochemicals, preliminary data showed the possibility of miRNA molecules from these plants having an anti-cancer role to play.

List of Contents

List of Figures

xiii

List of Tables

List of Abbreviations

Acetone-d_6	Deuterated acetone
ATCC	American Type Cell Culture
brs	Broad singlet
BSA	Bovine Serum Albumin
CC	Column Chromatography
CDCl$_3$	Deuterated Chloroform
cDNA	Complementary Deoxyribonucleic Acid
CD63	Cluster Differentiation protein 63
COSY	^{1}H-^{1}H COrrelation SpectroscopY
CT	Cycle Threshold
d	Doublet
DEPT	Distortionless Enhancement by Polarisation Transfer
dd	Doublet of a doublet
DMSO	Dimethyl sulphoxide
DMSO-d_6	Deuterated dimethyl sulphoxide
DNA	Deoxyribonucleic Acid
EtOAc	Ethyl acetate
FAO	Food and Agriculture Organization
FCS	Foetal Calf Serum
HREI-MS	High-resolution Electrospray Ionization Mass Spectrometry
HMBC	Heteronuclear Multiple Bond Coherence
HMQC	Heteronuclear Multiple Quantum Coherence
hPRLR	human Prolactin Receptor
Hz	Hertz

ISSR-PCR	Inter-simple Sequence Repeat- Polymerase Chain Reaction
kD	Kilodaltons
LC-MS	Liquid Chromatography- Mass Spectroscopy
m	Multiple
MeOH	Methanol
MIC	Minimum Inhibitory Concentration
miRNA	microRibonucleic Acid
mRNA	Messenger Ribonucleic Acid
MS	Mass Spectroscopy
MTT	3-[4,5-Dimethylthiazol-2-yl]-2,5 diphenyl tetrazolium bromide
NMR	Nuclear Magnetic Resonance
NOESY	Nuclear Overhauser Enhancement SpectroscopY
PBS	Phosphate-Buffered Saline
PPIB	Peptidylprolyl Isomerase B
PCR	Polymerase Chain Reaction
RPMI	Roswell Park Memorial Institute
PTLC	Preparative Thin Layer Chromatography
qRT-PCR	Quantitative Real Time Polymerase Chain Reaction
Rf	Retardation Factor
RNA	Ribonucleic Acid
S	Singlet
siRNA	small interfering Ribonucleic Acid
SEC	Size-Exclusion Chromatography
TBE	Tris-borate-EDTA buffer
TLC	Thin Layer Chromatography
UV	Ultraviolet light
VLC	Vacuum Liquid Chromatography

Chapter 1 Introduction

The introduction will consist of four parts; general introduction contains background information about the therapeutic importance of camel milk and urine, phytochemical analysis of desert plants used in camel fodder, molecular analysis of these plants and camel milk and urine samples, and the aims of this project.

1.1 General introduction

Camels have been domesticated for thousand years and used for their milk, meat, wool, transportation, and in agricultural work for ploughing and water extraction (Andah *et al*., 2014). Camel milk is the most important camel product and has been consumed by many Bedouin cultures for generations (Raziq *et al*., 2008). These animals are a reliable source of milk production during dry seasons and contribute up to 50% of the nutrient intake of the nomads (Seaman *et al*., 1978; Farah *et al*., 2007).

Historical texts, dating back hundreds of years, reveal traditional medicine in desert regions has made use of camel milk and urine as treatments for various diseases such as asthma, cancer, common cold, diabetes, jaundice, and hypertension and its use continues today (Yardav *et al.,* 2015). The Holy Qur'an mentions the camel several times in different contexts and refers to the camel as a very important animal. Traditionally (Al Hadith), the Prophet Muhammad (S.A.W) recommended camel milk and urine to his followers as a medicine for different health problems. In addition, the consumption of camel milk and/or urine is considered a natural remedy in Arabic medicine to treat several diseases for Bedouin communities (Kaskous, 2016). There are many modern scientific studies that have examined the efficacy of camel milk, urine, and milk-urine mixtures against a range of diseases (Introduction Section 1.1.1 and 1.1.2).

The potential efficacy of camel milk and urine therapy could depend on desert plants found in camel fodder, which may be a source of therapeutically active compounds that could be transferred to the camel milk and urine following digestion. There is evidence of the benefit of using some supplements to animal food to ensure quality animal products for human consumption. Reports have demonstrated that selenium,

which has antioxidant properties, when used as an animal feed supplement can deliver nutritional benefit to human consumers of animal products (Sretenović *et al*., 2007). Dietary selenomethionine-containing plant or yeast protein can also be stored in animal proteins to offer nutritional content of selenium in animal products. Consequently, supplemented animal feed can lead to production of antioxidant-enriched eggs, milk, and meats for human consumption (Surai *et al*., 2006; Ravn-Haren *et al*., 2008; Fisinin *et al*., 2009; Navas-Carretero *et al*., 2010).

On the other hand, milk and milk products have been linked with some diseases due to infected foods and contaminated water. One example is *Pteridium aquilinum* (bracken fern), known to be the cause of acute or chronic toxic syndromes of livestock that ingest it (Yamada *et al*., 2007; Vetter, 2009). A norsesquiterpene glucoside (ptaquiloside) has been found to be the major toxin and carcinogen of *P. aquilinum* (Niwa *et al*., 1983). This compound is transformed to pterosin B in acidic solution (such as stomach acid) and it can form an unstable dienone, which is immediately converted to pterosin B under alkaline conditions (as found in lower parts of the intestinal tract) (Yamada *et al*., 2007). Both compounds have been reported to induce DNA damage and mutations (Matoba *et al*., 1987; Freitas *et al*., 2002). Ptaquiloside has been detected in the milk of cows fed with *P. aquilinum* (Alonso- Amelot, 1998). Humans can be exposed to *P. aquilinum* either by eating the plant or indirectly by the consumption of contaminated milk (Haenszel *et al*., 1976; Shahin *et al*., 1999; Gomes *et al*., 2012).

Coumarin is one of the ingredients in sweet clover and it is converted to a toxic substance, dicoumarol, in spoiled sweet clover (Wyllie *et al*, 1978). This toxin causes a bleeding disorder in animals by interfering with the synthesis and metabolism of vitamin K1, which is essential for normal blood clotting. Dicoumarol can pass through milk to calves when the cows ingest mouldy sweet clover. This causes death in new-born calves (Fraser and Nelson, 1959). Oleander (*Nerium oleander*) is an ornamental plant and commonly exists in the southern United States and contains oleandrin which is a toxic cardiac glycoside found in the aerial parts of this plant

(Langford and Boor, 1996). Oleander poisoning of humans and different domestic animals is common in regions where this plant grows (Aslani *et al*., 2004; Soto-Blanco *et al*., 2006). Just a few leaves of this plant can cause death in horses and cattle (Galey *et al*., 1996); while, a single leaf may be lethal for children (Shaw and Pearn, 1979). It is not only the consumption of plant materials that can pass on compounds harmful to the health of animals that ingest cattle products. Other studies have shown that livestock feeds contaminated with aflatoxin B1 lead to excretion of the metabolite (aflatoxin M1) in animal milk, resulting in a potent liver carcinogen in humans through the consumption of contaminated milk (Massey *et al*., 1995; Kang and Lang, 2009). Finally, some antibiotics that are used in livestock feed to prevent or treat bacterial infections, or promote growth, are reported to cause allergies or bacterial infection in humans who consume the contaminated milk (Phillips *et al*., 2004).

In arid zones, camels browse mainly on plants that are high in salt, thorny bushes and bitter plants including *Tamarix aphylla*, *Haloxylon aphyllum*, *Astragalus spinosus* and *Aristida karelinii*, which are generally avoided by other animals (Iqbal and Khan, 2001). This indicates that the difference of composition of camel milk and urine compared with cattle and goats could, in part, be due to the type of plants that are consumed. *T. aphylla* is a desert plant which is reported to have bioactive compounds such as ferulic acid derivatives, ellagic acid derivatives, flavonoids, phenolic aldehydes, terpenoids, and tannins (Souliman *et al*., 2012). Orabi *et al*. (2013) demonstrated significant human tumour-selective cytotoxic activity of isolated tannins from this plant.

Plants need to defend themselves from attack by micro-organisms, in particular fungi, and they do this by producing anti-fungal chemicals. Because fungal and human cells are similar at a biochemical level, it is often the case that chemical compounds intended for plant defence have an inhibitory effect on human cells, including human cancer cells (*Cardenas* et al., 1999).

The medicinal value of drinking camel milk and urine could also be attributed to a modern concept known as the dietary xenomiR hypothesis (Zhang *et al*., 2012a). This proposes a potential cross-kingdom action of plant-derived micro-ribonucleic acids (miRNAs) through dietary intake and their ability to regulate mammalian gene expression. Applying this xenomiR hypothesis here, one might suggest that the therapeutic value of camel milk and urine could be associated with the plant-derived miRNAs; these small nucleic acids could be passed through the food chain to humans via camel milk and/or urine and might regulate human gene expression.

Zhang *et al*. (2012a) determined the presence of several exogenous miRNAs, including osa-miR-168a, in the serum of mice via their food intake and they revealed that the plant miRNAs were able to inhibit mammalian gene expression in the liver. Further evidence comes from sequencing and microarray analysis of miRNAs in porcine milk exosomes has led to the detection of hundreds of miRNAs, which are potentially involved in regulation of immunity of newborn piglets (Chin *et al.*, 2014). More recently, a study demonstrated that the plant miRNA miR-159 is abundant in human serum and inversely associated with the incidence and progression of breast cancer in patients. The study revealed that the oral administration of a miR159-mimic significantly inhibited the growth of xenograft breast tumours in mice. These findings suggest the ability of plant miRNAs to inhibit cancer growth in mammals (Chin *et al*., 2016). The above observations support the dietary xenomiR hypothesis and suggest that the plants could be a source of mammalian tumour suppressor miRNAs and may provide a new treatment for human diseases.

1.1.1 The camel

According to the Food and Agriculture Organization (FAO, 2012), the estimated global camel population is 20 million. There are two major species of camels: 89% are Arabian dromedary camels (*Camelus dromedarius*) which are characterised by a single hump, that live in North Africa and the Middle East; and 11% are Bactrian camels (*C. bactrianus*) that have two humps and exist only in China and Central Asia (Peters and Driesch, 1997). A full-grown dromedary camel grows to a shoulder

height of 2 meters and weighs 300 to 600kg while Bactrian camels stand 1.85 meters at the shoulder and weigh 300 to 1000kg (Khanvilkar *et al*., 2009).

1.1.2 Dietary and therapeutic properties of camel milk

The estimation of daily production of camel milk depends on many factors such as age, feeding conditions, calving number, and stage of lactation (Khaskheli *et al.*, 2005). According to the FAO (2012), daily milk production in a lactation period of 8-18 months ranges between 1.0 and 2.7 litres in Africa while in South Asia reaches up to 12.0 litres. The world production of camel milk is 1,300,000 tonnes per year including about 850,000 tonnes in Somalia 89,000 tonnes in Saudi Arabia and 40,000 tonnes in the United Arab Emirates (UAE) (FAO, 2012).

In many African and Asian countries, camel milk production is growing due to increased demand (Al-Otaibi and El-Demerdash, 2013). The production of pasteurised camel milk and other dairy products made from camel milk has also increased in super markets (Iqbal and Khan, 2001; El-Agamy, 2006). The popularity of camel milk has reached countries beyond Africa and Asia. In 2013, the European Community licenced the importation of camel milk from the UAE. The main supplier of camel milk is the Dubai-based Emirates Industry for Camel Milk and Products (EICMP), which produces trademarked camel milk known as *Camelicious*. It is on sale currently in some European countries such as England, Denmark, and the Netherlands. In addition, a chocolate manufacturer, Al Nassma, sells camel milk chocolate through the Harrods store in London (Abdel Gader and Alhaider, 2016).

Camel milk has been reported to have a high vitamin, mineral, and immunoglobin content (Table 1.1, Hamad *et al*., 2011). Farah *et al.* (1992) found that the milk of dromedary camels contains water-soluble vitamin C at an average three times higher than that of bovine milk, but less fat soluble vitamin A and B2. In addition, Al-Humaid (2010) reported high levels of minerals and vitamins in camel milk, as well as reports of low cholesterol levels (Yagil and Van Creveld, 2000).

Table 1.1: Vitamin and mineral content of camel and bovine milk.

Name of component	Camel milk (mg/100ml±SD)	Bovine milk (mg/100ml±SD)
Vitamin A	0.04±0.002	0.36±0.02
Vitamin C	4.51±0.24	1.58±0.81
Vitamin E	0.26±0.03	0.11±0.01
Sodium	40.00±3.01	39.00±2.67
Zinc	2.21±0.17	2.01±0.14
Copper	0.17±0.02	0.11±0.01
Magnesium	12.12±1.00	13.12±1.00
Chloride	123.00±8.31	120.00±9.99

Camel milk is a rich source of proteins and the total protein content of camel milk ranges from 2.15 to 4.90% with potential antimicrobial, antioxidant, and immuno-modulatory activities (FitzGerald and Meisel, 2000; Iqbal and Khan, 2001; Konuspayeva et al., 2009). The main components of camel milk proteins are casein and whey. The casein varies between 52-87% of the total proteins while the content of whey protein is about 20 to 25% (Khaskheli et al., 2005). Caseins are easily digested in the intestine and they are a rich source of essential amino acids required for infant growth. Casein fractions are α_{s1}, α_{s2}, β and κ-casein and camel milk has a higher content of β-casein (65%) and lower content of other casein fractions than bovine milk (Kappeler et al., 2003). The high concentration of β-casein could be the reason that camel milk is more digestible and reduces allergic reactions in infants (El-Agamy et al., 2009). Camel whey proteins are lactoferrin, immunoglobulins, lysozyme, α-lactalbumin, peptidoglycan recognition proteins, and serum albumin (Merin et al., 2001; Kappeler et al., 2004). In camel milk, the major whey protein is α-lactalbumin, while β-lactoglobulin is the major bovine milk portion, which exists in low amounts in camel milk (Kappeler et al., 2003; Laleye et al., 2008). It has been reported that camel milk has a low level of two proteins that are responsible for allergies (β-lactoglobulin and β-casein) and only a few allergic cases have been reported in camel milk consumers (Merin et al., 2001; El-Agami et al., 2009; Al-alawi and Laleye et al., 2011). An earlier study demonstrated that dromedary camel

milk had a positive effect in eight children (4 months-10 years) with severe food allergies (Shabo *et al*., 2005). High levels of immunoglobulin G, secretory immunoglobulin A, and lactoperoxidase are also reported in camel milk with antimicrobial activity (Mona *et al*., 2010). Additionally, camel milk has shown higher antibacterial properties than bovine milk and that could be attributed to the concentration of lactoferrin (220mg/l) and lysozyme (2880mg/l) which were higher in camel milk than in bovine milk (110mg/l and 130mg/l) (El-Agami *et al*., 2009; El-Said *et al*., 2010).

Several scientific studies have demonstrated the antihyperglycemic effect of camel milk and its effect on diabetic complications including liver and kidney diseases, delayed wound healing, high cholesterol levels and decreased oxidative stress. In 2005, Agrawal *et al*. found that dromedary camel milk was a useful adjunct to parenteral insulin administration in the management of type 1 diabetes. In that study, a significant reduction in the dose of insulin was required for maintaining long-term glycaemic control. Hamad *et al*. (2011) evaluated the effects of camel milk on liver function by treating diabetic rats with camel, buffalo, and bovine milk. The study found that the highest enhancement of liver enzymes was reported in rats fed camel milk with 41% improvement for alanine transaminase (ALT) and 38% improvement for aspartate transaminase (AST). Both enzymes are useful in diagnosing and monitoring liver disease where they are detected at higher levels (Hall and Cash, 2012). Similarly, Khan *et al*. (2013) reported a decrease in the elevated levels of liver enzymes in streptozotocin (STZ)-induced diabetic rats fed camel milk for 1 month. In addition, camel milk reduced microalbuminuria levels in diabetic patients treated with camel milk, from 92.08 ± 15.18 to 75.75 ± 3.17, after 24h (Mohamad, 2009). Microalbuminuria refers to an increase in urinary albumin excretion usually associated with renal failure and cardiovascular disease and a decrease in microalbuminuria can delay organ damage (Koroshi, 2007).

In another study, camel milk was added to the usual diet of diabetic patients for 6 months and exhibited a significant reduction in microalbuminuria levels (from 119.48 ± 1.68mg/dl to 22.52 ± 2.68mg/dl, $p < 0.001$). In 2013, Badr showed an

accelerated wound healing in STZ-induced diabetic mice after treatment with camel milk for a month. This result was related to the significant elevation in hydroxyproline, an essential component in collagen that may be associated with tissue regeneration in diabetic mice. Another study conducted by Al-Numair (2011) reported that the level of hydroxyproline and total collagen content was increased to normal levels in STZ-diabetic rats fed camel milk.

Several studies have shown the efficacy of camel milk in reducing hyperlipidemia in diabetic patients. In one study, a significant reduction in the total cholesterol (TC) and triacylglycerols (TG) (25% and 37%, respectively) were observed in young type 1 diabetic patients after being treated with camel milk for 16 weeks. There were no significant changes in high density lipoprotein (HDL), low density lipoprotein (LDL), and very low-density lipoprotein (VLDL) levels after treatment (Mohamad *et al*., 2009). Another study conducted by El-Said *et al*. (2012) revealed an improvement in lipid levels in type 1 diabetic patients injected with a mixture of insulin and camel milk for three months. A significant reduction (45% and 30%, $p < 0.001$) in TG and TC, respectively and a significant ($p < 0.001$) increase in HDL-C levels was shown (from 41mg/ dl to 49mg/dl) compared to the control group.

1.1.3 Therapeutic properties of camel urine

In Mediterranean countries and some parts of Asia, camel urine has also been used traditionally as a treatment for different diseases including hair problems, skin injuries, snake bites, stomach pain, the common cold, and diarrhoea (Al-Awadi and Al-Judaibi, 1999; Bakhsh *et al*., 2012; Baesmel, 2014). One study showed that camel urine had an inhibitory effect on fungal growth of *Candida albicans* (45%±0.89), *Aspergillus niger* (43%±1.16) and *Fusarium oxysporum* (39%±0.89) after treatment with fresh camel urine (Al-Awadi and Al-Judaibi, 2015). Another study conducted by Kabbashi and Alfadhil (2016) evaluated the efficacy of camel urine in the treatment of dermatomycosis caused by dermatophyte fungi. The results showed stronger antifungal activity of camel urine compared with the antifungal drug fluconazole. Another study revealed that in rabbits and albino mice, liver and

stomach tissues infected with *Escherichia coli* recovered with no histopathological effects after treatment with camel urine (El-Elyani and Khalifa, 2006).

Al-Yousef (2012) found that dromedary camel urine possessed anti-cancer and potent immuno-modulatory properties. A dose containing 216mg/ml of lyophilised camel urine inhibited cell proliferation and caused more than 80% apoptosis in a number of cancers, including breast carcinomas and medulloblastomas ($p \leq 0.05$). The urine had no cytotoxic effect against peripheral blood mononuclear cells and had strong immunological activity in terms of inducing interferon gamma and inhibiting T helper 2 cytokines interleukin-4, interleukin-6, and interleukin-10. In addition, *in vitro* investigations have reported anti-cancer activity of camel urine against human lung adenocarcinoma cells (A549) (Alghamdi and Khorshid, 2012). Romli *et al*. (2016) examined the potential anti-cancer effect of camel urine against Mouse 4T1 breast tumour cells. The results demonstrated that camel urine is able to inhibit the proliferation and metastasis of 4T1 cells *in vitro* and *in vivo*. Alhaidar *et al*. (2011) investigated the potential antiplatelet activity of camel urine against adenosine diphosphate (ADP)-induced and arachidonic acid (AA)-induced platelet aggregation. The results demonstrated that camel urine had a potent antiplatelet activity similar to the activity of drugs such as aspirin and clopidogrel.

1.2 Phytochemistry analysis

1.2.1 Desert plants

The food of camels consists of dry grasses and available desert vegetation; mainly thorny plants. Many plant species have been recorded as fodder for the dromedary camel, including *A. spinosus, C.colocynthis, R. epapposum,* and *T. aphylla* which are detailed below.

1.2.1.1 *Rhanterium epapposum*

R. epapposum Oliv. (Figure 1.1) is called Arfaj in Arabic and belongs to the family Asteraceae. The plant is native to the deserts of Saudi Arabia and Kuwait, is indigenous and widespread throughout tropical and subtropical regions and is considered one of the main desert fodder plants for camels and sheep. *R. epapposum* is a bushy shrub approximately 80cm in height and it starts flowering from April and May. The flower is yellow in colour and is the national flower of Kuwait. The plant has small fruits in the form of a nut surrounded by membranous wings, which form in late spring (Ageel *et al.,* 1987; Suleiman *et al.,* 2009).

A   **B**
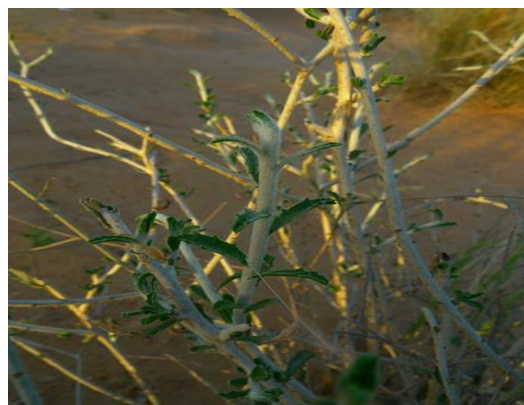
Figure 1.1A: The growing plant of *Rhanterium epapposum*, **1.1B:** stem with flowers (Pictures provided by Dr. Rothwelle Tate, Kuwait, 2012).

1.2.1.1.1 Historical use

People in rural areas from various countries consider Arfaj the main desert plant for grazing camels. It is also used as a source of fuel. In Arabic folk medicine, Bedouin people use *R. epapposum* in the treatment of gastrointestinal disturbances, skin infections, as an insecticide, and the flowers can be added to tea as a flavouring agent (Ageel *et al.,* 1987; Al-Yahya *et al.,* 1990).

1.2.1.1.2 Active ingredients and biological activities

Al-Yahya *et al*. (1990) demonstrated the presence of volatile oils, flavonoids, tannins, sterols and triterpenes in the aerial parts of *R. epapposum* using various qualitative chemical tests to detect the chemical constituents. There are no scientific studies reporting any medicinal activities for *R. epapposum*.

The Asteraceae family is reported to produce valuable phytochemicals, such as terpenoids (AF-1-AF-4), lignans (AF-5-AF-7), polyphenols (AF-8-AF-14), carbohydrates **(**AF-15**)**, sterols (AF-16 and AF17**)** and alkaloids (AF-18-AF-21) (Table 1.2). This family has also been reported to have biological ffects including antimicrobial, anti-cancer, anti-inflammatory and insecticidal activities (Lin *et al.*, 2004; Keyhanfar *et al*., 2011; He *et al*., 2012). The sesquiterpene lactone onopordopicrin (AF-4) showed protective effects in acute experimental colitis (de-Almeida *et al*., 2012). Arctiin (AF-5), a lignan isolated from Asteraceae plants such as burdock, was reported to have anti-cancer properties in humans and rats (Huang, Guh *et al*. 2004, Matsuzaki *et al*. 2008). Chlorogenic acid (AF-8) is reported to have different biological activities including antimicrobial activities against *E. coli*, *Staphylococcus aureus* and *Micrococcus luteus* (Lin *et al*. 2004). Chiang *et al*. (2002) reported antiviral activities of caffeic (AF-9) and chlorogenic (AF-8) acids against herpes simplex viruses (HSV-1, HSV-2) and adenoviruses (ADV-3, ADV-11).

Table 1.2: Selection of phytochemicals previously isolated from the Asteraceae family. AF: refers to the name of the plant Arfaj (*R. epapposum*).
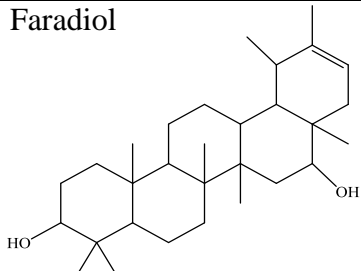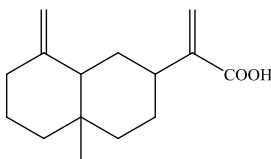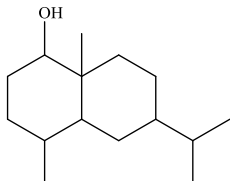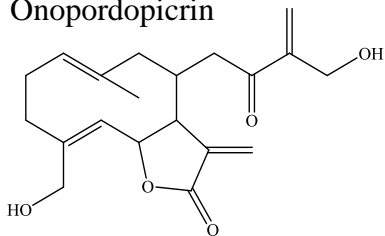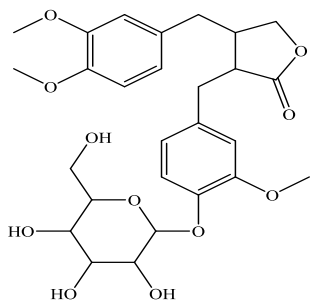
Compound	Code	Parts of the plant	Reference
Faradiol	AF-1	Leaves	(Liu *et al*., 2006)
Costus acid	AF-2	Leaves	(Barnes *et al*., 2007)
β-Eudesmol	AF-3	Fruits, leaves	(Tsuneki *et al*., 2005)
Onopordopicrin	AF-4	Leaves	(Barbosa *et al*., 1993)
Arctiin	AF-5	Seeds, fruits, leaves, roots	(Kamkaen *et al*., 2006; Matsumoto *et al*.. 2006)

Table 1.2 (continued): Selection of phytochemicals previously isolated from the Asteraceae family. AF: refers to the name of the plant Arfaj (*R. epapposum*).
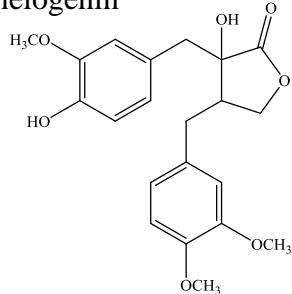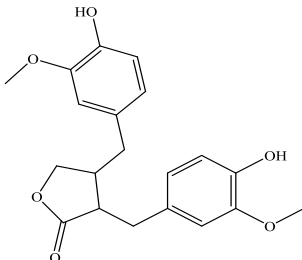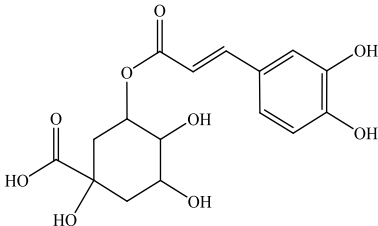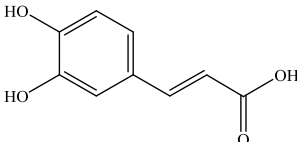
Compound	Code	Parts of the plant	Reference
Trachelogenin	AF-6	Fruits	(Chan *et al.*, 2011)
Matairesinol	AF-7	Fruits, seeds	(Wang and Yang 1993; Matsumoto *et al.*, 2006)
Chlorogenic acid	AF-8	Roots, leaves, seeds	(Chen *et al.*, 2004 **;** Lin *et al.*, 2003)
Caffeic acid	AF-9	Roots, leaves, seeds	(Pari and Prasath, 2008)

Table 1.2 (continued): Selection of phytochemicals previously isolated from the Asteraceae family. AF: refers to the name of the plant Arfaj (*R. epapposum*).
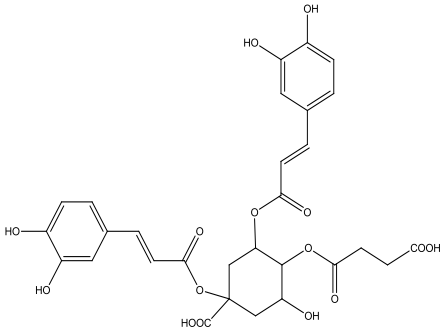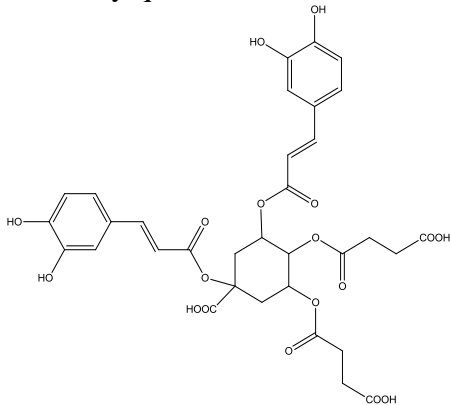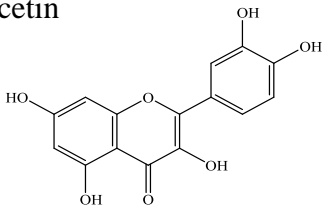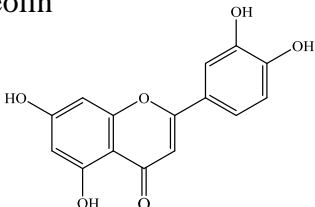
Compound	Code	Parts of the plant	Reference
1-*O*-,5 -*O*-dicaffeoyl-4-*O*-succinylquinic acid	AF-10	Roots	(Maruta *et al.*, 1995)
1-*O*-,5 -*O*-dicaffeoyl-3-*O*-, 4-*O*-disuccinylquinic acid	AF-11		
Quercetin	AF-12	Lower buds, roots, leaves	(Ferracane *et al.*, 2010)
Luteolin	AF-13	Roots, leaves	(Ferracane *et al.*, 2010)

Table 1.2 (continued): Selection of phytochemicals previously isolated from the Asteraceae family. AF: refers to the name of the plant Arfaj (*R. epapposum*).
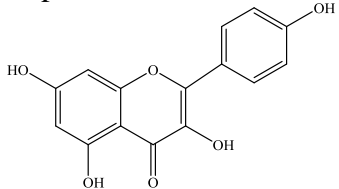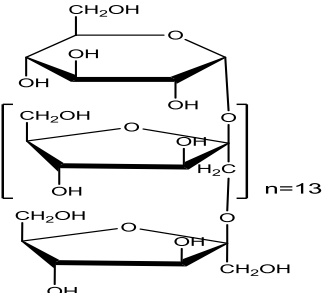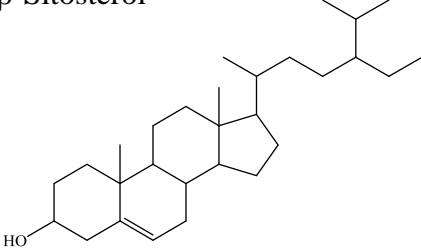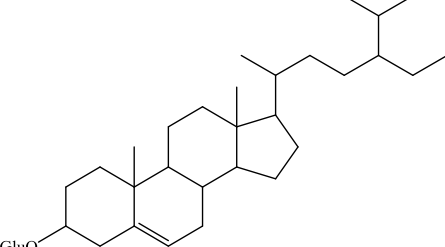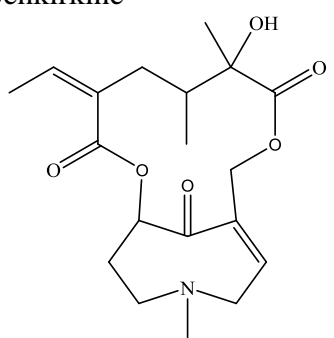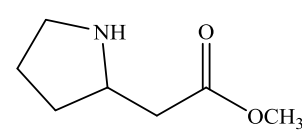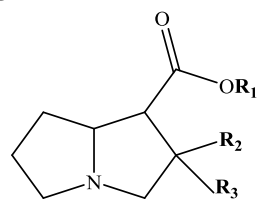
Compound	Code	Parts of the plant	Reference
Kaempferol	AF-14	Roots	(Okunade, 2002; Shi-xiong *et al.*, 2011)
ALF (Fructan)	AF-15	Roots	(Lei, 2009)
β-Sitosterol	AF-16	Aerial parts	(Kamboj and Saluja, 2011)
Sitosterol-β-D-glucopyranoside	AF-17	Roots, seeds	(Schütz *et al.*, 2006)

Table 1.2 (continued): Selection of phytochemicals previously isolated from the Asteraceae family. AF: refers to the name of the plant Arfaj (*R. epapposum*).

Compound	Code	Parts of the plant	Reference
Senkirkine	AF-18	Flower buds	(Roder and Wiedenfeld, 2011)
2-Methylpyrrolidine	AF-19	Flower buds	(Luethy *et al.*, 1980)
Tussilagine, **R₁**= Me, **R₂**= OH, **R₃**=Me Isotussilagine, **R₁**= Me, **R₂**= Me, **R₃**=OH	AF-20 AF-21	Flower buds	(Rizk, 1990; Roeder *et al.*, 2015)

1.2.1.2 *Astragalus spinosus*

A. spinosus Forssk. is known as Kitad (Figure 1.2) (Fabaceae). It is indigenous and widespread throughout tropical, subtropical, and the Mediterranean regions such as Iran, Kuwait, Libya, Egypt, Saudi Arabia, and Syria. It is an ascending branched spiny shrub, about 20-70cm in high, with apical leaves 3-5cm long, with 4-5 pairs of small leaflets that soon drop off leaving the rachises to become spines (El-Sebakhy *et al*., 1990).

A   **B**

Figure 1.2A: The growing plant of *Astragalus spinosus* (Pictures provided by Dr. Rothwelle Tate, Kuwait, 2012), **1.2B:** Stem with leaves and flowers. https://commons.wikimedia.org/wiki/File:Astragalus_spinosus_1.JPG

1.2.1.2.1 Historical use

There is no specific traditional use of *A. spinosus,* but several species of *Astragalus* exist in the Middle East, including *A. adscendens*, *A. gummifer*, and *A. brachycalyx*, that have been used to make the natural gum, tragacanth (Phillips and Williams, 2009). In Bangladesh, many plants of the Fabaceae family have been reported to have a traditional use to treat many diseases such as asthma, coughs and colds, fever, diarrhoea, heart disease, eczema, ulcers, snake-bites, kidney disease, high blood pressure, malaria, syphilis, and cholera (Rahman and Parvin, 2014).

1.2.1.2.2 Active ingredients and biological activities

A. spinosus mainly contains cycloartane triterpene oligoglycosides (Table 1.3). The isolated saponin glycosides have been used in the treatment of induced hepatic, renal and cardiac toxicities (Yusufoglu *et al*., 2014). The administration of carbon tetrachloride (CCl_4) is one of the most used methods of induction of liver cirrhosis. Darwish (2002) examined the effect of the isolated glycosides of *A. spinous* in reducing CCl_4-induced mortality. The study revealed that cycloastragenol-6-*O*-glycoside (AST-1) showed higher activity than isoastragaloside I (AST-3) and trigonoside I (AST-2). It has been demonstrated that astragaloside IV (AST-5) has therapeutic effects in cardiovascular diseases. In 2002, Li and Cao reported that AST-5 enhances the cardiac function of myocardial infarction and ischemic myocardium in rats. It has also been found that AST-5 can help in suppression of myocardial oxidative injury (Li *et* al., 2006). It was established that AST-5 has potential to prevent myocardial cell damage resulting from lack of oxygen in rats (Hu *et* al., 2009). In addition, AST-5 was reported to have antiviral activity against hepatitis-B virus (Wang *et al*., 2009), and was used to treat mice with type 2 diabetes (Lv *et al*., 2010). Furthermore, AST-5 showed biological activity in treatment of Parkinson's disease when examined on 6-hydroxydopamine (6-OHDA)-induced loss of dopaminergic neurons in primary nigral culture (Chan *et al*., 2009).

Table 1.3: Selection of phytochemicals previously isolated from *Astragalus spinosus*. AST: refers to the name of the plant Astragalus.

Compound	Code	Parts of the plant	Reference
Cylcoastragenol-6-*O*-glycoside, **R**= H, **R₁**= glucose	AST-1	Aerial parts	(Abdallah *et al.*, 1993)
Trigonoside I, **R**= H, **R₁**= xylose	AST-2	Aerial parts, Roots	(Abdallah *et al.*, 1993; Darwish, 2002)
Isoastragaloside I, **R**= β-D-xyl (2, 4 di Ac), **R₁**= glucose	AST-3	Aerial parts	(Abdallah *et al.*, 1993)
Astragaloside I, **R**= β-D-xyl (2, 3 di Ac), **R₁**= glucose	AST-4	Aerial parts, Roots	(Abdallah *et al.*, 1993; Darwish, 2002)
Astragaloside IV, **R**= β-D-xylopyranosyloxy, **R₁**= glucose	AST-**5**	Aerial parts, Roots	(Darwish, 2002)

1.2.1.3 *Tamarix aphylla*

T. aphylla (L.) Karsten (Figure 1.3) is the largest known species of the *Tamarix* and belongs to the family Tamaricaceae. The species has a variety of common names, including Athel pine, Athel tree, Athel tamarisk, and salt cedar. *T. aphylla* is an evergreen tree, up to 18 metres high with an erect tapering trunk. The fruit consists of a small narrow pointed capsule, 5mm long, splitting into 3 parts. Seeds are 0.5mm long; brown, each with a tuft of 3mm long whitish hairs. The specific name means without leaves. It is native across North, East and Central Africa, through the Middle East, and into parts of Western and Southern Asia (Merfort *et al*., 1992).

A   **B**
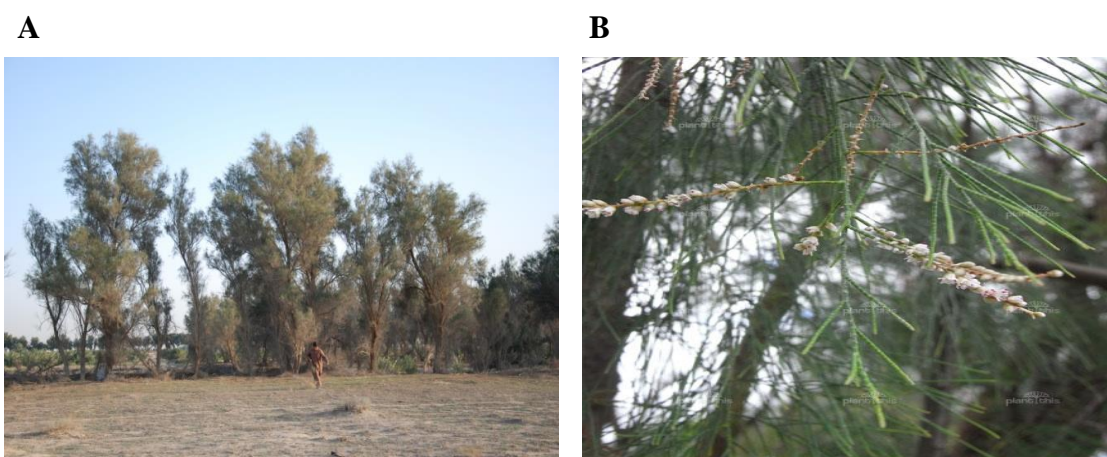
Figure 1.3A: *Tamarix aphylla* growing as a hedge, **1.3B:** Stem with leaves (pictures provided by Dr. Rothwelle Tate, Kuwait, 2012).

1.2.1.3.1 Historical use

T. aphylla has been used as an ornamental, windbreak and shade tree in agriculture especially in dry areas (Figure 1.3A). The species is highly valued for stabilising sand dunes due to its fast growth, deep and extensive root system. Also, Tamarisk is used as a plant indicator for soil type in agricultural surveys. *T. aphylla* is mentioned in the Holy Qur'an and prescribed in Al Hadith as a general tonic (Marwat *et al*., 2008). It is a traditionally used plant in Middle Eastern countries; for example flower galls are used as an astringent and for gargles, while the bark is used for treating eye

inflammation, rheumatism, fever, eczema, and other skin diseases (Azaizeh *et al*., 2006; Marwat *et al.,* 2008; Yusufoglu and Alqasoumi, 2011). In Saudi Arabia, *T. aphylla* is used as a treatment for allergic dermatitis in camels (Abbas *et al.,* 2002).

1.2.1.3.2 Active ingredients and biological activities

Various phytochemicals, mainly phenolic acids, terpenoids, and sterols have been isolated from different parts of *T. aphylla* (Table 1.4).

The aqueous extract of the leaves, possess antioxidant, anti-inflammatory and wound healing activities (Yusufoglu and Alqasoumi, 2011; Auribie, 2011). In a carrageenan-induced paw oedema model and excision wound model, a formulation of herbal gel containing 15 and 25% *T. aphylla* extract in a gel base were prepared and tested for anti-inflammatory activity. It showed optimum percentage inhibition of 53.1% and 89.6% with 15 and 25% gel formulation which was comparable to the standard Diclomax® (1% Diclofenac sodium) and Betadine® (10% Povidone-Iodine), respectively (Yusufoglu and Alqasoumi, 2011). In addition, strong antibacterial and anti-fungal activities of an aqueous bark and leaf extracts of *T. aphylla* were reported (Vadlapudi *et al*., 2009; Iqbal *et al*., 2015; Alrumman, 2016). In 2014, a study conducted by Qadir *et al*. revealed that an aqueous ethanolic extract of *T. aphylla* showed antipyretic and analgesic activity.

Nawwar *et al*. (2013) evaluated cytotoxicity activity of tamarixellagic acid (TAM-5) against breast (MCF-7), prostate (PC-3) and liver (Huh 7) cancer cell lines. The study revealed that tamarixellagic acid exhibited *in vitro* activity against all tested cell lines with an IC_{50} value of 0.16, 0.13, and 0.03μg/ml, respectively.

Table 1.4: Selection of phytochemicals previously isolated from *Tamarix aphylla*.
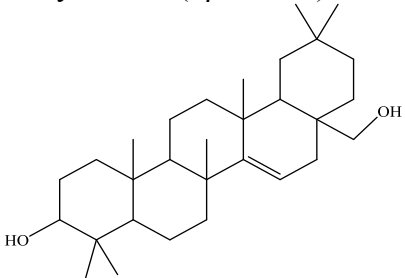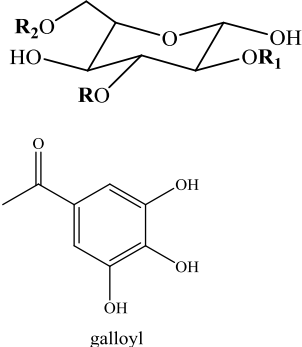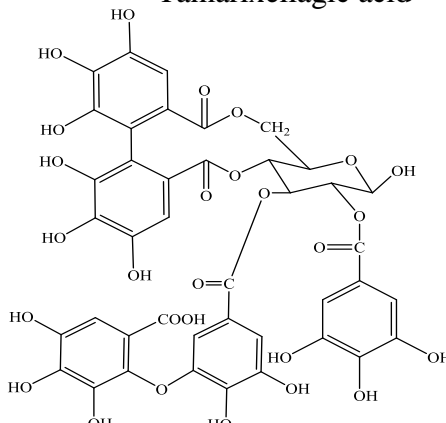
Compound	Code	Parts of the plant	Reference
Myricadiol Isomyricadiol (3β isomer) 	TAM-1 TAM-2	Bark	(Merfort *et al.*, 1992)
2, 6-Digalloyl glucose, **R**=H, **R₁**=**R₂**= galloyl 3, 6-Digalloyl glucose, **R₁**=**H, R**= **R₂**=galloyl galloyl	TAM-3 TAM-4	Galls	(Nawwar *et al.*, 1994)
Tamarixellagic acid 	TAM-5		

Table 1.4 (continued): Selection of phytochemicals previously isolated from *Tamarix aphylla*. TAM: refers to the name of the plant Tamarix.
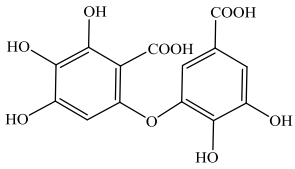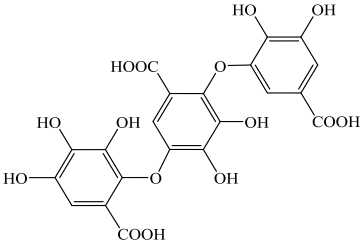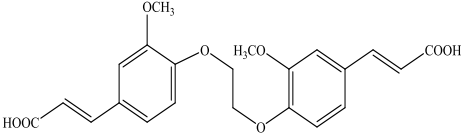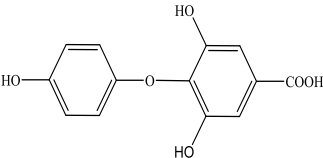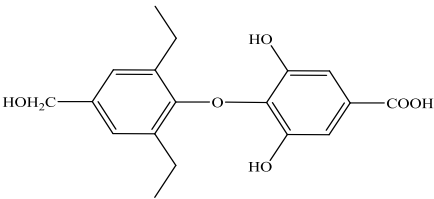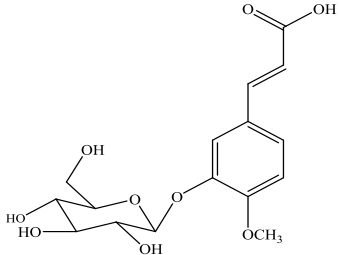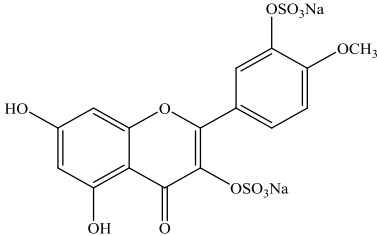
Compound	Code	Parts of the plant	Reference
Dehydrodigallic acid	TAM-6	Galls	(Nawwar *et al*., 1994)
Dehydrotrigallic acid	TAM-7		
Dimethylene oxyferulic acid	TAM-8	Stem galls	(Akhlaq and Mohammed, 2011)
Aphyllaoic acid	TAM-9		

Table 1.4 (continued): Selection of phytochemicals previously isolated from *Tamarix aphylla*. TAM: refers to the name of the plant Tamarix.

Compound	Code	Parts of the plant	Reference
Tamarixoic acid	TAM-10	Steam galls	(Akhlaq and Mohammed, 2011)
Isoferulic acid 3-*O*-β-glucopyranoside	TAM-11	Flowers	(Nawwar *et al.*, 2009)
Tamarixetin 3, 3`-di-sodium sulphate	TAM-12		

1.2.1.4 *Citrullus colocynthis*

C. colocynthis (L.) Schrad is known as Bitter apple, Wild water melon, Handal or Shaira (Figure 1.4). It belongs to the family Cucurbitaceae. It has yellow-coloured flowers, triangular-shaped leaves and yellow-green fruit. This plant is found in arid or semi-arid regions and is widely distributed especially in South Africa and Mediterranean regions (Bolous, 1983).

A   B
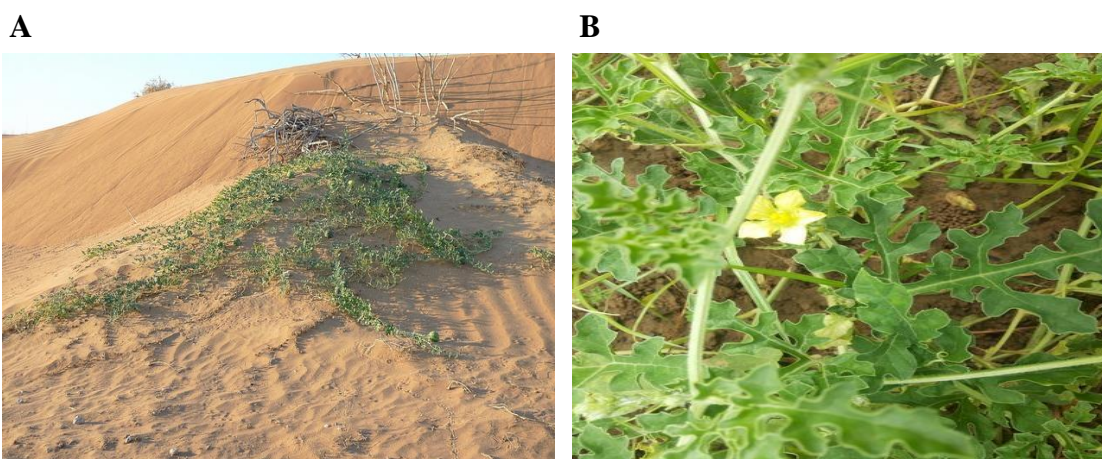
Figure 1.4A: The growing plant of *Citrullus colocynthis*, **1.4B:** Stem with leaves and flowers. https://en.wikipedia.org/wiki/Citrullus_colocynthis

1.2.1.4.1 Historical use

In traditional medicine, indigenous people from Mediterranean countries and some parts of Asia use different parts of this plant such as the leaves, fruits and seeds as an anti-inflammatory, a purgative for constipation, and for anti-rheumatic and antidiabetic treatments. Additionally, the fruits have been used by some women to terminate pregnancy in the first trimester (Hussein, 1985; Marzouk *et al*, 2012; Sebbagh, *et al*., 2009).

1.2.1.4.2 Active ingredients and biological activities

Previous studies concerning the chemical constituents of *C. colocynthis* have demonstrated the existence of cucurbitacin, cucurbitacin glycosides, *C-p-*hydroxybenzyl derivatives, phenolic acids, and flavonoids (Table 1.5). Studies have identified a range of potential biological properties and applications for extracts from *C. colocynthis*.

1.2.1.4.2.1 *C. colocynthis* antimicrobial properties

Gurudeeban *et al*. (2010) observed that a methanol extract of *C. colocynthis* leaves had *in vitro* antimicrobial activity against various pathogenic bacteria such as *S. aureus*, *Salmonella typhi*, *Bacillus subtilis*, *Streptococcus pyogenes* and *E. coli*. It also showed high antifungal activity against *C. albicans*, *Mucor* species, and *Aspergillus fumigatus* (Khatibi and Teymorri, 2011). Antibacterial effects have been evaluated for gluco-cucurbitacin E (CIT-4) and cucurbitacin I (CIT-2) against Gram-positive bacteria; *S. aureus* and *Klebsiella pneumonia*. Results revealed that gluco-cucurbitacin E showed strong antibacterial activity with minimum inhibitory concentration (MIC) values ranging from 1.25 to 2.5mg/ml while cucurbitacin B and I exhibited antibacterial effects (Chawech *et al*., 2015a). The antimicrobial activity of flavonoids has been widely documented. For example, flavonoids such as quercetin (CIT-28) and myricetin (CIT-30) showed antitubercular activity (MIC=50μg/ml, for both) at concentration of 100μg/ml (Yadav *et al*., 2013).

1.2.1.4.2.2 *C. colocynthis* anti-inflammatory properties

C. colocynthis extracts have anti-inflammatory activity and have been found to significantly ($p < 0.05$) inhibit serotonin and prostaglandin E_1 in carrageenan-induced oedema in the hind paw of rats (Rajamanickam *et al*., 2010). Cucurbitacins E (CIT-2) and I (CIT-2) have been reported to have anti-inflammatory activity by inhibiting cyclooxygenase (COX)-2 enzymes with no effect on COX-1 enzymes (Jayaprakasam *et al*., 2003). In 2013, Qiao *et al*. evaluated anti-inflammatory effects of cucurbitacin

E (CIT-1) in Lipopolysaccharide (LPS)-stimulated RAW 264.7 cells. The study reported anti-inflammatory effects of this compound through suppression of NF-κB nuclear translocation. Thus, CIT-1 decreased expression of TNF-α and IL-1β in LPS-activated cells in dose dependent manner.

1.2.1.4.2.3 *C. colocynthis* antidiabetic properties

Huseini *et al.* (2009) reported significant decrease in Haemoglobin A1c (HbA1c) and fasting blood glucose levels in *C. colocynthis* treated patients (receiving 100mg fruit capsules). Another study confirmed the antidiabetic property of *C. colocynthis* in which a significant reduction in blood glucose (from 381±34 to 105±35mM/l) was observed in diabetic patients treated with an oral dose (250mg and 500mg) of aqueous plant leaf suspension (Gurudeeban and Ramanathan , 2010).

1.2.1.4.2.4 *C. colocynthis* antitumour activity

Antitumour activity of cucurbitacin compounds is widely documented through different mechanisms, mainly by inhibiting the Janus kinase/signal transducer and activator of transcription pathways (Lee *et al*., 2010). Cucurbitacin E (CIT-1) is one of the cucurbitacins which is widely studied for anti-cancer activity. It was reported that cucurbitacin E is able to inhibit cell proliferation in many cancer cells such as bladder cancer, pancreatic cancer, breast cancer, hepatocellular carcinoma, oral squamous cell carcinoma and leukemia (Hung *et al*., 2013; Feng *et al*., 2014). In 2013, Lan *et al*. stated the inhibitory activity of cucurbitacin E against human breast cancer cells *in vitro* by inducing apoptosis and cell cycle arrest through the inhibition of signal transducer and activator of transcription 3 function. A study conducted by Kong *et al*. (2014) demonstrated inhibitory effect of cucurbitacine E toward triple negative breast cancer by inducing cell cycle G2/M phase arrest and apoptosis. Recent reports demonstrated cytotoxic effects of cucurbitacin I (CIT-2) on chondrosarcoma SW 1353, SW480 and Colo205 colorectal cancer cell lines (Abbas *et al*. 2013; Kim *et al*., 2014). Cucurbitacin I derivative (CIT-5) was shown to be specifically cytotoxic for Caco-2 cells (Song *et al*., 2014). In addition, Yuan *et al*.

(2014) analysed the inhibitory effect of CIT-2 in patients with glioblastoma multiforme (GBM). The results revealed that CIT-2 suppressed GBM growth by inducing apoptosis through regulating bcl-2 family proteins *in vitro* and *in vivo*.

1.2.1.4.2.5 Other *C. colocynthis* activities

Different extracts of *C. colocynthis* have been shown to display hypolipidaemic, laxative, larvicidal and anti-alopecia activity (Daradka *et al.*, 2007; Rahuman and Venkatesan, 2008; Dhanotia *et al.*, 2011). Studies have established the antioxidant activity of cucurbitacin I (CIT-2) (Jayaprakasam, *et al*., 2003) and its glucosides (CIT-5) (Delazar *et al*., 2006). Anti-artherosclerotic activity of 2-*O*-glucocucurbitacin E (CIT-4) was reported to cause a decrease in lipid oxidation products; malonaldehyde (MDA) and 4-hydroxynonenal (4-HNE) (Esterbauer, 1993; Tannin-Spitz *et al*., 2007). Torkey *et al*. (2009) reported insecticidal activity for 2-*O*-glucocucurbitacin E (CIT-4) on *Aphis craccivora*.

Table 1.5: Selection of phytochemicals previously isolated from *Citrullus colocynthis*. CIT: refers to the name of the plant Citrullus.
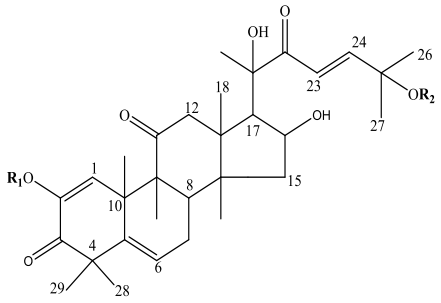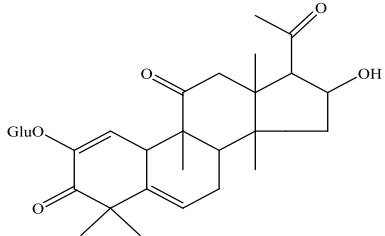
Compound	Code	Parts of the plant	Reference
Elaterin (cucurbitacin E); R_1=H, R_2=H	CIT-1	Fruits	(Lavie *et al.*, 1964; Seger *et al.*, 2005)
Elatericin B (cucurbitacin I); R_1=Glucose, R_2=Ac	CIT-2		
Dihydroelatericin B (cucurbitacin L); R_1=Glucose, R_2=H, 23,24-dihydro	CIT-3		
2-*O*-glucocucurbitacin E, R_1=Glucose, R_2=H	CIT-4		
2-*O*-glucocucurbitacin I; R_1=H, R_2=Ac	CIT-5		
2-*O*-β-D-glucopyranosyl-(22-27)-hexanorcucurbitacin	CIT-6	Fruits	(Lavie *et al.*, 1964)

Table 1.5 (continued): Selection of phytochemicals previously isolated from *Citrullus colocynthis*. CIT: refers to the name of the plant Citrullus.
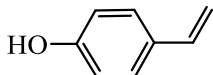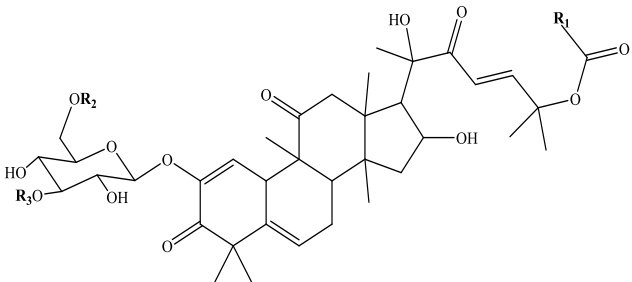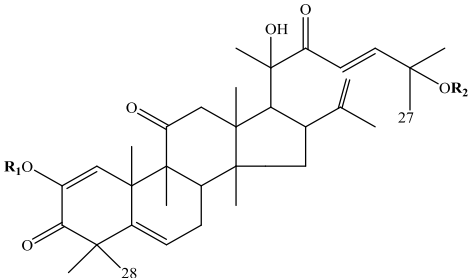
Compound	Code	Parts of the plant	Reference
6′-Acetyl-2-*O*-β-D glucocucurbitacin E; **R₁**=CH₃, **R₂**=Ac, **R₃**=H	CIT-7	Leaves	(Chawech *et al.*, 2015)
25-*p*-coumaroyl-3′-acetyl-2-*O*-β-D-glucocucurbitacin I;	CIT-8		
R₁= **R₂**= H, **R₃**=Ac 			
16-(2-Prop-1-enyl)-2-*O*-β-D-glucopyranosyl cucurbitacin I; **R₁**=Glu, **R₂**=H	CIT-9	Fruits	(Song *et al.*, 2015)
16-(2-Prop-1-en- yl)-25-*O*-acetyl-2-*O*-β- D-glucopyranosyl cucurbitacin I; **R₁**=Glu, **R₂**=Ac 	CIT-10		

Table 1.5 (continued): Selection of phytochemicals previously isolated from *Citrullus colocynthis*. CIT: refers to the name of the plant Citrullus.
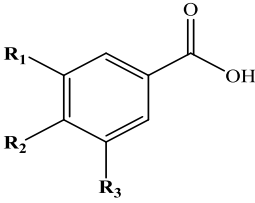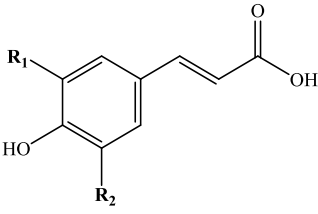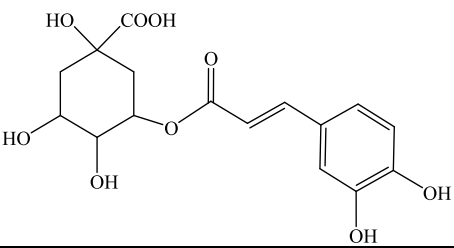
Compound	Code	Parts of the plant	Reference
Benzoic acid; $R_1=R_2=R_3=$ H	CIT-11	Fruit pulp	(Hussain *et al.*, 2014)
4-hydroxy-benzoic acid; R_1, R_3=H, R_2=OH	CIT-12		
Gallic acid; $R_1=R_2=R_3=$ OH	CIT-13		
Vanillic acid; R_1=H, R_2=OH, $R_3=$ OCH$_3$	CIT-14		
Ferulic acid; R_1=H, R_2=OCH$_3$	CIT-15	Fruit pulp	(Hussain *et al.*, 2014)
Sinapic acid; $R_1=R_2$=OCH$_3$	CIT-16		
p-Coumaric acid; $R_1=R_2$=H	CIT-17		
Chlorogenic acid	CIT-18	Fruit pulp	(Hussain *et al.*, 2014)

Table 1.5 (continued): Selection of phytochemicals previously isolated from *Citrullus colocynthis*. CIT: refers to the name of the plant Citrullus.
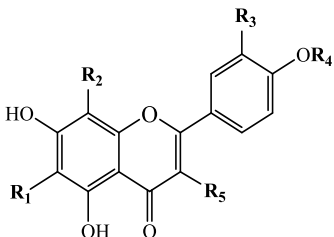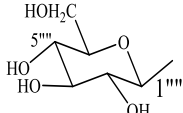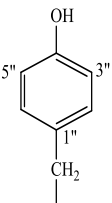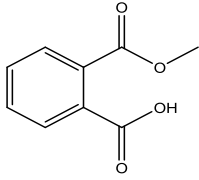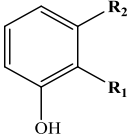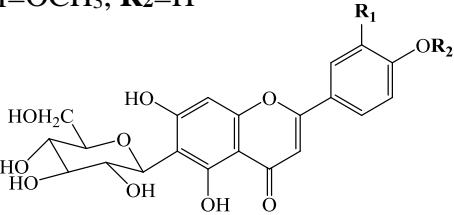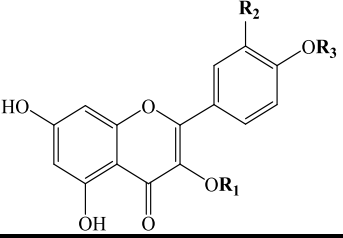
Compound	Code	Parts of the plant	Reference
8-*C*-*p*-hydroxybenzylisovitexin; R_1=Glucose, R_2=P-hydroxybenzyl, R_3= H, R_4=H, R_5=H	CIT-19	Aerial parts	(Maatooq *et al.,* 1997)
6-*C*-*p*-hydroxybenzylvitexin; R_1=P-hydroxybenzyl, R_2=Glucose, R_3= H, R_4=H, R_5=H	CIT-20		
8-*C*-*p*-hydroxybenzylisovitexin 4′-*O*-glucoside; R_1= Glucose, R_2= P-hydroxybenzyl, R_3= H, R_4=Glucose, R_5=H	CIT-21	Aerial parts	(Meena and patni, 2008)
phthalic acid methyl ester	CIT-22	Fruits	(Song *et al*., 2015)

Table 1.5 (continued): Selection of phytochemicals previously isolated from *Citrullus colocynthis*. CIT: refers to the name of the plant Citrullus.

Compound	Code	Parts of the plant	Reference
Catechol; R_1=OH, R_2=H Resorcinol; R_1=H, R_2=OH	CIT-23 CIT-24	Fruits	(Song *et al.*, 2015)
Isosaponarin; R_1=H, R_2=Glucosyl Isovitexin ; R_1=H, R_2= H Isoorientin 3-O-methylether; R_1=OCH$_3$, R_2=H	CIT-25 CIT-26 CIT-27	Fruits, seeds	(Delazar *et al.*, 2006; Gurudeeban *et al.*, 2010)
Quercetin; R_1=H, R_2=OH, R_3=H, R_4=H Catechin; R_1=H, R_2=H, R_3=H, R_4=OH Myricetin; R_1=H, R_2=OH, R_3=H, R_4=OH Kaempferol; R_1=H, R_2=H, R_3=H, R_4=H	CIT-28 CIT-29 CIT-30 CIT-31	Fruits Fruit pulp	(Meena and Patni, 2008; Hussain *et al.*, 2014) (Hussain *et al.*, 2014)

1.3 Molecular analysis

1.3.1 Exosomes

Exosomes are small vesicles (up to 100nm) containing nucleic acids and protein that are secreted by different cell types, and found in most body fluids including blood, saliva, urine, and breast milk (Thery, 2011). Recently, several studies demonstrated the existence of miRNAs in exosomes (Zhang *et al*., 2015; Izumi *et al.*, 2012; Cheng, *et al* 2014; Montecalvo *et al*., 2012). Exosomes work as a protective vesicle against degradation of transported miRNA by RNase (Cheng *et al*., 2014) and they can transport miRNAs directly to target cells (Montecalvo *et al*., 2012). They originate from the late endosomes and contain specific populations of mRNA, microRNA (miRNA), lipids, and proteins (Figure 1.5). They are released when a multivesicular endosome fuses with the plasma membrane (Harding *et al*., 1984). Although individual exosomal content may vary based on a variety of factors, there are common exosomal proteins that serve as markers: CD63, Alix, Rab 5, and Lamp 1 amongst others (Logozzi *et al*., 2009). Secreted exosomes can be internalized by recipient cells through endocytosis (Tian *et al*., 2010) where the release of exosomal contents can trigger a variety of responses in the target cell (Figure 1.5).
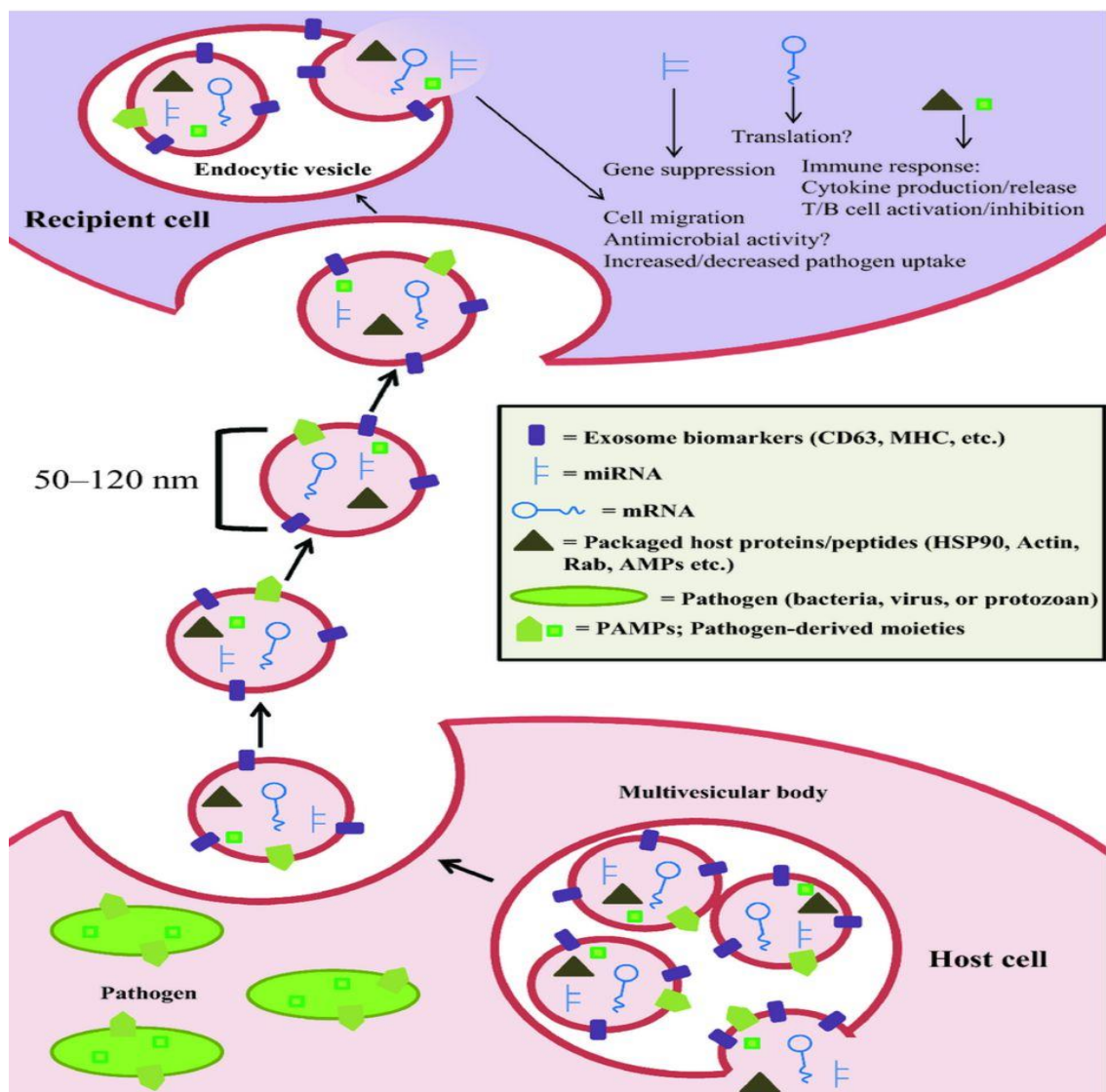
Figure 1.5: Diagram of exosome-mediated intercellular communication during infection. A model is presented for exosomal packaging and release, uptake by recipient cells, and known/potential effects of released exosomal contents on recipient cells during the course of pathogenic infection. Exosomes released by infected host cells carry a variety of host cargo molecules, including exosomal biomarkers, miRNA, mRNA, and antimicrobial peptides (AMPs). Pathogen-derived molecules (as indicated in inset) have also been shown to be incorporated into exosomes. Released exosomes are endocytosed by recipient cells for depositing their cargo. Released cargo molecules induce a variety of effects on the recipient cells, which vary depending on the pathogen causing the infection and the recipient cell type. These can include cytokine production, T-/B-cell activation/inhibition, cell migration and increased or decreased pathogen uptake (Fleming *et al*., 2014).

1.3.2 Plant miRNAs

Micro-ribonucleic acids (miRNAs) are non-coding small RNAs of 20-24 nucleotides in length. According to a recent study, about 17493 microRNAs have been identified in different plant species (Kozomara and Griffiths, 2014). Plant miRNAs are involved in plant development processes, including signal transduction, protein degradation, and the response to disease and pests. They play key roles in plants environmental stress responses such as oxidative stress, mineral nutrient deficiency, dehydration and even mechanical stimulus (Lima *et al*., 2012).

1.3.2.1 Dietary-derived miRNA regulation of human gene expression

Plant miRNAs are one of the most important gene regulators, involved mainly in those genes that are transcriptional factors (Hussain, 2012). The robustness of miRNA to degradation and their role as endogenous regulators of gene expression has, in recent years, led to the dietary xenomiR hypothesis (Witwer, 2012). This suggests that plant miRNAs are capable of cross-kingdom regulation gene expression through consumption of plant material, where the plant miRNAs may lead to an alteration in gene expression in the recipient cells of the mammalian consumer. On reaching the final recipient cells in organs such as liver, miRNAs are released and could regulate target genes in a sequence-specific manner (Melnik, *et al*., 2013; Witwer, 2012; Zhang *et al*., 2012a).

In 2014, Lukasik and Zielenkiewicz used high-throughput sequencing to establish that exogenous miRNAs from plants such as *Zea mays (Z. mays)*, *Arabidopsis thaliana (A. thaliana), Oryza sativa (O. sativa),* and *Citrus trifoliate (C. trifoliate)* were found in human plasma and porcine breast milk exosomes. The study detected 35 plant miRNAs in human breast milk and 17 in porcine breast milk, belonging to 25 and 11 miRNAs families, respectively. The largest amounts of ath-miR166a, bdi-miR168, ptc-miR472a and pab-miR951 were observed in the human samples, while in the porcine samples, zma-miR156a, ath-miR166a and zmamiR168a were detected in the highest abundance levels.

However, the xenomiR hypothesis is highly controversial (Zhang *et al*., 2012c). The first evidence for the absorption and bioactivity of a rice-derived miRNA in mice was provided by Zhang *et al*. (2012a). The authors reported high levels of exogenous plant miRNAs in the blood and tissues of ingesting organisms. They also suggested that a plant xenomiR could regulate a target transcript in the mouse. In contrast, Dickinson *et al*. (2013) repeated the original experiments and reported little uptake of plant xenomiRs and no regulation function was observed. Also other studies reporting investigations into the quantity and effects of dietary miRNAs, have shown different results in developing these findings (Wang *et a.l*, 2012; Snow *et al.*, 2013; Witwer *et al.*, 2013; Dickinson *et al.*, 2013; Chen *et al.*, 2013; Witwer and Hirschi, 2014; Liang, 2014). In 2014, Baier *et al*. revealed that after bovine milk consumption in humans, bovine milk miRNAs were demonstrated to survive in the gastrointestinal tract *in vivo* and transferred to systemic circulation, where they exert gene regulatory functions. In contrast, Aucherbach *et al*. (2016) reported that there is no evidence for transfer of bovine milk miRNAs into the circulation of adult humans when the authors analysed the samples provided by the laboratory of Baier.

However, several *in vitro* studies demonstrated that food-based miRNAs and miRNAs derived from commercially available bovine milk are able to enter into human and animal cells. They also reported the ability of these miRNAs to survive the gastrointestinal tract *in vivo* and then enter the systemic circulation to exert gene regulatory functions (Vaucheret *et al*., 2012; Jiang *et al*., 2012; Baier *et al*., 2014; Arntz *et al*., 2015; Wolf *et al*., 2015; Zhou *et al*., 2015). Some of these miRNAs were further shown to have therapeutic effects *in vivo*. A study conducted by Timms *et al*. (2014) demonstrated that plant-specific miR-168a is present in human maternal serum and can be detected in human placenta. In the same study, assessment of the potential role of miR-168a in regulating placental epidermal growth factor receptor (EGFR) signalling was conducted. They revealed that miR-168a overexpression resulted in reduced EGFR protein (62%; $p < 0.05$).

Supporting the above findings, there is evidence suggesting that the packaging of milk miRNA in exosomes offers the protection of these miRNAs from degradation and facilitates their absorption and their integration in mammals (Tian *et al*., 2014; Alsaweed *et al*., 2015; Pieters *et al*., 2015).

1.3.3 Bioavailability

Bioavailability refers to the proportion of a drug or other substance which enters the circulation when introduced into the body and able to have an active effect. In the current study, bioavailability assessement is required to detect plant-derived miRNAs in bovine milk following the gastric stage of human digestion sample using a drug dissolution tester TDT-08L. This would demonstrate their resilience and bioavailability and their potential for cross-kingdom gene regulation. The drug dissolution tester is usually used to predict *in vivo* drug release profiles by providing information about *in vitro* drug release. It is an industry standard system in complying with United States Pharmacopoeia specifications (USP). Recently, an *in vitro* study assessed the bioavailability of plant-derived miRNAs (miR-166, miR-167 and miR-168) in soybean and rice during storage, processing, cooking, and early digestion. The study demonstrated a significant bioavailability of measured plant miRNAs during all stages and after early digestion for 75 min (Philip *et al*., 2015). These results support the xenomiR hypothesis in which the xenomiRs show a robustness that could make them bioavailable for uptake during early digestion.

1.4 Project aims

One aim of this study was to establish whether the biological activities of camel milk and urine are derived from plants eaten by the camels as fodder, which may be a source of biologically active compounds. The concept was that bioactive compounds may be transferred to milk and urine to provide these products with potential medicinal properties for Bedouins and other communities.

This study also attempted to examine if the therapeutic value of camel milk and urine could be associated with plant-derived miRNAs; these small nucleic acids could be passed through the food chain to humans via camel milk and/or urine to regulate human gene expression according to the dietary xenomiR hypothesis (Zhang *et al*., 2012a). The first step was extraction of total RNA from the leaves of several desert plants using a number of commercially available extraction kits in order to identify the most effective method of extracting miRNAs from the plant samples. Examining the miRNAs present in these plants, camel urine and camel milk was the next step. That was followed by monitoring and comparing specific plant miRNA bioavailability in body fluids following the gastric stage of human digestion sample. Finally, an evaluation of the potential effect of selected plant miRNA to regulate the expression of a possible target human gene was carried out.

Chapter 2 Materials and methods

2.1 Solvents

A number of solvents were used for analytical and chromatographic purposes. All the solvents (VWR, Lutterworth, UK) were stored at low temperature and transferred to small bottles for routine use. Deuterated (99.9%) solvents (Sigma-Aldrich, Irvine, UK) were used for all the NMR analysis.

2.2 Reagents and chemicals

- 0.22μm filter (Merck, Darmstadt, Germany)
- 2x Fast SYBR Green Master Mix (Applied Biosystems, Renfrew, UK)
- 2x Luminaris Colour Probe High ROX Mastermix (Applied Biosystems, Paisley, UK)
- 20x TaqMan Assay primer/probe mix (Applied Biosystems, Renfrew, UK)
- 2-mercaptoethanol (Sigma-Aldrich, Poole, UK)
- AF488-labelled AllStars Negative Control siRNA (Qiagen, Manchester, UK)
- Agarose (Bioline, London, UK)
- AlamarBlue® Cell Viability Assay (Invitrogen, Renfrew, UK)
- AllStars Cell Death positive control siRNA (Qiagen, Manchester, Germany)
- Anti-bumping granules (Fisher Scientific, Leicestershire, UK)
- Bio-Rad Mini-PROTEAN 3® electrophoresis tank (Bio-Rad, Hemel Hempstead, UK)
- Column-grade silica gel (Silica gel 60, mesh size 20-200μm) (Merck, Darmstadt, Germany)
- Enhanced chemiluminescence (ECL) reagent (Thermo Fisher, Renfrew, UK)
- Ethidium bromide solution (Sigma-Aldrich, Steinheim, Germany)
- Experion™ RNA StdSens Analysis Kit (Bio-Rad, Hemel Hempstead, UK)
- Foetal calf serum (FCS) (Invitrogen, Renfrew, UK)
- GenElute™ Plant Genomic DNA Miniprep Kit (Sigma-Aldrich, Poole, UK)
- Haemocytometer (Hawksley, Lancing , UK)
- HiPerFect® transfection reagent (Qiagen, Manchester, UK)

- *PRLR* primers (Integrated DNA Technologies, Leuven, Belgium)
- Hyperladder™ DNA size marker (Bioline, London, UK)
- Isolate II RNA mini kit (Bioline, London, UK)
- L-glutamine (Invitrogen, Renfrew, UK)
- Lipophilic Sephadex LH-20 (GE Healthcare, Little Chalfont, UK)
- MagJET nucleic acid purification kit (Thermo Scientific, Renfrew, UK)
- miScript miRNA mimic (Qiagen, Manchester, UK)
- MirPremier microRNA isolation Kit (Sigma-Aldrich, Poole, UK)
- Mg^{2+}-Ca^{2+} -free Hank's balanced salt solution (HBSS) (Invitrogen, Renfrew, UK)
- Mouse monoclonal anti-CD63 antibody (Abcam, Cambridge, UK)
- Non-essential amino acids (Invitrogen, Renfrew, UK)
- Norgen Biotek Total RNA Purification Kit (Norgen Biotek Corp., Ontario, Canada)
- Nikon Eclipse TE300 Epifluorescent Inverted microscope (Nikon, Kingston upon Thames, UK)
- Oligonucleotide PCR primers (Integrated DNA Technologies, Leuven, Belgium)
- PowerPlant® RNA Isolation Kit (Mo Bio, Carlsbad, USA)
- PowerPlant® RNA Isolation Kit with DNase (Mo Bio, Carlsbad, USA)
- Polyacrylamide gel (Bio-Rad, Hemel Hempstead, UK)
- PureLink® RNA Mini Kit (Life Technologies, Renfrew, UK)
- Qiagen RNeasy Total RNA Purification Kit (Sigma-Aldrich, Poole, UK)
- Rabbit anti-Mouse IgG H&L (HRP) (Abcam, Cambridge, UK)
- RNA*later*® stabilization solution (Ambion, Austin, USA)
- RPMI 1640 (Lonza, Verviers, Belgium)
- Sodium pyruvate (Invitrogen, Renfrew, UK)
- Spectrum™ Plant Total RNA Kit (Sigma-Aldrich, Poole, UK)
- Streptomycin/ Penicillin (Invitrogen, Renfrew, UK)
- Sulphuric acid (VWR, Lutterworth, UK)

- TaqMan® MicroRNA Reverse Transcription Kit (Applied Biosystems, Renfrew, UK)

- miRNA PCR Assays (Thermo Fisher, Renfrew, UK)

- Tetro cDNA synthesis kit (Bioline, London, UK)

- TLC grade silica gel (60H, Merck, Darmstadt, Germany)

- TLC grade silica gel coated aluminium sheet (Precoated Silica gel PF254, Merck, Darmstadt, Germany)

- Total Exosome Isolation (from urine) Kit (Life Technologies, Renfrew, UK)

- Total Exosome Isolation (from other body fluids) Kit (Life Technologies, Renfrew, UK)

- Tris Acetate-EDTA buffer (Sigma-Aldrich, Steinheim, Germany)

- TRIzol® RNA Isolation Reagent (Invitrogen, Renfrew, UK)

- TrypLE Express (Invitrogen, Renfrew, UK)

- Virkon® (Antec International, Sudbury, UK)

2.3 Equipment

- $25cm^2$ and $75cm^2$ sterile flask (Thermo Fisher, Renfrew, UK)

- 12 and 96 well plates (Sigma-Aldrich, Poole, UK)

- Avance DRX500 MHz NMR (Bruker, Coventry, UK)

- MM300 Bead Milland cone balls (Retsch, West Yorkshire, UK)

- Beckman TLX ultracentrifuge with the TLA-55 rotor (Beckman Coulter, Inc., California)

- Bio-Ice cooling unit (Bio-Rad, Hemel Hempstead, UK)

- Biomax mbp 300 gel electrophoresis (Kodak, Watford, UK)

- Biotage Isolera™ Prime (Biotage, Uppsala, Sweden)

- Biotage SNAP C18 12g (Biotage, Uppsala, Sweden)

- Decon Sonicator (Decon laboratories, Hove, UK)

- Denali C18 Column 150 x 10mm 5μm column (Alltech Applied Science, Carnforth, UK)

- DNA Thermal Cycler 480 (Applied Biosystems, Warrington, UK)

- Drug dissolution tester TDT-08L (Pharma Alliance Group Inc., California, USA)
- Edwards freeze dryer (Edwards, Crawley, UK)
- Centrifuge 5415D (Eppendorf, Hamburg, Germany)
- Experion™ Automated Electrophoresis System (Bio-Rad, Hemel Hempstead, UK)
- IKA® Grinder (IKA® Werke GmbH & Co. KG, Staufen im Breisgau, Germany)
- Jeol Eclipse 400 NMR spectrometer (Jeol, Pleasanton, USA)
- KODAK M35-M X-OMAT processor (Kodak, Watford, UK)
- MTT solution (Biotium, Hayward, Canada)
- NanoDrop 2000c Spectrophotometer (Thermo Scientific, Loughborough, UK)
- NMR tubes (5mm x178 mm, Sigma-Aldrich, Poole, UK)
- Orbitrap HRESI mass spectrometer (Thermo Fisher, Hemel Hempstead, UK)
- Primus 96 *plus* thermal cycler (MWG-Biotech AG, Ebersberg, Germany)
- Reveleris® Prep Purification System (Grace, Columbia, USA)
- Rotary evaporator (Büchi, Flawil, Switzerland)
- Safety Cabinet (Walker, Glossop, UK)
- Soxhlet apparatus (Electrothermal, Staffordshire, UK)
- SpectraMax M5 Microplate Reader (Molecular Devices, Sunnyvale, USA)
- StepOne Plus Real time PCR System (Applied Biosystems, Renfrew, UK)
- Techne DRI-Block® (Camlab, Cambridge, UK)
- UV-detector 254nm and 364nm UVGL-58 (UVP, Chicago, USA)
- Vortex-Genie-2 (Scientific industries, New York, USA)
- Water Bath (Grant Instruments, Royston , UK)
- X-ray film (Santa Cruz Biotechnology, Heidelberg, Germany)

2.4 Sample collection

2.4.1 Plant material

Plant materials were collected from Libya in November, 2012 and January, 2013. Plants were identified by Dr Mohamad Ramadan, Faculty of Science, Zawia University, Zawia, Libya. Voucher specimens were deposited in the herbarium of the Faculty of Pharmacy, Zawia University, Zawia, Libya. The plants were air-dried to prevent mould and minimise degradation. The dried plant material was ground to a fine powder using an IKA® grinder. Extraction of the ground plant was performed using a Soxhlet apparatus by sequentially increasing the polarity of solvents every 3 days with each solvent (hexane, ethyl acetate, and methanol). The extracts were then evaporated to dryness at 40˚C under vacuum using a rotary evaporator.

2.4.2 Body fluid samples

Camel milk and urine samples were collected in January 2014 from Ghadamis / Libya. These samples were collected from one female dromedary camel (11 years old) that was mainly fed on *C. colocynthis* and *A. spinosus* leaves. The samples were mixed with RNA stabilisation reagent to minimise RNA degradation and kept at -80˚C until further use. Bovine whole milk was purchased from Tesco, UK.

2.5 Chromatographic techniques

2.5.1 Thin Layer Chromatography (TLC)

Thin layer chromatography (TLC) is one of the simplest forms of chromatographic separation techniques. This technique is essential for choosing suitable mobile phases for different separation methods such as column chromatography (CC), flash chromatography (FC), and vacuum liquid chromatography (VLC). TLC provides a quick way to analyse the components of a mixture or compare samples with standards. TLC was also used to examine the purity of isolated compounds. Plant crude extracts, fractions, or pure compounds were dissolved in a suitable (determined by trials and

errors) solvent and spotted 1cm above the bottom edge of a TLC-grade silica gel-coated aluminium sheet. A suitable solvent mixture was added to the TLC tank and left for a while to saturate the tank environment. Filter paper was placed inside the tank to aid the saturation. The spotted TLC plate was then placed in the TLC tank. When the solvent front had reached 1cm from the top of the plate, the TLC plates were taken out of the tank, the solvent front was marked with a pencil line and the plates air-dried immediately. They were then examined visually, under UV light (λ 254nm and 366nm) and sprayed with anisaldehyde-H_2SO_4 spray (5ml sulphuric acid, 85ml methanol, 10ml glacial acetic acid and 0.5ml anisaldhyde) and heated at 110°C for a minute.

The R_f value for each spot was calculated by dividing the distance the spot travelled, by the distance of the solvent front. This was used to pool similar fractions together, which were then dried and further analysed by nuclear magnetic resonance (NMR) to elucidate the structure of the compounds (Stahl and Mangold, 1975; Gray *et al.*, 2012).

2.5.2 Vacuum Liquid Chromatography (VLC)

A column was dry-packed with silica gel 60H (300g) under vacuum (via a water vacuum pump). Methanol extract (12g) was adsorbed on to a small amount of silica, allowed to dry and applied to the top of the VLC column. Elution was carried out with 400ml of different solvent systems according to the polarity and as determined by TLC (Coll and Bowden, 1986; Pelletier *et al.*, 1986).

2.5.3 Size-Exclusion Chromatography (SEC)

This technique is also known as gel filtration chromatography or molecular sieve chromatography. The principle of SEC is the separation of molecules according to their molecular size. In this work, a slurry of Sephadex LH-20 (35g) was added to a glass column of approximately 20.5cm height and 1.5cm diameter. Methanol extract (2g) was applied in a small quantity of methanol to the top of the column. Elution was commenced and completed with 100% MeOH and the fractions were collected in small vials (about 3 ml per fraction).

2.5.4 Column Chromatography (CC)

This technique was applied to fractionate polar and non-polar components, using an open glass column plugged with cotton wool. A glass column 55×3 cm was packed with 50g silica gel 60 and different crude extracts were eluted beginning with hexane after preadsorbing the extract on to silica gel introduced to the top of the column. The eluent was passed through the column with gradient elution. The polarity was subsequently changed to 5% (v/v) methanol in ethyl acetate to collect more polar compounds and 250-300ml of solvent system was used each time. Fractions were analysed by TLC and combined according to the band similarity and evaporated to dryness.

2.5.5 Preparative Thin Layer Chromatography (PTLC)

Preparative TLC (Prep. TLC) is a purification method carried out to isolate compounds from fractions in low quantities. Prep. TLC consists of TLC plates of 0.5mm thickness and 20g of silica gel (silica gel 60 PF_{254} containing gypsum), which is mixed with 40ml of distilled water. The formed slurry is then applied as a thin layer to a glass plate with a TLC applicator. The plates were allowed to air dry and then activated in an oven at 76°C (Sherma and Fried, 2006).

The mixture to be fractionated was dissolved in an appropriate solvent and spotted on the prepared plate as a narrow band. The plate was immersed in a previously determined solvent system. After drying, the plate was observed under UV light at λ 254nm and 366nm, and bands were marked for collection and carefully scraped with a spatula. Compounds were recovered from the silica gel by eluting the recovered stationary phase with 100% ethyl acetate (EtOAc), a mixture of EtOAc /methanol (MeOH) (50:50%), and finally with 100% MeOH for maximum recovery from the sorbent.

2.5.6 Biotage purification system

The Biotage system is an automated flash technology designed to fractionate crude extracts and isolate pure compounds from mixtures of small quantities (1mg to 150g). It works depending on detection of sample absorption of the light using two wavelengths

(254nm & 280nm) to detect sample components. This system consists of a cartridge of different sizes and types according to sample quantity and quality. A Biotage SNAP C18 12g (60mg-400mg) cartridge was used to purify 350mg of the mixture. Firstly, the sample was dissolved in a small quantity of MeOH and loaded onto the cartridge. This system has a fraction collector which collects fractions (5ml in each tube). The solvent system and the flow rate adjust automatically and each component of the sample is collected according to light absorption (Table 2.1).

Table 2.1: Shows the solvent mixtures used and the duration of each one at a flow rate of 8ml/m **(A)** and 7ml/m **(B)**.

A   **B**

No.	Mobile Phase (Water:Methanol)	Solvent Mix Length (min)	No.	Mobile Phase (Water:Methanol)	Solvent Mix Length (min)
1	15%-15%	10	1	5%-15%	5
2	15%-15%	10	2	5%-15%	10
3	15%-30%	30	3	15%-20%	10
4	30%-40%	1	4	15%-20%	15
5	40%-50%	9	5	20%-30%	15
6	50%-58%	5	6	30%-50%	5
7	58%-100%	5	7	50%-100%	5

2.5.7 Reveleris® Prep Purification System

The Reveleris® Prep Purification System is a high performance instrument designed with flash chromatography and preparative liquid chromatography modes. It allows the use of each mode independently or sequentially. This system has three channel variable UV-Vis wavelengths and Evaporative Light Scattering (ELS) detection that allow detection and collection of all components of various samples. A 100mg of a mixture of two compounds was dissolved in a suitable solvent and filtered using a 0.22μm filter

unit and finally injected into a Denali C18 Column 150 x 10mm 5μm column using preparative mode. The solvent system, collection volume, and the flow rate were adjusted automatically (Table 2.2).

Table 2.2: Gradient solvent mixture and the duration of each one at a flow rate of 4ml/m.

No.	Mobile Phase (Water: Acetonitrile)	Solvent Mix Length (min)
1	100%-0%	5
2	95%-5%	5
3	10%-90%	5
4	15%-85%	5
5	20%-80%	5
6	25%-75%	5
7	30%-70%	5

2.6 Spectroscopic examination

2.6.1 Nuclear Magnetic Resonance (NMR)

Nuclear magnetic resonance (NMR) spectra were obtained on a Jeol Eclipse 400 spectrometer operating at 400 MHz for ^{1}H and 100 MHz for ^{13}C and Distortionless Enhancement of Polarization Transfer (DEPT) spectra. A Bruker Avance DRX-500 (500MHz) spectrometer was used for heteronuclear multiple quantum coherence (HMQC) and heteronuclear multiple bond connectivity (HMBC). Each pooled fraction (15mg) was dissolved in 500μl of deuterated solvent; deuterated chloroform (CDCl$_3$) or dimethyl sulfoxide (DMSO-d_6), depending on the solubility of the compound and the extent of resolution obtained. The sample was then transferred to a 5mm internal diameter NMR tube and the structures of the compounds were elucidated from the resulting spectra. The NMR spectroscopic data were processed using MestReNova

software 8.1.2 (Mestrelab Research, A Coruña, Spain)) and ChemBioDraw Ultra, Version 14 (PerkinElmer, Yokohama, Japan), was used to draw compound structures.

2.6.1.1 One-Dimensional NMR (1D)

This is the simplest technique used in structure elucidation. ^{1}H NMR was used for the determination of the types of protons in the compounds and ^{13}C NMR for providing data on the number and kinds of carbon atoms in the compounds. Both ^{1}H and ^{13}C 1D NMRspectra can be less informative than two-dimensional (2D) NMR analysis especially in the case of some of the more complex organic molecules.

2.6.1.2 Two-Dimensional NMR (2D)

2D NMR includes COrrelation SpectroscopY (COSY), Nuclear Overhauser Enhancement SpectroscopY (NOESY), Heteronuclear Multiple Quantum Coherence (HMQC) and Heteronuclear Multiple Bond Coherence (HMBC).

COSY shows ^{1}H-^{1}H connectivities. The proton shifts are plotted on both axes with the contour plot along the diagonal of the square. NOESY records all the ^{1}H-^{1}H NOE correlations occurring in a molecule. HMQC was used to identify the correlation between protons and carbons atoms in samples through the ^1J coupling between them. HMBC provided the correlation between the chemical shift of the protons in the samples and the heteronucleus ^{13}C through ^2J and ^3J coupling interaction between the nuclei (long-range H-X-C-C-C correlations).

2.6.2 Mass Spectrometry (MS)

This technique is used to elucidate the elemental composition of a sample. One mg of each sample was dissolved in 1ml methanol and 10µL of the solution was injected along with a direct infusion of 0.1% (v/v) formic acid in acetonitrile: water (90:10) at a flow rate of 200µl/m. High resolution electron impact mass spectra were recorded on a Jeol 505HA spectrometer. Positive ion and negative ion mode ESI experiments were carried

out on a ThremoFinnigan LCQ-Decaiontrap or Orbitrap HRESI mass spectrometer. MS data acquisition was carried out by Dr. Tong Zhang (SIPBS, University of Strathclyde).

2.7 Bio-activity examination

2.7.1 Tissue culture

2.7.1.1 Maintenance of the cells

The cell lines used in this study, obtained from the European Collection Animal Cell Culture, (Public Health England, Salisbury, UK) were maintained at 37°C, 5% (v/v) CO_2, and 100% humidity. All cell lines were obtained from Prof. Robin Plevin and Mrs. Louise Young (University of Strathclyde, UK). Every 3-4 days, the cells were washed with 5ml of Mg^{2+}-Ca^{2+} -free Hank's Balanced Salt solution (HBSS) and trypsinised by adding 5ml of TryplE Express and then incubated at 37°C for 4 to 6 min according to the cell type. The cells were then observed under the microscope to ensure complete detachment of the cells. The action of TryplE Express was stopped by adding 10ml of complete culture medium (Table 2.3). The cells were then centrifuged at 1000×g for 2 min, the medium was removed, and the pellet resuspended in 10ml of fresh complete medium. The cell numbers were counted using a haemocytometer and adjusted to the required number according to the cell type.

2.7.1.2 Preparation of complete culture medium

The medium for each cell line was prepared in a sterile flow hood and was then stored at 4°C until required (Table 2.3). All the cell lines used in this study were adherent with an epithelial morphology (Figure 2.1).

Table 2.3: Cell culture media of the cell lines used in this study.

Cell lines	ECACC number	Complete Culture Medium
1. HeLa cells cervical cancer cells	93021013	500ml Eagle's Minimum Essential Medium (EMEM) supplemented with 50ml foetal calf serum 10% (v/v), 5ml penicillin/streptomycin, 5ml non-essential amino acids and 5ml L-glutamine
2. LNCaP cells prostate carcinoma	89110211	500ml RPMI 1640 medium supplemented with 50ml foetal calf serum 10% (v/v), 5ml penicillin/streptomycin, 5ml L-glutamine and 5ml sodium pyruvate.
3. ZR-75-1 cells breast carcinoma	87012601	500ml RPMI 1640 medium supplemented with 50ml foetal calf serum 10% (v/v), 5ml penicillin/streptomycin, 5ml L-glutamine and 5ml sodium pyruvate.
4. A2780 cells ovarian carcinoma	93112519	500ml RPMI 1640 medium supplemented with 50ml foetal calf serum 10% (v/v), 5ml penicillin/streptomycin, 5ml non-essential amino acids, 5ml L-glutamine and 5ml sodium pyruvate.
5. PANC-1 cells pancreatic carcinoma	87092802	500ml Dulbecco's Modified Eagle's Medium (DMEM) supplemented with 50ml foetal calf serum 10% (v/v), 5ml penicillin/streptomycin and 5ml L-glutamine.
6. A375 cells malignant melanoma	88113005	500ml RPMI 1640 medium supplemented with 50ml foetal calf serum 10% (v/v), 5ml penicillin/streptomycin, 5ml non-essential amino acids, 5ml L-glutamine and 5ml sodium pyruvate.
7. PNT2 cells normal prostate	95012613	500ml RPMI 1640 medium supplemented with 50ml foetal calf serum 10% (v/v), 5ml penicillin/streptomycin and 5ml L-glutamine.
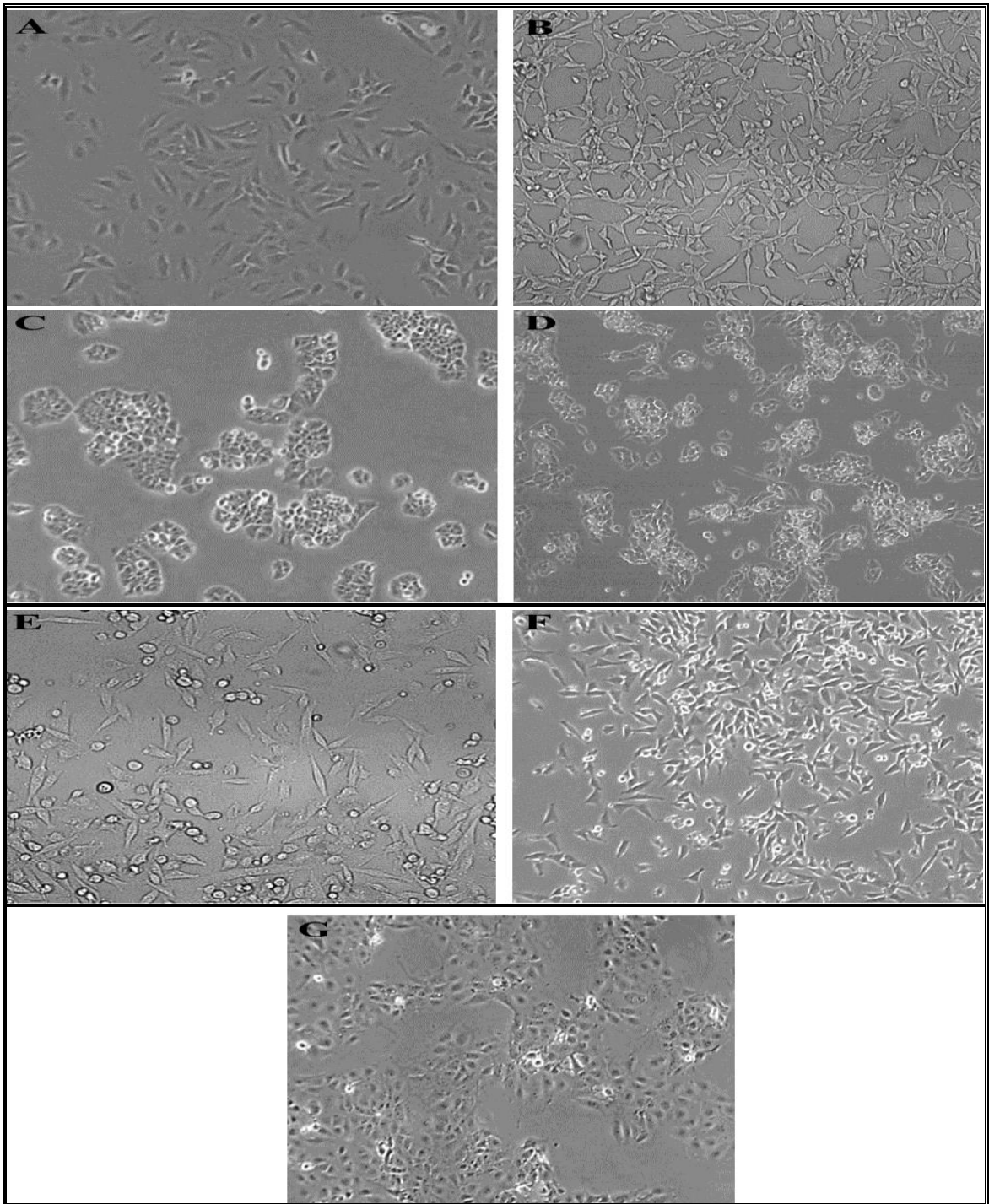
Figure 2.1: Morphology of the cell lines used in the present study; A: HeLa cells, B: LNCaP cells, C: ZR-75-1, D: A2780 cells, E: PANC-1 cells, F: A375, G: PNT2, Objective lens X10.

2.7.1.3 Seeding density optimisation

Each cell line was seeded in a 96-well plate at different seeding densities of 3000, 5000, 7000, and 10000 cells per well and allowed to attach overnight. An AlamarBlue® assay (Section 2.7.1.4) was used to examine the differences between the four seeding densities.

2.7.1.4 Cytotoxicity assay

The AlamarBlue® assay is a fluorometric measurement of metabolic activity and it was used to detect the effect of isolated compounds on cell viability. In metabolically active cells, AlamarBlue® can be reduced to resorufin and the dye appears changed from blue to pink. Initial cytotoxicity screening was performed at a concentration of 500μg/ml against the six tumour cell lines and one normal cell line. Two milligrams of each compound tested was dissolved in either 100% serum-free medium or 1% (v/v) DMSO in medium according to the solubility of each compound. Each compound solution (100μl) was then added to the first well of rows A, B, C, and G of a 96-well tissue culture plate. Row G contained compound and medium only and acted as a background control for coloured material. DMSO (100μl) was added to the first wells of rows D and E (solvent control). Medium containing 10% (v/v) AlamarBlue® solution (100μl/well) was then added to row F which contained cells only. After that, medium in row H containing 10% (v/v) AlamarBlue® solution was added (negative control). The plate was placed in an incubator overnight at 37°C, 5% (v/v) CO_2 and 100% humidity before the addition of 10μl of AlamarBlue®. After addition of AlamarBlue®, the plates were incubated at 37°C in 5% (v/v) CO_2 and 100% humidity for 4h. The plates were then read using a SpectraMax M5 micro-plate reader at 570nm and 600nm. The percentage proliferation was calculated and plotted as the percentage of metabolically active cells relative to the control. The statistical analysis was performed using GraphPad Prism version 5.0 for Windows (GraphPad Software, San Diego, CA, USA). The values were presented as the mean ± SEM of triplicate readings and three separate assays set up.

2.8 Molecular biology assays

2.8.1 Total RNA extraction

2.8.1.1 Plant total RNA extraction

Extraction of total RNA from the leaves of several desert plants was carried out using a number of commercially available extraction kits in order to identify the most effective method of extracting miRNAs from the plant samples (Table 2.4).

Table 2.4: Comparison of RNA extraction using different RNA extraction kits.

Name of RNA Extraction kit	Mechanism of RNA Purification	Extracted Nucleic Acid	Name of Extracted Plant
PureLink RNA Mini Kit	Spin column chromatography	Total RNA	*T. aphylla, A. spinosus, C. colocynthis* and *R. epapposum.*
Cambio PowerPlant RNA isolation Kit with DNase	Spin column chromatography	Total RNA	*A. spinosus* and *C. colocynthis.*
Cambio PowerPlant RNA isolation Kit	Spin column chromatography	Total RNA	*T.aphylla, A. spinosus* and *C. colocynthis.*
Qiagen Total RNA Purification Kit	Spin column chromatography	Total RNA	*T. aphylla, A. spinosus* and *C. colocynthis.*
MirPremier microRNA isolation Kit	Spin column chromatography	Small RNA	*T. aphylla, A. spinosus, C. colocynthis* and *R. epapposum.*
Invitrogen PureLink Kit with MirPremier flowthrough	Spin column chromatography	Small RNA from Total RNA	*T. aphylla, A. spinosus, C. colocynthis* and *R. epapposum.*
Spectrum Plant Total RNA Kit (Protocol A)	Spin column chromatography	Total RNA from difficult plant tissue	*T. aphylla, A. spinosus, C. colocynthis* and *R. epapposum.*
Spectrum Plant Total RNA Kit (Protocol B)	Spin column chromatography	Total RNA	*T. aphylla, C. colocynthis*
Thermo Scientific MagJET nucleic acid purification kit	Magnetic bead	Total RNA	*A. spinosus* and *C. colocynthis.*
Norgen Biotek Total RNA Purification Kit	Spin column chromatography	Total RNA	*A. spinosus* and *C. colocynthis.*
Invitrogen TRIzol® RNA Isolation Reagent	Organic extraction	Total RNA	*C. colocynthis.*
Ambion *mir*Vana™ miRNA Isolation Kit	Organic extraction	Total RNA & Small RNA	*T. aphylla, C. colocynthis*

A comparative study between the above kits was conducted. Due to the size of the miRNAs and the capture limits of the purification systems, some total RNA extraction kits require additional steps to improve the recovery of these small RNAs. For example, the Spectrum kit had two protocols (A&B). Protocol A is designed specifically for plant tissues with high water content and low RNA content to increase microRNA yield. Protocol B is recommended for plant tissues with normal water content. The PureLink, Plant RNeasy kit, and Norgen Total RNA kit disrupt and homogenise samples in the presence of the chaotropic salt, guanidinium isothiocyanate to overcome RNases. These kits utilise the selective nucleic acid binding properties of silica-based membranes with the speed of micro spin technology without using of phenol or chloroform. The MagJET kit employs magnetic bead technology to enable high yields of purified RNA from plant material. RNA extraction using TRIzol® Reagent is based on organic solvent purification. It is a solution of phenol, guanidine isothiocyanate, and other components which facilitate the isolation of RNA. Other extraction kits are specifically designed to only purify small RNAs such as the MirPremier and *mir*Vana™ kits. Some extraction kits require additional steps to improve the recovery of small RNAs.

All the spin column protocols include four main steps: disruption and lysing of tissue; binding of RNA to an affinity column step; washing away of contaminants; and a final elution step. The plant leaves (40-70mg) were first disrupted in sterile, RNase–free 2ml tubes using a 6mm coneball and beadmill (Retsch, West Yorkshire, UK) at a shaking frequency of 30 Hz for 30 seconds. This was repeated four times. A lysis solution containing 2-mercaptoethanol mixture (lysing step) was added to the plant material and mixed thoroughly by vortexing. The lysate was then filtered and centrifuged to pellet any cell debris and transferred to another RNase-free microcentrifuge tube. Next, ethanol was added to precipitate the RNA to facilitate binding to the column (binding step) and most of the contaminants were removed in the flowthrough following centrifugation. The bound RNA was then washed by adding a washing solution to remove any remaining impurities (washing step), the columns were centrifuged again, and the flowthrough discarded. This step was

repeated and the tubes were re-centrifuged to ensure that the column was completely dry and free of any residual wash solution. Finally, the purified RNA was eluted using the provided elution buffer or water (eluting step). The last step was repeated to improve the total yield. The purified RNA sample was placed at −80°C for long term storage.

2.8.1.2 Total RNA extraction from body fluids

Total RNA was extracted from camel milk and urine samples using a Norgen Biotek Total RNA purification kit, which has specific protocols for small RNAs co-purification from body fluids. Total RNA from store-bought, pasteurised whole cow milk was also extracted using the same kit for comparison purposes. This assay has a workflow similar to that of other extraction kits used for plant total RNA extraction (Figure 2.2).
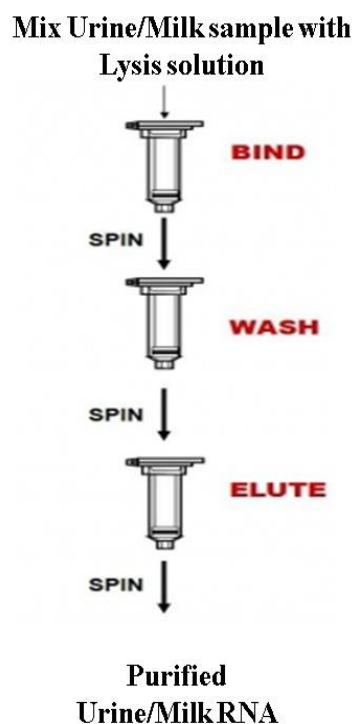
Figure 2.2: Norgen RNA extraction workflow for body fluids.

2.8.1.3 Total RNA extraction from exosomes

These microvesicles have been identified in body fluids and blood, indicating that this exchange of information between different organs could occur by exosomes (Qazi *et al*., 2010). Total RNA extraction from exosomes was applied to maximise recovery of intact total RNA obtained by using commercial total RNA extraction kits.

2.8.1.3.1 Total exosome isolation from milk

As detailed in the Total Exosome Isolation (from other body fluids) kit procedure, camel and bovine whole milk samples (500µl) were centrifuged using a bench centrifuge at 2000 × g for 10 min at room temperature to remove cells and debris. The supernatant was transferred to a new tube without disturbing the pellet which contains contaminants and centrifuged again at 10,000 × g for 30 min at 4°C. A clarified milk sample was transferred to a new tube and equal volume (500µl) of 1X Phosphate-buffered saline (PBS) (137mM NaCl, 2.7mM KCl, 10mM Na_2HPO_4, 2mM KH_2PO_4, pH7.4) was added to it. A sample of milk was mixed with total exosome isolation reagent by vortexing. The mixture was incubated at room temperature for 30 min and then centrifuged at 10,000 × *g* for 10 min. Exosomes were contained in a pellet at the bottom of the tube. The pellet was then resuspended in PBS and stored at -80°C until further analysis.

2.8.1.3.2 Total exosome isolation from urine

Following the Total Exosome Isolation (from urine) kit procedure, 500µl of camel urine sample was centrifuged at 2000 × g for 30 min at 4°C and then the supernatant was transferred to a new tube. An equal volume of total exosome isolation (from urine) reagent was added to the sample and mixed well by vortexing and inverting of the tube. The sample was then incubated at room temperature for 1h. After incubation, centrifugation of the sample at 10,000 × *g* for 1h at 4°C was carried out

to form a pellet which contains exosomes. RNA lysis buffer was immediately added to the exosome pellet to prevent nucleic acid degradation. Total RNA was then isolated from the lysed exosomes using the Norgen Biotek Total RNA purification kit.

2.8.1.3.3 Exosome isolation by ultracentrifugation

Pasteurised whole bovine milk sample was subjected to centrifugation at 4°C for 30 min at 2000 x g to remove fats followed by centrifugation at 12,000 x g for 30 min at 4°C to eliminate cell debris. The supernatant was removed to a new tube and then subjected to ultracentrifugation at 110,000 x g for 2h using a Beckman TLX ultracentrifuge with a TLA-55 rotor. RNA lysis buffer was immediately added to the exosome pellet to prevent nucleic acid degradation. Total RNA was then isolated from the lysed exosomes using Norgen Biotek Total RNA purification kit.

2.8.1.4 Exosome detection by Immunoblotting (Western Blot)

Characterisation of purified exosomes can be carried out using different techniques such as Western blotting, flow cytometry, or electron microscopy. In this study, immunoblotting analysis was applied.

2.8.1.4.1 Preparation of exosome sample

The exosome pellet was dissolved in 200μl of RIPA (Radio-Immunoprecipitation Assay) Buffer (150mM NaCl, 1.0% (v/v) IGEPAL® CA-630, 0.5% (w/v) sodium deoxycholate, 0.1% (w/v) SDS, and 50mM Tris, pH 8.0) by pipetting thoroughly, followed by vortexing. To ensure complete lysis of the exosomes, the sample was sonicated in a water bath for 10-15 min with vortex-mixing in between. The sample was then centrifuged at 13,000 x g for 5 min at room temperature, and the supernatant transferred to a new microcentrifuge tube, before storing at -20°C until use.

2.8.1.4.2 SDS-PAGE Polyacrylamide Gel Electrophoresis

In order to separate the proteins by gel electrophoresis, 10% (w/v) polyacrylamide gel was assembled in a Bio-Rad Mini-PROTEAN 3® electrophoresis tank with both reservoirs filled with running buffer (25mM Tris, 190mM glycine, 0.1% (w/v) SDS). Thirty µl/well of each sample was loaded into the wells along with a molecular weight marker using a micro-syringe. A negative control (without protein sample) was loaded as well to ensure that there was no non-specific binding. Loaded samples were electrophoresed at a constant voltage of 120V for one hour, until the marker dye had reached the bottom of the gel.

2.8.1.4.3 Protein transfer from SDS-PAGE to nitrocellulose membrane

Following separation of the proteins on the polyacrylamide gel, the protein bands were transferred to a nitrocellulose membrane using electrophoretic blotting. In a transfer cassette sandwich, the gel was pressed against a nitrocellulose sheet between two filter papers and two sponge pads. The cassette was then assembled in a Bio-Rad Mini-PROTEAN 3® electrophoresis tank filled with transfer buffer (25mM Tris, 190mM glycine, 20% (v/v) methanol) and cooled in presence of Bio-Ice cooling unit. This step was performed by applying a constant current of 100V for an hour.

2.8.1.4.4 Immunological detection of protein

Detection involves probing the membrane with a primary antibody specific to the protein of interest, followed by incubating the membrane with an appropriate conjugated secondary antibody (indirect detection of target antigen) and developed to allow visualisation of that protein. The common exosomal proteins that can be identified by immunoblotting include tetraspanin proteins; CD63, CD81, and CD9 (Gross *et al*., 2012; Mathivanan & Simpson, 2010; Simons & Raposo, 2009). Tetraspanins are highly expressed transmembrane proteins (25–50 kD) and include at least 28 different family members in mammals (Todres *et al*., 2000). Mouse monoclonal anti-CD63 antibody was used as primary antibody and Rabbit anti-

Mouse IgG H&L (HRP) as secondary antibody. The detection step included incubation of the membrane in a blocking buffer of 3% (w/v) Bovine Serum Albumin (BSA) in NaTT buffer (150mM NaCl, 20mM Tris, pH 7.4, 0.2%, v/v Tween-20) for 90 m with gentle agitation to reduce non-specific binding of the antibody to the membrane. After blocking, the membrane incubated overnight with the primary antibody (diluted to 1:1000 in NaTT buffer containing 0.2%, w/v, BSA) to form an antigen-antibody complex specific to the target protein. The next day, the membrane was washed three times in NaTT every 15 min with gentle agitation on a platform shaker. The membrane was then incubated at room temperature for 90 min with secondary antibody diluted to 1:10000 in NaTT buffer containing 0.2% (w/v) BSA. After incubation, the membrane was washed in NaTT for 90 min. Finally, detection of immunnoreactive protein bands was carried out by membrane incubation for 2 min in an enhanced chemiluminescence (ECL) reagent. The membrane was then developed in dark room by exposure to X-ray film for the required time using a KODAK M35-M X-OMAT processor.

2.8.2 Assessment of extracted RNA purity

The RNA concentrations of all samples were measured spectrophotometrically using a NanoDrop 2000c Spectrophotometer. It can measure 0.5-2µl of the RNA samples across the ultraviolet-visible spectrum range and allows assessment of the purity of extracted RNA through calculation of absorbance ratios (260/280nm and 260/230nm). Ratios of 1.8-2 suggest pure RNA low in protein and chemical contaminants (Figure 2.3).
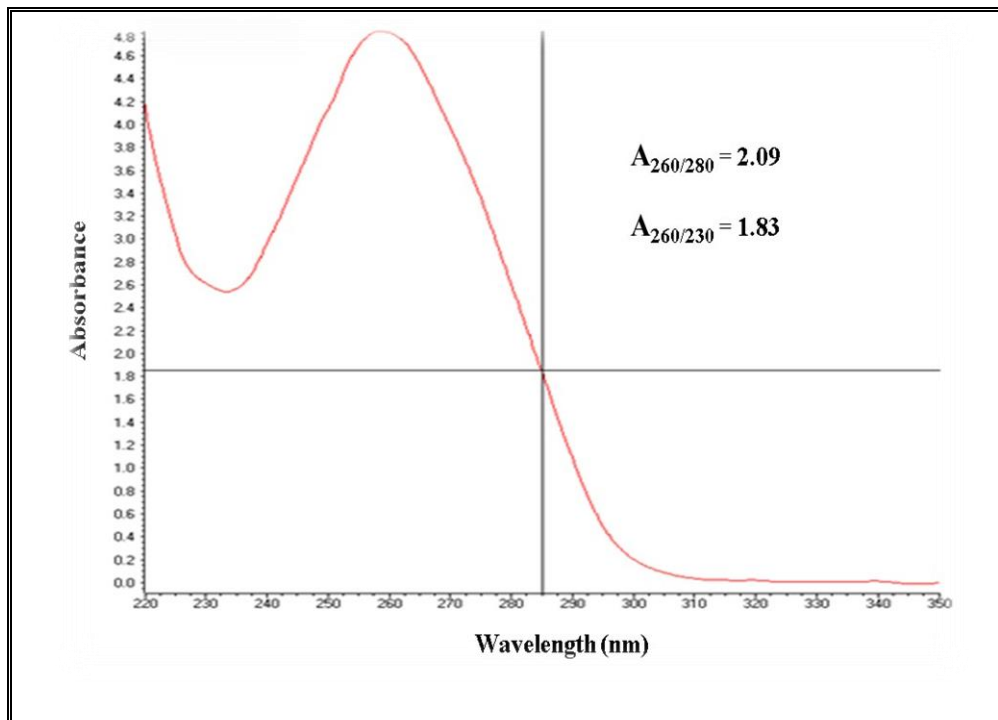
Figure 2.3: Pure RNA absorbance curve on a NanoDrop 2000c Spectrophotometer.

2.8.3 Integrity analysis

Evaluation of the total RNA integrity and purity is essential to provide quality assessment and assurance that the RNA is suitable for downstream applications. Assessment of the extracted RNA integrity was examined by micro-fluidic capillary electrophoresis using a Bio-Rad Experion Automated Electrophoresis System in which 1μl of each RNA sample was electrophoretically separated on a microfluidic RNA lab-chip and subsequently detected via laser-induced fluorescence. Figure 2.4 shows an electropherogram of total RNA with two high-molecular weight bands comprising the 28S and 18S ribosomal RNA (rRNA) species and other bands for smaller RNA species. RNA is considered of high quality with good integrity when the ratio of 28S:18S bands is about 2 and higher. The Experion system also provides

a RNA Quality Indicator (RQI). This is a scale from one, which reports highly degraded RNA, up to ten which is from intact RNA. With extracted RNA, an RQI value of 8 or more is indicative of high integrity RNA (Denisov *et al.*, 2008).
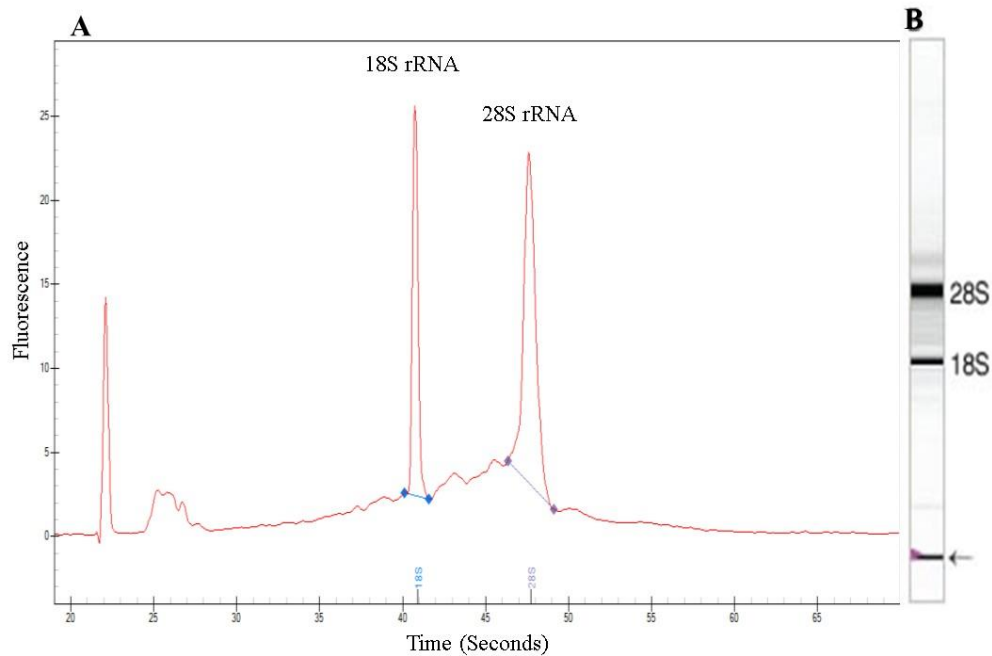
Figure 2.4: Experion total RNA analysis. A: an Experion electropherogram and B: Experion virtual gel, showing total RNA of high quality.

2.8.4 Quantitative Real Time PCR of miRNAs

This method for the quantification of specific miRNAs in samples is a two-step process (Figure 2.5). The first required step is a stem-loop reverse transcription reaction (RT) to convert the miRNAs to cDNA and the second step is the quantitative polymerase chain reaction using the cDNA as the template (qRT-PCR).
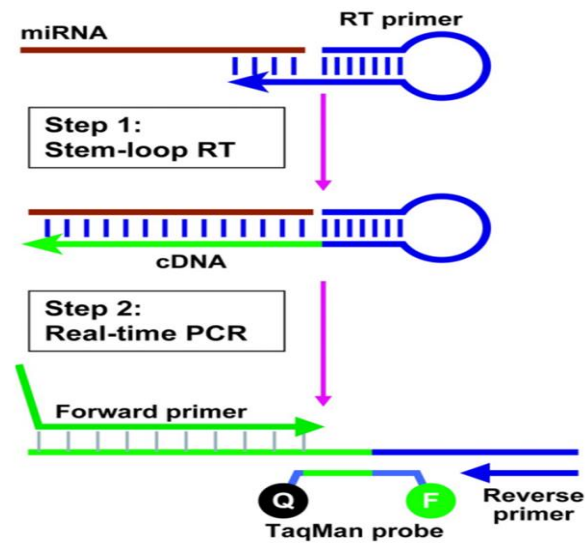
Figure 2.5: Schematic description of TaqMan-based, quantitative miRNA RT-PCR assay method (Chen *et al*., 2005a).

Three plant miRNAs were selected for this initial study based on both their likelihood of expression in the particular plants under study and their potential to regulate human gene expression. The miRNAs chosen were: miR-166a, miR-167a, and miR-168a (Table 2.5) as they are found to be highly conserved across plant species and have had human gene targets identified or predicted (Zhang, 2010a). This assay only requires 10ng of the extracted total RNA. Aerosol-resistant filter pipette tips were used in both steps to protect samples from any cross-contamination that may occur because of aerosol transfer.

Table 2.5: Applied BioSystems TaqMan Small RNA assays used in this study.

miRNA	Assay Name	Applied BioSystems Assays ID	The miRNA has been identified in
miR-166a	ath-miR166a	000347	*Aquilegia caerulea, Brachypodium distachyon, Brassica napus, Citrus sinensis, Digitalis purpurea, Glycine max, Manihot esculenta.*
miR-167a	ath-miR167a	000348	*Brachypodium distachyon, B. napus, B. rapa, Cucumis melo, D. purpurea, Theobroma cacao, Triticum aestivum, Vitis vinifera, Zea mays.*
miR-168a	ath-miR168a	000351	*B. napus, C. clementine, C. reticulata, Cynara cardunculus, Vigna unguiculata, V. vinifera*

2.8.4.1 Stem-loop Reverse Transcription reaction

This complementary DNA (cDNA) synthesis method is required to allow the assessment of specific miRNA levels or expression by converting the extracted miRNA to single-stranded cDNA. This reaction is carried out using the Taq-Man® miRNA Reverse Transcription Kit and miRNA-specific RT primers as per the manufacturer's instructions and contained:

1. Each RNA sample reaction (RT+) includes: 3µl of 5x specific miRNA assay primer, 10ng RNA sample, and 7µl of ABI TaqMan Small RNA Master Mix which consists of 0.15µl of 100Mm dNTP, 50U Multiscribe™ reverse transcriptase, 10x reverse-transcription buffer, 20U RNase-Inhibitor, and 4.16µL nuclease free water. The contents were mixed by pipetting followed by brief centrifugation. These samples were labelled RT+ samples.

2. RT- samples contain the same reagents in the same quantities except water is used instead of Multiscribe reverse transcriptase. This provides a no-template

or genomic DNA control sample. When used in qRT-PCR, this sample should not generate a signal as no cDNA should be present. If a signal is obtained then that may have come from genomic DNA contaminating the RNA sample or reaction. The contents were mixed by pipetting followed by brief centrifugation. These samples were labelled RT- samples.

3. RT+ and RT- samples were incubated in a DNA Thermal Cycler 480 to carry out the reverse transcription reaction using the following conditions: 16° C for 30 min, 42° C for 30 min, 85° C for 5 min, and hold at 4° C.

4. Both RT+ and RT- samples were stored at -20° C before running the real-time PCR assays.

2.8.4.2 TaqMan Probebased quantitative real-time reverse transcribed polymerase chain reaction (qRT-PCR) for miRNA expression analysis

TaqMan gene expression assays provide a quantitative detection of target RNA transcript expression levels and it is comprised of two unmodified oligonucleotides and a TaqMan probe. The intact TaqMan® oligonucleotide probe consists of a fluorescent reporter dye at its 5` terminus and a quencher dye at its 3′ end. The closeness between two dyes leads to suppress the reporter fluorescence, thus the cleavage of this probe during the polymerization step, separates two dyes. The 3′ end of the probe is blocked to prevent extension of the probe during PCR. The increase in the reporter dye fluorescence refers to the accumulation of amplified products during each cycle of the PCR (Bustin and Mueller, 2005).

This assay was performed in triplicate for RT+ and RT- samples, and includes a positive control (PC) and a negative control (NC). The total volume of reaction in each tube was (20μL) using 1.33μL RT product, 10μL Luminaris Colour Probe High ROX Mastermix (2×), and 1μL miRNA-specific TaqMan primer/probe mix (20x) per reaction. To reduce the risk of cross-contamination, aerosol-resistant pipette tips were used through the procedure. Real-time PCR was carried out on an Applied BioSystems StepOne Plus Real-time PCR system using the following conditions: 95 °C for 10 min, followed by 40 cycles of 95 °C for 15 s and 1 min at 60 °C. The PCR

was stopped by a hold at 4 °C. Raw data was then analysed with ABI StepOne Software version 2.1 (Applied BioSystems, Renfrew, UK), using the automatic cycle threshold (Ct) determination. The Ct was defined as the cycle number at which the reporter fluorescence was greater than the threshold (Bustin and Mueller, 2005).

With the appropriate internal reference control targets or concentration curves, accurate quantification, whether relative or absolute, can be obtained (Livak and Schmittgen, 2001; Pfaffl, 2001). Applying this practice across multiple sample types, species, and experimental conditions can be challenging so approximate measure of the concentration of target in the PCR reaction can be given by the Ct value. A Ct value of 29 or less suggests an abundance of target nucleic acid in the sample. A sample Ct of 30-37 would suggest moderate amounts of target nucleic acid present and Cts of 38-40 are indicative of minimal amounts of the target nucleic acid. Comparative graphs were created using Graphpad Prism Version 5 (GraphPad Software, La Jolla, USA).

2.8.5 Agarose gel electrophoresis

Horizontal submarine agarose gel electrophoresis is a common molecular technique for separating nucleic acids under the influence of an electric field and determining their size. Agarose gel was used as a separation medium and prepared by suspending dry agarose in 1x Tris-borate-EDTA buffer (TBE) and heating until the agarose melts. A DNA stain such as ethidium bromide is added, and the gel solution is then pour into a casting tray and allowing it to cool and set. The agarose gel was submersed under 1x TBE running buffer in an electrophoresis tank. The PCR products were mixed with a loading buffer which increases the density of the sample and contains a tracking dye. DNA is negatively charged and will move to the positive electrode under an electrical field. It also binds with the stain to fluoresce under UV light on a gel documentation system.

A DNA ladder or DNA marker was usually loaded on a gel with the DNA samples. It contains a set of known DNA fragments with different sizes in base pairs (bp) or kilo

bases (kb) of a range appropriate for the sample size. These DNA fragments were separated and visualised as DNA bands on the gel. Determination of the size and quantity of the DNA fragments were achieved by comparing with the size and quantity of the DNA bands in the DNA ladder.

2.8.6 *In vitro* digestion of bovine milk

Therefore the objective of this section was to detect plant-derived miRNAs in bovine milk following the gastric stage of human digestion sample using a drug dissolution tester TDT-08L. This would demonstrate their resilience and bioavailability and their potential for cross-kingdom gene regulation. The drug dissolution tester is usually used to predict *in vivo* drug release profiles by providing information about *in vitro* drug release. It is an industry standard system in complying with United States Pharmacopoeia specifications (USP). The system was used with simulated human gastric fluid (SGF) with a pH of 1.2 at a temperature of 37°C and gut movement was simulated with the help of paddles rotating at 50 rpm. The SGF contained 3.2mg/ml pepsin and 0.03M NaCl at pH of 1.2. The half gastric emptying time (T1/2) of a liquid test meal is 19 min (Ziessman, *et al* 2016). The levels of specific plant miRNA were measured at the beginning of digestion (t=0) and at time intervals of 19 (t=19) and 38 min (t=38) of incubation. Sample aliquots of 100μL were collected for total RNA extraction. A stem-loop reverse transcription of extracted total RNA samples was carried out using Taq-Man® miRNA Reverse Transcription Kit and miRNA-specific RT primers followed by quantitative real-time PCR to measure the quantity of target plant miRNAs using TaqMan miRNA assays. Comparison of multiple samples was performed by one-way ANOVA followed by Tukey's post hoc tests to calculate *p* values. Values of $p < 0.05$ were considered significant.

2.8.7 Quantification of human prolactin receptor (*PRLR*) in several cancer cell lines

2.8.7.1 miRNA target gene prediction

As little as only 6bp complementary binding between a miRNA and its mRNA target can reduce its expression (Thomson *et al.,* 2011). There are a number of research tools available to help identify miRNAs that target specific gene transcripts (Wang and El Naqa, 2008). These systems do not consider a xenomir model and can only screen miRNAs for targets gene targets within the same organism and not for plant miRNAs to animal gene targets. There are accepted rules for miRNA target prediction (Lewis *et al*., 2003; Doench and Sharp, 2004; Brennecke *et al*., 2005). As these rules may not apply for plant miRNA:human mRNA targets, a BLAST (basic local alignment search tool (Johnson *et al*., 2008) was conducted using the sequences of a number of miRNAs found in the plants in this study to see if there was any possibility of complementary pairing. Human Prolactin receptor (*PRLR*) variants 1 (NM-000949.5) and 6 (NM-001204314.1) were high-scoring hits on the BLAST search with 15 base complementarity. This analysis was performed in an earlier target gene prediction study in our research group by Anna Philip.

To see if these plant miRNAs could have an effect on the expression of the prolactin receptor, a human cell line which natively expressed *PRLR* was transfected with synthetic miRNA or "mimic" versions of these plant miRNAs and the *PRLR* expression levels measured.

2.8.7.2 Total RNA isolation

Total RNA from six cancer cell lines was extracted using Isolate II RNA mini kit and the concentration of isolated total RNA was then measured using a NanoDrop 2000c Spectrophotometer.

2.8.7.3 Complementary DNA synthesis

The complementary DNA (cDNA) synthesis method is required to generate cDNA from an RNA template using an Oligo (dT) 18 primer. This primer method makes use of the poly-A tail on the 3` end of eukaryotic mRNAs to help ensure the cDNA produced is derived from transcripts in the RNA sample, and provides an indication of their expression. The resultant cDNA is suitable for use in qRT-PCR with gene-specific primers. For this study, this reaction is carried out using the Tetro cDNA synthesis kit as per the manufacturer's instructions:

1. Each RT+ samples include 100ng of total RNA, 1μL oligo (dT), 1X RT buffer, 0.5mM of dNTPs, 200 U of Tetro reverse transcriptase and 10 U of RNase inhibitor. The contents were mixed by pipetting followed by brief centrifugation.

2. RT- samples contain the same reagents in the same quantities except water is used instead of Tetro reverse transcriptase. This provides a no-template or genomic DNA control sample. When used in qRT-PCR, this sample should not generate a signal as no cDNA should be present. If a signal is obtained then that may have come from genomic DNA contaminating the RNA sample or reaction. The contents were mixed by pipetting followed by brief centrifugation.

3. RT+ and RT- samples were incubated in a Model 480 thermocycler (Applied Biosystems, Warrington, UK) for 30 min at 45°C. The cDNA synthesis reaction was stopped by incubating at 85°C for 5 min. The cDNA reactions were stored at -20°C until required.

2.8.7.4 Quantitative real-time reverse transcribed polymerase chain reaction (qRT-PCR)

This assay is reliant on SYBR® Green dye binding to double-stranded DNA. SYBR green is useful in monitoring the accumulation of PCR products in quantitative real-time PCR. In every cycle, DNA polymerase amplifies the target sequence to increase

the amount of PCR products. With SYBR green present in the reaction, binding between SYBR® dye and double-stranded PCR products results in an increase in fluorescence intensity proportioned to the amount of PCR product produced. The assay was conducted to measure the level of *PRLR* mRNA expression in several cancer cell lines (A375, PANC-1, A2780, ZR-75-1, LNCaP, and HeLa). The selection of appropriate reference genes for normalisation of the data is essential to ensure precise quantification of *PRLR* mRNA expression level (Bustin and Mueller, 2005). Peptidylprolyl isomerase B (*PPIB*), a housekeeping gene used in case of comparing mRNA expression in different experimental conditions in which the expression of a target gene has to be normalized to this gene (Pachot *et al*., 2004). It has been identified as a suitable reference gene in an earlier study, a typical reaction comprised of 1pM forward and reverse primers (2µl each) of *PRLR* (target) or *PPIB* (Table 2.6), 10µL of 2x Fast SYBR Green master mix, and 1.33µL cDNA in a reaction volume of 20µL. The RT-PCR reactions were carried at 95°C for 20 sec followed by 40 cycles of 95°C for 3 sec and 60°C for 30 sec in a StepOnePlus RT-PCR system. This was followed by melt curve analysis to detect any issues with mispriming or multiple amplicons.

Table 2.6: Sequences of *PPIB* and *PRLR* primers.

Name	Sequence-(5`- 3`)	Amplicon size (bp)	Genebank accession number
PPIB forward primer	CAGTGGATAATTTTGTGGCCTTAG	149	NM-000942
PPIB reverse primer	CTCACCGTAGATGCTCTTTCC		
PRLR forward primer	TGGCAAGCAGTACACCTCCATGTG	136	NM-000949
PRLR reverse primer	CAGCTCCAAAGGAGGGTCTGGC		

2.8.7.5 Delta delta Ct method

This delta-delta Ct (ΔΔCt) method is used to calculate the relative changes in the gene expression determined from real-time quantitative PCR experiment (Livak and Schmittgen, 2001). The ΔΔCt method normalises the Ct values of the target gene to the Ct values of the reference gene to determine the fold changes in the gene expression between the control and treated samples using the following equations:

- The difference between the Cts for the target gene and the reference gene for the treated and the control samples (ΔCt):

  ΔCt = Ct target – Ct reference gene

- The difference between the ΔCts between the treated and control samples (ΔΔCt):

  ΔΔCt = ΔCt treated – ΔCt control

- Fold change (FC) in the treated sample was equal to $2^{-\Delta\Delta Ct}$

2.8.8 Effect of plant miR-167 on *PRLR* expression in cancer cell lines

2.8.8.1 Small RNA transfection of mammalian cells

2.8.8.1.1 Transfection validation

Transfection validation was carried out to ensure an effective transfection method for small RNAs for studied cell lines. Transfection efficiency was measured using AllStars Hs Cell Death positive Control siRNA and Alexa Fluor-488 labelled (AF488) AllStars Negative Control under different conditions to determine the optimal conditions for maximum transfection efficiency. Three concentrations of each control were carried out in each experiment and a control (non-transfected cells) was involved. Each experiment was performed in triplicate for each cell line.

2.8.8.1.1.1 Transfection examination by AllStars Hs Cell Death positive control siRNA

2.8.8.1.1.1.1 AllStars Hs Cell Death positive control siRNA

The AllStars Hs Cell Death positive control siRNA is a siRNAs mixture which is able to target and knockdown human cell survival genes when transfected to the cell effectively, causing cell death. An optimised number of cells from each cell line (Table 2.7) were seeded in a 96-well plate and the transfection complexes were added to the cells using a range of concentrations of the positive control (Table 2.8). The efficacy of this control was assessed by the methyl-thiazolyl-tetrazolium 3-(4, 5-dimethylthiazol-2-yl)-2, 5-diphenyltetrazolium bromide (MTT) cell viability assay and observing the cells under a light microscope, 72h after transfection. The concentration of the control at which 50% of its maximum response is observed (EC_{50}), was determined.

Table 2.7: Cell line densities in 96-well plates.

Cell line	Cell density/well
A375	7000
PANC-1	10000
HeLa	10000
A2780	7000
LNCaP	10000
ZR-75-1	7000

Table 2.8: Transfection optimisation of AllStars Hs Cell Death positive Control siRNA.

Condition 1	Condition 2	Condition 3
31.25ng siRNA (12.5nM*)	62.5ng siRNA (25nM*)	125ng siRNA (50nM*)
1µl HiPerFect	1µl HiPerFect	1µl HiPerFect

* Refers to the final miRNA concentration in each well.

2.8.8.1.1.1.2 MTT assay

The MTT assay was used to detect the effect of AllStars Hs Cell Death Control on cell viability. It measures the mitochondrial activity of the viable cells based on the conversion of MTT into formazan crystals. After 72h of treatment with the transfection complexes, 100µl of 5mg/ml MTT solution is added to the media in each well and incubated for up to 4h under normal growth conditions. After 4h, the media was removed from all the wells and replaced with 100µl DMSO to stop the reaction. Finally, the absorbance at 570nm was read using a SpectraMax M5 micro-plate

reader. The percentage viability was calculated as the absorbance for treated cells divided by the absorbance for control (untreated) cells.

2.8.8.1.1.1.3 Transfection examination by AF488-labelled AllStars Negative Control siRNA

Transfection of each cell line was performed at various concentrations of AllStars Negative Control and at different quantities of transfection reagent to identify the optimum transfection conditions for small RNAs into the cell lines in this study (Table 2.9). The performance of this control was evaluated by detection of the cellular uptake of AF488-labelled AllStars Negative Control siRNA using a Nikon Eclipse TE300 Epifluorescent Inverted microscope, 6, 12, 24, 48, and 72h after transfection. The cell images were captured using MetaMorph software (MetaMorph, London, UK).

Table 2.9: Transfection optimisation of AllStars Hs Negative Control siRNA.

Condition 1	Condition 2	Condition 3	Condition 4
75ng siRNA (10nM*)	75ng siRNA (10nM*)	150ng siRNA (20nM*)	150ng siRNA (20nM*)
6µl HiPerFect	12µl HiPerFect	6µl HiPerFect	12µl HiPerFect

* Refers to the final miRNA concentration in each well.

2.8.8.2 Effect of plant miR-167 mimic on *PRLR* expression in cancer cell lines

This experiment was carried out to assess the possible regulatory impact miR-167 might have on *PRLR* mRNA expression in several tumour cell lines. Each cell line was transfected using the optimised conditions and transfection complex. After 72h of transfection a complex of 150ng of a miR-167 mimic and 12µl HiPerFect, the cancer cell lines were collected and total RNA was extracted. The concentration and the purity of total RNA were determined and total RNA samples were reverse

transcribed to prepare the cDNA for qRT-PCR using selected primers for *PRLR* as described in Section 2.8.7.3. Relative expression levels of *PRLR* mRNA transcripts were normalised to the reference gene *PPIB* using the ΔΔCt method (Section 2.8.7.5) and the significant changes in fold difference were measured by one-way ANOVA followed by Tukey's post hoc tests to calculate *p* values.

2.8.8.3 Effect of plant total RNA on *PRLR* expression in cancer cell lines

This experiment was carried out to examine the effect of plant total RNA sample (containing miR-167) on the expression of *PRLR* mRNA. First, total RNA samples were extracted from *A. spinosus* and *C. colocynthis* using PureLink® RNA Mini Kit. Next, a 10ng of each total RNA sample and also from miR-167 mimic was reverse transcribed. The cDNA samples were used as template of qRT-PCR and the level of miR-167 in each sample was quantified. The required amount of miR-167 in the plant total RNA samples was calculated (Section 2.8.8.3.1). The plant derived total RNA showed such low levels of the miR-167 and a large quantity would have to be used in order to deliver the same amount as 10ng of the mimic. This amount is far in excess of what is practical in a transfection-based cell culture experiment and what was available from the limited amount of plant material. More manageable amounts were selected (150 and 300ng/µl), recognising that the effect could be a fraction of what the mimic could achieve.

Each tested cancer cell line was transfected with two different concentrations (150 and 300ng/µl) of total RNA sample (extracted from *C. colocynthis*). 72h after transfection, cells were collected and total RNA was extracted. The concentration and purity of total RNA were determined and then reverse transcribed to provide the cDNA as template of qRT-PCR. The expression level of *PRLR* mRNA was quantified using selected primers for *PRLR* as described in Section 2.8.7.4. Relative expression levels of *PRLR* mRNA transcripts were normalised to the reference gene *PPIB* using the ΔΔCt method (Section 2.8.7.5). The significant changes in fold difference were measured by one-way ANOVA followed by Tukey's post hoc tests to calculate *p* values.

2.8.8.3.1 Calculating the amount of miR-167 in plant total RNA samples

Based on the comparative miR-167 levels, the amount of miR-167 in plant total RNA samples was calculated. As shown in Table 2.10, the level of miR-167 in *C. colocynthis* sample was higher than that in the other plant and it was selected for further analysis. The following equations were used to calculate the required quantity of the miR-167 in the sample comparing with miR-167 mimic amount:

1. Calculation of the difference between the Cts for the miR-167 mimic and the total RNA sample (ΔCt):

$$\Delta Ct = 19 - 6.9$$
$$\Delta Ct = 12.1$$

2. Calculation of fold difference between miR-167 in plant material and 10ng of mimic (FD= $2^{-\Delta Ct}$)

$$FD = 2^{-12.1}$$

$$FD = 4390$$

Quantity of Plant material needed to have the same amount of miR-167 as 10ng of mimic based on Ct= FD × 10ng

1× (43.9µg from total RNA sample) ≡ 10ng (miR-167 mimic)

Table 2.10: Comparison of Ct values of each sample.

Sample Name	Ct value
miR-167 mimic	6.9
Total RNA from *A. spinosus*	21
Total RNA from *C. colocynthis*	19

2.8.9 Plant genotyping

Some plant samples were collected from different places in Libya because of the extreme hazards and difficulties in obtaining the plant material. In order to ensure that plant samples tested were of the same species, plant genotyping was conducted. This was done on extracted plant DNA using Inter-simple Sequence Repeat-PCR (ISSR-PCR).

2.8.9.1 Plant genomic DNA isolation

Genomic DNA was extracted from two samples (each sample was collected from different cities in Libya) of each plant (*T. aphylla* and *C. colocynths*) according to the manufacturer's instructions using GenElute™ Plant Genomic DNA Miniprep Kit. Following DNA extraction, DNA concentration of each sample was then measured using a NanoDrop 2000c Spectrophotometer.

2.8.9.1.2 The Inter-Simple Sequence Repeat-PCR (ISSR-PCR)

The Inter-simple Sequence Repeat-PCR (ISSR-PCR) is a PCR-based assay that can enable one to visualise plant genetic variation (Zietkiewicz *et al*., 1994). SSR are microsatellites or simple sequence repeat and they can be detected by PCR. They are abundant and scattered throughout the eukaryotic genomes analysed. ISSR primers contain one to three bases for primer annealing to either the 5` or 3` end of the SSR (Charters *et al*., 1996). The ISSR primers anneal to and amplify DNA sequence between the two adjacent and oppositely oriented SSRs (Zietekiewicz *et al*. 1994). In this study, five ISSR primers were chosen from Primer Set #9 of the University of British Columbia (UBC) Biotechnology Laboratory (Table 2.11). PCR amplifications were carried out in a reaction containing 2μl of 10ng of purified plant genomic DNA, 12.5μl of Promega Go-Taq Green mastermix, 1.25μl of the 10pmol/μl solution of the ISSR primer and 9.25μl water. The 25μL reactions were incubated in a Primus 96 *plus* thermal cycler using the following conditions: 95°C for 2 min, followed by 35 cycles of 95°C for 30 sec, 50°C for 30 sec and 1m at 72°C. No-template negative controls which contain the same reagents in the same

quantities, but water is used instead of plant genomic DNA to detect any contamination. The PCR products were electrophoresed on a 0.3% (w/v) TBE agarose gel and visualised under UV light. The obtained banding patterns were analysed to estimate genetic relationships between the plant samples. The bands with strong intensities and clearly distinctive bands were scored only. While the smeared or faint bands could be the result of unspecific binding of ISSR primers and should be excluded. When comparing band profile of the samples, the sample with the highest number of bands was considered as a reference sample and the other was considered as compared sample. Thus, the bands which were visible in the reference sample only are called polymorphic bands. The increase of the number of the polymorphic bands refers to the increase of genetic variability between samples.

Table 2.11: Nucleotide Sequences of ISSR primers used in this study.

ISSR Primer	
UBC Code	**Sequence (5`- 3`)**
UBC-801	ATATATATATATATATT
UBC-807	AGAGAG AGAGAGAGAGT
UBC-816	CACACACACACACACAT
UBC-845	CTCTCTCTCTCTCTCTRG
UBC-849	GTGTGTGTGTGTGTGTYA

Chapter 3 Results

Part 1: Phytochemistry and biology results

3.1 Fractionation of *T. aphylla* crude extracts

The methanol extract (22g, 3.66%) of *T. aphylla* was subjected to VLC (Methods Section 2.5.2). Fraction-(5) coded TA-1 was obtained as a white crystalline solid (250mg, 1.13%) identified as a mixture of two compounds while fraction-(6) (2g, 9.09%) coded TA-2 was obtained as a white powder of a single compound. Other fractions were identified as mixtures of two or three compounds and were subjected to further fractionation using Sephadex coloumn. Fractions were assessed using NMR and it also enabled elucidation of the structure of TA-3 (25mg, 0.11%) and TA-4 (11mg, 0.05%). The ^{1}H NMR spectrum of the hexane and EtOAc extracts of *T. aphylla* showed signals suggesting the presence of mixtures of triglycerides and fats. No single compound was separated from the fractionation of the latter extracts.

3.1.1 Characterisation of TA-1 as a mixture of *trans*-coniferyl alcohol-4-*O*-sulphate (TA-1a) and *trans*-coniferyl acetate-4-*O*-sulphate (TA-1b)

The compounds TA-1a and TA-1b (Figure 3.1) were isolated as a mixture from the methanol extract of the leaves of *T. aphylla* by VLC. Using 30% (v/v) MeOH in EtOAc as the mobile phase for TLC (Method Section 2.5.1), the mixture appeared as a violet spot (R_f= 0.74) after spraying with *p*-anisaldehyde-sulphuric acid reagent and heating.

The ^{1}H NMR spectrum of the major compound TA-1a (Figure 3.2, Table 3.1) revealed the presence of an aromatic ring with protons at δ_H 7.39 (1H, *d*, *J* = 8.3 Hz, H-5), δ_H 7.02 (1H, *d*, *J* = 2.0 Hz , H-2), and δ_H 6.87 (1H, *dd*, J_1 = 8.3 Hz, J_2 = 2.0 Hz, H-6). The coupling constants and multiplicity of these signals indicated an aromatic ABX spin system. The spectrum also showed the presence of *trans* olefinic protons at δ_H 6.48 (1H, *dt*, J_1 = 15.9 Hz, J_2 = 5.2 Hz) and δ_H 6.30 (1H, *dt, J_1* = 15.9, J_2 = 5.2 Hz) were assigned to H-7 and H-8, respectively. A signal for a 3H singlet at δ_H 3.76 represented a methoxy group.

A DEPTq-135 NMR spectrum (Figure 3.2B, Table 3.1) indicated the presence of ten carbon atoms including one methylene carbon at 62.0 ppm, one methoxy carbon at 56.1 ppm, three quaternary carbons at 132.8, 142.5, 151.0 ppm and five CH carbons at 110.5, 121.3, 118.8, 129.0, 129.8 ppm.

The HMBC spectrum (Figure 3.3B, Table 3.2) showed ^2J correlation between δ_H 7.39 (H-5) and carbon signal at δ_C 142.5 (C-4) and ^3J correlations to the carbons at δ_C 132.8 (C-1) and δ_C 151.0 (C-3). The protons at δ_H 7.38 (H-5) showed a ^3J correlation to C-3. The proton signal at δ_H 7.02 (H-2) showed direct correlation to δ_C 110.5 in the HMQC spectrum (Figure 3.3A). The singlet of the methoxy group showed a ^3J correlation with an aromatic carbon bearing it at δ_C 151.0. The ^3J correlations between the proton signals at δ_H 7.02 (H-2), δ_H 6.87 (H-6) and the signal at δ_C 129.0 and ^2J correlation between the proton signal at δ_H 6.30 (H-8) and the carbon at δ_C 129.0 which therefore confirmed the position of δ_C 129.0 at C-7. Protons H-7 and H-8 showed ^3J and ^2J correlations to the carbon at 62.0 ppm which was assigned to C-9.

The HREI-MS data showed pseudo molecular ion [M] $^-$ at *m/z* 259.0605 suggesting the molecular formula of $C_{10}H_{12}O_6S$. The above data suggests TA-1a to be a *trans*-coniferyl alcohol-4-*O*-sulphate or Phenol, 1-(3-hydroxy-1-propen-1-yl)-3-methoxy-, 4-(hydrogen sulfate). The spectral data were consistent with those reported in literature and this compound was previously isolated from the stem bark of other *Tamarix* species; *T. gallica*, *T. africana* and *T. bobeana* (Tomás-Barberán *et al.*, 1990). However, this is the first report of the isolation of *trans*-coniferyl alcohol 4-*O*-sulphate from *T. aphylla*.

The ^{1}H and DEPTq-135 NMR (Table 3.1) spectra for the minor compound TA-1b (Figure 3.1) followed the same pattern as that of TA-1a except for the presence of an acetate group instead of a hydroxyl group at C-9 and the protons at this position were deshielded by 0.56 ppm comparing with the same protons in TA-1a (Table 3.1). The ^{1}H NMR spectrum of TA-1b (Figure 3.2A, Table 3.1) indicated the presence of an aromatic ring with proton signals at δ_H 7.42 (1H, *d, J* = 8.3 Hz, H-5), 7.07 (1H, *d, J* =

2.0 Hz, H-2) and 6.92 (1H, *dd*, J_1 = 8.3 Hz, J_2 = 2.0 Hz, H-6). The presence of two protons at δ_H 6.60 (1H, *m*) and 6.26 (1H, *dt*, J_1 = 15.9 Hz, J_2 = 5.2 Hz) also suggested a *trans*-olefinic H-7 and H-8 in the compound. The spectrum also showed a singlet for 3H at δ_H 2.06 (H-11) representing the methyl of an acetate group. This methyl group showed a direct correlation with the carbon at δ_C 21.2 in the HMQC spectrum (Figure 3.3A) and a ^2J correlation with a carbonyl carbon at δ_C 170.6 in the HMBC spectrum (Figure 3.3B, Table 3.2). Therefore, this carbon was assigned to C-10 in the compound. ^2J and ^3J correlations were observed between protons at δ_H 6.60 (H-7) and 6.26 (H-8) to the carbon at 64.9 ppm which therefore was assigned to C-9. The other signal at δ_C 56.1 ppm was assigned to the methoxy carbon attached to C-3 of the aromatic ring. This carbon signal showed HMQC correlation with the signal at δ_H 3.77 in the spectrum (Figure 3.3A). Additionally, in the HMBC spectrum, a ^3J correlation between the signal at δ_H 3.77 and δ_C 151.0 confirmed the assignment of this carbon signal to C-3. The proton at δ_H 7.07 showed ^2J and ^3J correlation to C-3 and C-4 at 151.0 and 142.5 ppm, respectively.

The HREI-MS data showed pseudo molecular ion [M] ‾ at *m/z* 301.2014, suggesting the molecular formula of $C_{12}H_{14}O_7S$. On the basis of the above data, TA-1b was identified as *trans*-coniferyl-4-*O*-sulphate-9-acetate. This compound has not been previously reported.

TA-1a: R= OH, **TA-1b:** R= OCCH₃
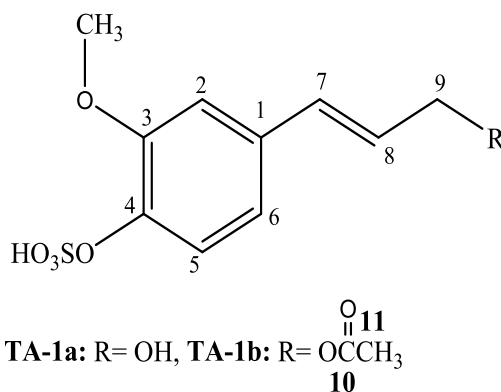
Figure 3.1: Structure of *trans*-coniferyl alcohol-4-*O*-sulphate (TA-1a) and *trans*-coniferyl acetate-4-*O*-sulphate (TA-1b).

Table 3.1: [1]H (400MHz) and DEPTq-135 (100MHz) data of TA-1a and TA-1b in DMSO-d_6.

Position	TA-1a		TA-1b	
	δ_H	δ_C	δ_H	δ_C
1	-	132.8	-	131.8
2	7.02 (1H, *d*, *J* = 2.0 Hz)	110.5	7.07 (1H, *d*, *J* = 2.0 Hz)	110.7
3	-	151.0	-	151.0
4	-	142.5	-	142.5
5	7.39 (1H, *d*, *J* = 8.3 Hz)	121.3	7.42 (1H, *d*, *J* = 8.3 Hz)	121.1
6	6.87 (1H, *dd*, J_1 = 8.3 Hz, J_2 = 2.0 Hz)	118.8	6.92 (1H, *dd*, J_1 = 8.3 Hz, J_2 = 2.0 Hz)	119.3
7	6.48 (1H, *dt*, J_1 = 15.9 Hz, J_2 = 5.2 Hz)	129.0	6.60 (1H, *m*)	133.6
8	6.30 (1H, *dt*, J_1 = 15.9 Hz, J_2 = 5.2 Hz)	129.8	6.26 (1H, *dt*, J_1 = 15.9, J_2 = 5.2 Hz)	122.8
9	4.11 (2H, *m*)	62.0	4.67 (1H, *dd*, J_1 = 5.2, J_2 = 1.4 Hz)	64.9
10	-	-	-	170.6
11	-	-	2.06 (1H, *s*)	21.2
3-OCH$_3$	3.76 (3H, *s*)	56.1	3.77 (3H, *s*)	56.1
9-OH	4.84 (1H, *broad s*)	-	-	-

Table 3.2: Selected HMBC correlations of TA-1a and TA-1b in DMSO-d_6.

Proton	TA-1a		TA-1b	
	^2J	^3J	^2J	^3J
H-2	C-1, C-3	C-4, C-6, C-7	C-3	C-4, C-6, C-7
H-5	C-4	C-1, C-3	C-4	C-1, C-3
H-6	-	C-2, C-4, C-7	-	C-2, C-4, C-7
H-7	C-8	C-6, C-2, C-9	-	C-2, C-6,C-9
H-8	C-7, C-9	C-1	C-9	-
H-9(b)	-	C-7(b)	C-8(b),C-10	C-7(b)
H-11(b)	-	-	C-10(b)	-
3-OCH$_3$	-	C-3	-	C-3

A

B
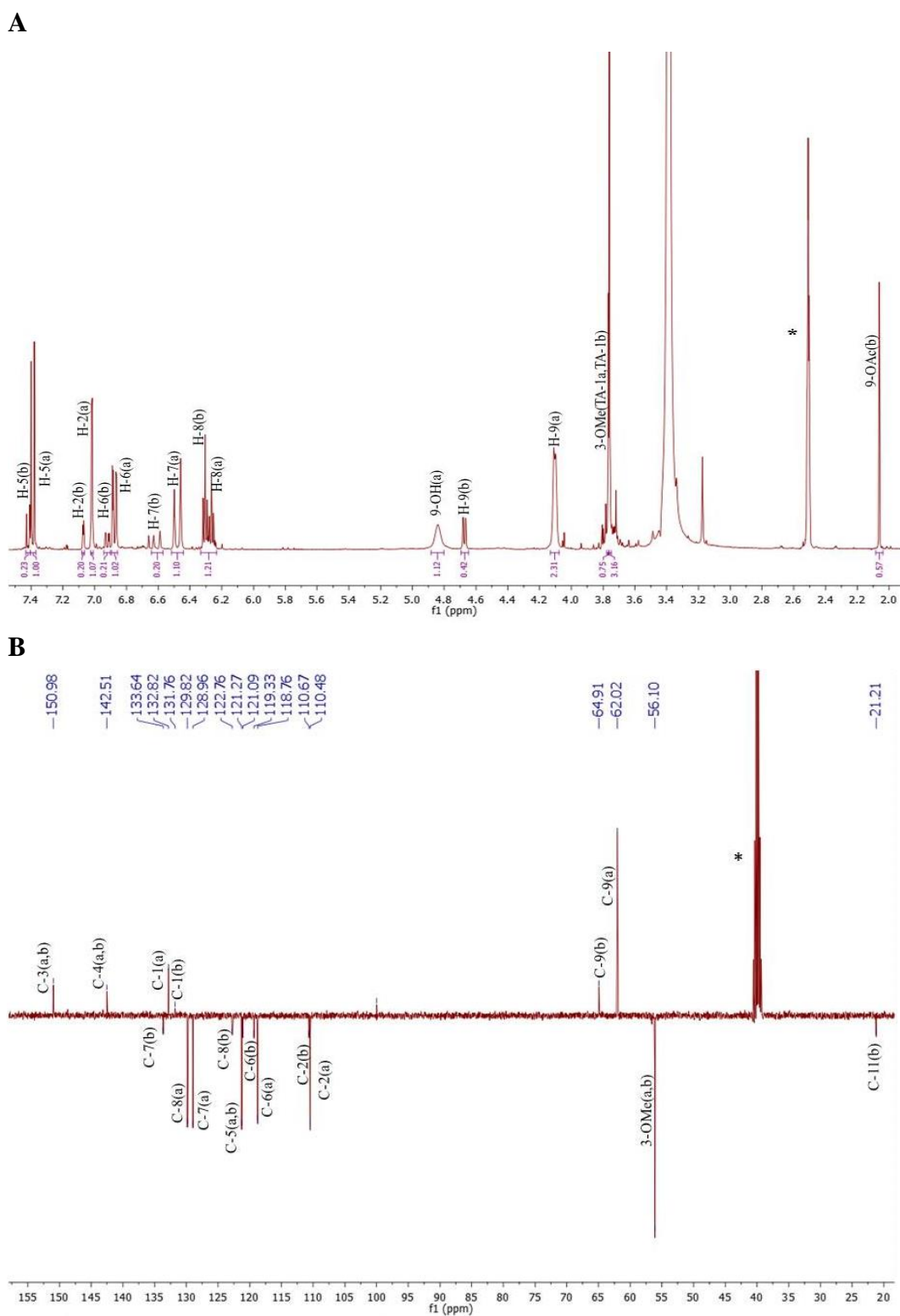
Figure 3.2A: ^{1}H NMR (400 MHz) and **3.2B:** DEPTq-135 NMR (100 MHz) spectra of the mixture TA-1a (labelled as a) and TA-1b (labelled as b) in DMSO-d_6*.

A
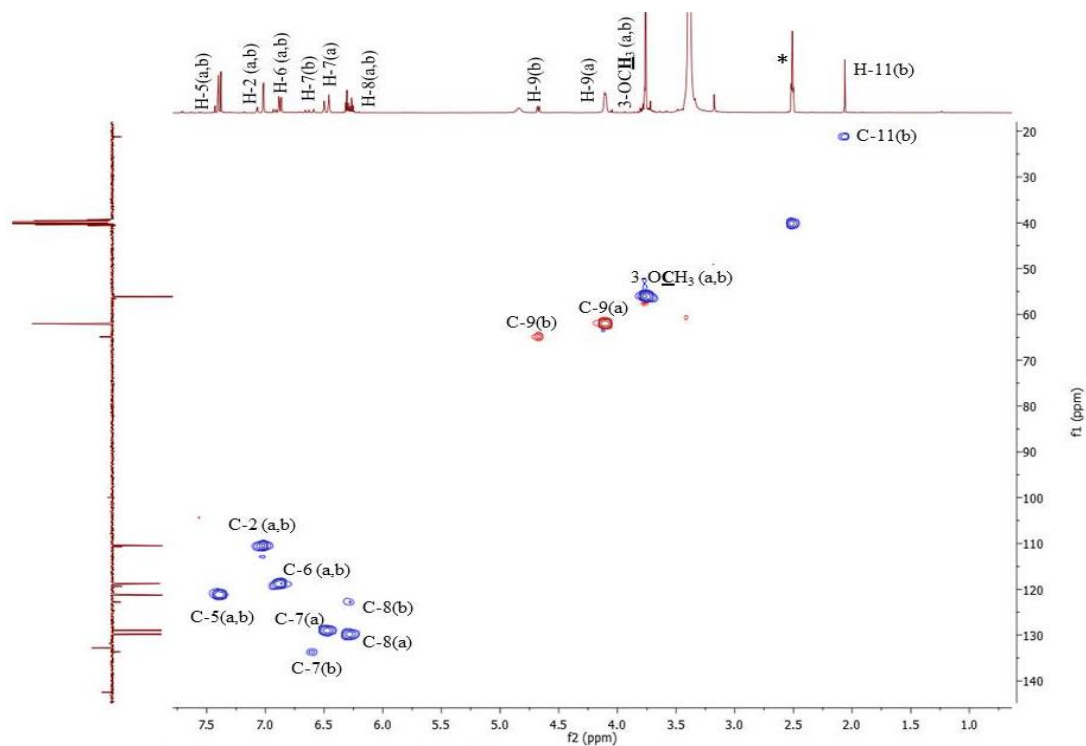
B
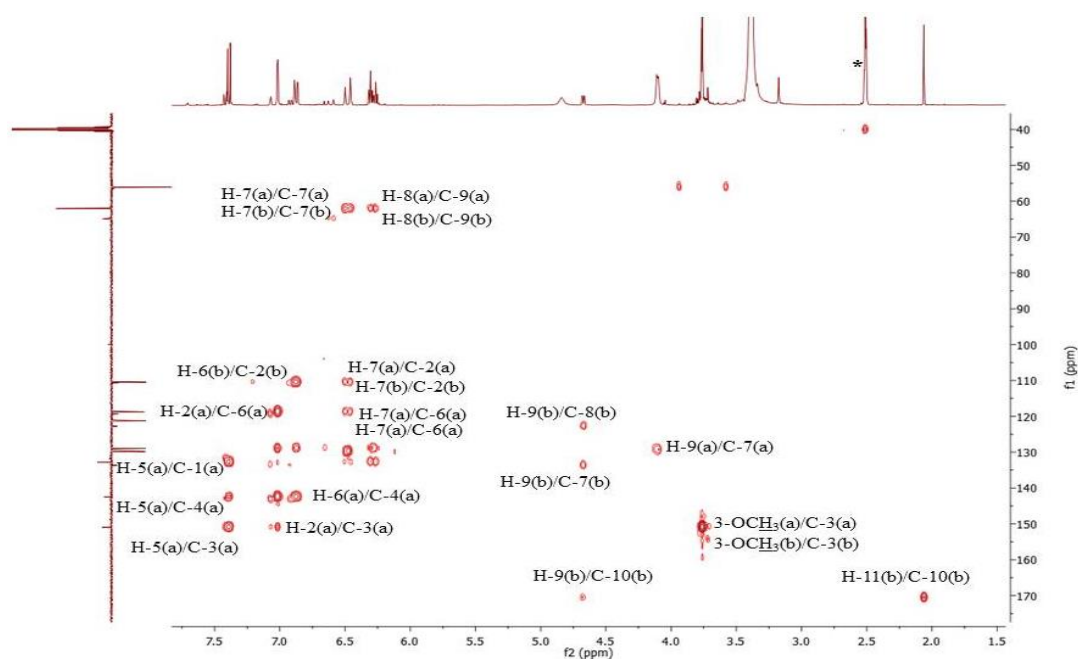
Figure 3.3A: HMQC and **3.3B:** HMBC spectra (400 MHz) of the mixture TA-1a (labelled as a) and TA-1b (labelled as b) in DMSO-d_6*.

To purify this mixture of TA-1a and TA-1b, different separation methods were carried out. Sephadex column was used with methanol as the eluting solvent and 28 vials (3ml each) were collected. Identical spots were obtained on the TLC plate of all fractions. Vials 1, 10, 15, 20 and 28 were subjected to ^{1}HNMR analysis and the results indicated the same mixture in the vials. Next, prep. TLC was performed using different solvent mixtures (10% MeOH: 90% EtOAc, 20% methanol: 80% EtOAc, 30% MeOH: 70% EtOAc) and only one spot appeared on TLC each time. Thirdly, a Biotage purification system was employed twice using different solvent systems to isolate the compounds. The first time, 113 fractions were collected and the absorption spectrum of the mixture showed that there was a separation between the two compounds (Figure 3.4A). Also, the TLC of these fractions showed two different spots with different R_f values (Figure 3.5). The ^{1}HNMR showed two compounds together with a different quantity each time. A second Biotage purification was attempted using a different gradient system (Methods Section 2.5.6). Similarly, the UV absorption spectrum showed that there were two peaks with different absorptions (Figure 3.4B) and the ^{1}HNMR revealed that there was no separation between the two compounds. Finally, the REVELERIS® PREP purification system was applied. A sample of 100mg of the mixture was dissolved in methanol and injected into a Denali C18 Column 150 x 10mm 5µm column and run in the preparative mode. The solvent system, elute volume, and the flow rate were adjusted automatically (Methods Section 2.5.7). However, the ^{1}H NMR spectra of the fractions obtained showed minor differences from the original spectrum, therefore, the separation process should be repeated in the future using different conditions. However, the limited time prevented this from being carried out. Therefore, if further work is to be carried out on the mixture, a large quantity of plant material should be used.
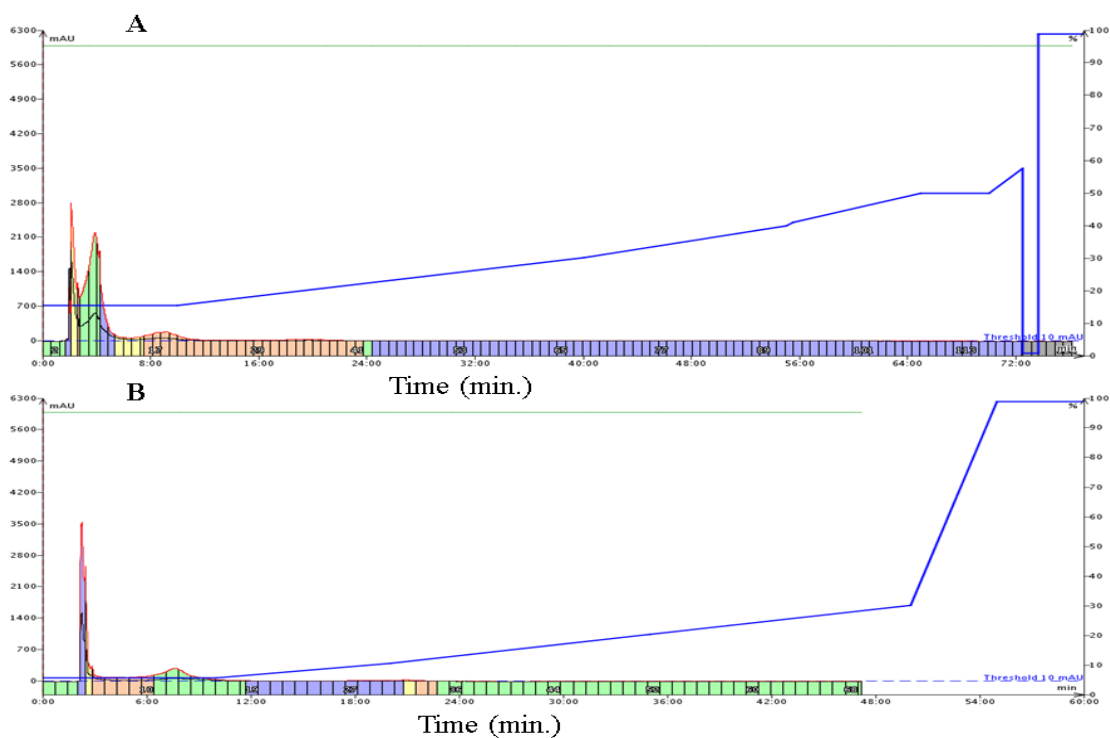
Figure 3.4A&B: Shows Biotage absorption spectra of the mixture TA-1a and TA-1b.
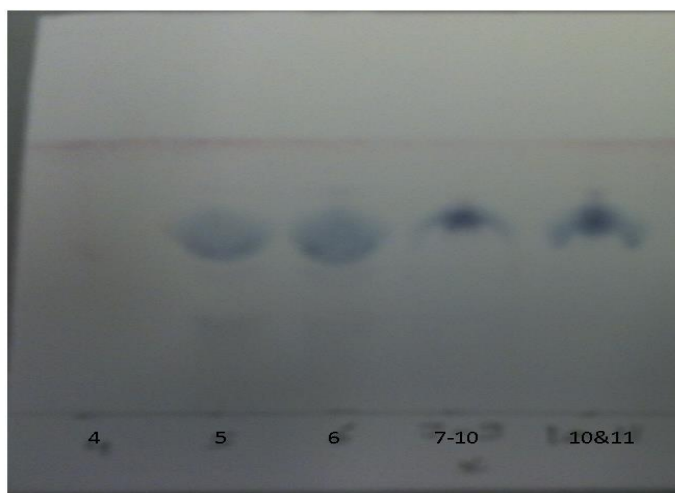
Figure 3.5: TLC of the two peaks resulting from the Biotage purification system. A 30:70% MeOH/EtOAc mixture was used as a mobile phase. The spots were visible after spraying with anisaldehyde-H_2SO_4.

3.1.2 Characterisation of TA-2 as isoferulic acid-3-*O*-sulphate

The compound TA-2 (Figure 3.6) was obtained from the methanol extract of the leaves of *T. aphylla* using VLC. After spraying with *p*-anisaldehyde-sulphuric acid reagent and heating, a yellow spot appeared with R_f value of 0.49 using 30% MeOH in EtOAc as the mobile phase on TLC.

The ^{1}H NMR spectrum (Figure 3.7A, Table 3.3) revealed a 1, 3, 4-trisubstituted aromatic ring with the proton signals at δ_H 7.52 (1H, *d*, *J* = 2.0 Hz, H-2), 7.04 (1H, *d*, *J* = 8.6 Hz, H-5), and 7.36 (1H, *dd*, *J* = 8.6, 2.0 Hz, H-6). The spectrum also showed the presence of *trans*-substituted olefinic protons at δ_H 7.48 (1H, *d*, *J* = 15.9 Hz) and 6.27(1H, *d*, *J* = 15.9 Hz) were assigned to H-7 and H-8 in the compound.

The DEPTq-135 spectrum (Figure 3.7B, Table 3.3) showed ten carbon atoms made up of one a methoxy group at 56.1 ppm and six aromatic carbons at 113.3, 122.0, 127.1, 128.1, 140.0, 153.3 ppm (carbons at 153.3 and 140.0 ppm were observed to be oxygen bearing carbons), and two olefinic carbons at 115.9 and 145.2, and a carbonyl carbon at 170.0 ppm.

Using 2D NMR (COSY, HMQC and HMBC) the structure of the compound was elucidated as follows: The long range correlation (HMBC, Figure 3.8B) of the proton at δ_H 7.36 (H-6) showed [3]*J* correlation to the carbon at δ_C 153.3 (C-4) while the proton at δ_H 7.50 (H-2) showed [2]*J* correlation to δ_C 140.0 (C-3) in the aromatic ring. The proton at δ_H 7.48 (H-7) had a [3]*J* correlation to δ_C 171.1 which was assigned as carboxylic acid carbon C-9. The protons at δ_H 6.27 (H-8) and at δ_H 7.04 (H-5) showed [3]*J* correlations to the carbon at δ_C 127.1 and was assigned as C-1 in the aromatic ring.

The HREI-MS data showed pseudo molecular ion [M] $^-$ at *m/z* 273.0332 which showed that the molecular formula of this compound was $C_{10}H_{10}O_7S$. This compound was previously isolated from the flowers of *T. amplexicaulis* (El-

Moussallami *et al.*, 2000) and from *T. nilotica* (Abouzid *et al.*, 2009). This is the first report of isoferulic acid-3-*O*-sulphate from *T. aphylla*.
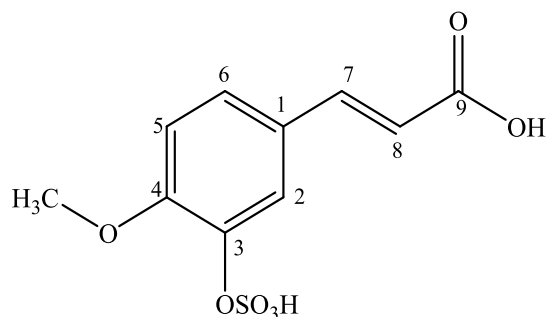
Figure 3.6: Structure of isoferulic acid-3-*O*-sulphate.

Table 3.3: ^{1}H (400MHz), DEPTq-135 (100MHz) and HMBC data of TA-2 in D_2O.

Position	^{1}H	^{13}C	HMBC	
			^2J	^3J
1	-	127.1	-	-
2	7.52 (1H, *d*, *J* = 2.0 Hz)	122.0	C-3	C-4, C-2, C-7
3	-	140.0	-	-
4	-	153.3	-	-
5	7.04 (1H, *d*, *J* = 8.6 Hz)	113.3	C-4	C-1, C-3
6	7.36 (1H, *dd*, *J* = 8.6, 2.0 Hz)	128.1	-	C-2, C-4, C-7
7	7.48 (1H, *d*, *J* = 15.9 Hz)	145.2	C-8	C-2, C-6, C-9
8	6.27 (1H, *d*, *J* = 15.9 Hz)	115.9	C-7, C-9	C-1
9	-	171.1	-	-
4-OCH$_3$	3.84 (3H, *s*)	56.1	-	C-4

A

B
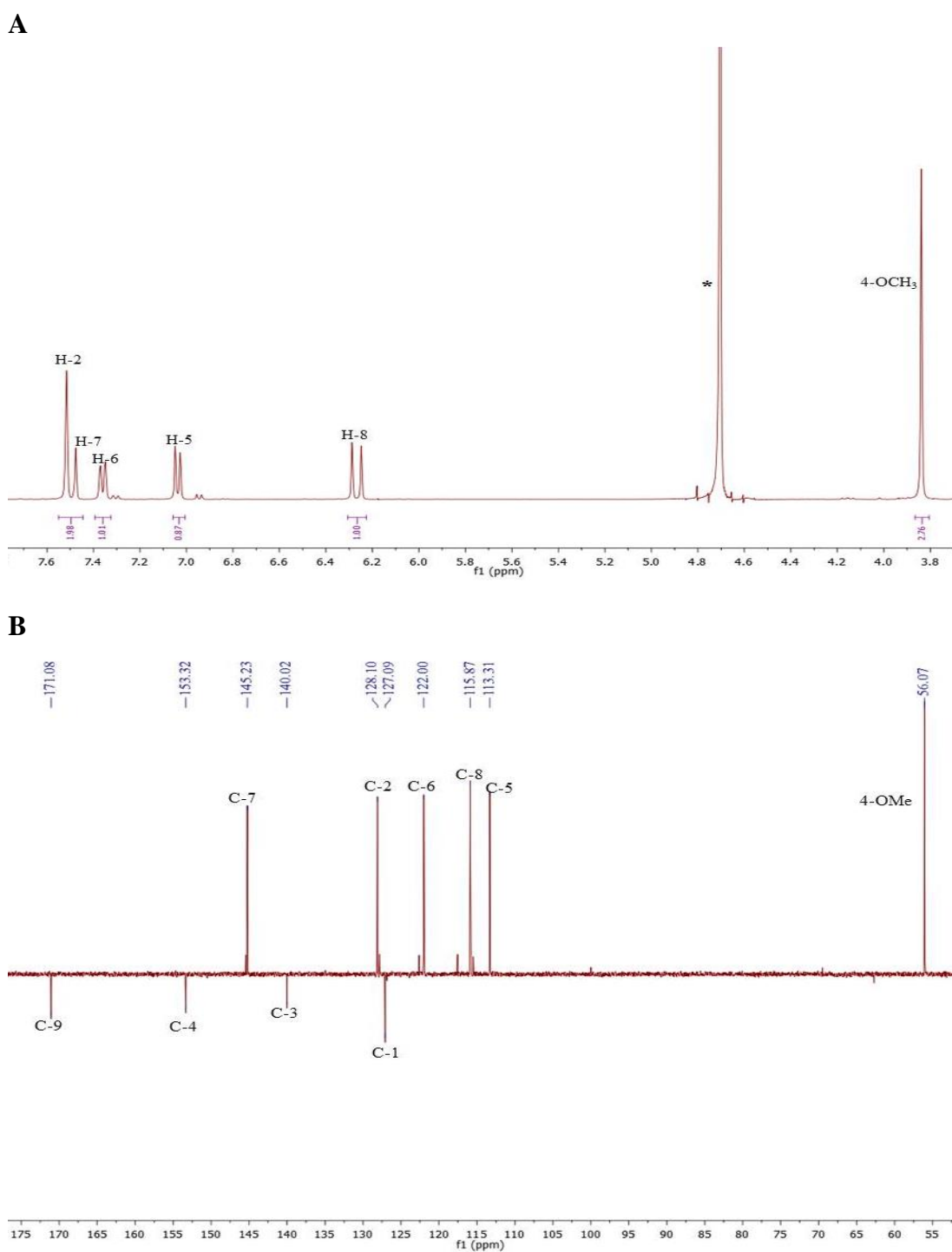
Figure 3.7A: 1H (400 MHz) and **3.7B:** DEPTq-135 (100 MHz) NMR spectra of TA-2 in D_2O*.
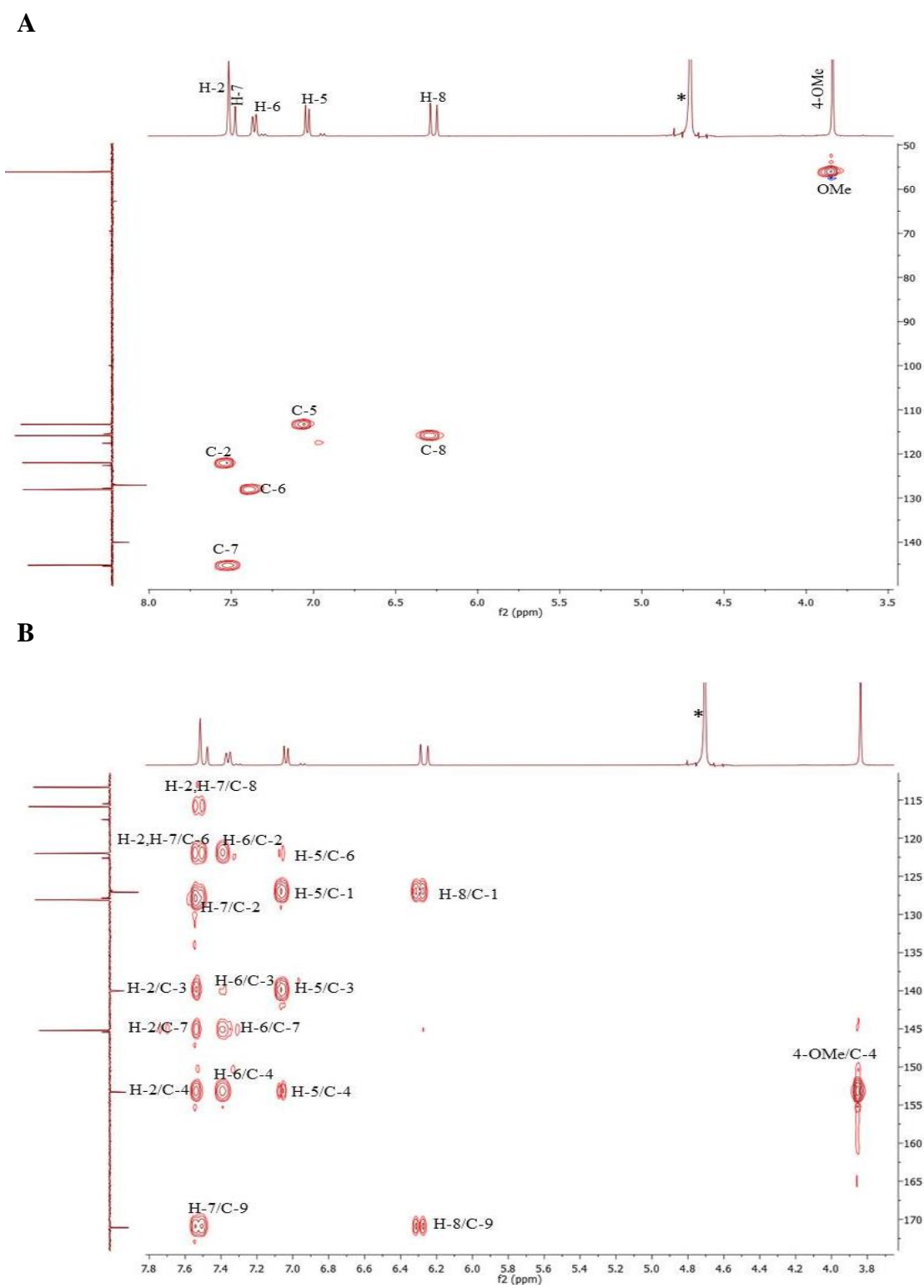
Figure 3.8A: HMQC (A) and **3.8B:** HMBC (400 MHz, D₂O*) spectra of TA-2.

3.1.3 Characterisation of TA-3 as 3`, 4`, 5, 7-tetrahydroxyflavone (Luteolin)

The compound TA-3 (Figure 3.9) was isolated from the methanol extract of *T. aphylla* leaves using Sephadex column. After spraying with *p*-anisaldehyde-sulphuric acid reagent and heating, a yellow spot appeared with R_f value of 0.60 using 20% methanol in EtOAc as the mobile phase on TLC.

The ^{1}H NMR spectrum (Figure 3.10A, Table 3.4) showed the protons at δ_H 6.19 (1H, *d*, *J* = 2.1 Hz) and 6.45 (1H, *d*, *J* = 2.1 Hz) were for the flavone A-ring as H-6 and H-8 protons, respectively and a proton singlet at δ_H 6.69 (1H, *s*, H-3) of ring C, while H-2', H-5' and H-6' of ring B appeared at δ_H 7.43 (1H, *dd*, *J* = 8.3, 2.3 Hz), 6.86 (1H, *d*, *J* = 8.3 Hz) and 7.40 (1H, *d*, *J* = 2.3 Hz).

The DEPTq-135 NMR spectrum (Figure 3.10B, Table 3.4) indicated the presence of 15 carbon atoms including a carbonyl at δ_c 181.6 (C-4) and six aromatic CH at 102.8, 99.2, 94.1, 119.0, 116.0 and 113.6 ppm (C-3, C-6, C-8, C-2`, C-5` and C-6`, respectively). Six phenolic carbons were observed at 164.1, 161.4, 163.8, 157.8, 145.7, and 149.6 ppm (C-2, C-5, C-7, C-9, C-3` and C-4`) and two quaternary carbons at 103.6, and 121.4 ppm (C-10 and C-1`).

Using 2D NMR (HMQC and HMBC) the compound was confirmed as follows: The A ring protons at δ_H 6.19 (H-6) and δ_H 6.45 (H-8) both showed ^3J correlation to the same quaternary carbon at δ_C 103.6 (C-10). The proton at δ_H 6.45 (H-8) displayed a ^2J coupling to a carbons at δ_c 163.8(C-7) and 157.8 (C-9). This proton also showed weak ^4J correlation to a carbon at δ_c 181.6 (C-4). The B ring proton at δ_H 6.86 (H-5`) showed $^3J$ correlation to the quaternary carbon at $\delta_c$ 145.7 (C-3`) and ^2J correlation to the carbon at δ_c 149.6 (C-4`). The proton at $\delta_H$ 7.43 (H-2`) correlated via ^3J coupling to C-4` and C-6`. Protons H-2` and H-6` showed ^3J correlation to the carbon C-2 of C ring. Couplings between the -OH in C-5 and its neighbouring carbons were also detected, including a ^3J correlation to C-6 at δ_c 99.2, C-10 at δ_c 103.6, and a ^2J correlation to C-5 (161.4 ppm).

Protons at δ_H 6.69 (H-3) and 6.86 (H-5`) displayed $^3J$ correlation to the carbon at $\delta_C$ 121.4 (C-1`) and confirmed the assignment of this carbon signal to the C-1` of the aromatic ring B.

The HREI-MS data showed pseudo molecular ion [M] $^+$ at *m/z* 287.0549 which indicated that the molecular formula of this compound was $C_{15}H_{10}O_6$. This compound was previously isolated from *T. aphylla* leaves (Mahfoudhi *et al.*, 2014). The ^{1}H &^{13}C NMR spectral data are in agreement with those reported earlier (Boersm *et al.*, 2002) and the structure identified as 3`, 4`, 5, 7-tetrahydroxyflavone.
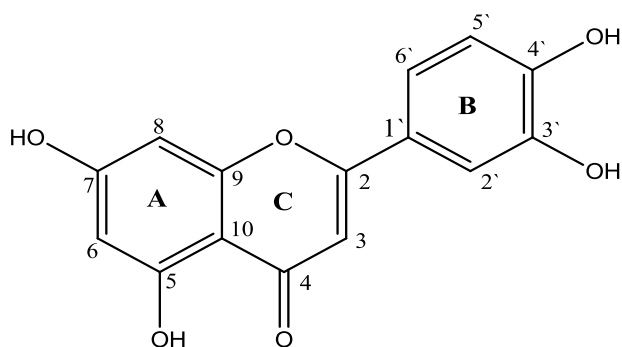
Figure 3.9: Structure of 3`, 4`, 5, 7-tetrahydroxyflavone.

Table 3.4: [1]H (400MHz) and DEPTq-135 (100MHz) and HMBC data of TA-3 in DMSO-*d6.*

Position	[1]H	[13]C	HMBC [2]J	HMBC [3]J
1	-	-	-	-
2	-	164.1	-	-
3	6.69 (1H, *s*)	102.8	C-4	C-1`, C-10
4	-	181.6	-	
5	-	161.4	-	
6	6.19 (1H, *d*, *J* = 2.1 Hz)	99.2	C-5, C-7	C-8, C-10
7	-	163.8	-	
8	6.45 (1H, *d*, *J* = 2.1 Hz)	94.1	C-9, C-7	C-6, C-10
9	-	157.8	-	-
10	-	103.6	-	-
1`	-	121.4	-	-
2`	7.43 (1H, *dd*, *J* = 8.3, 2.3 Hz)	119.0	-	C-2, C-4`, C-6`
3`	-	145.7	-	-
4`	-	149.6	-	-
5`	6.86 (1H, *d*, *J* = 8.3 Hz)	116.0	C-4`	C-1`, C-3`
6`	7.40 (1H, *d*, *J* = 2.3 Hz)	113.6	-	C-2, C-2`, C-4`
5-OH	13.0 (1H, *s*)	-	C-5	C-6, C-10

A
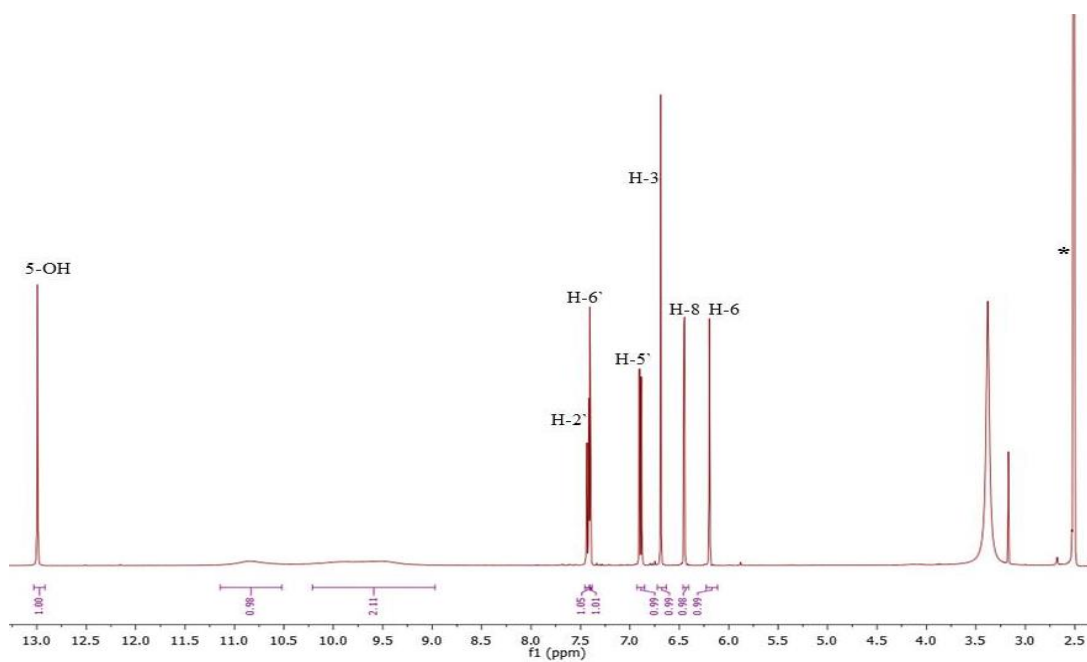
B
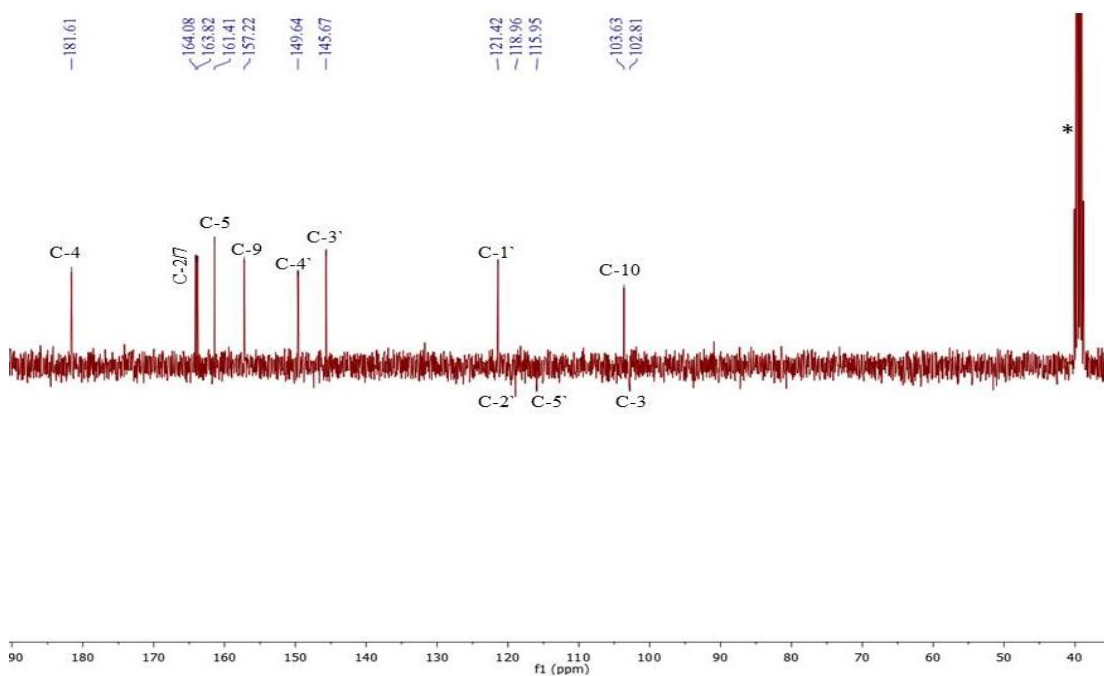
Figure 3.10A: ¹H (400 MHz) and **3.10B:** DEPTq-135 (100 MHz) NMR spectra of TA-3 in DMSO-*d₆**.

A
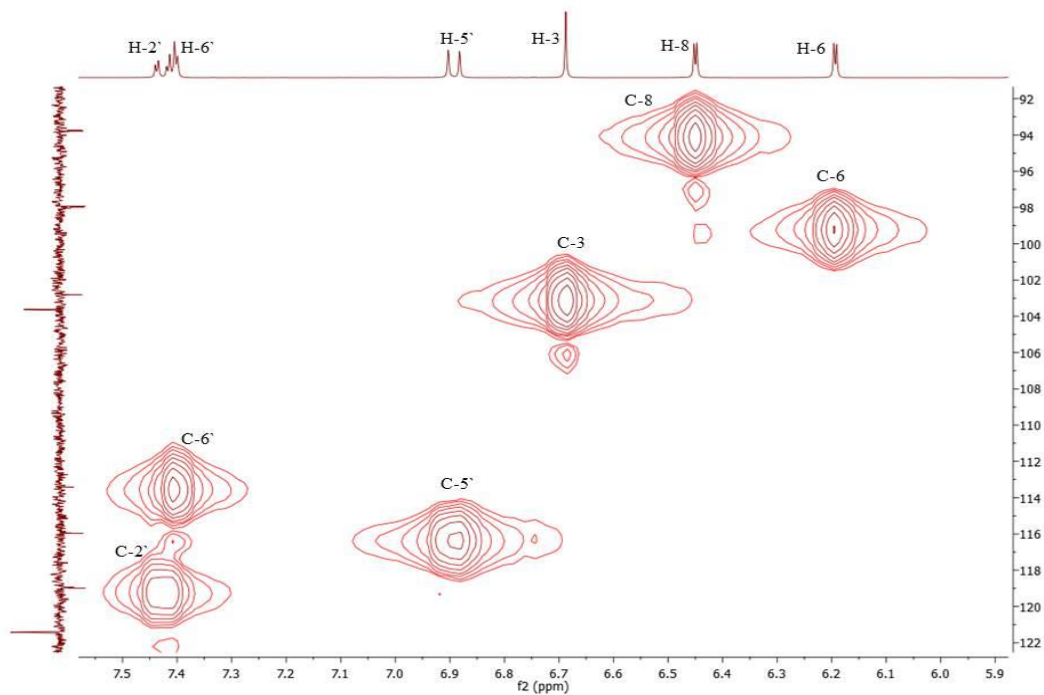
B
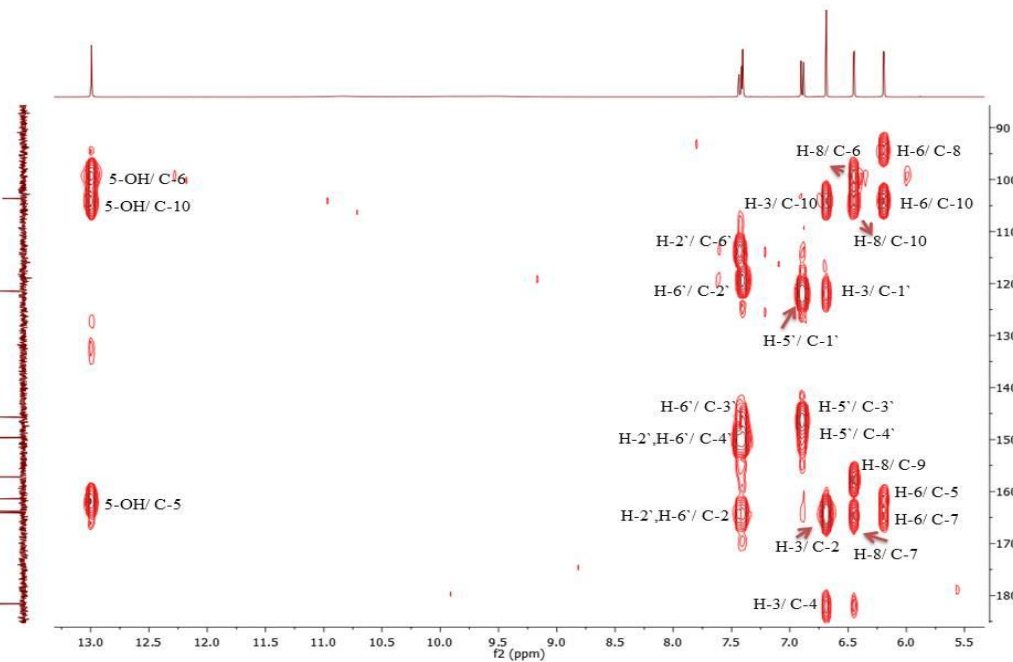
Figure 3.11A: HMQC and **3.11B:** HMBC (400 MHz, DMSO-d_6*) spectra of TA-3.

3.1.4 Characterisation of TA-4 as *N*-methyl-4-hydroxyproline

The compound TA-4 (Figure 3.12) was obtained from the methanol extract of *T. aphylla* leaves using Sephadex column. It appeared as a yellow spot (R_f= 0.39) after spraying with *p*-anisaldehyde-sulphuric acid reagent and heating, using 30% MeOH in EtOAc as the mobile phase on TLC.

The ^{1}H NMR spectrum (Figure 3.13A, Table 3.5) showed methylene protons at δ_H 2.16 (1H, *ddd*, *J* = 14.2, 7.5, 2.0 Hz, H-3a), 2.40 (1H, *ddt*, *J* = 14.2, 7.5, 2.0 Hz, H-3b) and 3.12 (1H, *m*, H-5a), 3.88 (1H, *dd*, *J*= 13.0, 4.6 Hz, H-5b) and a proton singlet at δ_H 2.95 (3H, *s*) for a methyl group. While H-2 and H-4 appeared at δ_H 4.12 (1H, *dd*, *J* = 11.1, 7.5 Hz) and 4.55 (1H, *tt*, *J* = 4.6, 2.0 Hz), respectively.

The DEPTq-135 NMR spectrum (Figure 3.13B) indicated the presence of six carbon atoms including a methyl carbon (C-6) at δ_c 42.8 and a carboxylic acid at δ_c 172.4 (C-7). Two deshielded methine carbons were been observed at δ_c 69.5, and 69.0 (C-2 & C-4) and two methylene carbons (C-3 and C-5) at δ_c 37.7 and 62.2, respectively.

In the HMBC spectrum (Figure 3.14B, Table 3.5), the proton at δ_H 4.12 (H-2) showed ^2J correlations to carbons at δ_C 37.7 (C-3) and 172.4 (C-7), respectively and ^3J coupling to δ 42.8 (C-6). Protons H-3b and H-5a are correlated via ^2J couplings to the carbon at δ_C 69.0 (C-4). Other important correlations observed were for the proton signal at δ_H 2.95 (H-6) which showed ^3J correlations to the methine carbon at δ_C 69.5 (C-2) and methylene carbon at δ_C 62.2 (C-5). This further confirming the *N*-methyl group is at position 1.

The HREI-MS data showed pseudo molecular ion [M] $^+$ at *m/z* 146.0811 which showed that the molecular formula of this compound was $C_6H_{11}O_3N$. This compound has been previously isolated from a dichloromethane extract of *Trichilia lepidota* leaves (Pupo *et al*., 2002). The data were in agreement with those reported earlier (Sciuto *et al*., 1983) and led to the identification of TA-4 as *N*-methyl-4-hydroxyproline. This is the first report of this compound from *T. aphylla*.
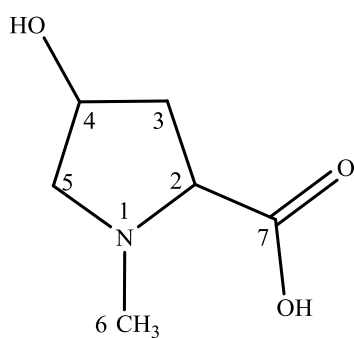
Figure 3.12: Structure of *N*-methyl-4-hydroxyproline.

Table 3.5: [1]H (400MHz) and DEPTq-135 (100MHz) and HMBC data of TA-4 in D$_2$O.

Position	[1]H	[13]C	HMBC [2]J	HMBC [3]J
1	-	-	-	-
2	4.12 (1H, *dd*, J = 11.1, 7.5 Hz)	69.5	C-3, C-7	C-6
3	2.16 (1H, *ddd*, J = 14.2, 7.5, 2.0 Hz, H-3a) 2.40 (1H, *ddt*, J = 14.2, 7.5, 2.0 Hz, H-3b)	37.7	C-2 C-2, C-4	C-7 C-5
4	4.55 (1H, *tt*, J = 4.6, 2.0 Hz)	69.0	C-5	C-2
5	3.12 (1H, *m*, H-5a) 3.88 (1H, *dd*, J = 13.0, 4.6 Hz, H-5b)	62.2	C-4 -	C-2,C-3, C-6 C-3, C-6
6	2.95 (3H, *s*)	42.8	-	C-5, C-2
7	-	172.4	-	-

A
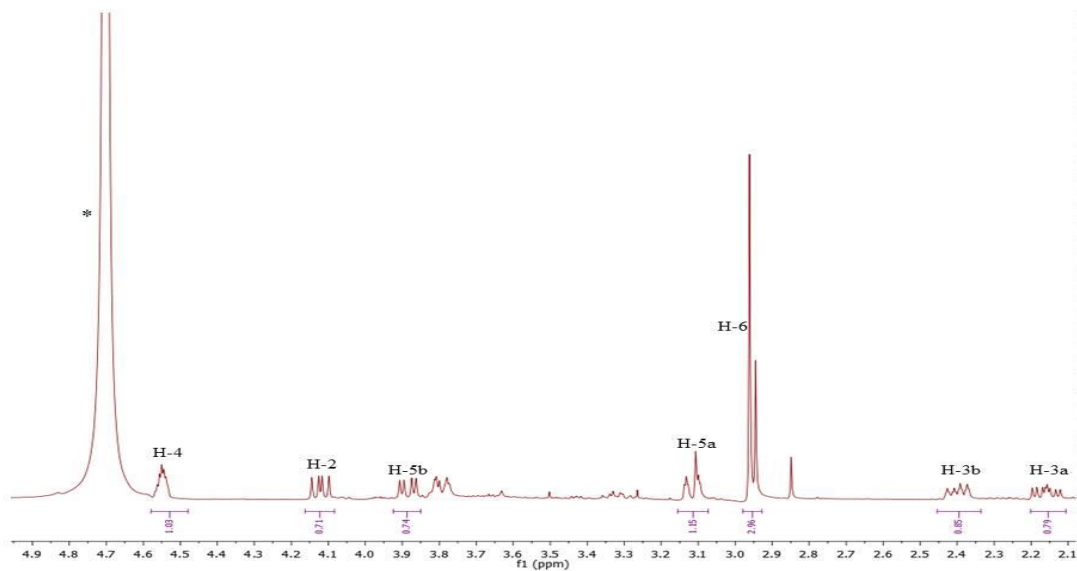
B
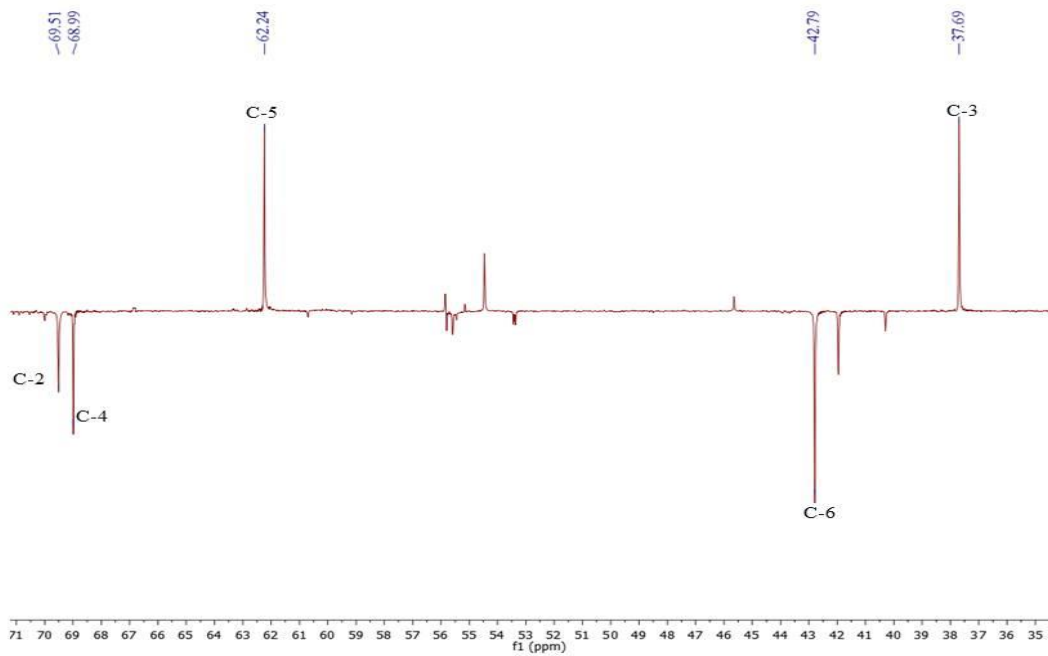
Figure 3.13A: ¹H (400 MHz) and **3.13B:** ¹³C (100 MHz) NMR spectra of TA-4 in DMSO-*d₆**.

A

B
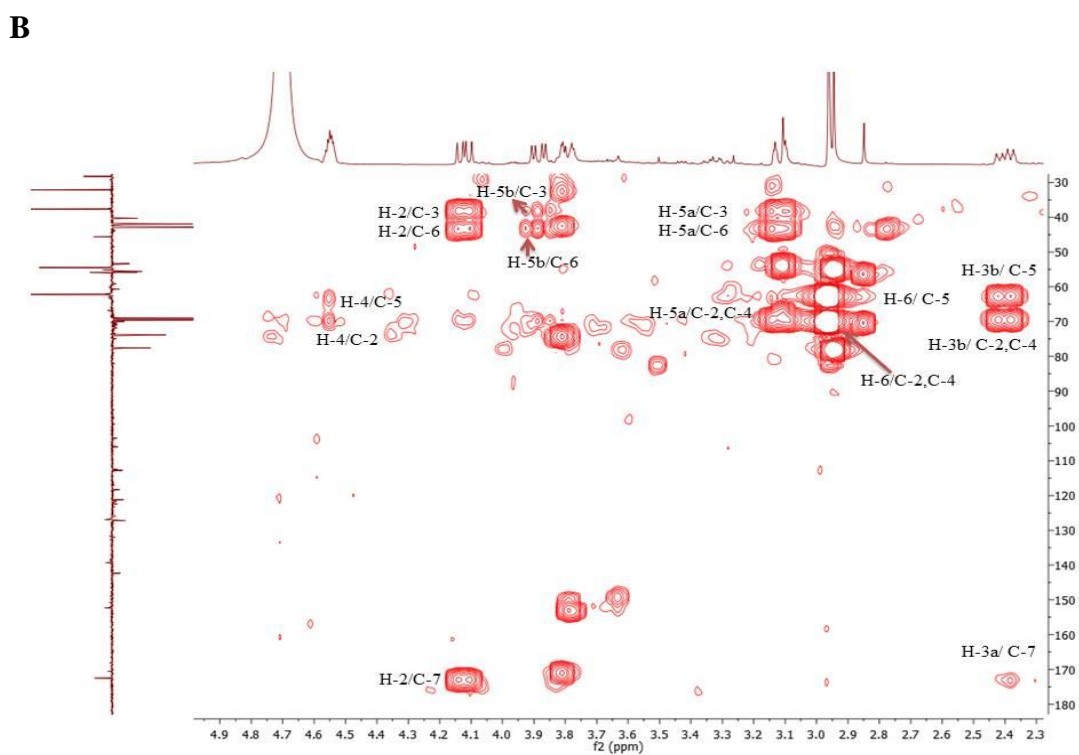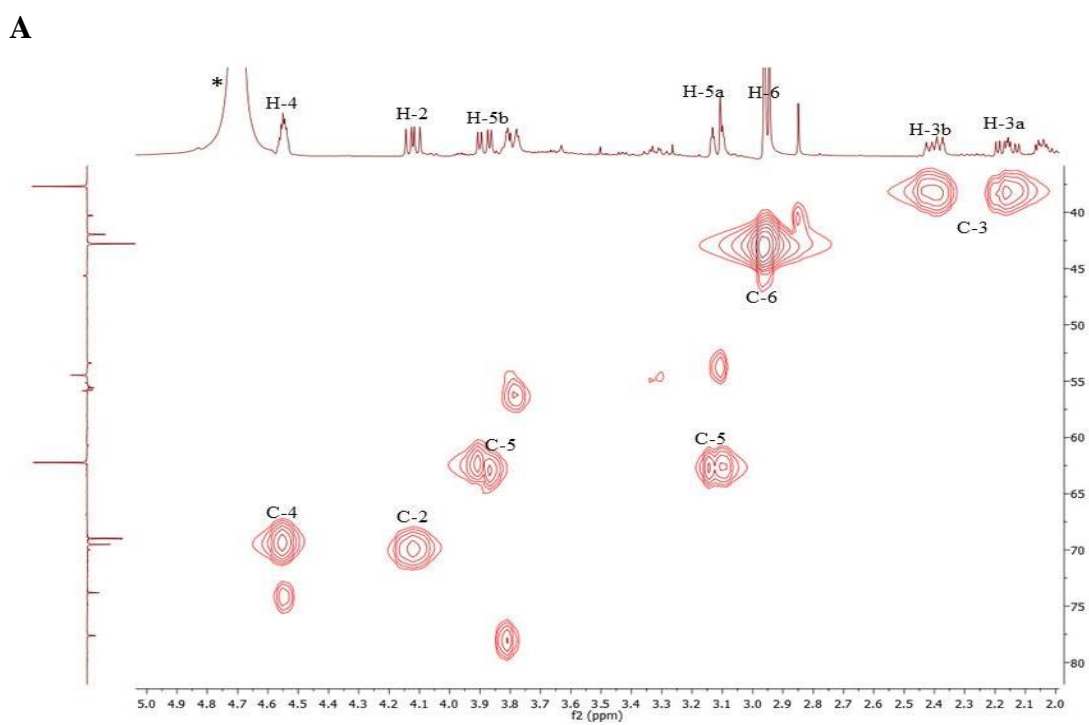
Figure 3.14A: HMQC and **3.14B:** HMBC (400 MHz, DMSO-d_6*) spectra of TA-4.

3.2 Fractionation of *Astragalus spinosus* crude extracts

A. spinosus methanol extract (26g, 6.5%) was divided into two parts for further fractionation. A VLC column was used to fractionate the first part of the extract (24g). The ^{1}HNMR enabled elucidation of a compound, coded AS-1 (18mg, 0.07%). The second part of the extract (2g) was subjected to further fractionation using Sephadex column as described before and lead to the isolation of two compounds AS-2 (24mg, 1.20%) and AS-3 (31mg, 1.55%). Fractionation of the EtOAc extract (6g, 1.50%) of *A. spinosus* led to identification of one compound named AS-4 (13mg, 0.21%). No compounds were separated from the fractionation of *A. spinosus* hexane extract using CC and the ^{1}H NMR spectrum of this crude showed signals indicating a mixture of fats.

3.2.1 Characterisation of AS-1 as 3-*O*-methyl-inositol (Pinitol)

The compound AS-1 (Figure 3.15) was obtained from the methanol extract of *A. spinosus* leaves using VLC. After spraying with *p*-anisaldehyde-sulphuric acid reagent and heating, a purple spot appeared with R_f of 0.66 using 30% MeOH in EtOAc as the mobile phase on TLC.

The ^{1}H NMR spectrum (Figure 3.16A, Table 3.6) had proton signals between 3.0 and 3.63 ppm. The proton at δ_H 3.0 was assigned to H-3, the methoxy group at δ_H 3.44 (3H, *s*, 3-OCH$_3$) integrated for 3H, while five protons at δ_H 3.44, 3.35, 3.50, 3.63 and 3.63 were attributed to H-1, H-2, H-4, H-5 and H-6, respectively.

The ^{13}C spectrum (Figure 3.16B, Table 3.6) showed seven carbon atoms at δ_C 60.2 (O$\underline{C}$H$_3$), 71.5 (C-1), 73.2 (C-2), 84.4 (C-3), 70.6 (C-4), 73.0 (C-5), 72.5 (C-6).

Using 2D NMR (COSY, HMQC and HMBC), the structure of the compound was elucidated as follows: The long range correlation (HMBC, Figure: 3.17B) for the proton at δ_H 3.00 (H-3) showed ^2J correlation to the carbons at δ_C 70.6 (C-4), δ_C 73.2 (C-2) and a ^3J correlation to the carbon 3-O$\underline{C}$H$_3$. The methyl protons 3-OC$\underline{H}$$_3$ and

the proton H-1 showed ^3J correlation to the carbon at δ_C 84.3 and was assigned as C-3.

The HREI-MS data showed pseudo molecular ion [M] $^+$ at *m/z* 195.0878 which revealed that the molecular formula of this compound was $C_7H_{14}O_6$. The ^1H & ^{13}C NMR spectral data are in agreement, even though the data were obtained in different NMR solvents, with those reported earlier (Raya-Gonzalez *et al*., 2008). This compound was previously isolated from different plant families such as Asteraceae, Caryophyllaceae, Leguminosae, Pinaceae, Sapindaceae, and Zygophyllaceae (Poongothai and Sripathi, 2013). This is the first report of pinitol from *A. spinosus*.
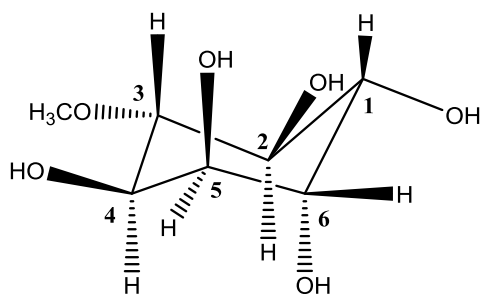
Figure 3.15: Structure of pinitol.

Table 3.6: ^1H (400MHz), DEPTq-135 (100MHz) and HMBC data of AS-1 in DMSO-d_6.

Position	^1H	^{13}C	HMBC ^2J	HMBC ^3J
1	3.42 (1H, *s*)	71.5	-	C-3
2	3.35 (1H,*dt*, *J* = 16.1 Hz)	73.2	-	-
3	3.0 (1H, *t*, *J* = 9.3 Hz)	84.4	C-2, C-4	3-OCH$_3$
4	3.50 (1H, *brm*, *J* = 3.5 Hz)	70.6	-	-
5	3.63 (1H, *d*, *J* = 2.2 Hz)	73.0	-	-
6	3.63 (1H, *d*, *J* = 2.2 Hz)	72.5	-	-
1-OH	4.35 (1H, *brd*, *J* = 5.3 Hz)	-	-	-
2-OH	4.52 (1H, *d*, *J* = 4.6 Hz)	-	-	-
4-OH	4.48 (1H, *d*, *J* = 6.4 Hz)	-	-	-
5-OH	4.64 (1H, *s*)	-	-	-
6-OH	4.73 (1H, *s*)	-	-	-
3-OCH$_3$	3.44 (3H, *s*)	60.2	-	C-3

A
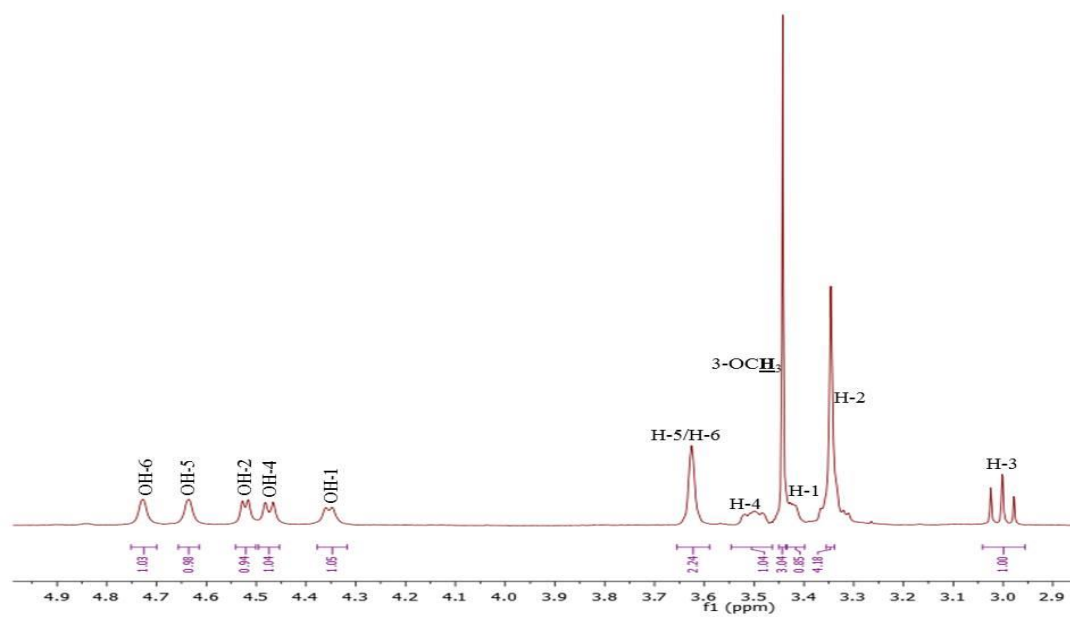
B
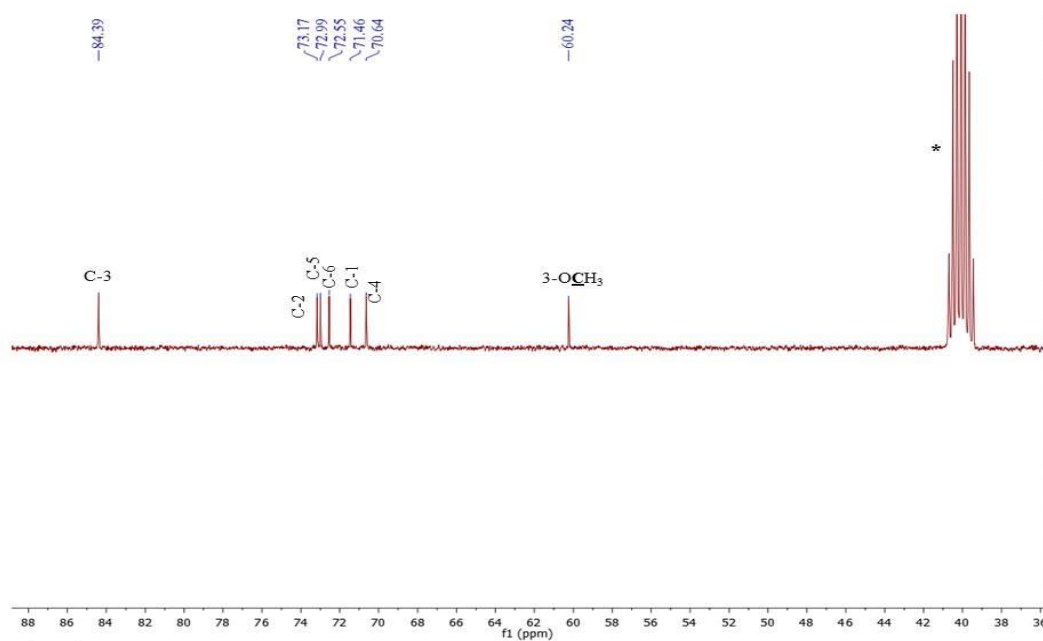
Figure 3.16A: ^{1}H (400 MHz) and **3.16B:** ^{13}C (100 MHz NMR spectra of AS-1 in DMSO-d_6*.

A
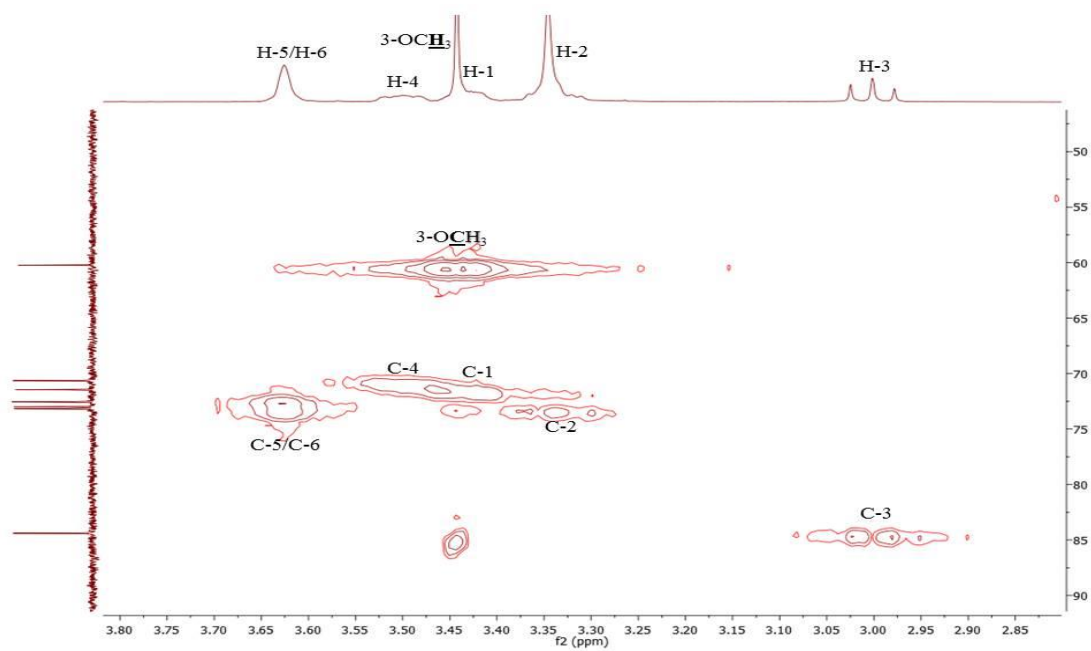
B
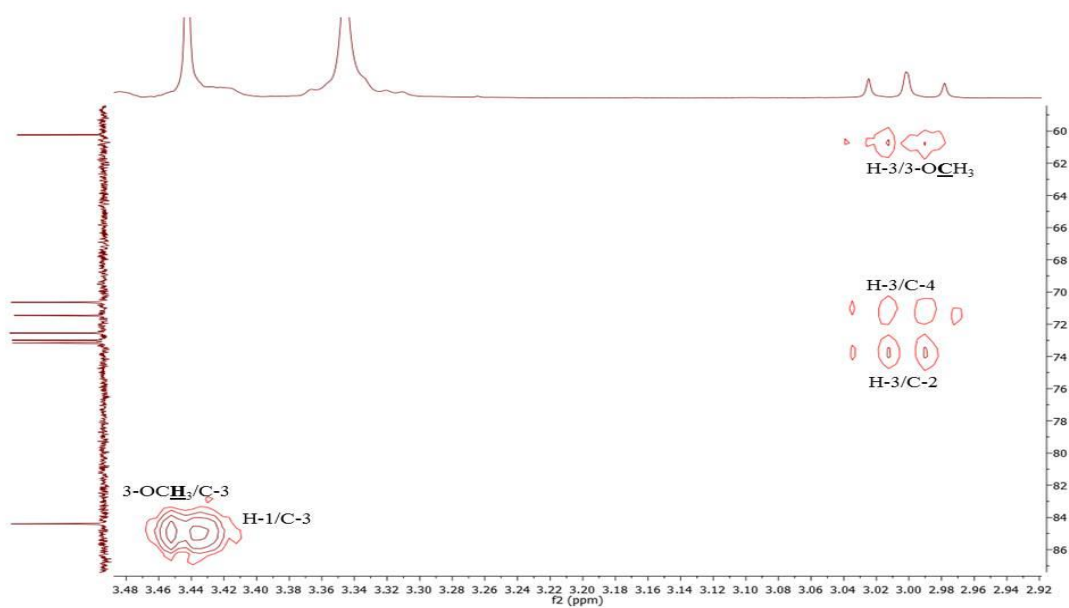
Figure 3.17A: HMQC and **3.17B:** HMBC (400 MHz, DMSO-*d₆**) spectra of AS-1.

3.2.2 Characterisation of AS-2 as Cycloastragenol

The compound AS-2 (Figure 3.18) was obtained from the methanol extract of *A. spinosus* leaves using Sephadex column. After spraying with *p*-anisaldehyde-sulphuric acid reagent and heating, a purple spot was obtained with R_f value of 0.61 using 100% EtOAc as the mobile phase on TLC (Methods Section 2.5.1).

The ^{1}H NMR spectrum (Figure 3.19A, Table 3.7) showed signals due to a cyclopropane methylene at δ_H 0.40 and 0.54 (1 H each, *d*, *J* = 4.5 Hz) and methylene signals at H-1, H-2, H-7, H-11, H-12, H-15, H-22 and H-23. Seven methyls at δ_H 1.25 (H-21), 1.32 (H-18 & H-27), 1.17 (H-26), 1.28 (H-28), 0.99 (H-29) and 0.97 (H-30) and seven methines at δ_H 3.33 (1H, *m*, H-3), 1.38 (1H, *m*, H-5), 3.55 (1H, *m*, H-6), 1.81 (1H, *m*, H-8), 4.70 (1H, *m*, H-16), 2.35 (1H, *d*, *J* = 7.9 Hz, H-17), 3.78 (1H, *t*, *J* = 7.3 Hz, H-24).

The DEPTq-135 NMR spectrum (Figure 3.19B, Table 3.7) displayed 30 carbon signals; seven attributable to methyls at δ_C 21.5 (C-18), 27.7 (C-21), 26.4 (C-26), 27.8 (C-27), 28.2 (C-28), 15.3 (C-29), 20.0 (C-30). Nine methylene signals at 32.1, 30.3, 37.9, 26.2, 33.0, 46.5, 31.5, 34.4, 25.6 ppm and seven signals were assigned to the methine carbons including three carbon bearing oxygen at 78.3, 69.2, and 73.4 ppm (C-3, C-6, C-16, respectively). Seven quaternary carbons were observed at 41.5, 20.7, 29.4, 45.0, 47.9, 87.1 and 71.8 ppm.

In the HMBC (Figure 3.20B), the geminal methyls at 1.28 and 0.99 ppm (H-28 & H-29) showed ^2J correlations to carbon at 41.5 ppm (C-4) and to ^3J correlations to each other and to the oxymethine carbon at 78.3 ppm (C-3), indicating C-3 as the position of attachment of the hydroxyl group while both germinal methyls at H-26 (1.17 ppm) and H-27 (1.32 ppm) had ^2J couplings to C-25 (71.8 ppm). Furthermore, the cyclopropane methylene doublets at C-19 showed ^2J correlations to C-9 at 20.7 ppm and ^3J correlations to two methylene carbons at 32.1 (C-1) and 26.2 ppm (C-11). The proton H-5 showed ^2J correlation to the oxymethine at 69.2 ppm establishing the hydroxyl group to be at C-6.

The HREI-MS data showed pseudo molecular ion [M] [+] at *m/z* 491.3729 suggesting the molecular formula of $C_{30}H_{50}O_5$. Thus, AS-2 was identified as cycloastragenol. This compound has previously been reported from the aerial parts of *A. spinosus* (Abdallah *et al.*, 1993) and all spectral data were in agreement with those previously reported (Nartop *et al.*, 2014).

3.2.3 Characterisation of AS-3 as cycloastragenol 6-*O*-glucoside (Brachyoside B)

The compound AS-3 (Figure 3.18) was obtained from the methanol extract of *A. spinosus* leaves using Sephadex column. After spraying with *p*-anisaldehyde-sulphuric acid reagent and heating, a purple spot was observed with R_f value of 0.44 using 100% EtOAc as the mobile phase on TLC.

The ^{1}H and DEPTq-135 NMR spectra for the compound AS-3 (Figure 3.19 A&B) followed a similar pattern to that of AS-2 except for the presence of a sugar moiety instead of a hydroxyl group at C-6. The ^{1}H NMR spectrum (Figure 3.19A, Table 3.7) revealed a doublet at δ_H 4.42 (1H, *J* = 7.7 Hz, H-1`) was assigned to the anomeric proton of the sugar, three oxymethines at $\delta_H$ 3.37 (1H, *m*, H-3`), 3.37 (1H, *m*, H-4`), 3.32 (1H, *m*, H-5`) and an oxymethylene group at δ_H 3.84 (1H, *d*, J_1=11.4 Hz, J_2 = 4.1Hz) and 3.66 (1H, *m*, H-6`).

The ^{13}C NMR spectrum (Figure 3.19B, Table 3.7) confirmed the presence of 36 carbon atoms including an anomeric carbon at δ_C 103.8 (C-1`), four oxymethines at $\delta_C$ 74.5 (C-2`), 77.6 (C-3`), 71.1 (C-4`), 76.2 (C-5`) and an oxymethylene at $\delta_C$ 62.4 (C-6`) was assigned to the glucose unit. The carbon resonance attributed to C-6 (78.6 ppm) was deshielded by 9.4 ppm, in comparison with those of cycloastragenol, suggesting that C-6 was the site of glycosylation.

The attachment of the glucose moiety at C-6 of the aglycone was further confirmed from the HMBC correlations (Figure 3.21B). The anomeric proton at δ_H 4.42 (H-1`) showed [3]*J* correlation to the oxygen-bearing carbon at $\delta_C$ 78.6 (C-6), indicating its connectivity to that carbon at C-6 of the aglycone. Also, proton H-5` showed [3]*J*

111

correlation to H-1` and proton H-3` displayed ^2J correlation to H-4`. Major HMBC correlations is given in Figure 3.23.

The HREI-MS data showed pseudo molecular ion [M] $^+$ at *m/z* 653.4259 suggesting the molecular formula of $C_{36}H_{60}O_{10}$. The mass spectrum supported the above data since the molecular weight of AS-3 was found to be 162 units higher than AS-2. This unit was identified to be a glucose moiety with the help of its COSY and HMBC data. Thus, all the above information led to the conclusion that AS-3 was cycloastragenol-6-*O*-glucoside. This compound has previously been reported from the aerial parts of *A. spinosus* (Abdallah *et al.*, 1993) and the roots of *A. brachypterus* and all spectral data were in agreement with those previously reported (Bedir *et al.*, 1998).
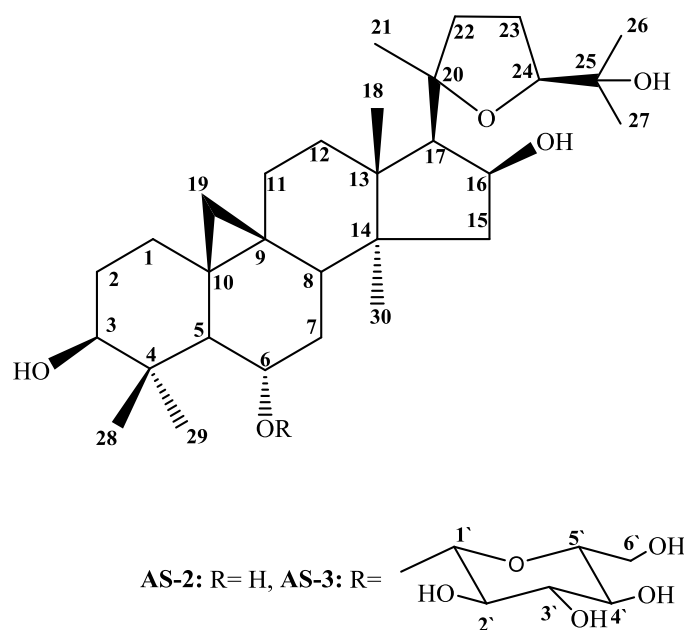
Figure 3.18: Structure of cycloastragenol (AS-2) and cycloastragenol 6-*O*-glucoside (AS-3).

Table 3.7: [1]H (400MHz) and DEPTq-135 (100MHz) data of SA-2 (CDCl$_3$) and SA-3 (Acetone-d_6).

Position	AS-2		AS-3	
	δ_H	δ_C	δ_H	δ_C
1	1.28 (2H, *d*, *J* = 1.5 Hz)	32.1	1.27 (1H, *s*) 1.60 (1H, *m*)	31.8
2	1.63 (1H, *m*) 1.81 (1H, *m*)	30.3	1.60 (1H, *m*) 1.70 (1H, *m*)	30.3
3	3.33 (1H, *m*)	78.3	3.22 (1H, *m*)	77.6
4	-	41.5	-	41.5
5	1.38 (1H, *m*)	53.7	1.60 (1H, *m*)	51.8
6	3.55 (1H, *m*)	69.2	3.56 (1H, *s*)	78.6
7	1.38 (1H, *m*) 1.52 (1H, *s*)	37.9	1.60 (1H, *m*) 1.90 (1H, *m*)	34.0
8	1.81 (1H, *m*)	47.0	1.88 (1H, *dd*, *J$_1$* = 11.7 Hz, *J$_2$* = 4.1 Hz)	45.4
9	-	20.7	-	20.8
10	-	29.4	-	29.0
11	2.01(2H, *m*)	26.2	1.90 (1H, *m*) 1.38 (1H, *m*)	25.8
12	1.63 (1H, *m*) 1.75 (1H, *s*)	33.0	1.60 (1H, *m*) 1.70 (1H, *m*)	33.0
13	-	45.0	-	44.6
14	-	47.9	-	45.7
15	1.47 (1H, *m*) 2.01 (1H, *m*)	46.5	1.38 (1H, *m*) 2.00 (1H, *m*)	45.4
16	4.70 (1H, *m*)	73.4	4.64 (1H, *m*)	72.9
17	2.35 (1H, *d*, *J* = 7.9 Hz)	57.5	2.33 (1H, *d*, *J* = 7.7 Hz)	57.8
18	1.32 (3H, *s*)	21.5	1.27 (3H, *s*)	20.3
19	0.40 (1H, *d*, *J* = 4.5 Hz) 0.54 (1H, *d*, *J* = 4.5 Hz)	31.5	0.27 (1H, *d*, *J* = 4.4 Hz) 0.60 (1H, *d*, *J* = 4.4 Hz)	27.8
20	-	87.1	-	86.7
21	1.25 (3H, *s*)	27.7	1.26 (3H, *s*)	27.5
22	2.58 (1H, *t*, *J* = 9.5 Hz) 1.65 (1H, *t*, *J* = 5.5 Hz)	34.4	2.71 (1H, *q*, *J* = 10.6 Hz) 1.60 (1H, *m*)	34.2
23	2.01 (1H, *m*) 2.15 (1H, *m*)	25.6	2.00 (2H, *m*)	25.5
24	3.78 (1H, *t*, *J* = 7.3 Hz)	81.4	3.75 (1H, *dd*, *J$_1$* = 8.5 Hz, *J$_2$* = 6.0 Hz)	80.9
25	-	71.8	-	71.0
26	1.17 (3H, *s*)	26.4	1.14 (3H, *s*)	26.1
27	1.32 (3H, *s*)	27.8	1.27 (3H, *s*)	26.9
28	1.28 (3H, *s*)	28.2	1.19 (3H, *s*)	27.5

Table 3.7: (continued).

29	0.99 (3H, *s*)	15.3	0.96 (3H, *s*)	15.0
30	0.97 (3H, *s*)	20.0	1.01 (3H, *s*)	19.3
1`			4.42 (1H, *d*, *J* = 7.7 Hz)	103.8
2`			3.22 (1H, *m*)	74.5
3`			3.37 (1H, *m*)	77.6
4`			3.37 (1H, *m*)	71.1
5`			3.32 (1H, *m*)	76.2
6`			3.84 (1H, *d*, J_1 = 11.4 Hz, J_2=4.1 Hz) 3.66 (1H, *m*)	62.4

A
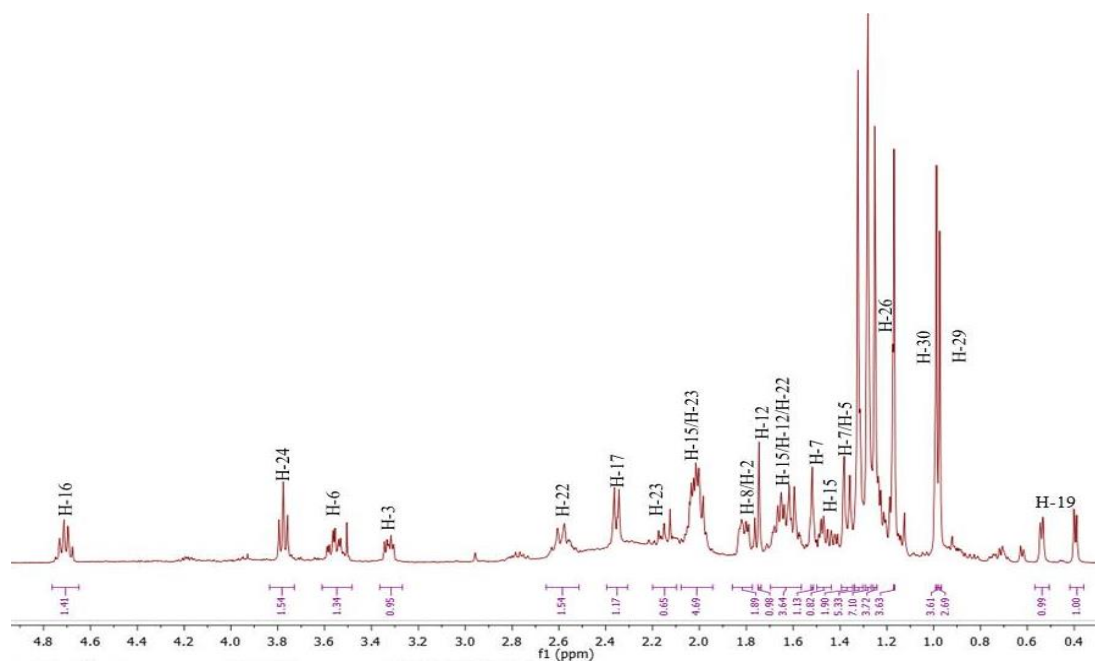
B
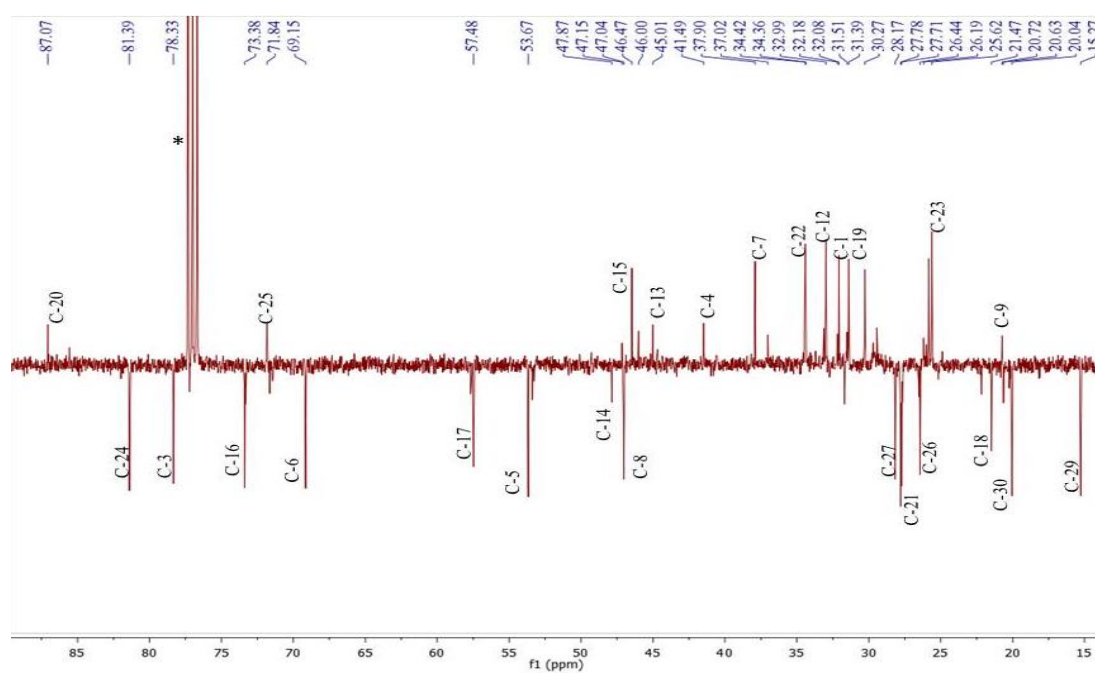
Figure 3.19A: [1]H (400 MHz) and **3.19B:** DEPTq-135 (100 MHz) NMR spectra of AS-2 in CDCl$_3$*.
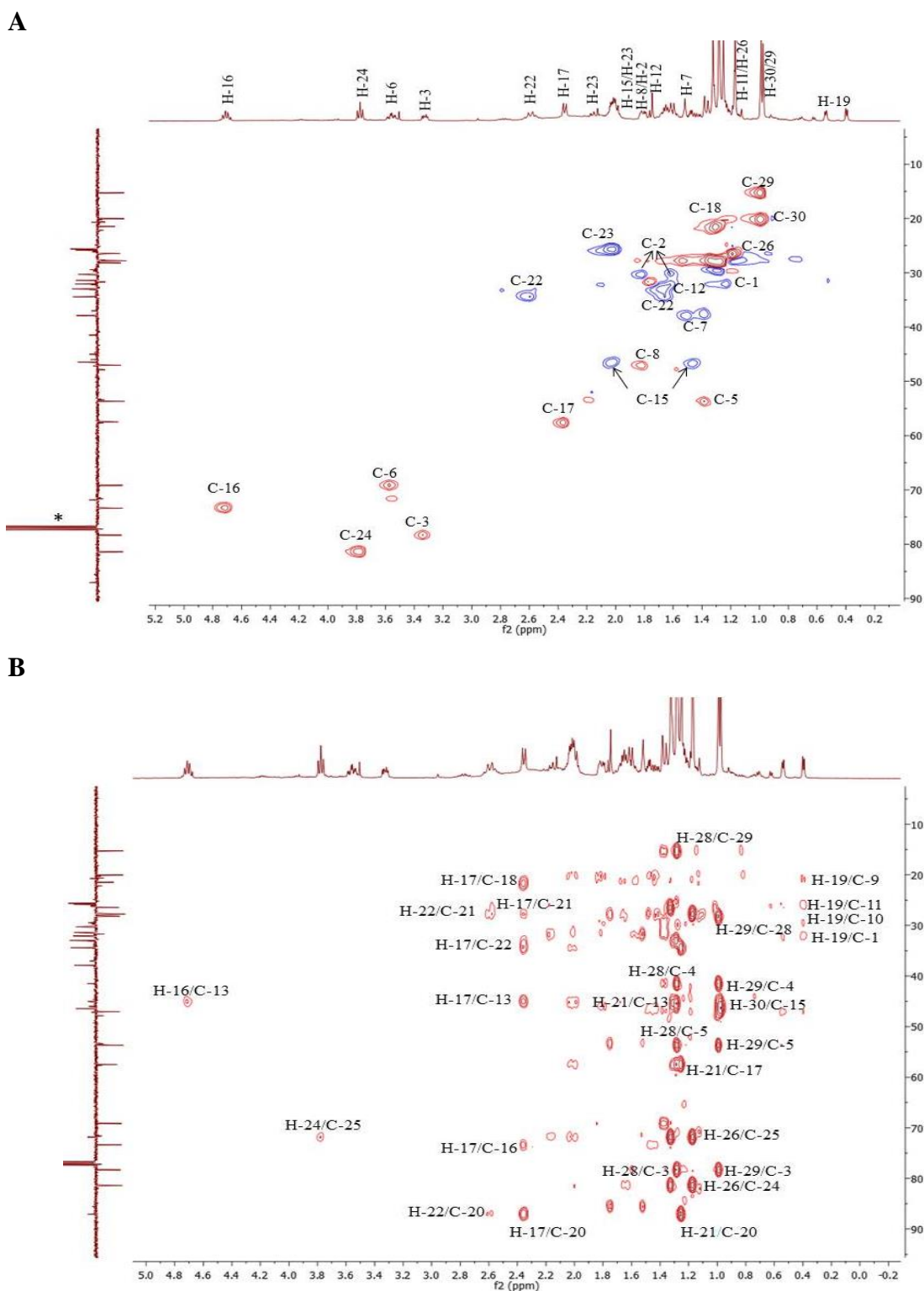
Figure 3.20A: HMQC and **3.20B:** HMBC (400 MHz, CDCl$_3$*) spectra of AS-2.

A

B
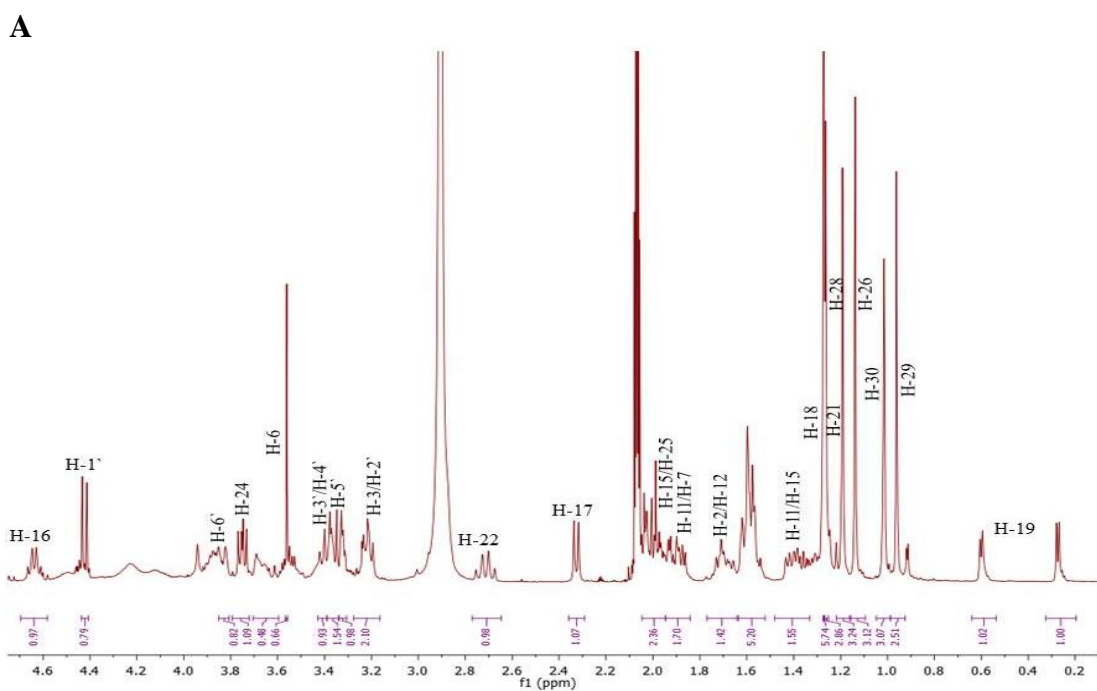
Figure 3.21A: ^{1}H (400 MHz) and **3.21B:** ^{13}C (100 MHz) NMR spectra of AS-3 in Acetone-d_6*.
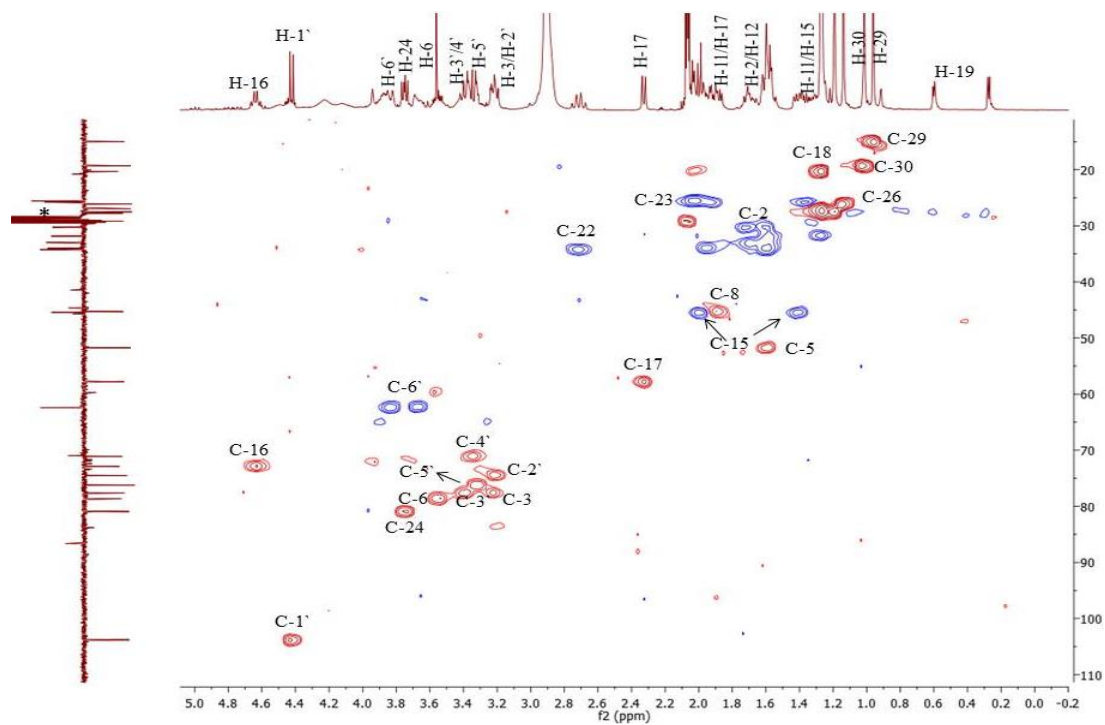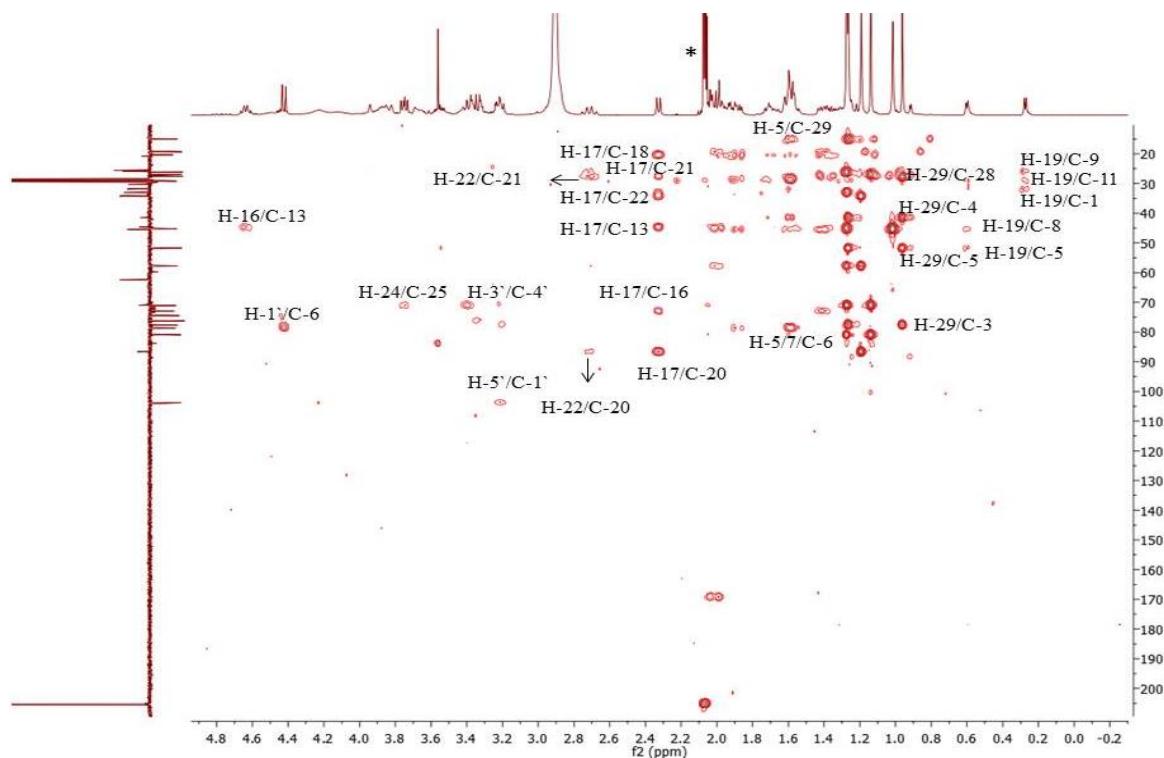
Figure 3.22A: HMQC and **3.22B:** HMBC (400 MHz, Acetone-d_6^*) spectra of AS-3.
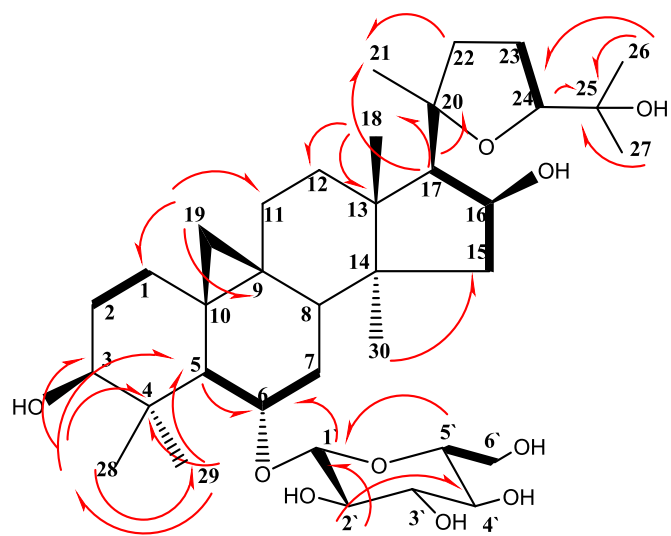
Figure 3.23: Key COSY (▬▬▬) and HMBC (⌒➔) correlations observed in AS-2 (aglycone) and AS-3.

3.2.4 Characterisation of AS-4 as maackiain (Inermine)

The compound AS-4 (Figure 3.24) was obtained from the ethyl acetate extract of *A. spinosus* leaves using CC (Methods Section 2.5.4). Using 100% EtOAc as the mobile phase for TLC, the compound appeared as a brown spot (R_f= 0.74) after spraying with *p*-anisaldehyde sulphuric acid reagent and heating.

The ^{1}H NMR (Figure 3.25A, Table 3.8) spectrum revealed characteristic signals belonging to a pterocarpan skeleton; the protons at δ_H 5.49 (1H, *d*, *J* = 6.9 Hz, H-11a), 4.24/3.67 (1H each, *dd*, *J* = 11.2, 5.0 Hz, H-6) and 3.50 (1H, *ddd*, *J* = 11.2, 6.9, 5.0 Hz, H-6a). The ^{1}H NMR also showed an aromatic ABX spin system for the ring D with a set of doublets at δ_H 7.39 (1H, *d*, *J* = 8.4 Hz, H-1) and 6.44 (1H, *d*, *J* = 2.5 Hz, H-4) and a doublet of doublets at δ_H 6.57 (1H, *J* = 8.4, 2.5 Hz, H-2). The signals at δ_H 6.74 (1H, *brs*, H-7), 6.46 (1H, *brs*, H-10) and 5.92, 5.94 (2x *d*, *J* = 1.4 Hz, H-12) were assigned to a methylenedioxy moiety in the ring A.

The DEPTq-135 NMR spectrum (Figure 3.25B) showed 16 carbon atom signals including seven methines at 132.1, 109.8, 103.7, 40.2, 104.7, 93.8 and 78.5 ppm (C-1, C-2, C-4, C-6a, C-7, C-10 and C-11a, respectively). Seven quaternary carbons were observed at 157.0, 156.5, 117.9, 141.5, 147.9, 154.3, and 112.7 ppm (C-3, C-4a, C-6b, C-8, C-9, C-10a and C-11b), and two signals were assigned to the methylene carbons at δ_C 66.5 (C-6) and 101.1 (C-12).

Using 2D NMR (COSY, HMQC and HMBC) the compound was characterised as follows: The long range correlations [3]*J* (Figure 3.26B) of H-12 to the quaternary carbons at δ_C 141.5 and 147.9 indicated they were C-8 and C-9, respectively, while the proton at δ_H 6.74 (H-7) had a [2]*J* correlation to C-8 and [3]*J* correlation to C-9. The doublets at δ_H 6.57 (H-2) and 6.44 (H-4) showed a [3]*J* correlation to the carbon at 112.7 ppm and was assigned C-11b. The protons H-2 and H-4 revealed [2]*J* correlations to the quaternary carbon at δ_C 157.0 which was assigned as C-3.

The HREI-MS data showed pseudo molecular ion [M] [+] at *m/z* 285.1203 which showed that the molecular formula of this compound was $C_{16}H_{12}O_5$. This compound has been previously isolated from the roots of *Sophora flavescens* (Park *et al*, 2003). This is the first report of maackiain from *A. spinosus*.
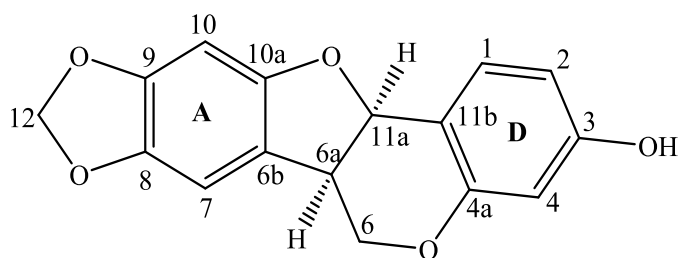
Figure 3.24: Structure of maackiain.

Table 3.8: ^{1}H (400MHz), DEPTq-135 (100MHz) and HMBC data of AS-4 in CDCl$_3$.

Position	^{1}H	^{13}C	HMBC	
			^2J	^3J
1	7.39 (1H, *d*, *J* = 8.4 Hz)	132.1	-	C-11a, C-3,C-4a
2	6.57 (1H, *dd*, *J* = 8.4, 2.5 Hz)	109.8	C-3	C-4, C-11b
3	-	157.0	-	-
4	6.44 (1H, *d*, *J* = 2.5 Hz)	103.7	C-3,C-4a	C-2, C-11b
4a	-	156.5	-	-
6	4.24 (1H, *dd*, *J* = 11.2, 5.0 Hz)	66.5	C-6a	C-11a, C-4a
	3.67 (1H, *dd*, *J* = 11.2, 5.0 Hz)		-	C-11a
6a	3.50 (1H, *ddd*, *J* = 11.2, 6.9, 5.0 Hz)	40.2	C-6b	-
6b	-	117.9	-	-
7	6.74 (1H, *brs*)	104.7	C-8	C-9,C-6a,C-10a
8	-	141.5	-	-
9	-	147.9	-	-
10	6.46 (1H, *brs*)	93.8	C-9,C-10a	C-6b, C-8
10a	-	154.3	-	-
11a	5.49 (1H, *d*, *J* = 6.9 Hz)	78.5	C-11b	C-1,C-6, C-4a
11b	-	112.7	-	-
12	5.92, 5.94 (2x *d*, *J* = 1.4 Hz)	101.3	-	C-8, C-9

A

B
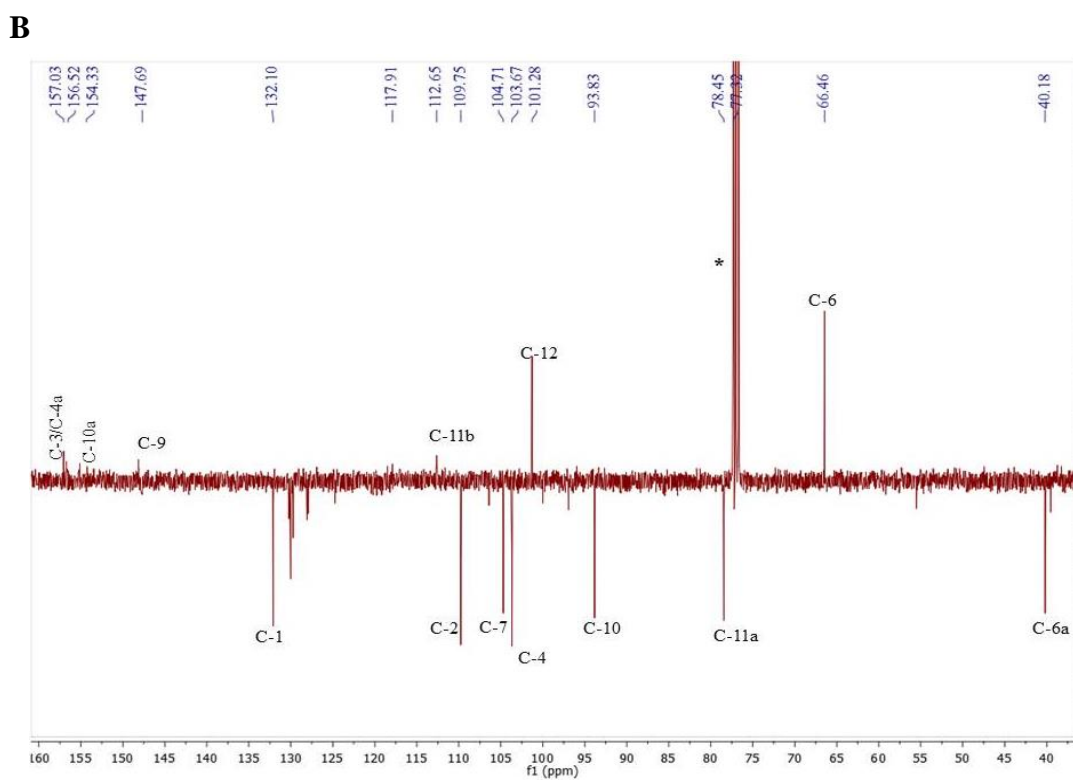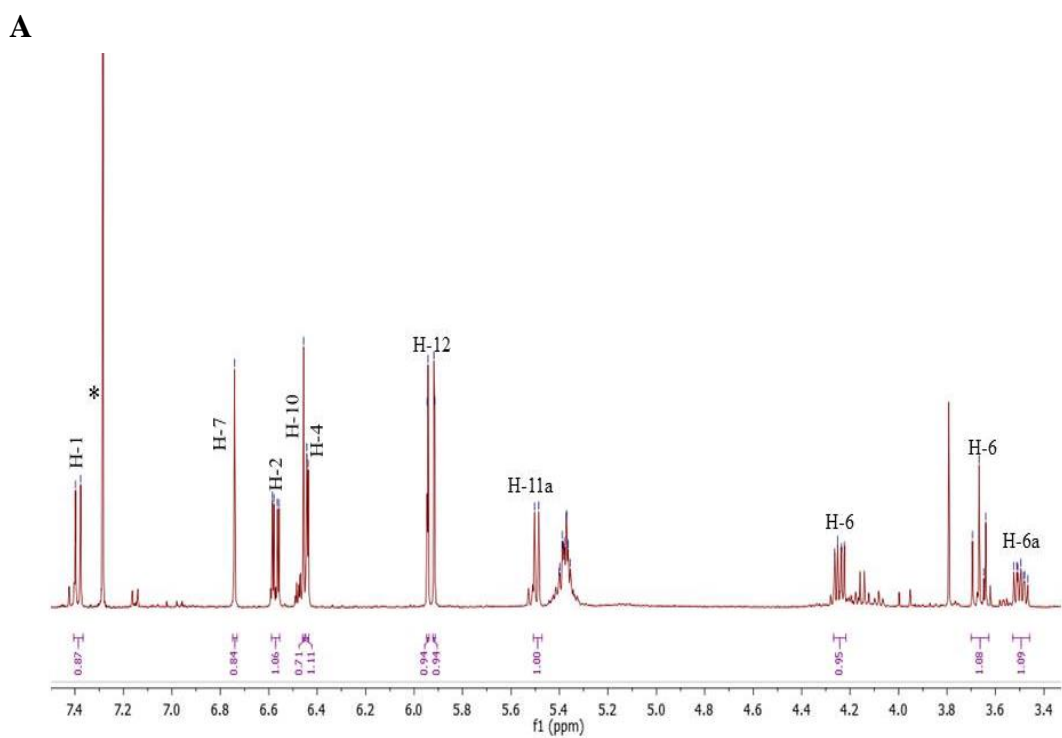
Figure 3.25A: ¹H (400 MHz) and **3.25B:** DEPTq-135 (100 MHz) NMR spectra of AS-4 in CDCl₃*.

A
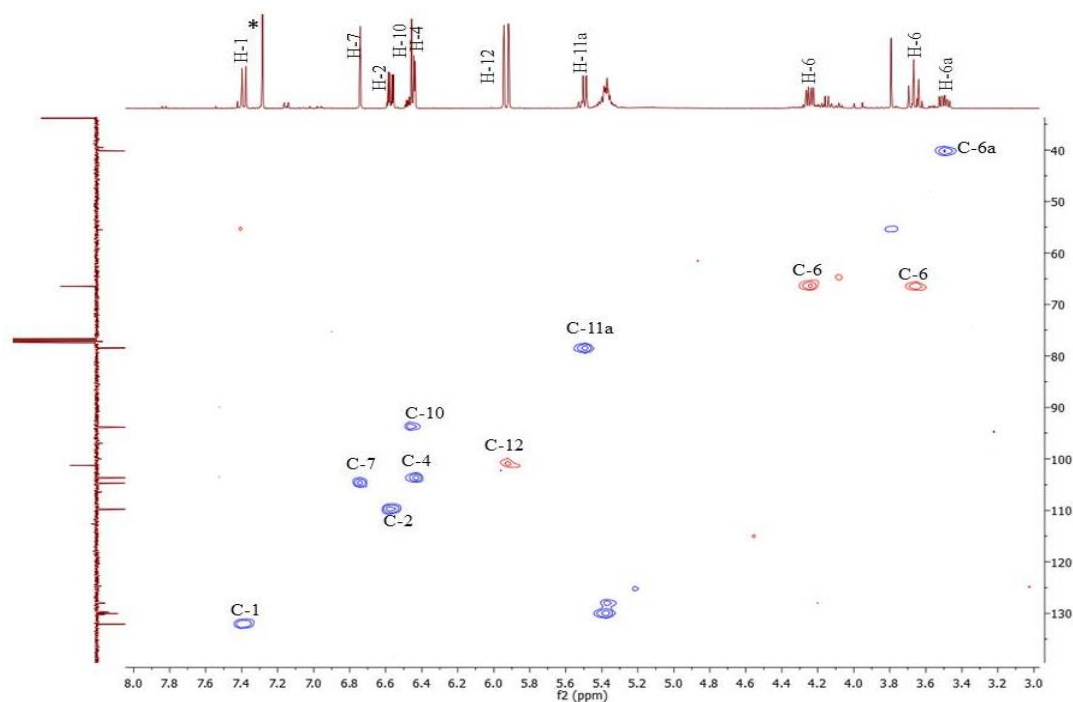
B
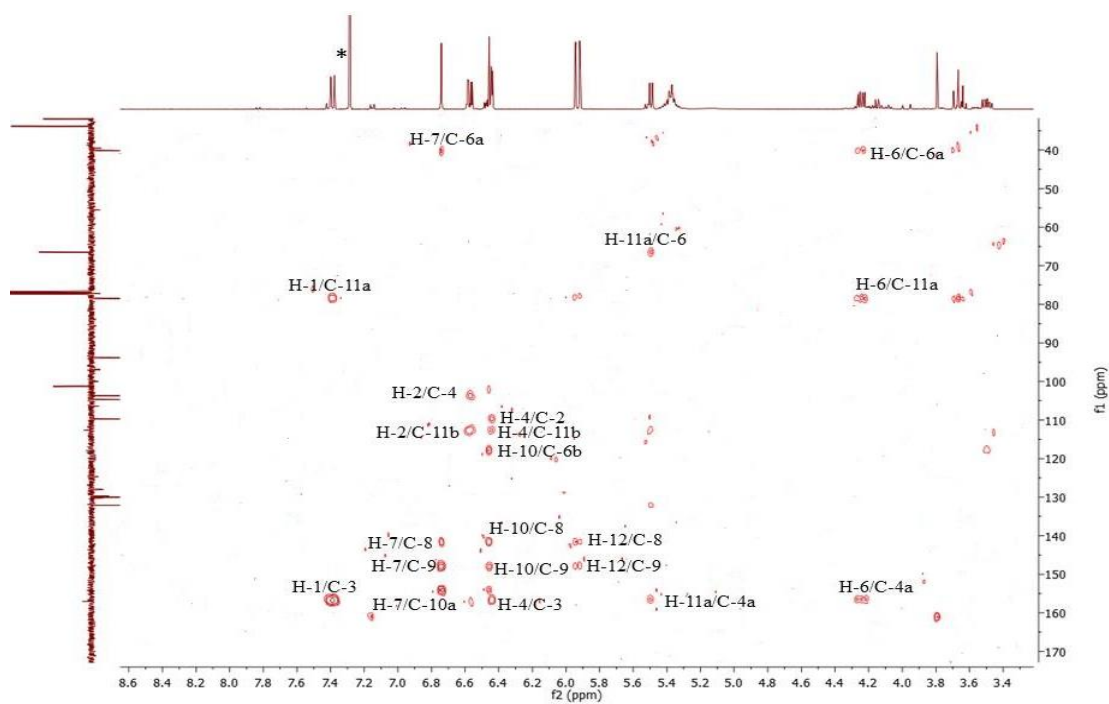
Figure 3.26A: HMQC and **3.26B:** HMBC (400 MHz, CDCl$_3$*) spectra of AS-4.

3.3 Fractionation of *Citrallus colocynthis* Extracts

CC was used to fractionate the hexane (7.6g, 1.68%), the EtOAc (8g, 1.77%) and the methanol extracts (13g, 2.88% w/w) of *C. colocynthis*. The fractions collected were assessed using NMR and enabled elucidation of the structure of one compound designated CC-1 (23mg, 0.28%) from the EtOAc extract. The same compound CC-1 (7.3mg, 0.05%) was also isolated from the methanol extract along with another compound coded CC-2 (3g, 23.07%). Compound CC-2 was further purified using Sephadex column. No single compound was obtained from the fractionation of the hexane extract of *C. colocynthis*.

3.3.1 Characterisation of CC-1 as Cucurbitacin E (Elaterin)

The compound CC-1 (Figure 3.27) was isolated from the EtOAc and from the early fractions of the methanol extract of *C. colocynthis*. It appeared as a yellow spot (R_f = 0.70) after spraying with anisaldehyde-sulphuric acid reagent followed by heating. EtOAc was used as the mobile phase for the TLC.

The ^{1}H NMR spectrum (Figure 3.29A, Table 3.9) indicated the presence of an olefinic proton at δ_H 5.83 (1H, *m*, H-6) and nine methyl singlets at δ_H 0.96 (3H, *d, J*=1.8 Hz, H-18), 0.98 (3H, *s*, H-19), 1.43 (3H, *s,* H-21), 1.57 (3H, *s*, H-26), 1.54 (3H, *s*, H-27), 1.32 (3H, *s,* H-28), 1.27 (3H, *s,* H-29), 1.49 (3H, *d, J*= 1.1Hz, H-30), and 1.98 (3H, *s,* COCH̲₃). The downfield shift of the latter methyl indicated it to be part of an acetyl group.

The DEPTq-135 NMR spectrum (Figure 3.29B, Table 3.9) showed a total of 32 carbon atoms made up of nine methyl carbons at δ_C 19.6 (C-18), 19.4 (C-19), 24.1 (C-21), 25.5 (C-26), 26.1 (C-27), 19.8 (C-28), 27.3 (C-29), 17.7 (C-30), and 21.0 (COC̲H₃). Eleven quaternary carbons were identified including four carbonyl carbons at C-3, C-11, C-22 and C̲OCH₃ were detected at 198.0, 212.6, 202.5, and 169.1 ppm, respectively. Three methylene carbons were observed at δ_C 23.4 (C-7), 48.7 (C-12), 45.8 (C-15). Nine methine carbon signals at δ_C (C-1, C-6, C-8, C-10, C-

16, C-17, C-20, C-23 and C-24) were also obtained. The major HMBC (Figure 3.30B) correlations are summarised in Table 3.10.

The HREI-MS data showed pseudo molecular ion [M]⁻ at *m/z* 555.0210 was observed suggesting the molecular formula of $C_{32}H_{44}O_8$. On the basis of these results and by comparison with previously published data (Seger *et al.*, 2005), CC-1 was identified as cucurbitacin E (elaterin).

3.3.2 Characterisation of CC-2 as Cucurbitacin E-2-*O*-β-D-glucoside

The compound CC-2 (Figure 3.27) was obtained from the methanol extract of *C. colocynthis*. After spraying with *p*-anisaldehyde-sulphuric acid reagent and heating, a brown spot (R_f= 0.32) appeared on the TLC. A 100% EtOAc was used as a mobile phase on TLC.

The ^{1}H and DEPTq-135 NMR spectra (Figure 3.31A and B, Table 3.9) for the compound were identical to CC-1 except for the presence of a glucose moiety instead of hydroxyl group at C-2. The proton spectrum with the aid of a COSY experiment, suggested the presence of a sugar molecule with an anomeric proton at δ_H 4.70 (1H, *d*, *J* = 7.8 Hz, H-1`), methine protons at $\delta_H$ 3.50 (1H, *d*, *J* = 2.7 Hz, H-3`), 3.40 (1H, *m*, H-4`), 3.53 (1H, *s*, H-5`) and an methylene proton at δ_H 3.84, 3.98 (1H, *dd*, J_1 = 11.8 Hz, J_2 = 2.7 Hz, H-6`).

The ^{13}C NMR spectrum (Figure 3.31B, Table 3.9) confirmed the presence of 38 carbon atoms. The anomeric carbon signal was obtained at δ_C 100.1 (1`), four oxymethines at $\delta_C$ 72.9 (2`), 76.7 (3`), 77.0 (4`), 69.6 (5`) and an oxymethylene at $\delta_C$ 61.4 (6`) and these were assigned to the sugar unit. The glycosylation site in CC-2 was identified by HMBC correlations (Figure 3.32B) as the anomeric proton at δ_H 4.70 (H-1`) showed ^3J coupling to the quaternary oxygen-bearing carbon at δ_C 145.4 (C-2), indicating a glycosidic linkage through oxygen to the carbon at position 2 of the aglycone.

The HREI-MS data showed pseudo molecular ion [M] [+] at *m/z* 719.3257 suggesting the molecular formula of $C_{38}H_{54}O_{13}$. The mass spectrum supported the above data since the molecular weight of CC-2 was found to be 162 units higher than CC-1. This extra fragment must be the attached glucose moiety. Thus, CC-2 was identified as cucurbitacin-E-2-*O*-β-D-glucoside. The NMR spectra were in agreement with literature reports and the compound has previously been reported from *C. colocynthis* (Hatam *et al*., 1989).

CC-1: R= H**, CC-2:** R=
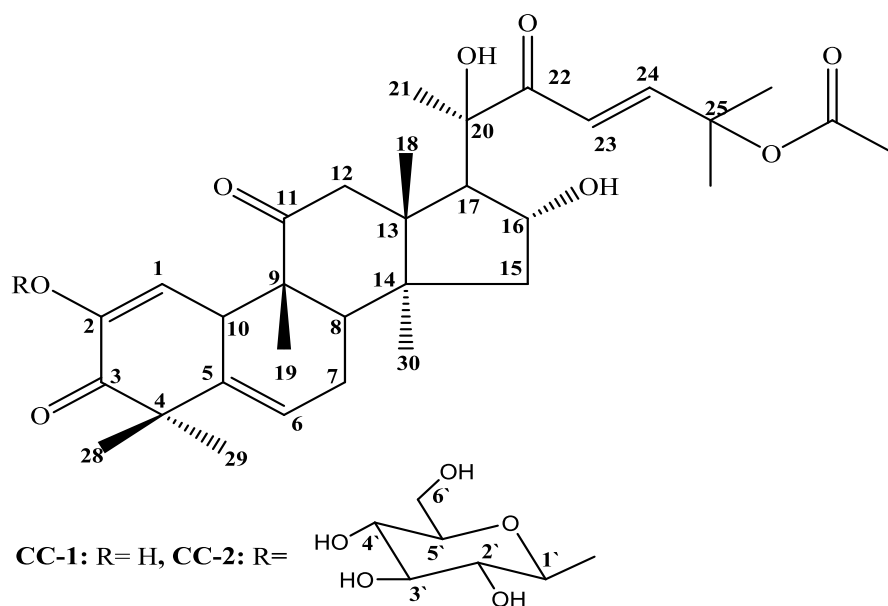
Figure 3.27: Structure of cucurbitacin E (CC-1) and cucurbitacin E -2-*O*-β-D-glucoside (CC-2).
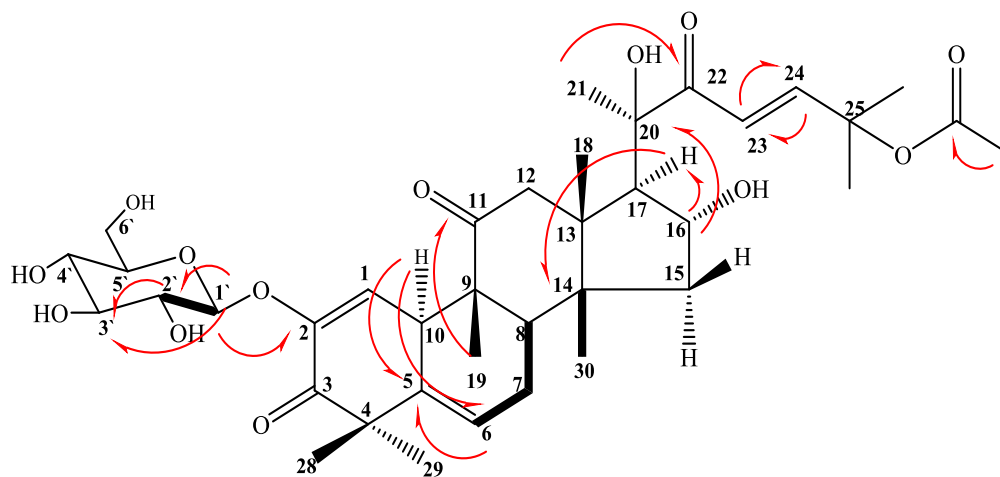
Figure 3.28: Key COSY (▬▬) and HMBC (⌒) correlations observed in CC-1(aglycone) and CC-2

Table 3.9: ^{1}H (400MHz) and DEPTq-135 (100MHz) data of CC-1 (CDCl$_3$) and CC-2 (Acetone-d_6).

Position	CC-1 δ$_H$	CC-1 δ$_C$	CC-2 δ$_H$	CC-2 δ$_C$
1	5.78 (1H, *dd*, J_1 = 2.8 Hz)	114.8	6.11(1H, *d*, J = 2.7 Hz)	124.0
2	-	145.2	-	145.4
3	-	198.0	-	197.5
4	-	49.0	-	48.7
5	-	137.1	-	136.0
6	5.83 (1H, *m*)	120.5	5.84 (1H, *dt*, J_1 = 5.1 Hz, J_2 = 2.5 Hz)	121.0
7	2.41 (1H, *ddt*) 2.08 (1H, *s*)	23.4	2.40 (1H, *m*) 2.09 (1H, *m*)	23.2
8	2.08 (1H, *s*)	41.7	2.09 (1H, *m*)	41.5
9	-	48.9	-	49.1
10	3.67 (1H, *d*, J_1 = 2.6 Hz)	34.4	3.72 (1H, *t*, J = 2.7 Hz)	35.2
11	-	212.6	-	213.8
12	2.57 (1H, *d*, J = 14.6 Hz) 3.40 (1H, *dd*, J_1 = 14.6 Hz, J_2 = 1.5 Hz)	48.7	2.60 (1H, *d*, J = 14.7 Hz) 3.40 (1H, *m*)	48.7
13	-	50.4	-	50.3
14	-	48.0	-	48.0
15	1.50 (1H, *s*) 1.89 (1H, *m*)	45.8	1.50 (1H, *d*, J = 1.1 Hz) 1.90 (1H, *m*)	45.8
16	4.52 (1H, *s*)	70.5	4.55 (1H, *d*, J = 7.1 Hz)	70.4
17	2.69 (1H, *d*, J = 7.1 Hz)	58.1	2.67 (1H, *d*, J = 7.1 Hz)	58.1
18	0.96 (3H, *s*)	19.6	0.95 (3H, *s*)	19.5
19	0.98 (3H, *s*)	19.4	0.99 (3H, *s*)	19.7
20	-	78.6	-	78.6
21	1.43 (3H, *s*)	24.1	1.43 (3H, *s*)	24.2

Table 3.9: (continued).

22	-	202.5	-	202.5
23	6.84 (1H, *d*, *J* = 15.8 Hz)	121.4	6.83 (1H, *d*, *J* = 15.8 Hz)	121.3
24	7.01 (1H, *d*, *J* = 15.8 Hz)	150.1	7.00 (1H, *d*, *J* = 15.8 Hz)	150.1
25	-	79.2	-	79.2
26	1.57 (3H, *s*)	25.5	1.57 (3H, *s*)	25.5
27	1.54 (3H, *s*)	26.1	1.53 (3H, *s*)	26.1
28	1.32 (3H, *s*)	19.8	1.28 (3H, *s*)	19.9
29	1.27 (3H, *s*)	27.3	1.28 (3H, *s*)	26.9
30	1.49 (3H, *s*)	17.7	1.48 (3H, *s*)	17.6
1`	-	-	4.70 (1H, *d*, *J* = 7.8 Hz)	100.1
2`	-	-	3.33 (1H, *s*)	72.9
3`	-	-	3.50 (1H, *d*, *J* = 2.7 Hz)	76.7
4`	-	-	3.40 (1H, *m*)	77.0
5`	-	-	3.53 (1H, *s*)	69.6
6`	-	-	3.84 (1H, *m*) 3.98 (1H, *dd*, J_1 = 11.8 Hz, J_2 = 2.7 Hz)	61.4
2-OH	6.97	-	-	-
<u>C</u>OCH₃	-	169.1	-	169.4
CO<u>CH</u>₃	1.98 (3H, *s*)	21.0	1.98 (3H, *S*)	21.0

Table 3.10: Selected HMBC correlations of CC-2 in CDCl$_3$[*].

Proton	Selected HMBC correlations	
	^2J	^3J
H-1	C-2	C-3, C-5, C-9
H-6	C-5	C-8, C-10, C-4
H-7	C-6	-
H-10	C-1, C-5	C-6
H-12	C-11, C-13	C-9, C-14, C-17, C-18
H-15	C-14, C-16	C-8, C-13, C-30
H-16	C-17	C-20
H-17	C-16	C-14, C-18, C-22
H-18	-	C-14,C-17
H-19	-	C-8, C-10, C-11
H-21	C-20	C-17, C-22
H-23	C-22, C-24	C-25
H-24	C-23, C-25	C-22
H-26	C-25	C-24, C-27
H-27	C-25	C-24, C-26
H-28	C-4	C-3, C-5, C-29
H-29	C-4	C-3, C-5, C-28
H-30	C-14	C-8, C-15, C-13
H-1`	C-2`	C-2, C-3`, C-5`
COC**H**$_3$	**C**OCH$_3$	-

A

B
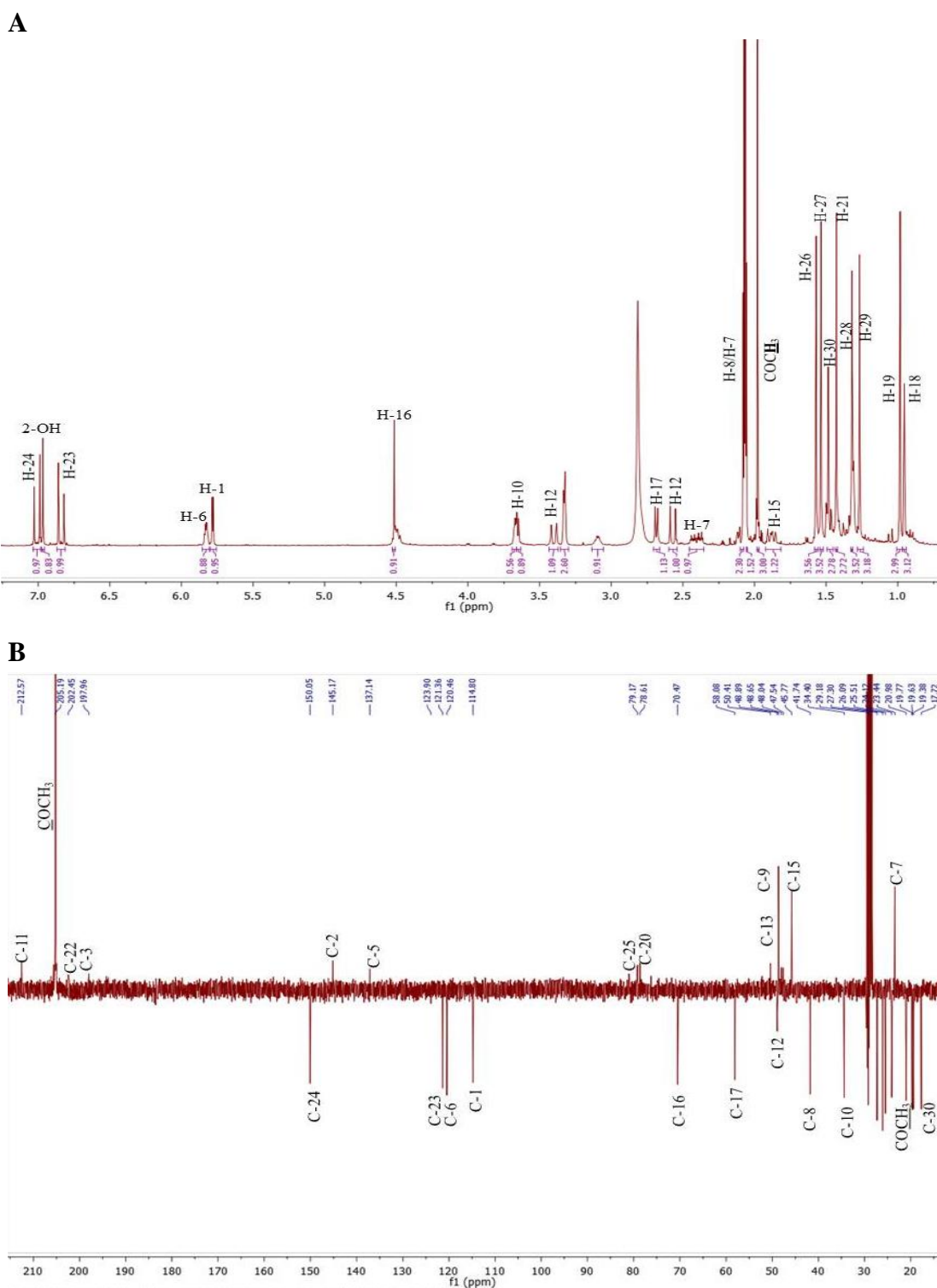
Figure 3.29A: ^{1}H (400 MHz) and **3.29B:** DEPTq-135 (100 MHz) NMR spectra of CC-1 in CDCl$_3$*.

A

B
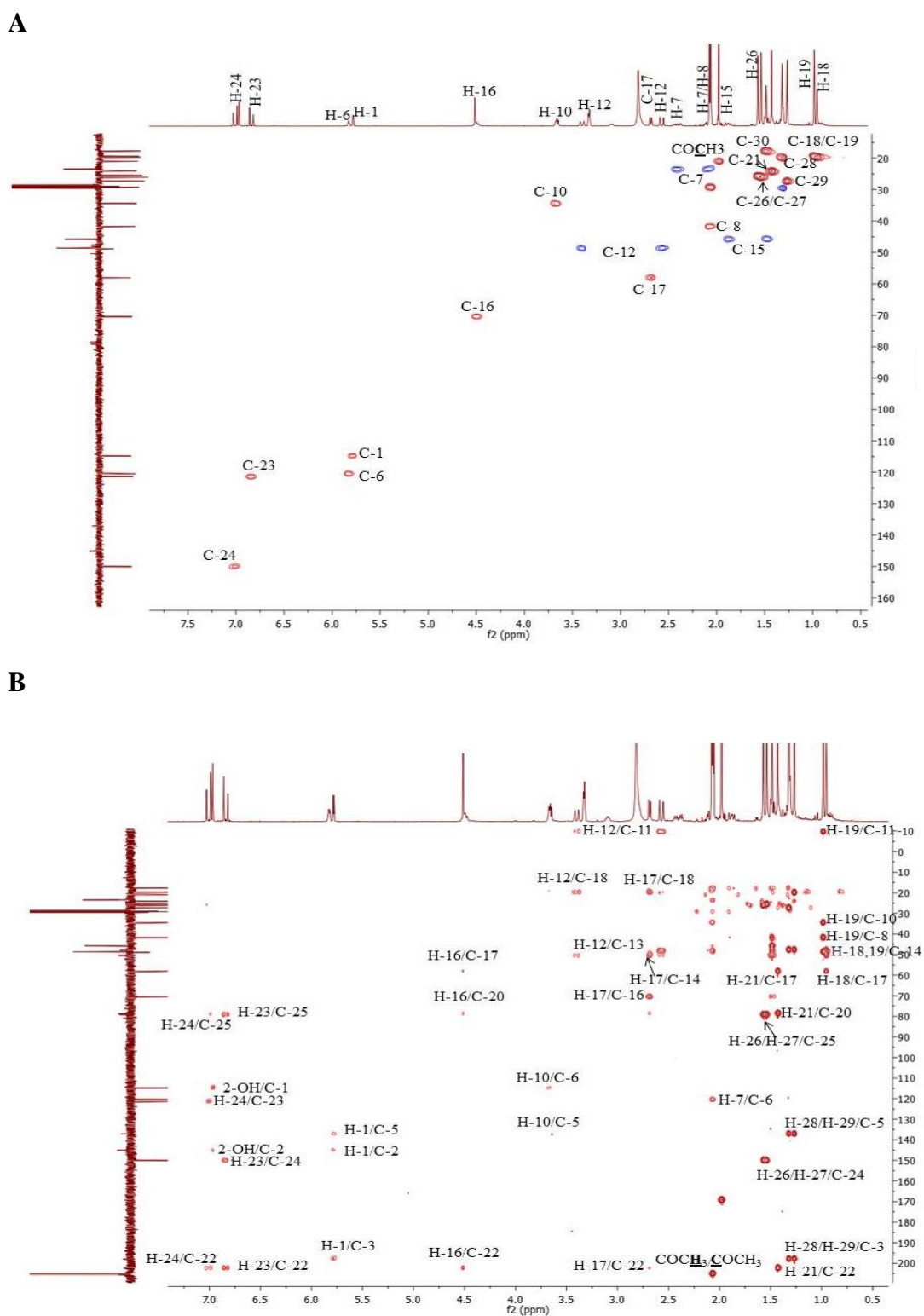
Figure 3.30A: HMQC and **3.30B:** HMBC (400 MHz, CDCl₃*) spectra of CC-1 *C-11 folded to -10 ppm due to smaller window˝F1˝in the down field region of HMBC (B).

133

A

B
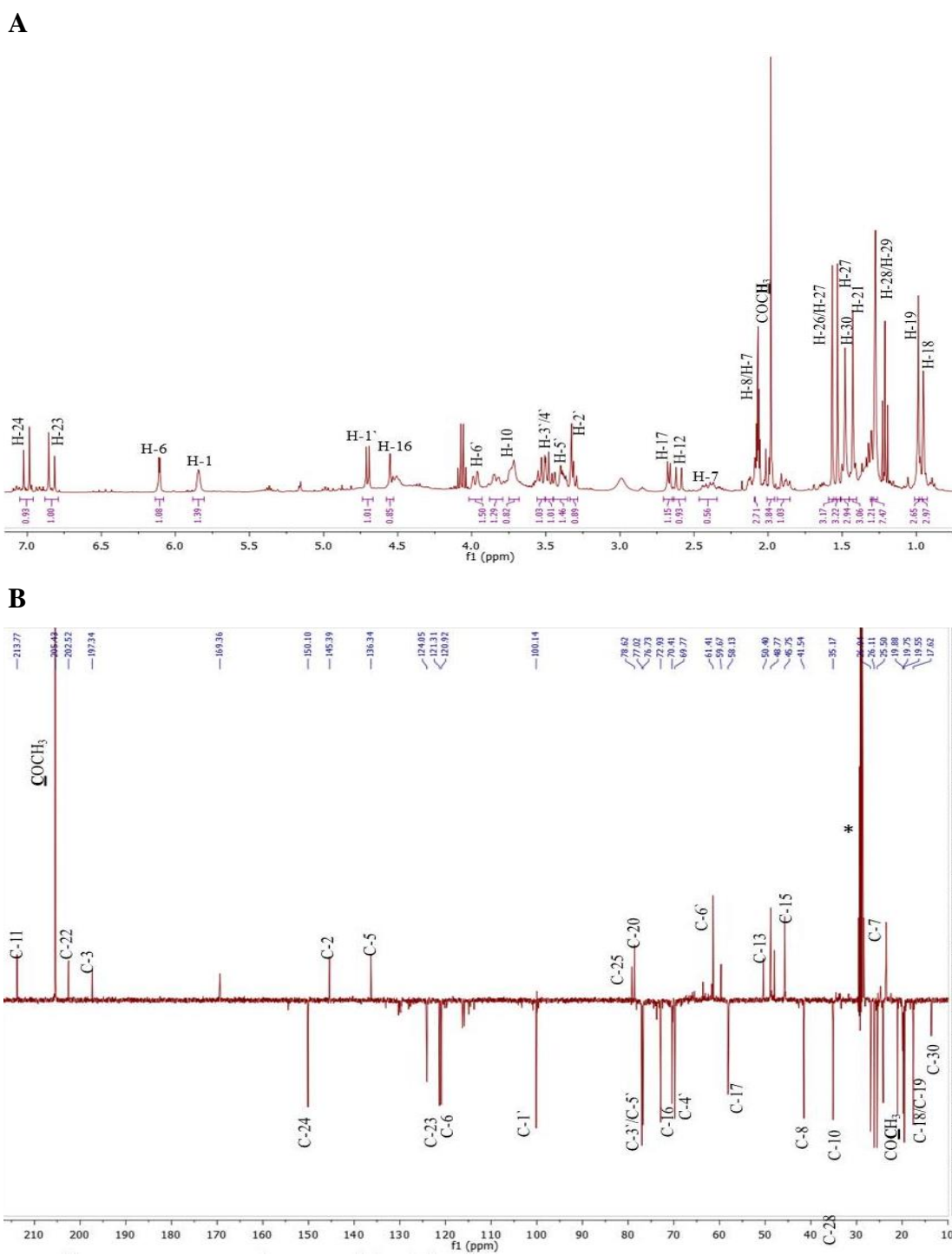
Figure 3.31A: ^{1}H (400 MHz) and **3.31B:** ^{13}C (100 MHz) NMR spectra of CC-2 in Acetone-d_6*.
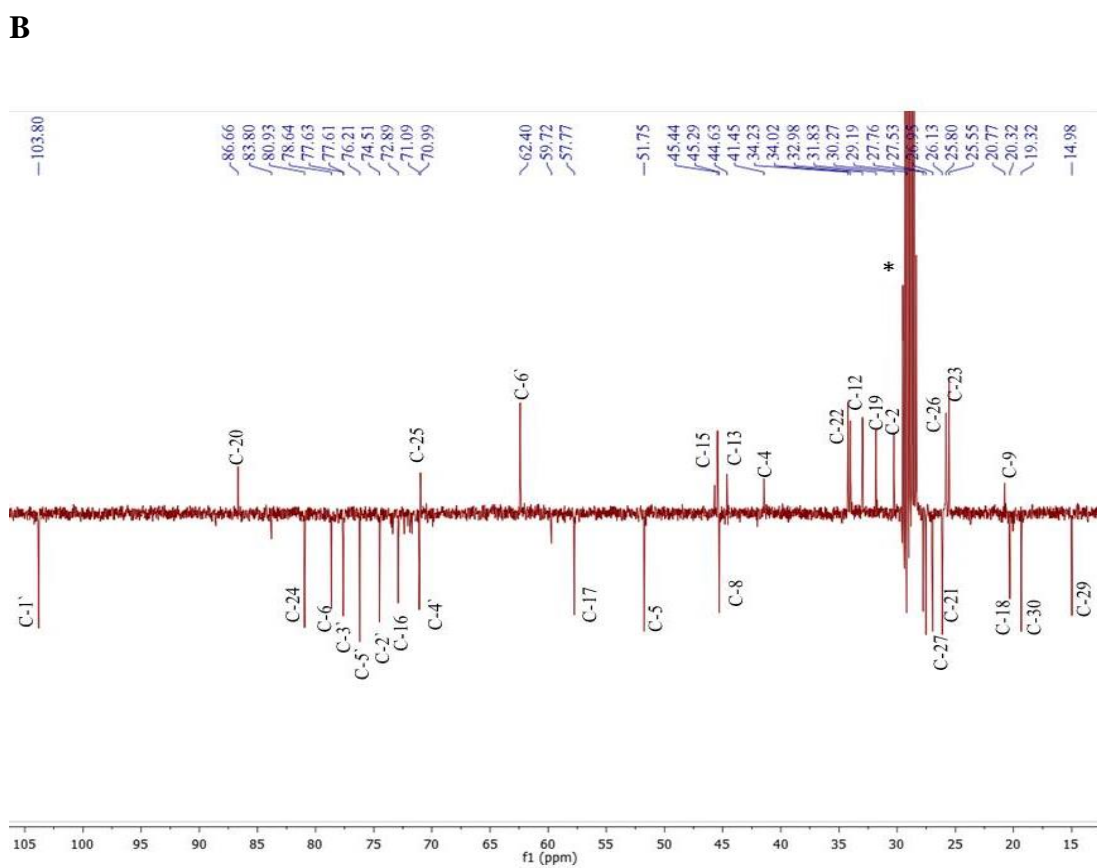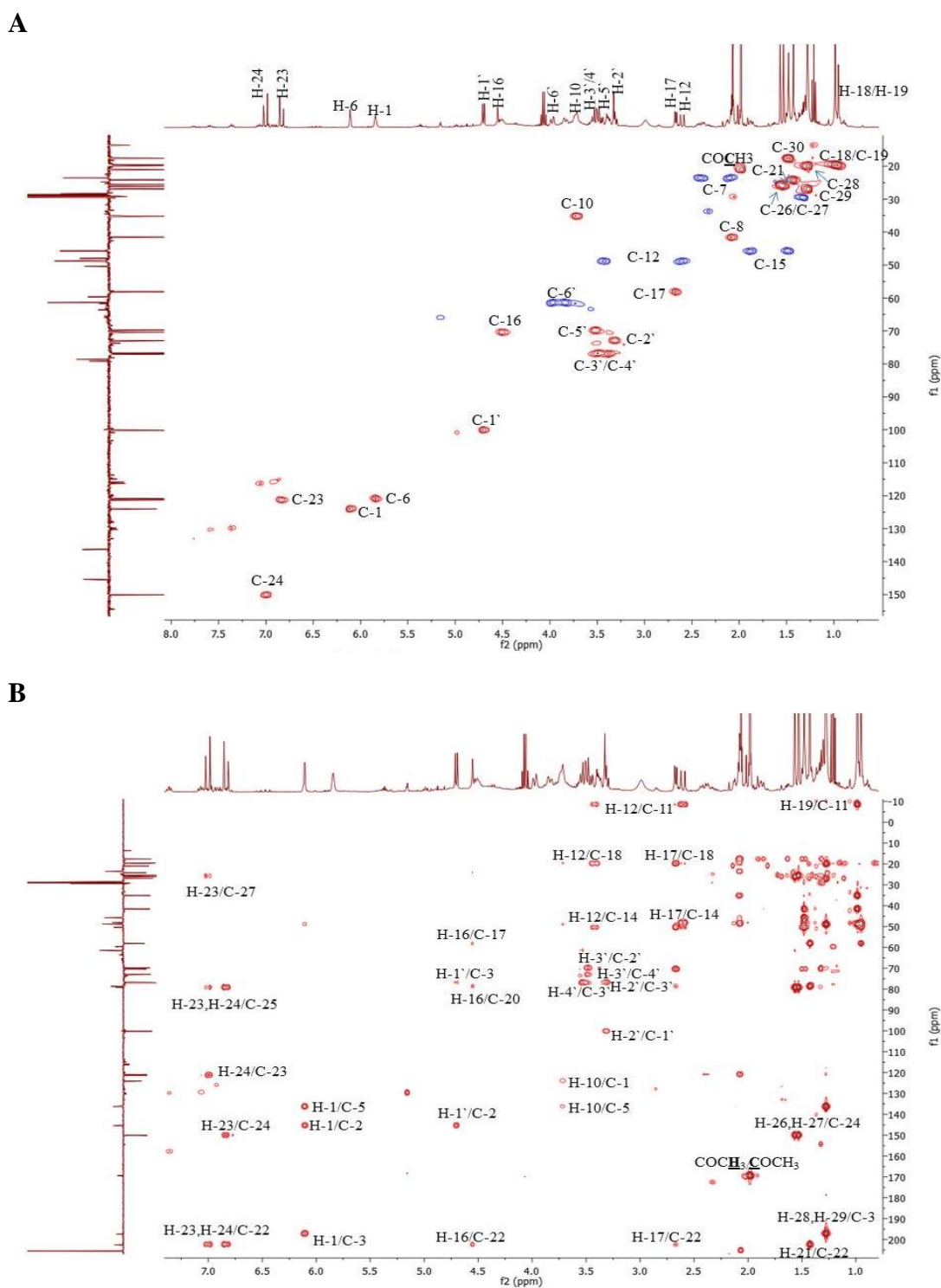
Figure 3.32A: HMQC and **3.32B:** HMBC (400 MHz, Acetone-d_6*) spectra of CC-2
*C-11 folded to -10 ppm due to smaller window″F1`in the down field region of
HMBC (B).

3.4 Fractionation of *Rhanterium epapposum* Extracts

Silica gel CC (Methods Section 2.5.4) was used to fractionate *R. epapposum* hexane extract (8g, 2%), while the EtOAc extract (2g, 0.5%) and the methanol extract (2g, 0.5%) were fractionated using Sephadex column. The collected fractions were examined using NMR and enabled the elucidation of the structure of the following compounds; RE-1 (38mg, 0.47%) from the hexane extract, RE-2 (352mg, 16.25%) and RE-3 (61mg, 3.05) from the EtOAc extract and RE-4 (14mg, 0.7%) from the methanol extract.

3.4.1 Characterisation of RE-1 as 2-hydroxyalantolactone

The compound RE-1 (Figure 3.33) was obtained from the hexane extract of *R. epapposum* leaves using CC. After spraying with *p*-anisaldehyde-sulphuric acid reagent and heating, a yellow spot appeared with R_f value of 0.52 using 100% EtOAc as the mobile phase on TLC.

^{1}H and DEPTq-135 carbon NMR spectra (Figure 3.34, Table 3.11) showed the presence of two methyls at δ_H 1.24 (3H, *s*, H-14) and δ_H 1.16 (3H, *d, J*= 7.7 Hz, H-15), one oxygenated methine at δ_H 4.19 (1H, *m*, H-2), one oxygenated quaternary carbon at δ_C 170.3 and these were evidence of a eudesmanolide type sesquiterpene lactone. The existence of a lactone moiety was confirmed from the protons at δ_H 5.66 (1H, *d, J* = 1.9 Hz, H-13a) and at δ_H 6.23 (1H, *d, J* = 1.9 Hz, H-13b) and one oxygen bearing methine at δ_H 4.83 (1H, *m*, H-8).

The ^{13}C NMR spectra (Table 3.11) displayed 15 signals and confirmed the presence of two methyl groups at δ_C 29.6 (C-14) and 23.4 (C-15); four quaternary carbons, including a carbonyl lactone at δ_C 170.3 (C-12), and an olefinic carbon at δ_C 139.4 (C-11); four methylenes, including one exocyclic olefinic at δ_C 122.2 (C-13); five methines, including an oxygen-bearing carbon at δ_C 75.8 (C-8).

Using 2D NMR (COSY, HMQC and HMBC) the compound was identified as follows: The long range correlation (HMBC, Figure 3.35B, Table 3.11) of the

protons at δ_H 5.66 and 6.23 (H-13) had ^3J correlations to the quaternary carbon at 170.3 ppm which was assigned as C-12. The protons at δ_H 1.50 (H-3), 1.60 (H-9) and 1.24 (H-14) all showed ^3J correlations to the carbon at δ_C 50.3 (C-1). ^2J couplings between the signal at δ_H 1.08 (H-1) and δ_C 63.3 confirmed the assignment of this carbon signal to be C-2. The proton at δ_H 1.24 (H-14) showed ^3J correlations to the carbons at δ_C 146.8 (C-5) and 42.4 (C-9) and correlated via ^2J coupling to the carbon at δ_C 33.6 (C-10).

The HREI-MS data showed pseudo molecular ion [M] $^-$ at *m/z* 247.0080 suggesting a molecular fomula of $C_{15}H_{20}O_3$. Thus RE-1 was identified as 2-hydroxyalantolactone and this is the first report of its isolation from *R. epappsum*. This compound has been previously isolated from *Francoeuria crispa*, family Asteraceae (Al-Yahya *et al*., 1984). All the spectral data were in agreement with those published in the literature (Al-Yahya *et al.*, 1984).
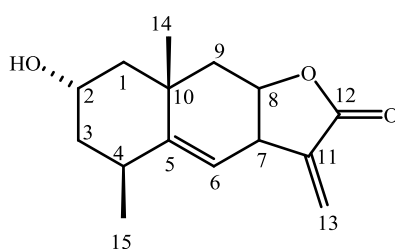
Figure 3.33: Structure of 2-hydroxyalantolactone.

Table 3.11: [1]H (400MHz) and DEPTq-135 (100MHz) data of 2-hydroxyalantolactone in CDCl[3].

Position	[1]H	[13]C	HMBC	
			^2J	^3J
1	1.08 (1H, *d, J* = 3.3 Hz) 1.98 (1H, *m*)	50.3	C-2 C-10	C-3,C-5,C-9 C-14
2	4.19 (1H, *m*)	63.3	-	-
3	1.50 (1H, *dd, J* = 11.9, 6.2 Hz) 1.94 (1H, *dt, J* = 4.4, 2.1 Hz)	41.7	C-2,C-4 C-2	C-1,C-5,C-15 C-1
4	2.66 (1H, *ddd, J* = 8.0, 6.3, 1.9 Hz)	38.5	C-3,C-5,C-15	C-2,C-10,C-6
5	-	146.8	-	-
6	5.25 (1H, *d, J* = 4.1 Hz)	119.7	C-7	C-4,C-8,C-11
7	3.63 (1H, *ddt, J* = 6.3, 3.8, 1.9	39.5	C-11	C-12
8	4.83 (1H, *m*)	75.8	C-7,C-9	C-6,C-10
9	1.60 (1H, *m*) 2.21 (1H, *m*)	42.4	C-10 C-8,C-10	C-1,C-14 C-5,C-7
10	-	33.6	-	-
11	-	139.4	-	-
12	-	170.3	-	-
13	5.66 (1H, *d, J* = 1.9 Hz) 6.23 (1H, *d, J* = 1.9 Hz)	122.2	- C-11	C-7,C-12 C-7,C-12
14	1.24 (3H, *s*)	29.6	C-10	C-1,C-5, C-9
15	1.16 (3H, *d, J* = 7.7 Hz)	23.4	C-4	C-3,C-5

A
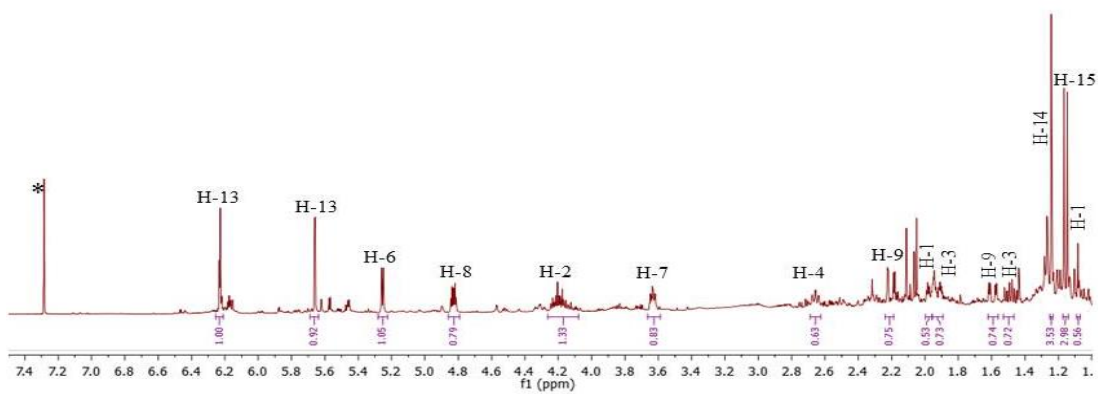
B
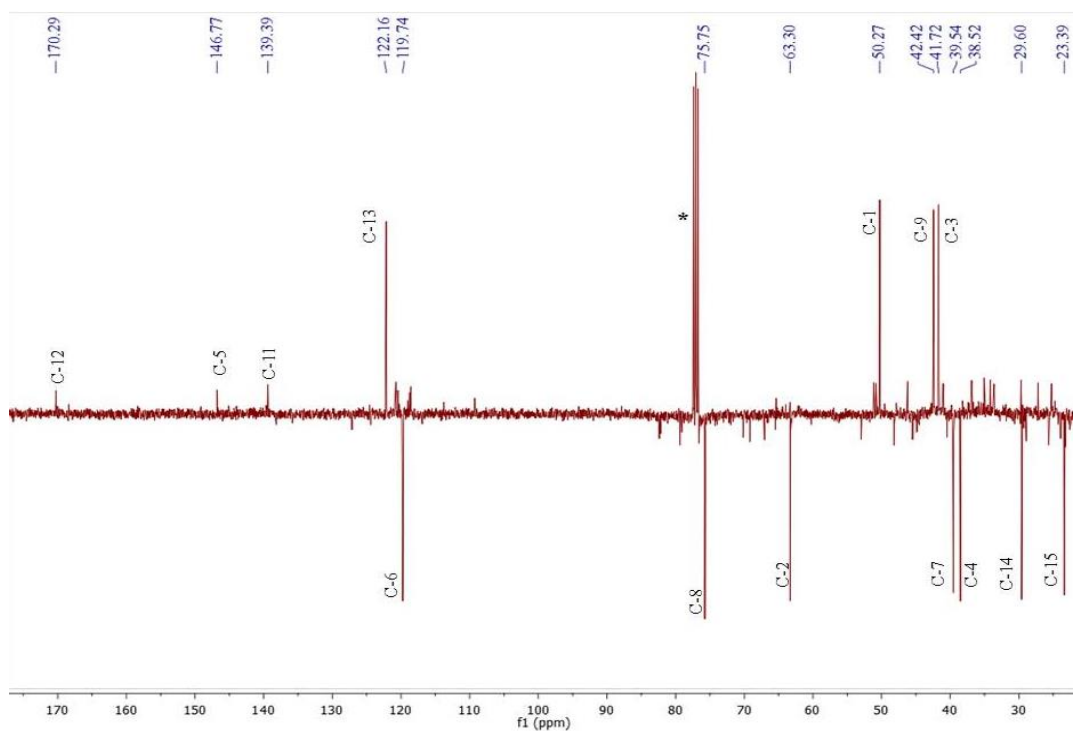
Figure 3.34A: ^1H (400 MHz) and **3.34B:** DEPTq-135 (100 MHz) NMR spectra of RE-1 in $CDCl_3$*.

A
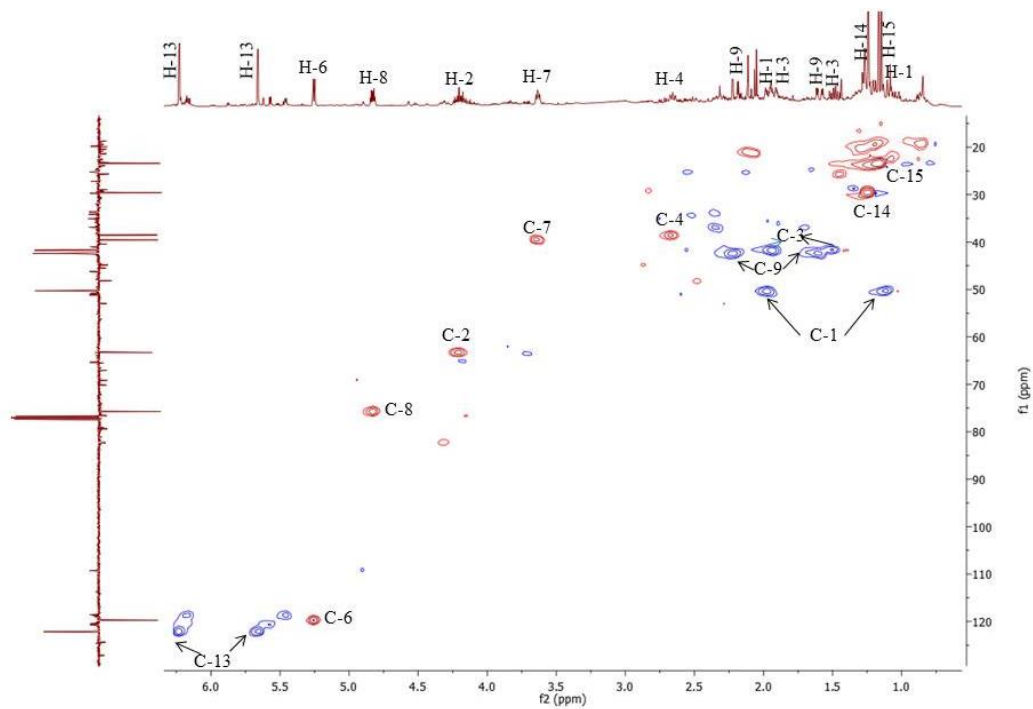
B
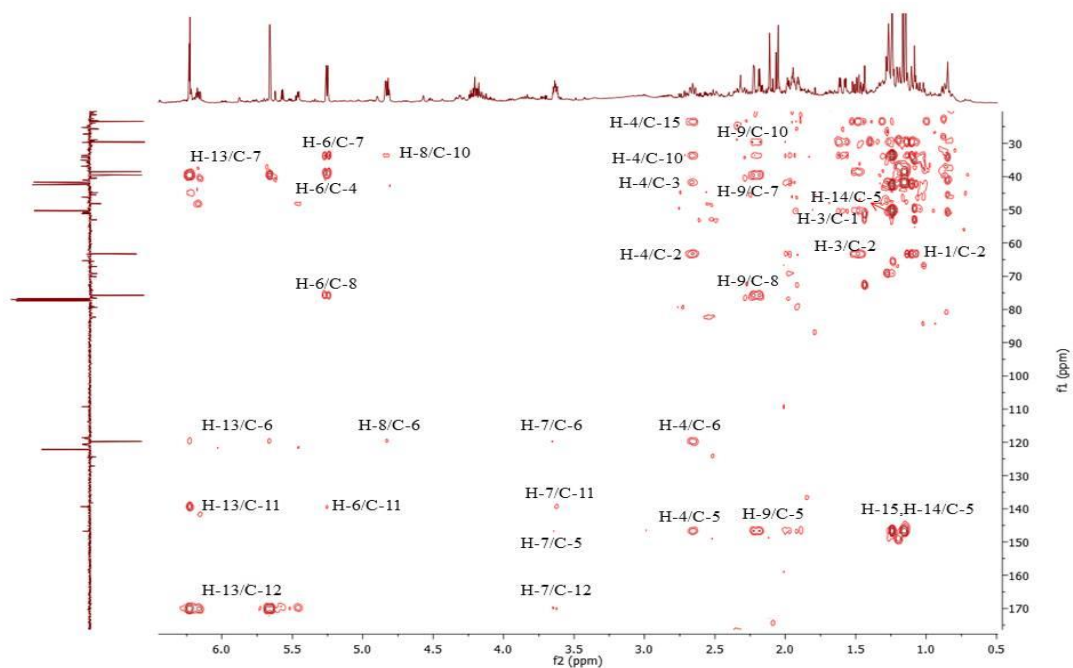
Figure 3.35A: HMQC and **3.35B:** HMBC (400 MHz, CDCl$_3$*) spectra of RE-1.

3.4.2 Characterisation of RE-2 as 5-Caffeoylquinic acid (Chlorogenic acid)

The compound RE-2 (Figure 3.36) was obtained as a dark green solid from the ethyl acetate extract of *R. epapposum* leaves through CC using Sephadex LH-20. After spraying with *p*-anisaldehyde-sulphuric acid reagent and heating, a yellow spot appeared with R_f value of 0.74 on TLC using EtOAc as the mobile phase.

The ^{1}H NMR spectrum (Figure 3.37A, Table 3.12) revealed one quinic acid moiety with three oxymethines at δ_H 3.47 (1H, *dd*, *J* = 9.6, 3.3 Hz, H-3), 3.90 (1H, *d*, *J* = 3.3 Hz, H-4), and 5.16 (1H, *ddd*, *J* = 11.1, 9.6, 5.1 Hz, H-5) and two methylenes at δ_H 1.63 (1H, *dt*, *J* = 14.3, 3.1 Hz), 1.98 (1H, *dd*, *J* = 14.3, 3.1 Hz) (H-2) and 1.78 (1H, *ddd*), 1.84 (1H, *dd*, *J*=12.7, 11.1 Hz) (H-6). One caffeoyl moiety was established with signals at δ_H 7.45 (H-7`), 6.23 (H-8`), 6.98 (H-2`), 7.07 (H-6`) and 6.76 (H-5`).

The DEPTq-135 NMR spectrum (Figure 3.37B, Table 3.12) showed sixteen carbon atoms made up of seven carbon atoms of the quinic acid moiety and nine carbons for the caffeoyl moiety. The quinic acid moiety showed two methylene carbons, C-2 and C-6 at 38.5 and 40.4 ppm respectively and three oxymethine carbons (C-1, C-3, C-4 and C-5) as well as quaternary carbon at 75.6 ppm along with carboxyl signal (C-7) at 176.7 ppm. The caffeoyl moiety includes a carbonyl at δ_C 166.8 (C-9`) and five methine carbons at 121.7, 116.3, 115.2, 145.1 and 115.0 ppm (C-2`, C-5`, C-6`, C-7` and C-8`, respectively). Three quaternary carbons were observed at 126.0, 146.1 and 148.9 ppm (C-1`, C-3` and C-4`).

Using 2D NMR (HMQC and HMBC) the compound was elucidated as follows: The long range correlation (HMBC, Figure 3.38B) of the proton at δ_H 7.07 (H-6`) showed $^3J$ correlations to the carbons at $\delta_C$ 121.7 (C-2`), 148.9 (C-4`) and 145.1 (C-7`) while the proton at δ_H 6.98 (H-2`) showed $^2J$ correlation to $\delta_C$ 146.1 (C-3`) and ^3J correlation to δ_C 148.9 (C-4`) in the aromatic ring. The proton at $\delta_H$ 6.23 (H-8`) had a ^2J correlation to δ_C 166.8 which was assigned as carboxylic acid carbon C-9`. The protons at $\delta_H$ 6.23 (H-8`) and at δ_H 6.76 (H-5`) showed $^3J$ correlation to the carbon at $\delta_C$ 126.0 while the proton at $\delta_H$ 7.45 (H-7`) had a ^2J correlation to δ_C 126.0 which

was assigned as C-1` in the aromatic ring. In the quinic acid moiety, the proton at δ_H 3.90 (H-4) showed ^3J correlations to methylene carbon at δ_C 38.5 (C-2), and ^2J correlations to the oxymethines at δ_C 72.1 (C-5) and δ_C 73.6 (C-3). The methylene protons at δ_H 1.63/1.98 (H-2a/b) and δ_H 1.78/1.84 (H-6a/b) displayed a ^2J correlation to the carbon at δ_C 75.6 (C-1). The proton signal (H-2b) had ^3J correlation to the carbonyl at δ_C 176.7 (C-7). The deshielded proton at δ_H 5.16 (H-5) correlated via ^2J coupling to C-6 at δ_C 40.4 and ^3J coupling to carbon at δ_C 73.6 (C-3). H-5 showed a ^3J correlation to the caffeoyl carbonyl at δ_C 166.8 (C-9`), confirming the presence of one caffeic acid unit in RE-2.

The HREI-MS data showed pseudo molecular ion [M] $^-$ at *m/z* 353.0885 which showed that the molecular formula of this compound was $C_{16}H_{18}O_9$. The ^1H &^{13}C NMR spectral data are in agreement with those reported earlier (Amin *et al*., 2013). This is the first report of 5-caffeoylquinic acid from *R. epapposum*.
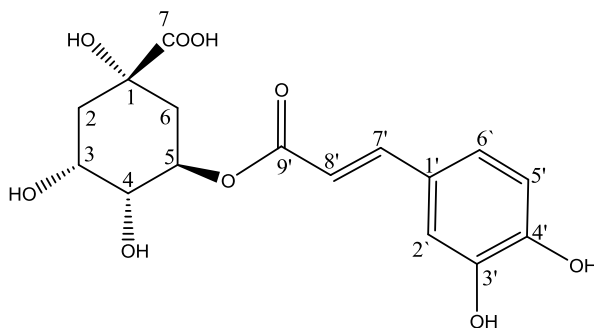
Figure 3.36: Structure of 5-caffeoylquinic acid.

Table 3.12: [1]H (400MHz), DEPTq-135 (100MHz), HMBC data of chlorogenic acid in DMSO-d_6.

Position	[1]H	[13]C	HMBC [2]J	HMBC [3]J
1	-	75.6	-	-
2	1.63 (1H, *dt*, *J* = 14.3, 3.3 Hz) 1.98 (1H, *dd*, *J* = 14.3, 3.1 Hz)	38.5	C-1 C-1	C-7 C-7
3	3.47 (1H, *dd*, *J* = 9.6, 3.1 Hz)	73.6	C-4	-
4	3.90 (1H, *d*, *J* = 3.3 Hz)	71.7	C-3,C-5	C-2
5	5.16 (1H, *ddd*, *J* = 11.1, 9.6, 5.1 Hz)	72.1	C-6	C-3,C-9`
6	1.78 (1H, *ddd*, *J* = 12.7, 5.1, 2.6 Hz) 1.84 (1H, *dd*, *J* = 12.7, 11.1 Hz)	40.4	C-1 C-1	C-2,C-4 C-2,C-4
7	-	176.7	-	-
1`	-	126.0	-	-
2`	6.98 (1H, *dd*, *J* = 8.2, 2.1 Hz)	121.7	C-3`	C-4`,C-6`
3`	-	146.1	-	-
4`	-	148.9	-	-
5`	6.76 (1H, *d*, *J* = 8.2 Hz)	116.3	C-4`,C-6`	C-1`,C-3`
6`	7.07 (1H, *d*, *J* = 2.1 Hz)	115.2	-	C-2`,C-4`,C-7`
7`	7.45 (1H, *d*, *J* = 15.8 Hz)	145.1	C-1`,C-8`	C-6`,C-9`
8`	6.23 (1H, *d*, *J* = 15.8 Hz)	115.0	C-9`	C-1`
9`	-	166.8	-	-

A
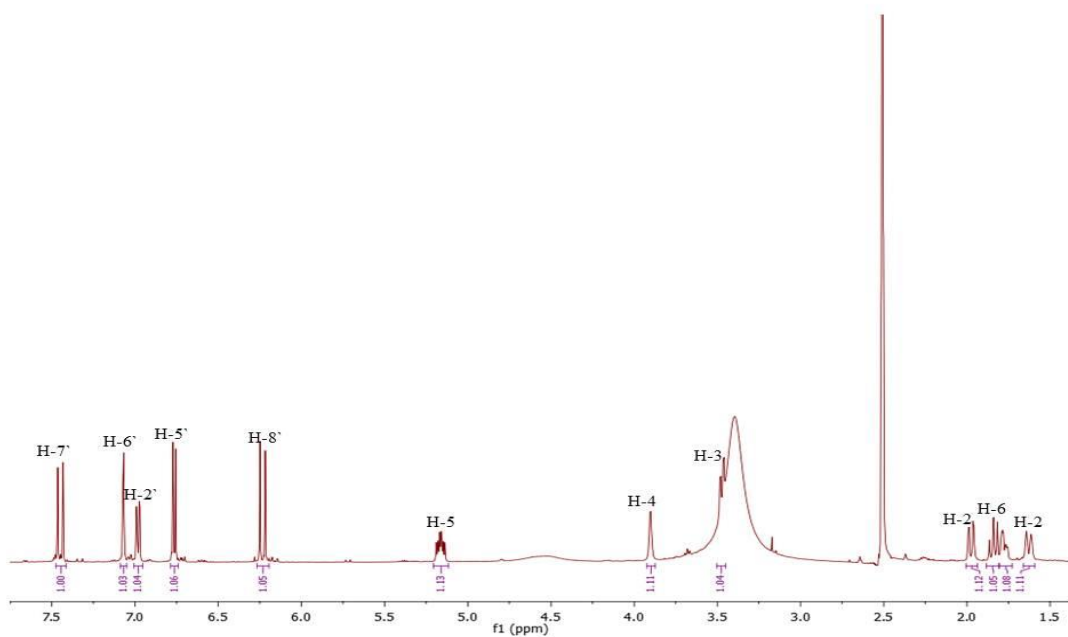
B
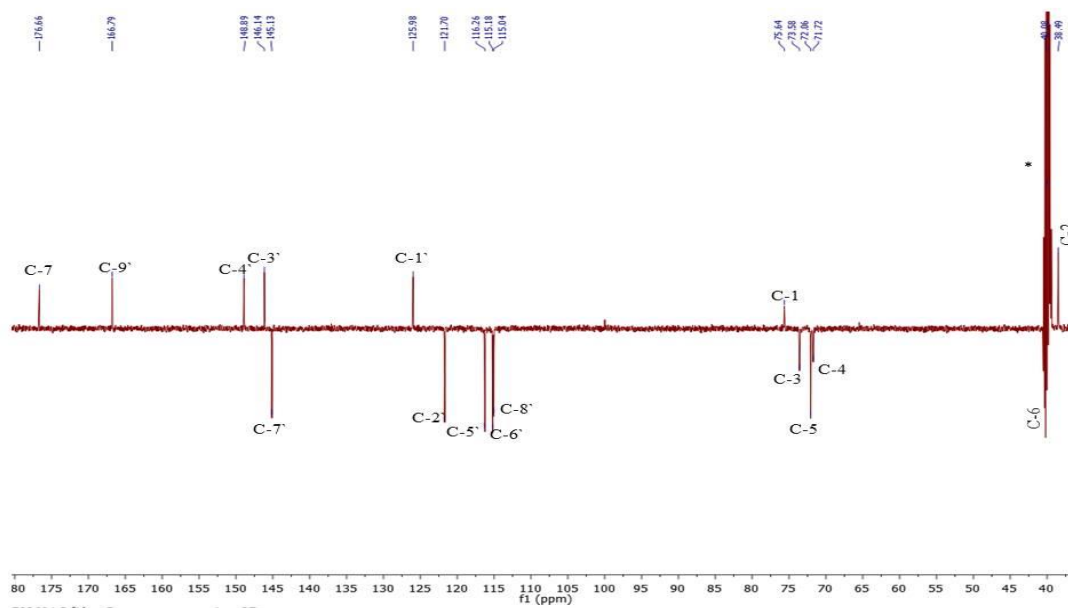
Figure 3.37A: ^{1}H (400 MHz) and **3.37B:** DEPTq-135 (100 MHz) NMR spectra of RE-2 in DMSO-d_6*.
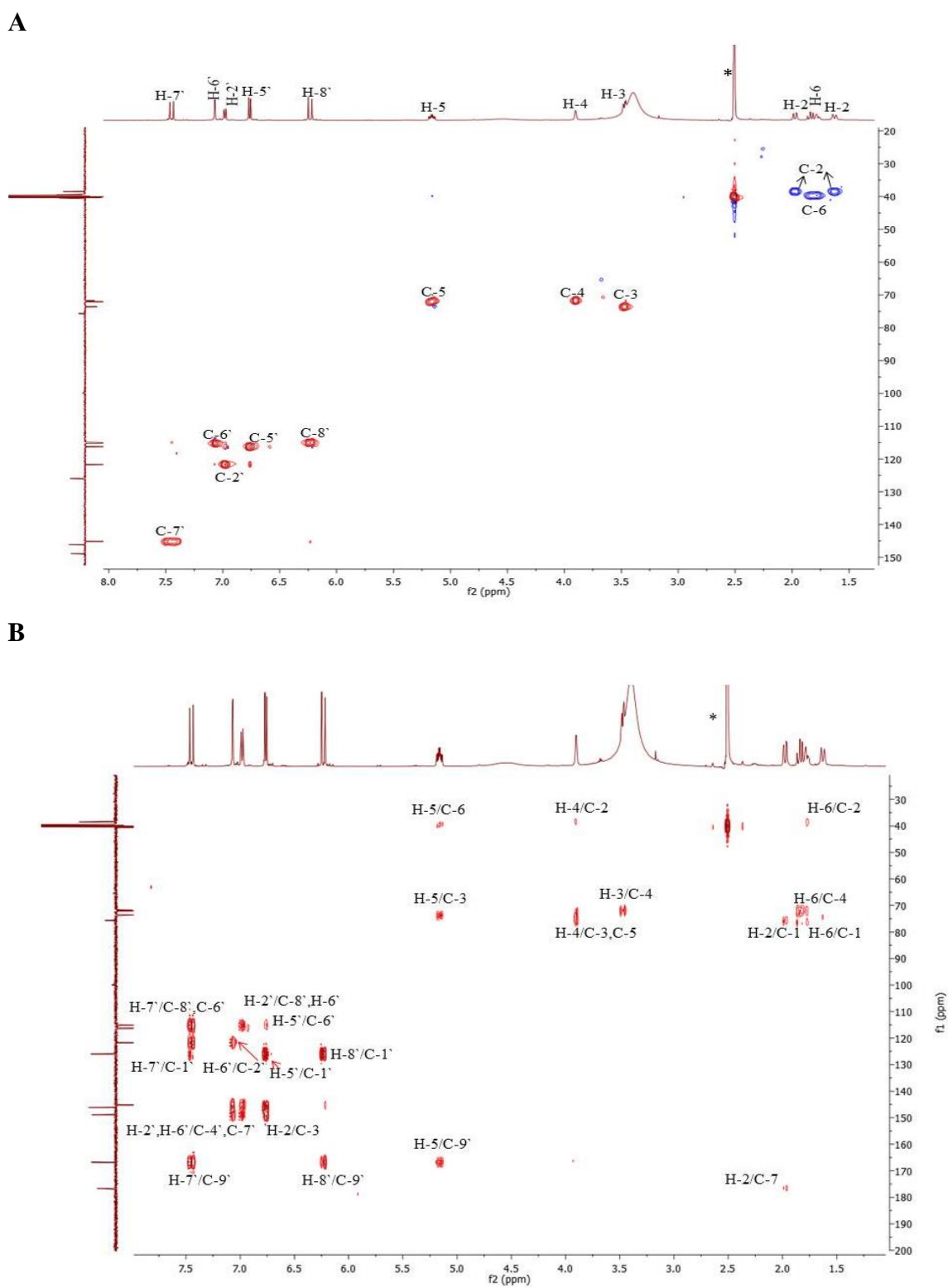
Figure 3.38A: HMQC and **3.38B:** HMBC (400 MHz, DMSO-*d₆**) spectra of RE-2.

3.4.3 Characterisation of RE-3 as 3, 4-dicaffeoylquinic acid

The compound RE-3 (Figure 3.39) was isolated from the methanol extract of *R. epapposum* as a brown amorphous solid. TLC analysis revealed a brown spot (R_f= 0.61) after spraying with anisaldehyde-sulphuric acid reagent followed by heating. 30% MeOH in EtOAc was used as mobile phase on TLC.

The ^{1}H NMR spectrum (Table 3.13, Figure 3.40A) showed one quinic acid moiety with three oxymethines at δ_H 5.52 (1H, *m*, H-3), 4.91 (1H, *dd*, *J* = 10.2, 2.9 Hz, H-4), and 4.12 (1H, *q*, *J* = 3.2 Hz, H-5), and two methylenes at δ_H 1.68 (1H, *dt*, *J* = 14.4, 3.2 Hz), 2.08 (1H, *m*) (H-2) and 1.88 (1H, *ddd*), 2.00 (1H, *d*, *J*= 12.1 Hz) (H-6). Two caffeoyl groups were established with signals at δ_H 7.42 (H-7`), δ 7.45 (H-7"), 6.23 (H-8`), 6.17 (H-8``), 7.02 (H-2`), 7.01 (H-2``), 6.96 (H-6`), 6.92 (H-6``), 6.72 (H-5`/H-5``).

The DEPTq-135 NMR spectrum (Table 3.13, Figure 3.40B) showed 25 carbons in total. Some distinctive signals from caffeoyl groups included two carbonyls at δ_C 166.7 (C-9") and 166.5 (C-9`), four olefinic carbons at $\delta_C$ 145.9 (C-7`), 145.8 (C-7"), 114.1 (C-8`) 114.2 (C-8") and six aromatic carbons at $\delta_C$ 121.8 (C-6`/C-6"), 115.3 (C-5`/5"), 116.3 (C-2`/C-2"). Three oxymethines at δ_C 68.7 (C-3), 76.4 (C-4) and 69.3 (C-5), two methylenes at δ_C 38.4 (C-2) and 40.3 (C-6) and one carbonyl at δ_C 176.2 (C-7) were also observed.

In the HMBC spectrum (Table 3.13, Figure 3.41B), the proton at δ_H 4.91 (H-4) showed ^2J correlation to carbons at δ_C 68.7 (C-3) and ^3J correlation to carbons at δ_C 40.3 (C-6) and 166.7 (9``). Protons at δ_H 1.68 (H-2) and 1.88, 2.00 (H-6) both correlated via ^2J couplings to the quaternary carbon at δ_C 75.4 (C-1). Two protons at δ_H 5.52 (H-3) and 4.12 (H-5) showed ^2J correlations to one oxymethine at δ_C 76.4 (C-4). The olefinic proton at δ_H 7.42 (H-7`) displayed a $^3J$ correlation to carbons at $\delta_C$ 121.8 (C-6`), δ166.5 (C-9`) and $^2J$ correlation to the carbonyl at $\delta_C$ 125.7 (C-1`). The olefinic proton at δ_H 6.22 (H-8`) showed a $^3J$ coupling to the quaternary carbon at $\delta_C$ 125.7 (C-1`). Proton at δ_H 7.42 (H-7`) correlated via ^2J coupling to carbon at δ_C

125.7 (C-1`), $^3J$ couplings to carbons at $\delta_C$ 115.3 (C-5`), 121.8 (C-6`) and the carbonyl at $\delta_C$ 166.5 (C-9`). Similarly, proton at δ_H 7.45 (H-7") correlated via ^2J coupling to carbon at δ_C 125.7 (C-1"), ^3J couplings to carbons at δ_C 115.3 (C-5"), 121.8 (C-6") and the carbonyl at δ_C 166.7 (C-9"). Protons at δ_H 6.92 (H-6") and 7.01 (H-2") both showed ^3J correlations to the carbon at δ_C 149.1 (C-4"). Other two important correlations observed were that the proton at δ_H 5.52 (H-3) showed a ^3J coupling to one caffeoyl carbonyl at δ_C 166.5 (C-9`) and the proton at δ_H 4.91 (H-4) correlated via a ^3J coupling to the other caffeoyl carbonyl at δ_C 166.7 (C-9"). This further confirmed that both hydroxyl groups at position 3 and 4 of the quinic acid moiety were esterified with caffeic acid units.

The HREI-MS data showed pseudo molecular ion [M] $^-$ at m/z 515.1199 which showed that the molecular formula of this compound was $C_{25}H_{24}O_{12}$. The above data led to the identification of RE-3 as 3, 4-dicaffeoylquinic acid in agreement with previous reports (Corse *et al.*, 1965). This is the first report of this compound from *R. epapposum*.
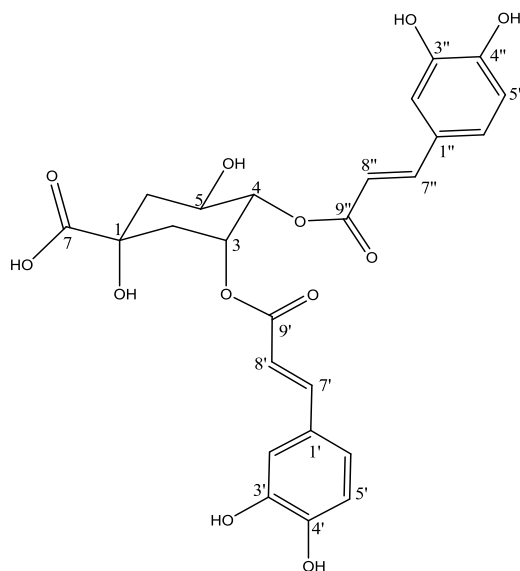
Figure 3.39: Structure of 3, 4-dicaffeoylquinic acid.

Table 3.13: [1]H (400MHz), DEPTq-135 (100MHz), HMBC data of 3, 4-dicaffeoylquinic in DMSO-d_6.

Position	[1]H	[13]C	HMBC [2]J	HMBC [3]J
1	-	75.4	-	-
2	1.68 (1H, *dt*, *J* = 14.4, 3.2 Hz) 2.08 (1H, *m*)	38.4	C-1, C-3	C-6
3	5.52 (1H, *m*)	68.7	C-4, C-2	C-9`
4	4.91(1H, *dd*, *J* = 10.2, 2.9 Hz)	76.4	C-3	C-6,C-9``
5	4.12 (1H, *q*, *J* = 3.2 Hz)	69.3	C-4	C-1,C-3
6	1.88 (1H, *ddd*, *J* =12.8,5.3, 2.7 Hz) 2.00 (1H, *d*, *J* = 12.1 Hz)	40.3	C-1, C-5 C-1, C-5	C-2 -
7	-	176.2	-	-
1`	-	125.7	-	-
2`	7.02 (1H, *s*)	116.3	C-3`	C-6`
3`	-	145.8	-	-
4`	-	149.1	-	-
5`	6.72 (2H, *dd*, *J* = 8.2, 7.1Hz)	115.3	C-4`	C-1`
6`	6.96 (1H, *m*)	121.8	C-1`, C-5`	C-4`, C-7`
7`	7.42 (1H, *d*, *J* = 16.1Hz)	145.9	C-1`	C-6`, C-9`
8`	6.23 (1H, *dd*, *J* = 16.1, 1.8 Hz)	114.1	C-9`	C-1`
9`	-	166.5	-	-
1"	-	125.7	-	-
2"	7.01 (1H, *s*)	116.3	C-3``	C-4``, C-6``
3"	-	146.1	-	-
4"	-	149.1	-	-
5"	6.72 (2H, *dd*, *J* = 8.2, 7.1 Hz)	115.3	C-4``	C-1``
6"	6.92 (1H, *d*, *J* = 2.1 Hz)	121.8	C-1``,C-5``	C-4``, C-7``
7"	7.45 (1H, *d*, *J* = 15.9 Hz)	145.8	C-1``	C-6``,C-9``
8"	6.17 (1H, *d*, *J* = 15.9 Hz)	114.2	C-9``	C-1``
9"	-	166.7	-	-

A
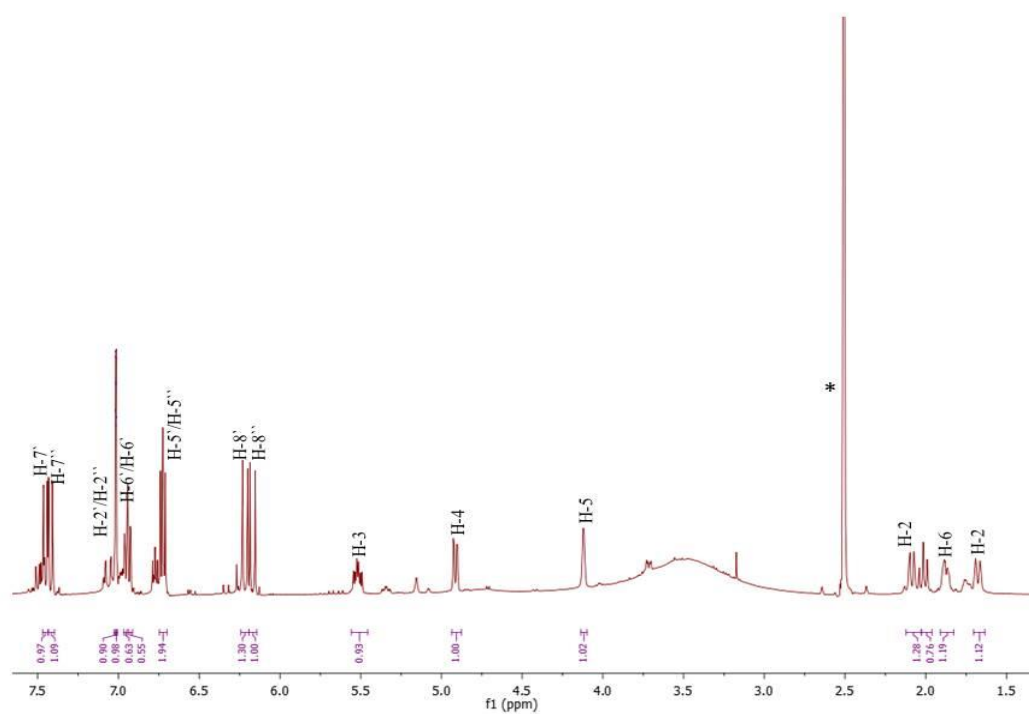
B
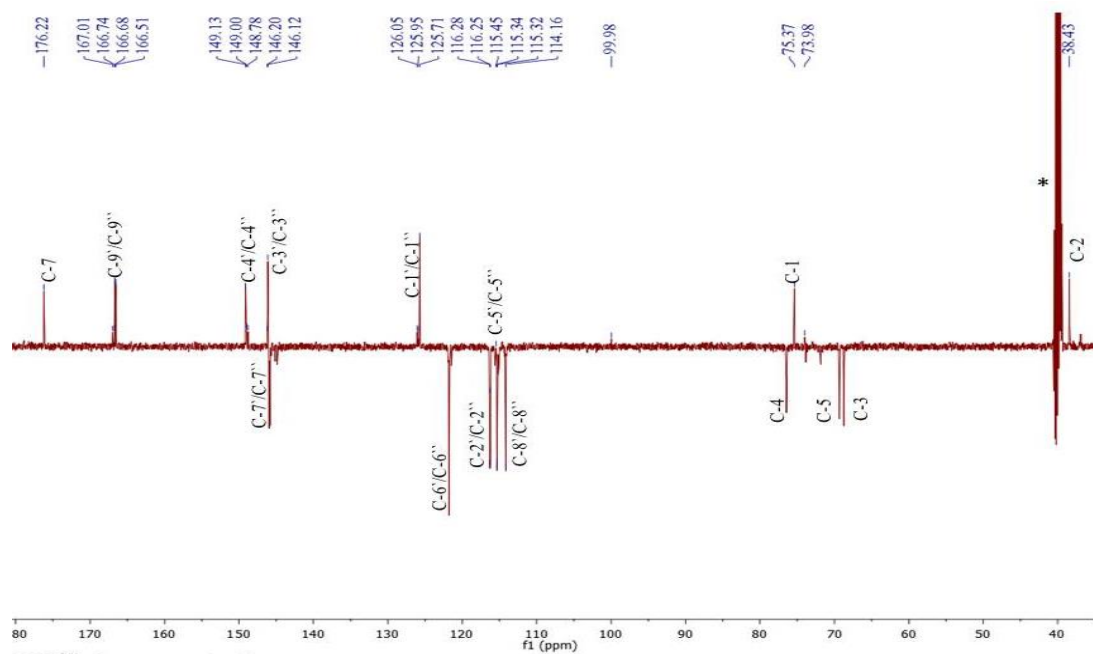
Figure 3.40A: ^{1}H (400 MHz) and **3.40B:** DEPTq-135 (100 MHz) NMR spectra of RE-3 in DMSO-d_6*.

A
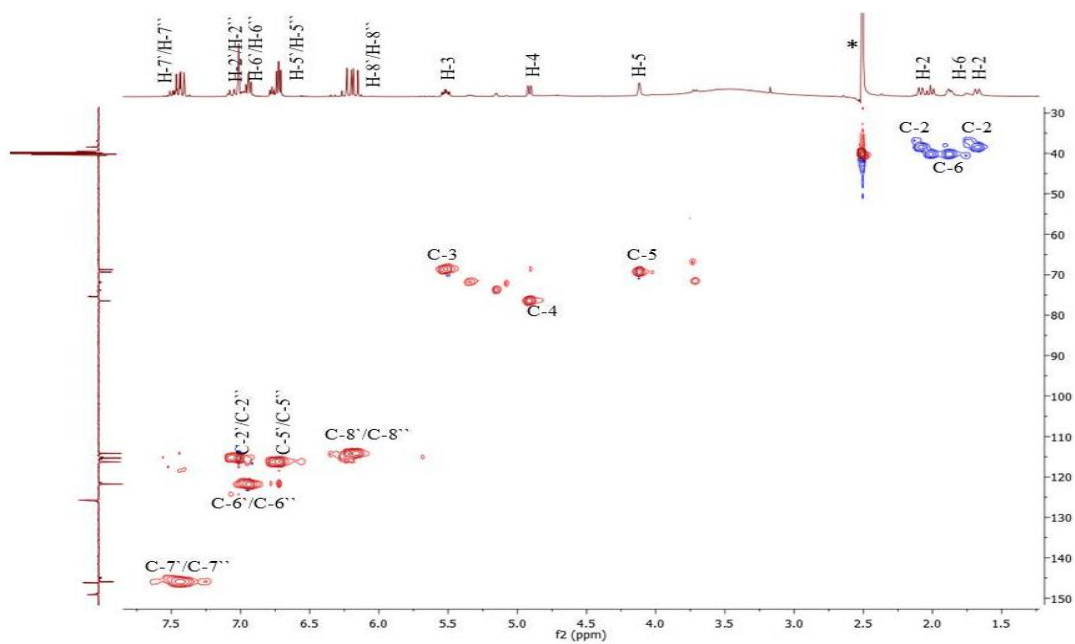
B
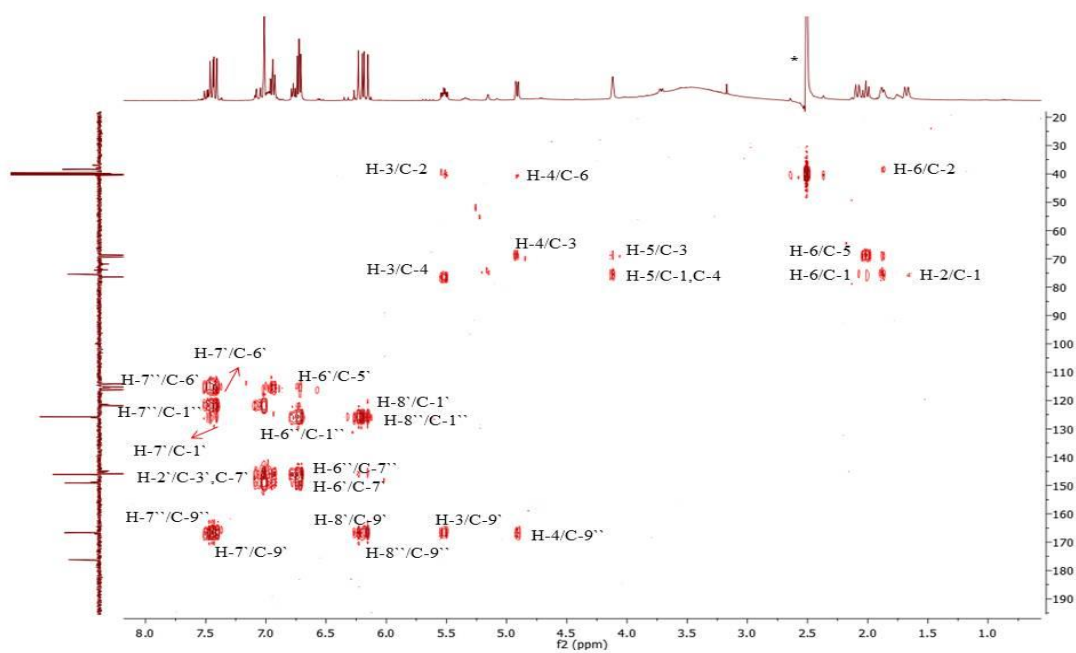
Figure 3.41A: HMQC and **3.41B:** HMBC (400 MHz, DMSO-*d₆**) spectra of RE-3.

3.4.4 Characterisation of RE-4 as a mixture of 3`,4`,5,7-tetrahydroxy-3,6-dimethoxyflavone (RE-4a) and 3`,4`,5,6-tetrahydroxy-3,7-dimethoxyflavone (RE-4b)

The fraction RE-4 (Figure 3.42) was isolated as a brown solid from the methanol extract of *R. epapposum* using Sephadex column. After spraying with *p*-anisaldehyde-sulphuric acid reagent and heating, a yellow spot appeared with R_f value of 0.62 using 20% methanol in EtOAc as the mobile phase on TLC.

The ^{1}H NMR spectrum (Figure 3.43A, Table 3.14) showed two downfield singlets at δ_H 12.80 and 12.38 attributed to a H-bonded phenolic hydroxyl proton usually found at position-5 of flavonoids and each signal was integrated for one. Hence, it is may be a mixture of two flavonoids. Four signals corresponding to methoxy groups was observed at δ_H 3.75, 3.78, 3.80 and 3.91. The protons at δ_H 6.52 (1H, *s*) and 6.85 (1H, *s*) accounted for the A-ring as H-8 for each flavonoid in the mixture. While the set of aromatic protons gave overlapping signals belonging to the aromatic ABX spin system at δ_H 6.90/6.92 (1H, *d*, *J* = 3.2 Hz, H-5`), 7.45/7.48 (1H, *dd*, *J* = 8.5, 2.3 Hz, H-6`) and 7.55/7.59 (1H, *d*, *J* = 2.3 Hz, H-2`).

Using DEPTq-135 NMR (Figure 3.43B) and 2D NMR (HMQC and HMBC), the identification of the compounds in the mixture was possible. The major constituent RE-4a showed a singlet at δ_H 6.52 attached to C-8 (94.3 ppm) and methoxy protons at δ_H 3.75 attached to 6-O<u>C</u>H$_3$ (60.4 ppm) in the A-ring (HMQC, Figure 3.44A). The downfield shift of this methoxy carbon indicated its attachment at sterically-hindered site.

The HMBC spectrum also showed a ^3J correlation of the methoxy protons with a carbon at δ_C 131.7, confirming the methoxy to be at C-6. The singlet at δ_H 12.80 (5-OH) correlated by ^2J to the carbon at δ_C 152.4 which was assigned to be C-5 and ^3J correlation to the carbon at δ_C 131.7 which further confirmed it to be C-6.

The minor constituent RE-4b showed a singlet at δ_H 6.85 attached to C-8 (91.3 ppm) and methoxy protons at δ_H 3.91 attached to 7-O<u>C</u>H$_3$ (56.8 ppm) in the A-ring. A ^3J correlation between the methoxy protons and the carbon at δ_C 155.0 was suggesting the methoxy to be at C-7. The singlet at δ_H 12.38 (5-OH) correlated by ^2J to the carbon at δ_C 146.3 which was assigned to be C-5 and ^3J correlation to the carbon at δ_C 130.0 which confirmed to be C-6.

The A-ring protons at δ_H 6.52 (H-8, RE-4a) and δ_H 6.85 (H-8, RE-4b) each showed ^3J correlations to the quaternary carbon at δ_C 105.2 and 106.2, respectively and ^2J correlations to C-9 (RE-4a, RE-4b) at 152.0 and 149.3 ppm. ^3J correlations between two signals at 12.80 (RE-4a) and 12.38 ppm (RE-4b) and carbons at δ_C 105.2 and 106.2, confirmed the assignment of this carbon signals to the C-10. Proton singlets of C-ring at δ_H 3.78 and 3.80 attributed to the methoxy group found at C-3 of flavonoids and integrated for three protons. Both signals revealed correlations to the carbon at 137.8 ppm which was assigned to be C-3 of ring-C for each flavonoid.

The B-ring protons (RE-4a, RE-4b) at δ_H 6.90/6.92 (H-5`) showed $^2J$ correlations to C-6` at 121.1/121.0 ppm and to the oxygen-bearing quaternary carbon at δ_C 149.2 (C-4`), indicating the presence of an -OH substituent in C-4` on the B-ring. The protons at δ_H 7.45/7.49 (H-2`) correlated via $^3J$ couplings to highly-deshielded C-2 (155.9/156.1 ppm) and had $^2J$ couplings to the quaternary carbons at $\delta_C$ 121.4/121.3 (C-1`) confirmed the assignment of this carbon signal to the C-1` of the aromatic ring B. A NOESY correlation (Figure 3.45 and 3.46) observed between H-8(b) and 7-OCH$_3$ (b) also supported the methoxy to be at C-7 in the compound RE-4b.

The HREI-MS data showed pseudo molecular ion [M] $^-$ at *m/z* 345.1200 which showed that the molecular formula of each compound in the mixture was C$_{17}$H$_{14}$O$_8$. The ^{1}H &^{13}C NMR spectral data are in good agreement with those reported earlier (Gebreheiwot *et al*., 2010; Hung *et al*., 2013) and the compounds identified as a mixture of 3`,4`,5,7-tetrahydroxy-3,6-dimethoxyflavone (axillarin) (RE-4a) and 3`,4`,5,6-tetrahydroxy-3,7-dimethoxyflavone (tomentin) (RE-4b). They are being

reported from this plant material for the first time. Further work is required to separate this mixture.
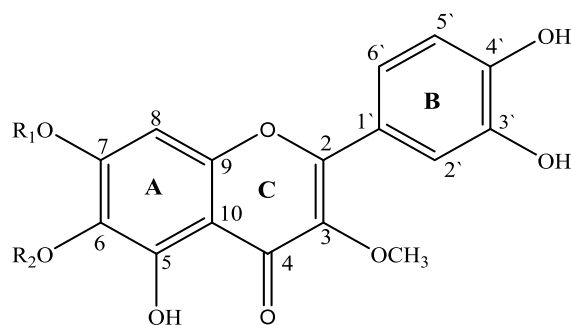
Figure 3.42: Structure of 3`,4`,5,7-tetrahydroxy-3,6-dimethoxyflavone (RE-4a) and 3`,4`,5,6-tetrahydroxy-3,7-dimethoxyflavone (RE-4b).

Table 3.14: [1]H (400MHz) and DEPTq-135 (100MHz) data of RE-4a and RE-4b DMSO-d_6.

Position	RE-4a		RE-4b	
	δ_H	δ_C	δ_H	δ_C
1	-	-	-	-
2	-	155.9	-	156.1
3	-	137.8	-	137.8
4	-	178.4		178.4
5	-	152.4	-	146.3
6	-	131.7	-	130.0
7	-	157.7	-	155.0
8	6.52 (1H, *s*)	94.3	6.85 (1H, *s*)	91.3
9	-	152.0		149.3
10	-	105.2		106.2
1`	-	121.4	-	121.3
2`	7.59/7.55 (1H, *d*, 2.3 Hz)	115.9/115.8	7.55/7.59 (1H, *d*, 2.3 Hz)	115.8/115.9
3`	-	145.9/145.7	-	145.7/145.9
4`	-`	149.2	-	149.2
5`	6.92/6.90 (1H, *d*, 3.2 Hz)	116.2	6.90/6.92 (1H, *d*, 3.2 Hz)	116.2
6`	7.48/7.45 (1H, *dd*, 8.5, 2.3 Hz)	121.1/121.0	7.45/7.48 (1H, *dd*, 8.5, 2.3 Hz)	121.0/121.1
3-OCH$_3$	3.80/3.78 (3H, *s*)	60.1	3.78/3.80 (3H, *s*)	60.1
5-OH	12.80 (1H, *s*)	-	12.38 (1H, *s*)	-
6-OCH$_3$	3.75 (3H, *s*)	60.4	-	-
7-OCH$_3$	-	-	3.91 (3H, *s*)	56.8

A
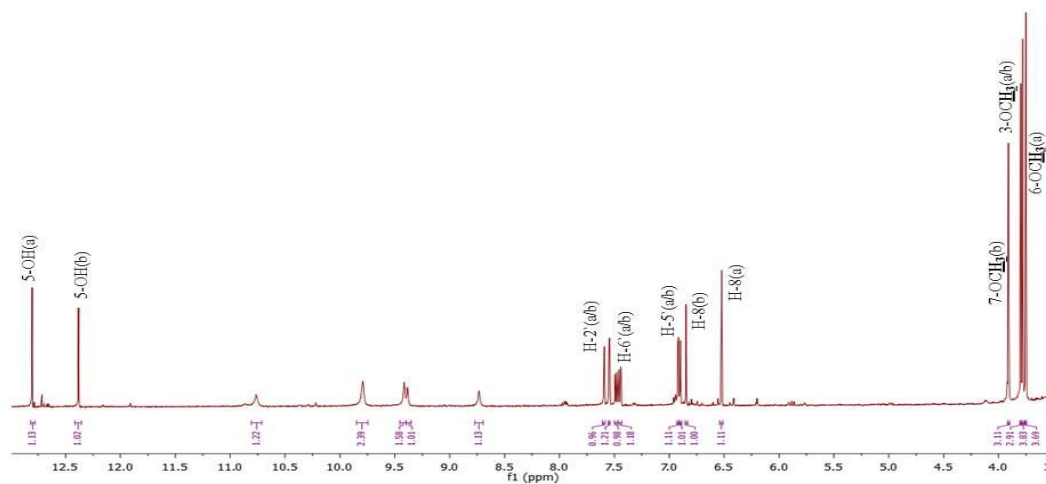
B
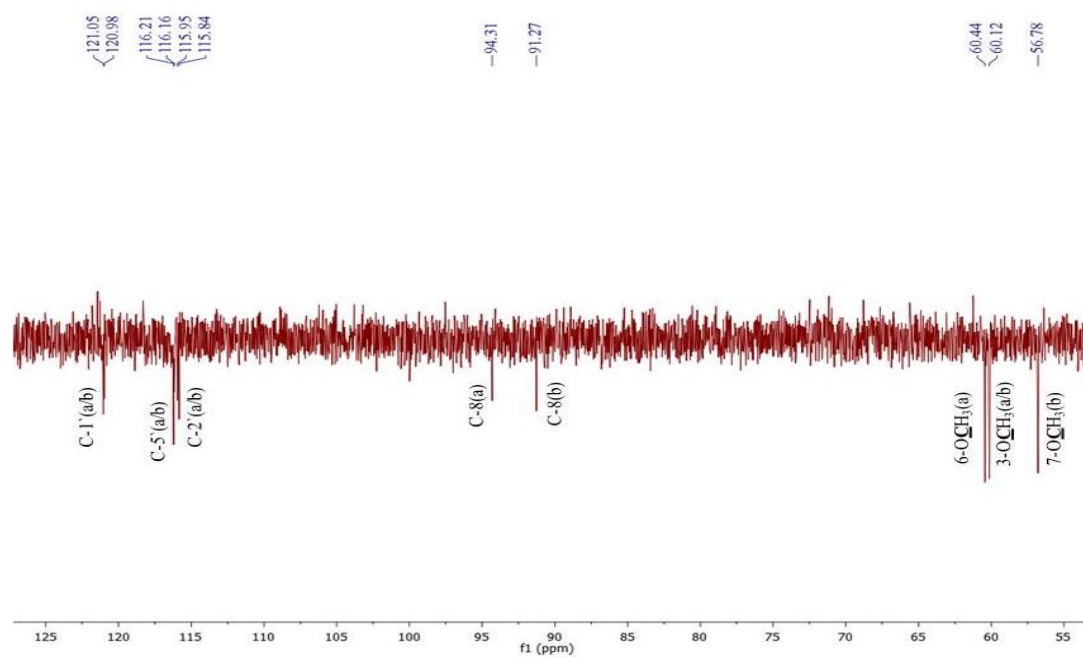
Figure 3.43A: ^{1}H NMR (400 MHz) and **3.43B:** DEPTq-135 NMR (100 MHz) spectra of the mixture RE-4a (labelled as a) and RE-4b (labelled as b) in DMSO-d_6*.

A
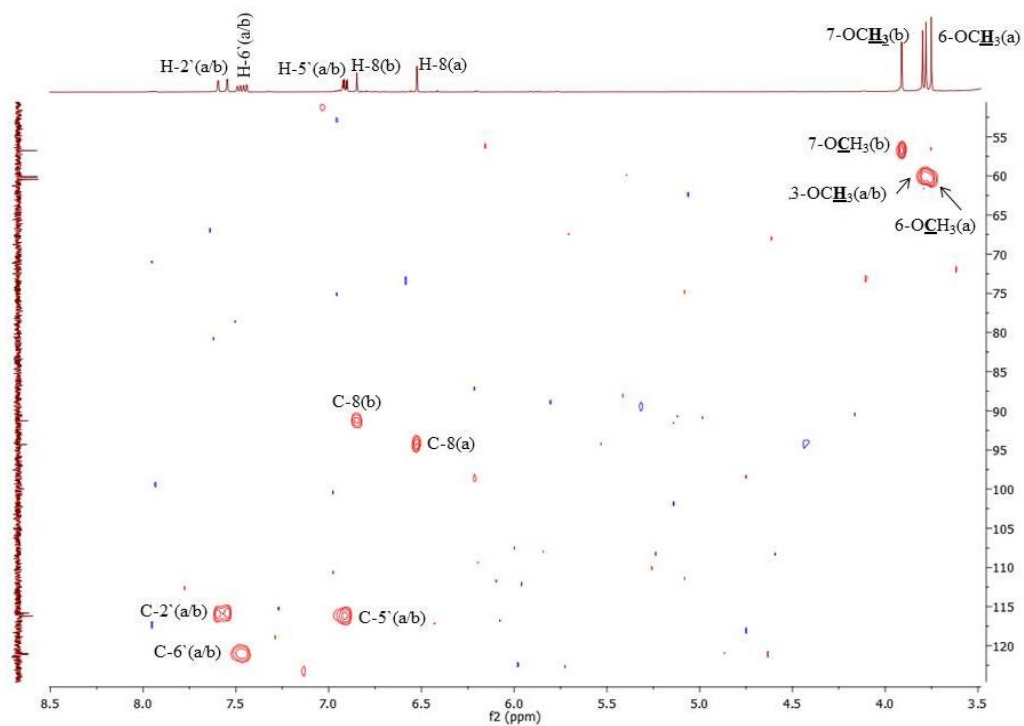
B
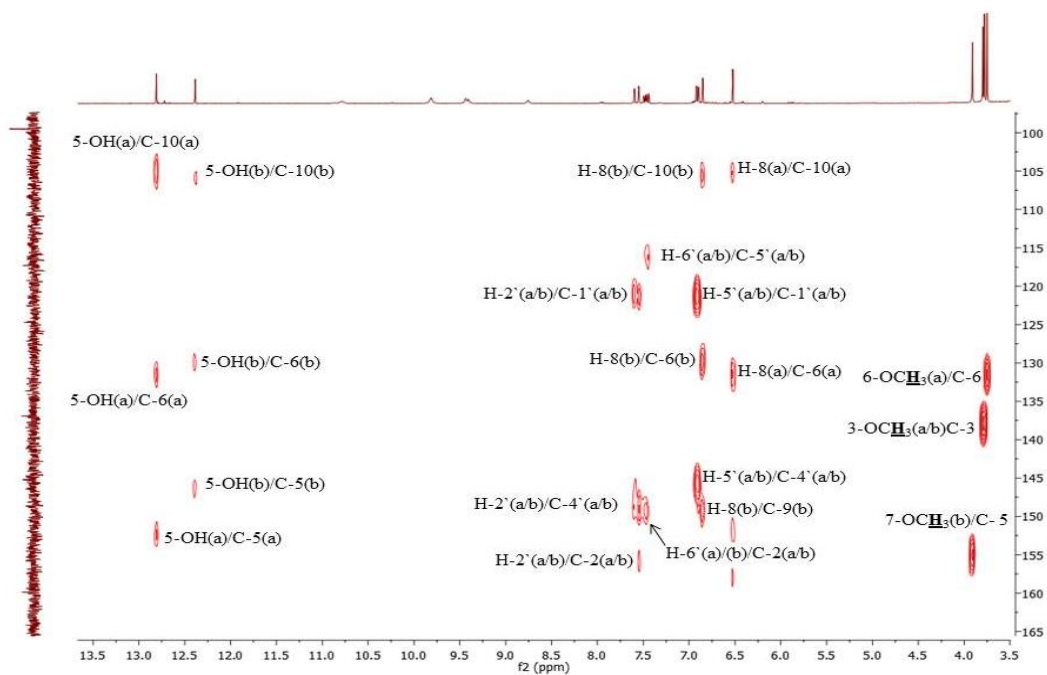
Figure 3.44A: HMQC and **3.44B:** HMBC spectra (400 MHz) of the mixture RE-4a (labelled as a) and RE-4b (labelled as b) in DMSO-d_6*.
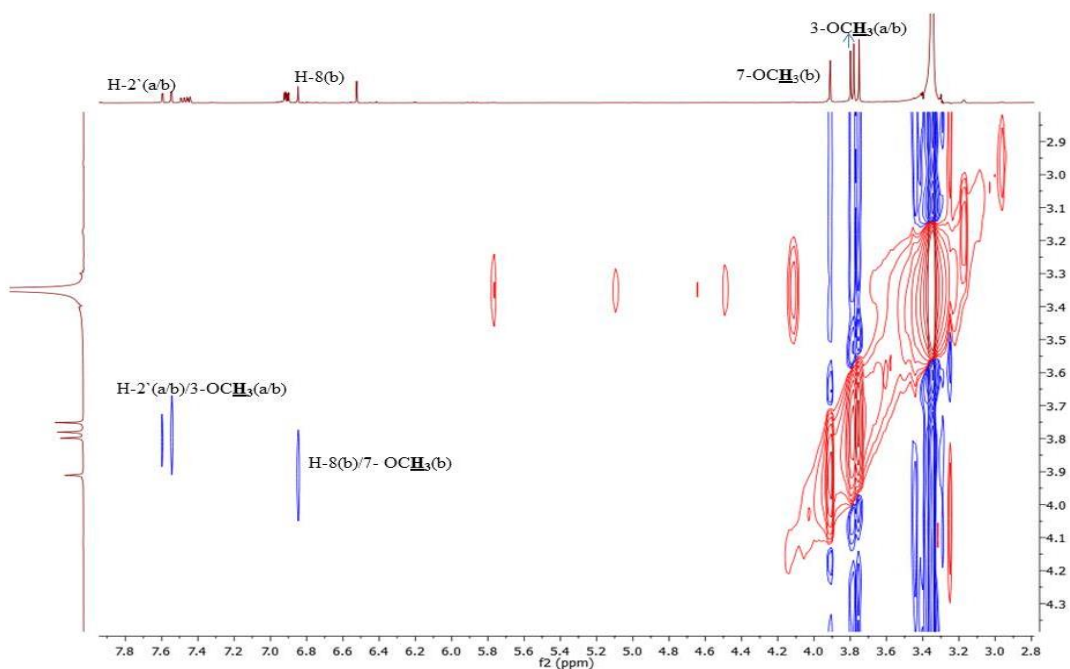
Figure 3.45: Selected expansion of NOESY spectrum (400 MHz) of RE-4a and RE-4b in DMSO-*d₆.*
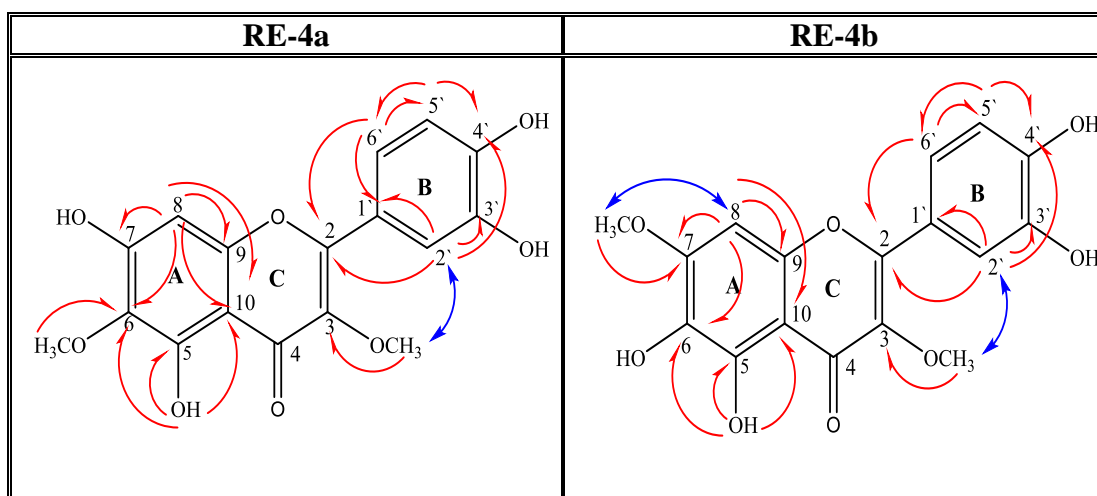
Figure 3.46: Key HMBC (⟶) and NOESY (⟵⟶) correlations observed in RE-4a and RE-4b.

3.5 Cytotoxicity secreening of isolated compounds using AlamarBlue®assay

3.5.1 Seeding density optimisation

This experiment was carried out to determine the best seeding density to be used in AlamarBlue®and MTT assays with tumor and non-tuomor cell lines. The optimum seeding density for each cell line was determined using an AlamarBlue® assay (Figure 3.47). As a result, 10^4 cells per well were chosen as an optimal number to be used in a 96-well plate for LNCaP, PNT2, HeLa and PANC-1 cells as the highest absorption was recorded at this number of the cells. By contrast, A375, A2780 and ZR-75-1 cells were seeded using 7 x 10^3 cells per well.

PNT2 Cells	
3000	5000
7000	10000
LNCaP Cells	
3000	5000
7000	10000
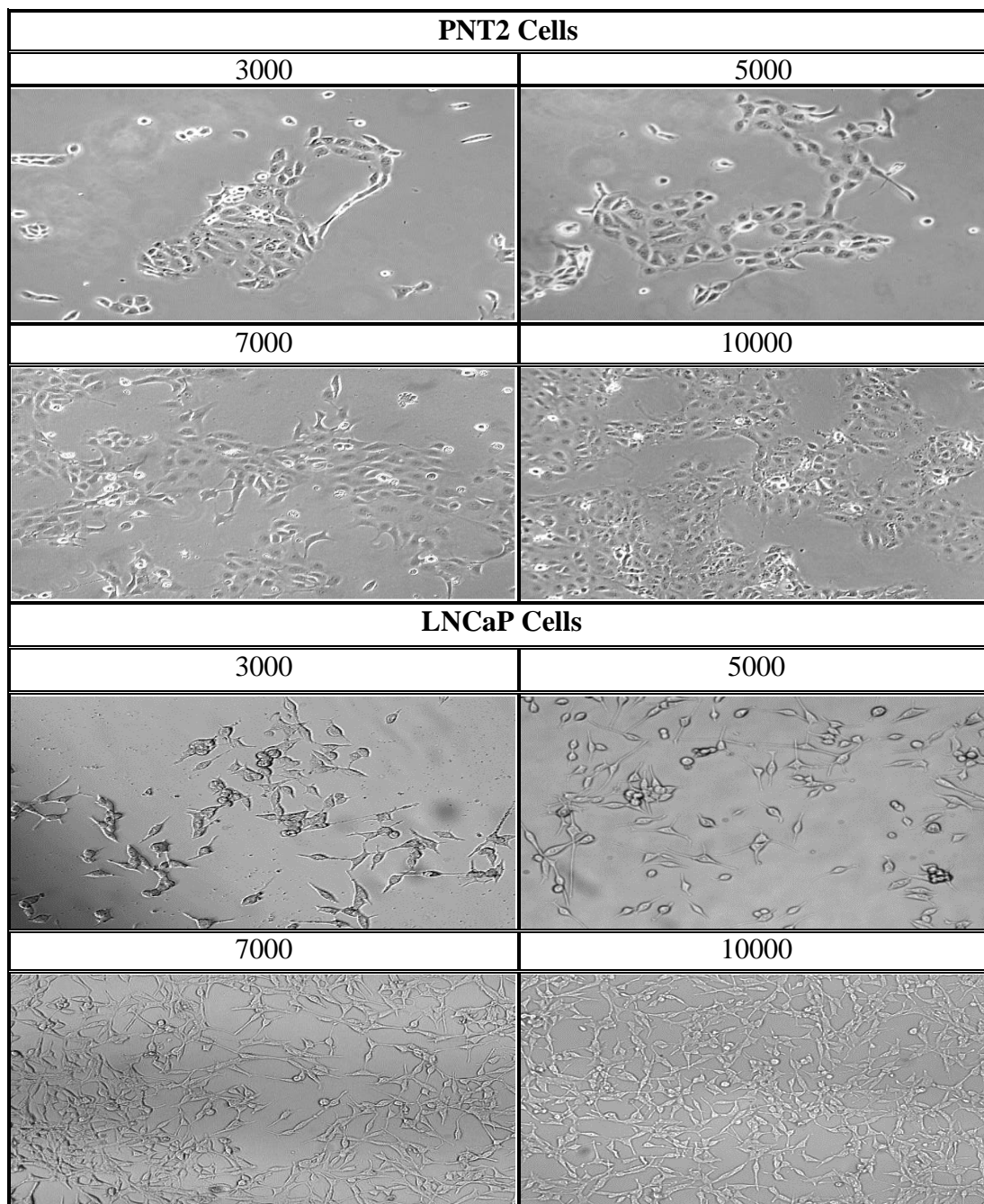
Figure 3.47: Cell line seeding density optimisation. Each cell line was seeded in different seeding densities (3000, 5000, 7000, 10000 cells per well) in 96 well plates and then incubated at 37°C, 5% CO_2 and 100% humidity, for 72h, and assayed for cell viability by AlamarBlue® assay. The images shows that 10000 cells per well were chosen as an optimum number to be used in a 96 well plate.

HeLa Cells	
3000	5000
7000	10000
PANC-1 Cells	
3000	5000
7000	10000
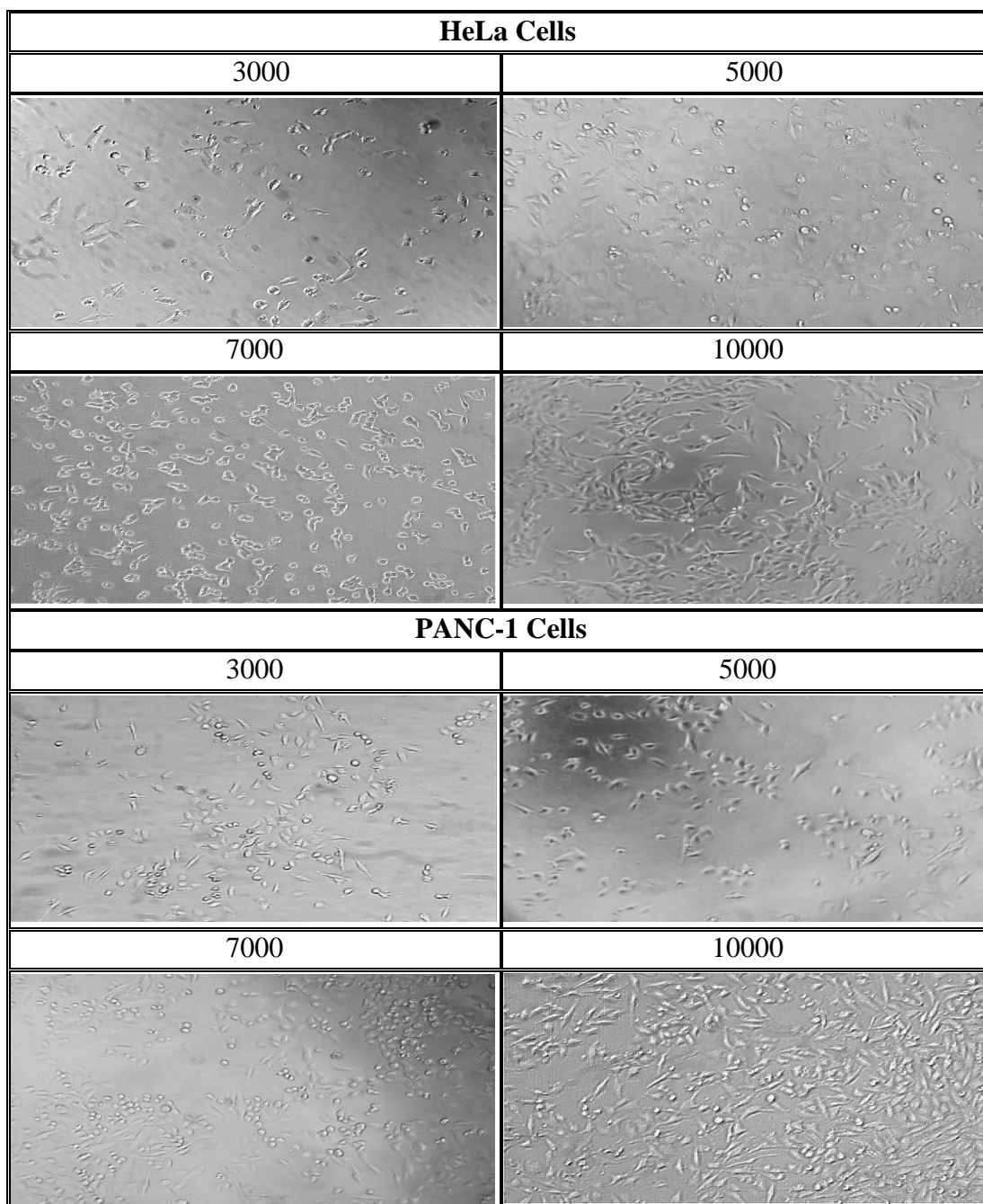
Figure 3.47 (continued): Cell line seeding density optimisation. The images show that 10000 cells per well were chosen as an optimum number to be used in a 96 well plate.
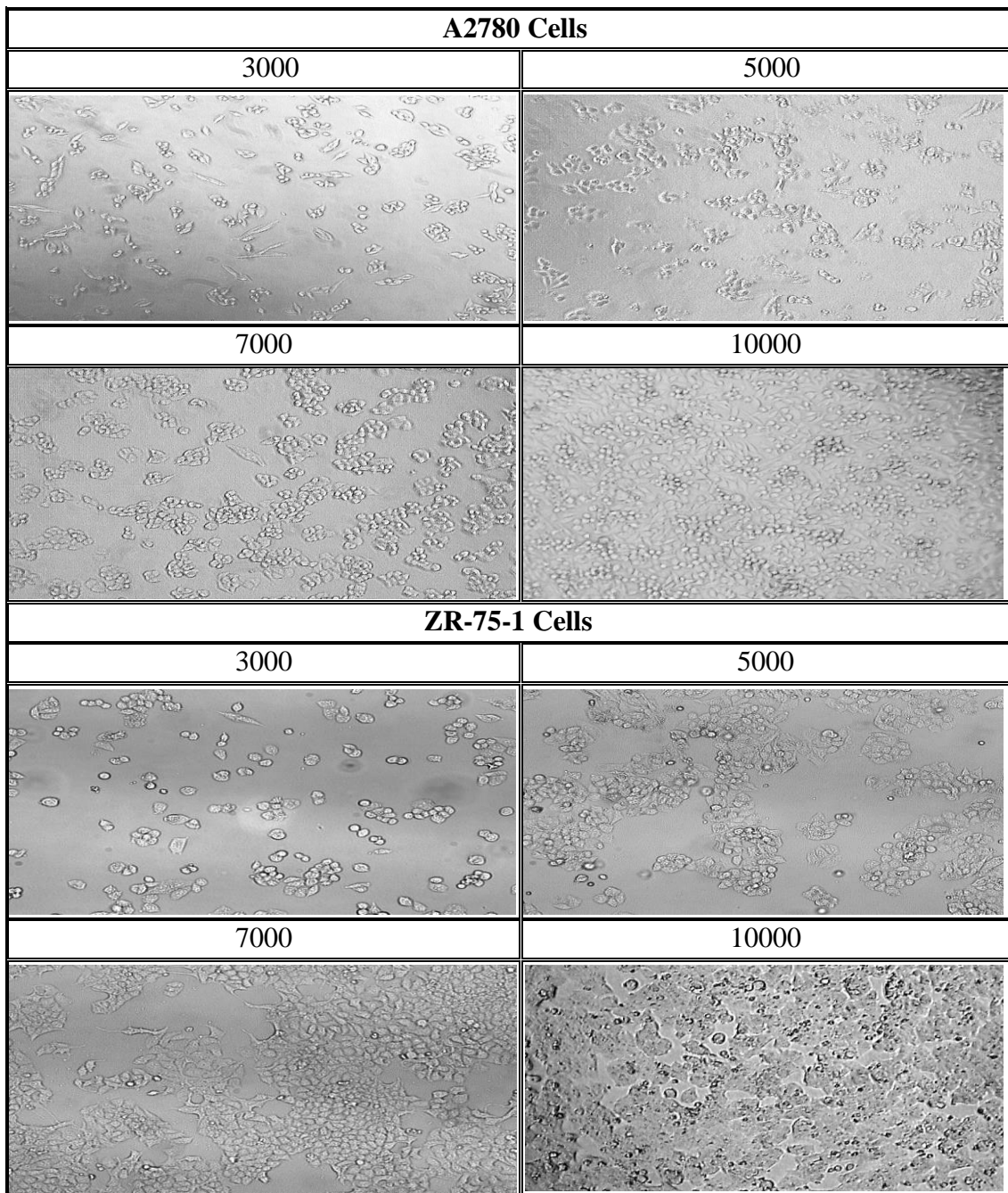
A2780 Cells	
3000	5000
7000	10000
ZR-75-1 Cells	
3000	5000
7000	10000

Figure 3.47 (continued): Cell line seeding density optimisation. The images shows that 7000 cells per well were chosen as an optimum number to be used in a 96 well plate.

A375 Cells	
3000	5000
7000	10000
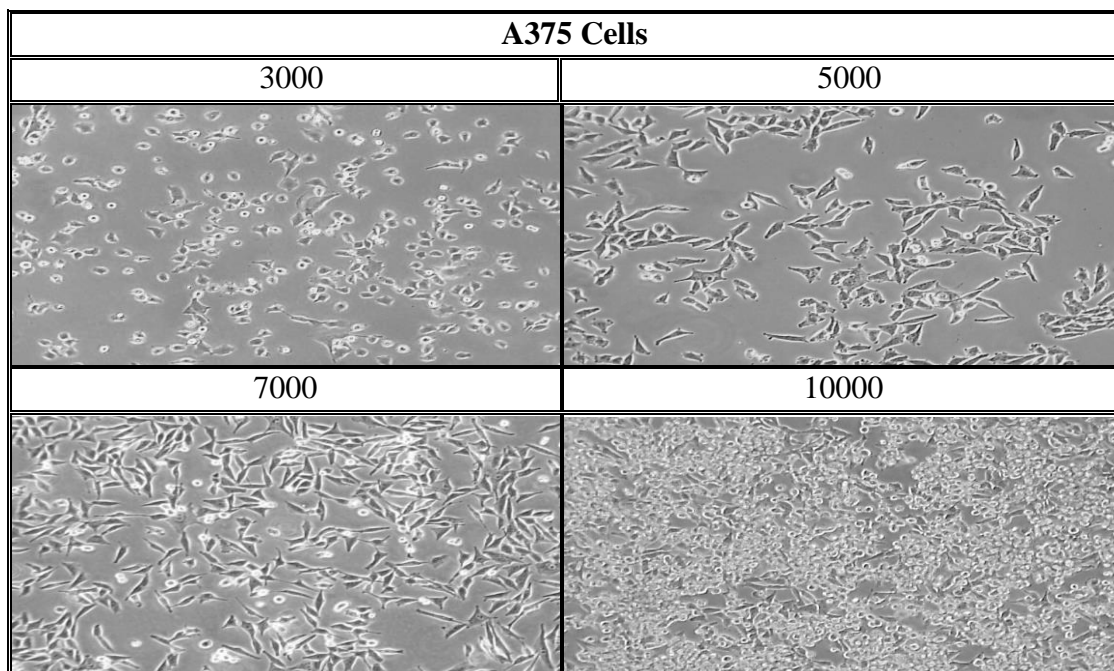
Figure 3.47 (continued): Cell line seeding density optimisation. The images shows that 7000 cells per well were chosen as an optimum number to be used in a 96 well plate.

3.5.2 Cytotoxicity evaluation

3.5.2.1 Cytotoxicity of isolated compounds

Cytotoxicity of the isolated compounds was evaluated against cancer (A375, PANC-1, A2780, ZR-75-1, LNCaP, and HeLa) and non-cancer (PNT2) cell lines using the AlamarBlue® assay (Table 3.15). Any compound that caused cell viability to decrease to less than 50% was considered cytotoxic and the concentration of each compound which gave 50% of the maximum response, the (EC_{50}) was calculated. The results, which can be seen in Table 3.15, show that among the isolated compounds from *T. aphylla*, TA-1 and TA-3 exhibited cytotoxic activity. Compared with the non-cancer cell line, fraction TA-1(a+b) (5:1)* presented cytotoxic effects against A375 cell line, with an EC_{50} of 25.18±1.5μg/ml. In contrast, the compound

TA-2 was not toxic to the cancer cell lines, with the majority of cells still viable. TA-3 exerted cytotoxic activity against HeLa cells ($86.50\pm0.51\mu M$) when compared to normal cell line (PNT2).

(*) According to the ^{1}H NMR spectrum of the mixture of the two compounds **TA-1a** and **TA-1b,** the peak which corresponds to H-5 of the compound **TA-1a** integrated for one proton when the peak of the H-5 for the compound **TA-1b** was integrated for 0.2, thus, the ratio of the two compounds in this mixture was 5:1 (**TA-1a: TA-1b**).

CC-1 and CC-2 were isolated from *C. colocynthis* and the best cytotoxicity against the cancer cell lines was observed with CC-2. It exhibited cytotoxic activity against A375, A2780 and ZR-75-1 cell lines, with EC_{50} values of $58.00\pm1.20\mu M$, $62.27\pm1.76\mu M$, and $55.25\pm1.15\mu M$, respectively. CC-1 was toxic to HeLa cancer cell line $85.11\pm1.20\mu M$ and also toxic to the normal cells (PNT2, $73.61\pm1.26\mu M$).

Some compounds isolated from *R. eppaposum* (RE-1, RE-2 and RE-3) *and A. spinosus* (AS-1, AS-2 and AS-3) were tested and no cytotoxicity was observed at concentrations up to $100\mu M$.

Other isolated compounds such as TA-4, AS-4, and RE-4 were not assessed for cytotoxicity due to the limited quantities and the prescence of some impurities. This study showed preliminary cytotoxic screening of isolated compounds on cancer cell lines and to study the mechanisms of action of these compounds, further investigations are required.

Table 3.15: EC$_{50}$ of the tested compounds on each cell line. The values are means ± SEM of at least three independent experiments performed in triplicates.

Treatment	EC$_{50}$ (μM)						Normal Cell Line
	Cancer Cell Lines						
	A375	HeLa	LNCaP	A2780	PANC-1	ZR-75-1	PNT2
TA-1	25.18 ±1.50*	-	-	-	>100	-	-
TA-3	>100	86.50 ±0.51	-	>100	>100	>100	-
CC-1	-	85.11±1.20	>100	-	-	-	73.61 ±1.26
CC-2	58.00 ±1.20	>100	>100	62.27 ±1.76	>100	55.25 ±1.15	-

*EC$_{50}$ of this fraction TA-1(a+b) was measured in μg/ml.
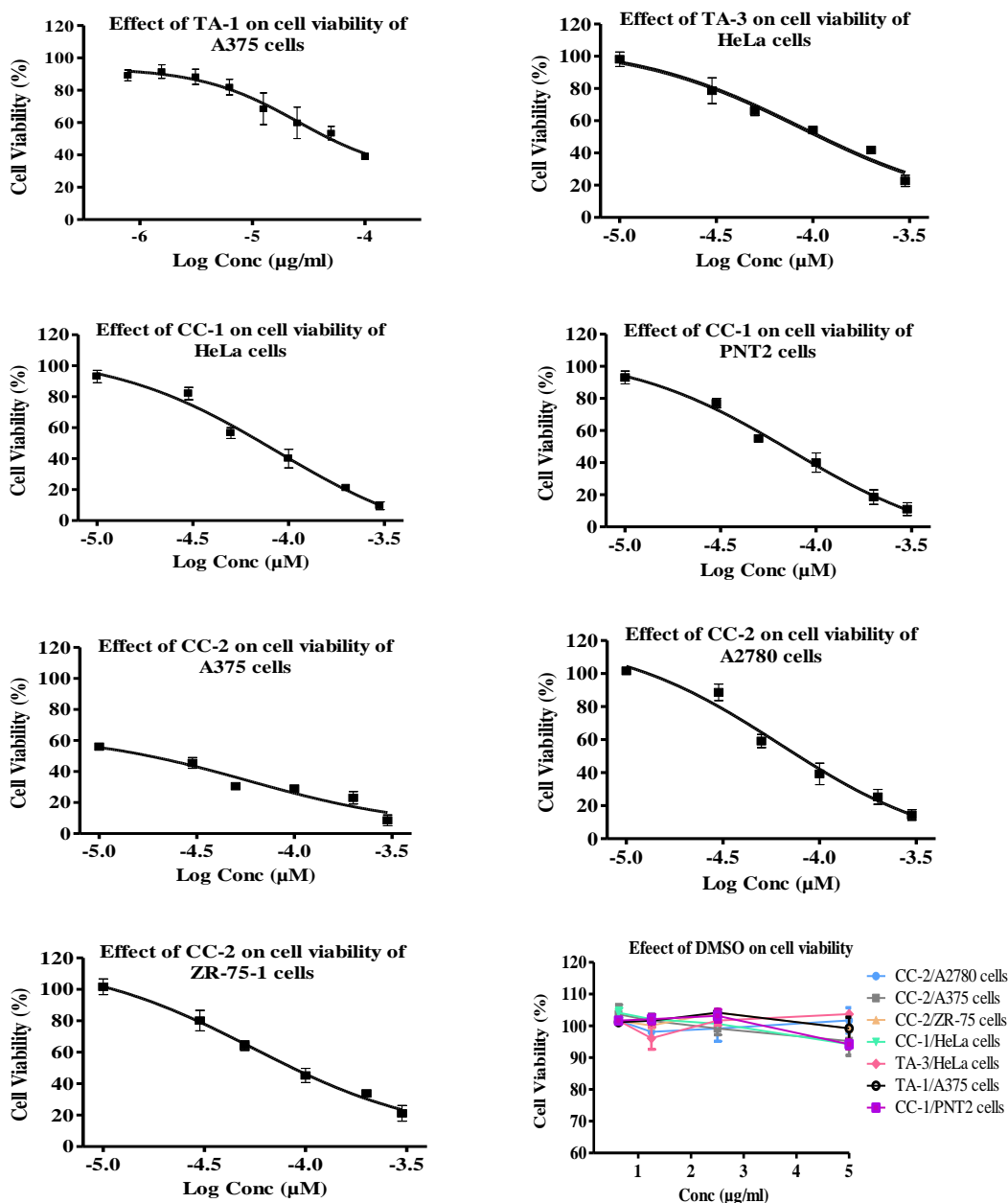
Figure 3.48: Cytotoxicity of isolated compounds. Determination of EC_{50} for compounds TA-1, TA-3, CC-1 and CC-2 using the dose-response curve and the effect of DMSO on cell viability at the equivalent DMSO content in the wells. Cellular viability was measured using an AlamarBlue® assay, values are the means of $n = 3 \pm$ SEM.

Part 2: Molecular Biology Results

3.6 RNA Extraction and Quality Assessment

3.6.1 Plant RNA Extraction and Quality Assessment

Researchers can face difficulties during the extraction process because some plants are rich in secondary metabolites which can interfere with RNA extraction. For example, plant tissues with large quantities of phenolic compounds that compromise downstream analysis. Also, the carry-over of genomic DNA in extracted plant RNA samples will affect gene expression studies, as it can lead to false-positive results because of an overestimation of transcript quantity.

Due to known issues regarding nucleic acid extraction from plant material, an early comparison between several RNA purification kits, including kits specifically designed for plant RNA isolation, was carried out using four plants. Of the plants in this study, some of the kits gave a low RNA yield per amount of starting material and the isolated RNA was contaminated, as indicated by the spectrophotometric $A_{260/230}$ and $A_{260/280}$ readings. The purified RNA samples should be free from genomic DNA, protein, enzyme inhibitors, or any salt or alcohol carry-over which could compromise RNA-based applications. Therefore, identifying and using an efficient RNA extraction method is an important factor to ensure total RNA of high quality.

The outbreak of war in the country of origin of the plants after the original, limited collection of plant material prevented their further collection. Constrained with only limited dried stocks and no fresh plant material, the further study of the RNA isolation methods had to be conducted with only two selected plants (*A. spinosus* and *C. colocynthis*) to identify the most effective method of extracting intact RNA from the plant samples. The extraction kits investigated in this study applied different strategies: silica-based capture column-based kits; magnetic bead-based kits; and organic solvent extraction kits. The yield and purity of the extracted total RNA from these RNA isolation procedures are listed in Table 3.16.

Table 3.16: Evaluation of competing methods for RNA isolation efficiency.

Extraction Kit	Plant	RNA Yield (μg)	$A_{260/280}$ Ratio	$A_{260/230}$ Ratio
Norgen Total RNA Kit	*A. spinosus*	69.23	1.93	1.49
	C. coloynthis	53.83	1.96	1.77
Qiagen Plant RNeasy Kit	*A. spinosus*	18.58	1.99	0.07
	C. coloynthis	33.00	1.46	0.24
Invitrogen PureLink Total RNA Kit	*A. spinosus*	471.75	2.23	3.48
	C. coloynthis	374.31	2.26	4.77
Cambio PowerPlant RNA Isolation Kit with DNase	*A. spinosus*	13.26	1.62	0.73
	C. coloynthis	5.04	1.64	1.02
Cambio PowerPlant RNA Isolation Kit	*A. spinosus*	283.86	1.47	0.54
	C. coloynthis	368.88	1.27	0.41
Thermo Scientific MagJET Plant RNA Kit	*A. spinosus*	28.50	1.0	0.10
	C. coloynthis	281.34	1.92	1.43
Sigma Spectrum Plant Total RNA Kit (Protocol A)[*]	*A. spinosus*	N/A	N/A	N/A
	C. coloynthis	4.85	0.61	0.20
Sigma TRIzol Reagent[*]	*A. spinosus*	N/A	N/A	N/A
	C. coloynthis	303.00	1.72	0.62
Ambion *mir*Vana[TM] miRNA Isolation Kit	*A. spinosus*	18.18	2.04	1.41
	C. coloynthis	59.62	1.87	0.47
MirPremier microRNA isolation Kit	*A. spinosus*	402.51	2.11	0.98
	C. coloynthis	697.20	2.07	1.95

[*]This protocol was not performed on *A. spinosus* due to limited quantity of the plant sample

The purified total RNA using the Norgen Kit was assayed spectrophotometrically and gave $A_{260/280}$ and $A_{260/230}$ values of 1.93 and 1.49 for *A. spinosus* and 1.96 and 1.77 for *C. colocynthis,* respectively. A typical RNA UV absorption spectrum was observed (Figure 3.49; A1&A2). It shows that the purified RNA sample has close to an ideal $A_{260/280}$ ratio, suggesting the lack of protein contaminants. However, with an $A_{260/230}$ ratio of less than 2.0 at 1.49, suggests salt contamination may be present in the sample. The yield of the extracted RNA samples is 69.23 and 53.83μg for both

plants, respectively and it is within the reliable detectable range of the Nanodrop spectrophotometer.

Most of the other purification kits isolated total RNA of lower purity. The Qiagen Plant RNA kit extracted total RNA with low yields of 18.58μg and 33.00μg of *As. spinosus* and *C. colocynthis*, respectively. The absorbance spectrum shows a high shoulder of the curve at 220nm. The $A_{260/230}$ values are significantly low (0.07 and 0.24) for both samples and these numbers are indicative of the contamination of the sample with reagents used in the isolation which absorb at 220nm (Figure 3.49; B1&B2).

The PureLink Kit purified total RNA with high yield values of 471.75μg and 374.31μg of *A. spinosus* and *C. colocynthis*, respectively (Figure 3.49; C1&C2). The $A_{260/280}$ ratios of both samples are higher than ideal (2.23 and 2.26, respectively) While the $A_{260/230}$ ratios are also higher than 2 (3.48 and 4.77, respectively). In addition the absorption curve is not typical of a pure RNA sample, lacking the 230nm dip before the 260nm peak.

The PowerPlant RNA Isolation Kit isolated total RNA samples with high quantities; 283.86μg of *A. spinosus* and 368.88μg of *C. colocynthis* and low $A_{260/280}$ and $A_{260/230}$ ratios. The UV curve (Figure 3.49; D1&D2) indicated a high concentration of protein in the sample as the large peak appears at 270nm. Additionally, a small shoulder of the curve was observed around 220nm which suggests salt carry-over contamination.

The PowerPlant Kit with DNase protocol purified total RNA samples with low quantity and quality. The absorbance curve (Figure 3.49; E1&E2) of both samples shows a small shoulder at 270nm and a small bulge at 220nm, suggesting to presence of salt impurities. Very low yield values of 13.26μg (*A. spinosus*) and 5.04μg (*C. colocynthis*) could be due to degradation of RNA samples.

The purified total RNA using the MagJET Plant RNA Kit gave $A_{260/280}$ and $A_{260/230}$ values of 1.00 and 0.10 for *A. spinosus* and 1.92 and 1.43 for *C. colocynthis*, respectively. RNA sample isolated from *A. spinosus* was from low quantity (28.50μg) and low $A_{260/280}$ and $A_{260/230}$ ratios. The absorbance spectrum (Figure 3.49; F1) shows a small shoulder of the curve that was observed at 220nm, indicating to salt contamination. A small bulge was observed at 270nm suggesting that the RNA sample is contaminated with protein. A good absorbance spectrum (Figure 3.49; F2) shows that the purified RNA sample of *C. colocynthis* has close to ideal $A_{260/280}$ ratio, however, the $A_{260/230}$ ratio of 1.43 is lower than 2, indicating to salt contamination. High yield of the extracted RNA sample (281.34μg) was measured.

The Spectrum Kit (Protocol A) purified total RNA from poor quality and quantity. The RNA sample was assayed spectrophotometrically and gave $A_{260/280}$ and $A_{260/230}$ values of 0.61 and 0.20, respectively. The absorbance curve (Figure 3.49; G) shows peak at 270nm and small bump at 220nm, indicating contamination of the isolated sample with kit reagent impurities.

Organic extraction with Invitrogen TRIzol Reagent purified RNA in a significant quantity of 303μg but of low quality as indicated by $A_{260/280}$ and $A_{260/230}$ values (1.72, 0.62, respectively). Additionally, the large peak is at 270nm. This curve (Figure 3.49; H) is typical of carry-over of phenol in the sample as a result of TRIzol RNA isolation protocols with poor removal of phenol during the organic phase separations.

The above results revealed that, based on the spectrophotometric analysis alone, the Norgen Total RNA kit would be a recommended extraction kit for *A. spinosus* and *C. colocynthis* as it isolated total RNA of reasonable quantity and quality. However, between the kits tested, there was no one kit that extracted total RNA with high quality and quantity from both plants.

Isolation of intact RNA from these samples was complicated and challenging because of several issues were observed during RNA purification process. First issue

was that the column-based methods would become clogged during the initial filtration step. That could be due to insufficient lysis of the plant tissues as a result of the disruption issues with of some plant samples. Also, blocking of the RNA binding columns occurred due to high viscosity of clarified lysate and binding solution mixture. RNA samples are likely to be degraded due to the degradation between harvesting the plant and RNA extraction. In this case, RNA stabilisation after plant harvesting would be recommended (e.g. freezing of plant samples or preserving with RNA*later*® solution). Moreover, contamination of purified RNA with genomic DNA and kit isolation solutions carry-over was also reported in some cases.
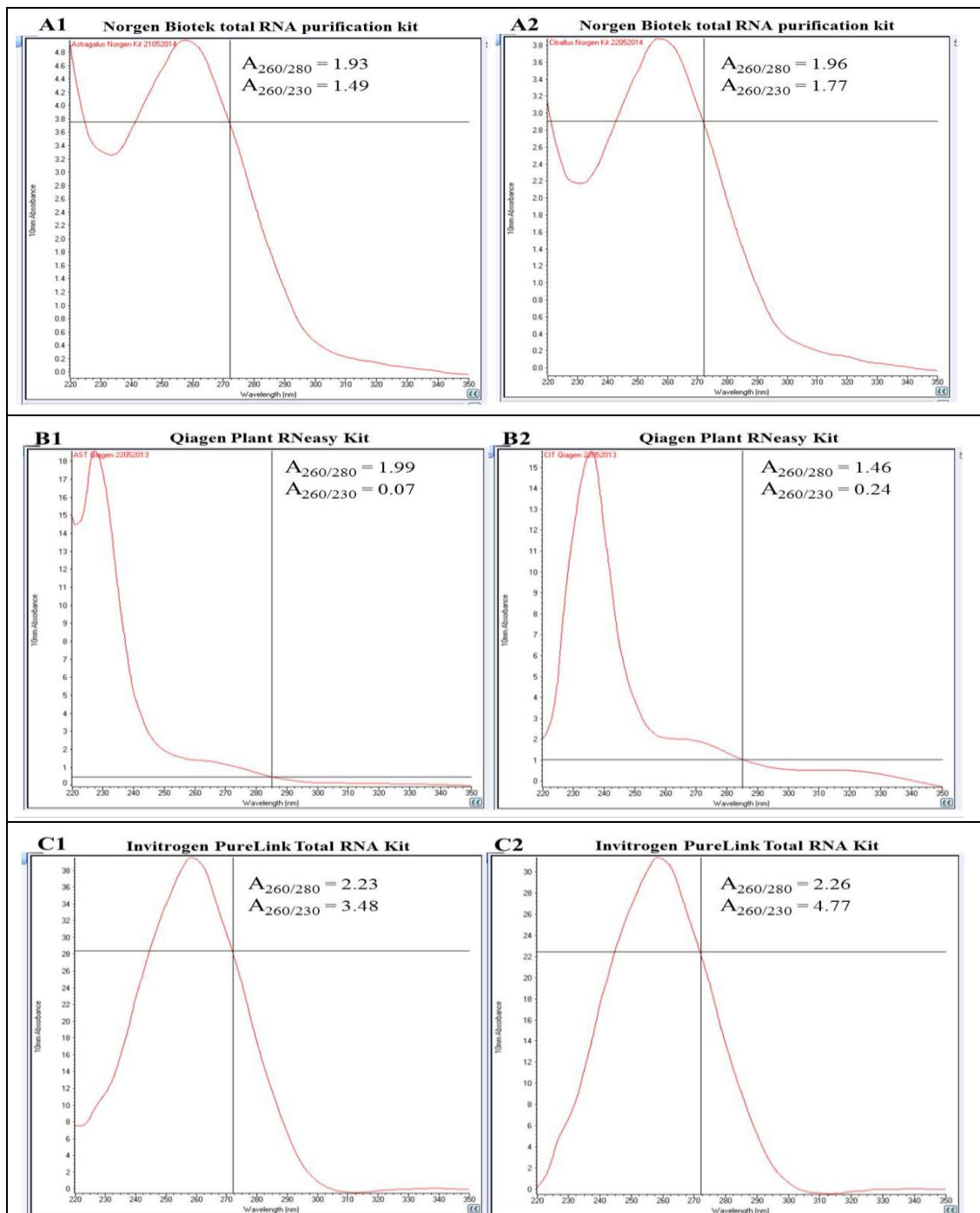
Figure 3.49: Assessment of extracted RNA purity. Absorption spectra in the UV-region for purified RNA of two plants: **A1, B1, C1** - *Astragalus spinosus* and **A2, B2, C2-** *Citrallus colocynthis* using Norgen Biotek total RNA purification kit, Qiagen Plant RNeasy Kit and Invitrogen PureLink Total RNA Kit for RNA extraction, respectively. 2μl of each sample was analysed using the NanoDrop 2000c spectrophotometer.
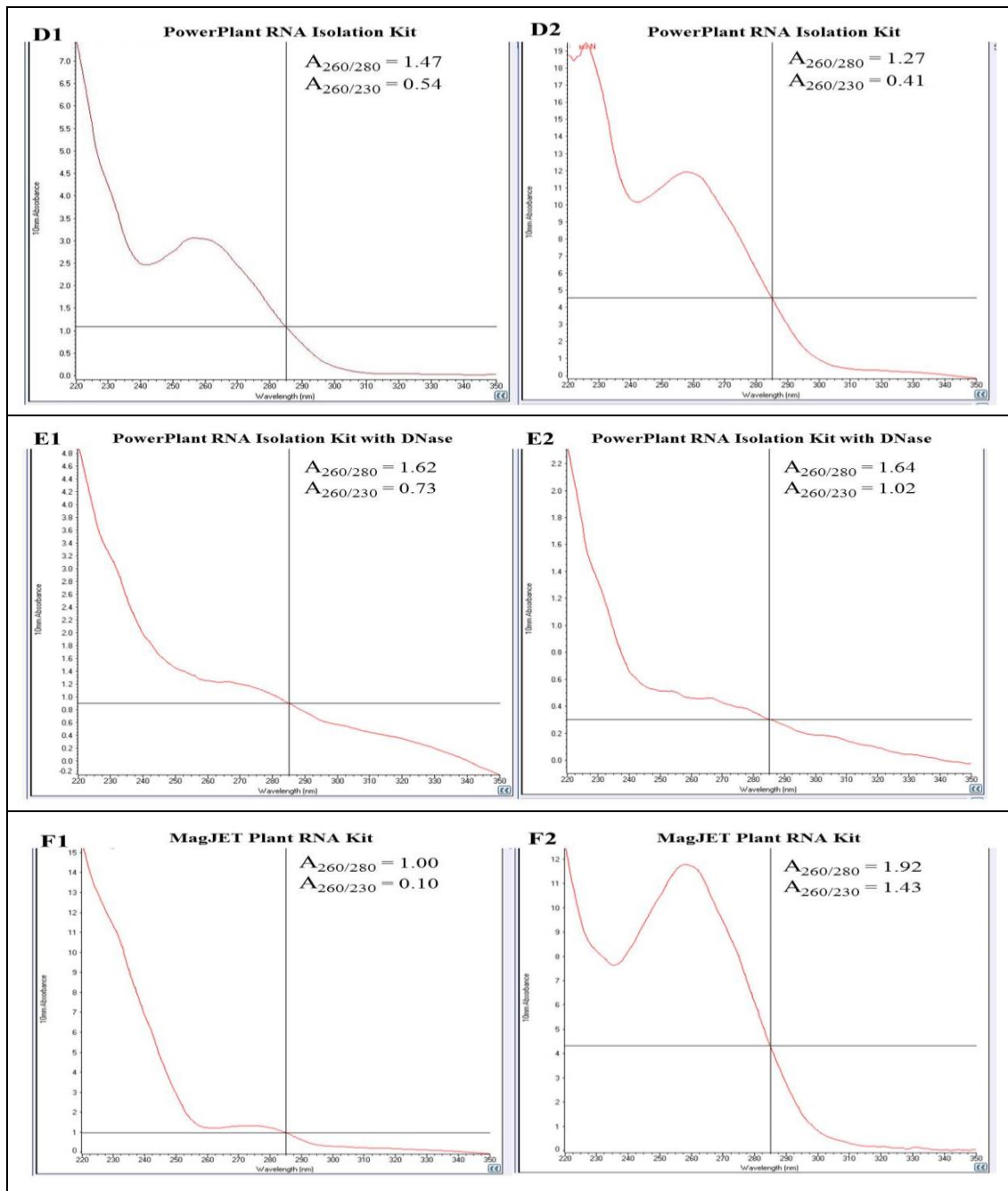
Figure 3.49 (continued): Assessment of extracted RNA purity. Absorption spectra in the UV-region for purified RNA of two plants: **D1, E1, F1** - *Astragalus spinosus* and **D2, E2, F2-** *Citrallus colocynthis* using PowerPlant RNA Isolation Kit, PowerPlant RNA Isolation Kit with DNase and MagJET Plant RNA Kit for RNA extraction, respectively. 2μl of each sample was analysed using the NanoDrop 2000c spectrophotometer.
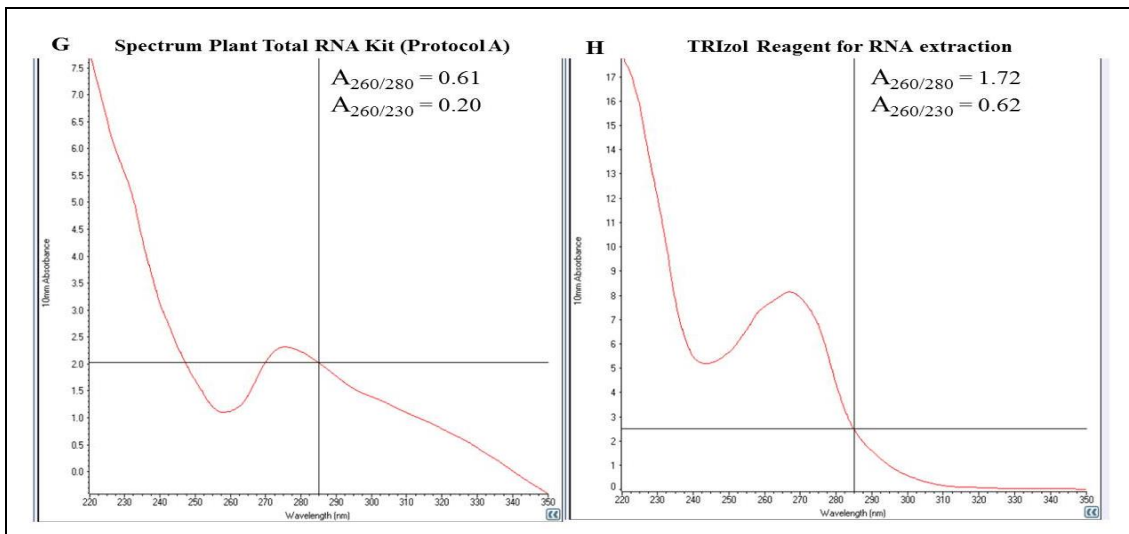
Figure 3.49 (continued): Assessment of extracted RNA purity. Absorption spectra in the UV-region for purified RNA of *Citrallus colocynthis*: using **G**: Spectrum Plant Total RNA Kit (Protocol A) and **H**: TRIzol Reagent for RNA extraction, respectively. 2μl of each sample was analysed using the NanoDrop 2000c spectrophotometer.

3.6.2 Total RNA Extraction from Body Fluids

Purification of total RNA and miRNA from camel milk and urine, and bovine milk was performed using a Norgen Biotek Total RNA kit. This kit states it is designed for total RNA and miRNA extraction from plant tissues, animal cells, and body fluids including milk, urine, and blood.

A preliminary study indicated that the Norgen kit was not effective and it produced RNA of low quantities and poor quality (Table 3.17). Further extraction work is needed using other extraction kits to identify the most effective method of RNA isolation from body fluids.

Table 3.17: Quantification of isolated RNA from body fluid samples using Nanodrop spectrophotometer. The highest RNA yield measured was from camel milk followed by bovine milk and camel urine.

No.	Sample Name	RNA Yield (µg)	$A_{260/280}$ Ratio	$A_{260/230}$ Ratio
1	Bovine Milk	6.40	1.30	0.34
2	Camel Milk	13.79	1.53	0.06
3	Camel Urine	4.37	1.36	0.50

3.6.2.1 Total RNA extraction from exosomes

3.6.2.1.1 Total exosome isolation from body fluids

RNA has been detected in exosomes isolated from different biological fluids (Qazi *et al*., 2010). Therefore, in order to improve the poor recovery of total RNA obtained using commercial kits, total exosome isolation from body fluids was carried out followed by total RNA extraction from exosomes.

A pellet of exosomes was purified from both camel milk and urine samples using a Total Exosome Isolation (From other body fluids) kit and Total Exosome Isolation (from urine) kit, respectively. As with the camel milk samples, bovine milk was subjected to exosomal extraction using the Total Exosome Isolation (from other body fluids) kit. However, no pellet of exosomes was formed. A pellet of exosomes from bovine milk was only obtained with use of the ultracentrifugation method.

3.6.2.1.2 Exosome detection by immunoblotting (Western Blot)

CD63 is a tetraspanin membrane protein which is commonly enriched in exosomes (Gross *et al*., 2012). Therefore, in order to confirm the identity of the purified pellet as exosomes, immunoblotting was conducted using an antibody against CD63 with different concentrations of pellet lysate. As shown in Figure 3.50, exosomes prepared from bovine milk (BM) by ultracentrifugation gave a stronger band comparing with other exosome samples isolated from camel milk (CM) and urine (CU). All the samples were shown to be positive for CD63. This result demonstrated the presence of exosomes in the isolates from all three body fluid samples.
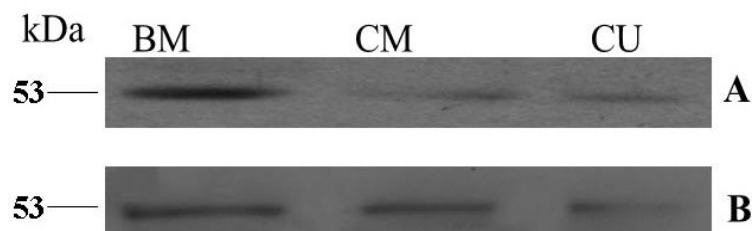
Figure 3.50: Western blot analysis of CD63 in purified exosomes from body fluids. A: 30μg/µl of total protein of each exosomal pellet lysates. **B:** 40μg/µl of total protein of each exosomal pellet lysates. **BM:** Bovine milk; **CM:** Camel milk; **CU:** Camel urine.

3.6.2.1.3 Total RNA extraction from exosomes

Total RNA was extracted from the exosomes using Norgen Biotek Total RNA purification kit and then the isolated total RNA was measured using a NanoDrop 2000c Spectrophotometer. Total RNA isolated from the three exosome samples was of low yield and poor quality (Table 3.18). In order to identify the most effective method of RNA extraction from body fluid, further extraction work is needed examining other RNA extraction kits.

Table 3.18: Quantification of isolated RNA from exosomes using Nanodrop spectrophotometer. The highest RNA yield measured was from the bovine milk sample followed by camel milk sample, while camel urine sample showed the lowest RNA yield.

No.	Sample Name	RNA Yield (µg)	$A_{260/280}$ Ratio	$A_{260/230}$ Ratio
1	Bovine Milk	18.37	1. 21	0.39
2	Camel Milk	11.2	0.79	0.29
3	Camel Urine	1.90	1.77	0.16

3.6.3 Experion™ Automated Electrophoresis System

The quality of the RNA isolated from the five plants using various extraction methods was assessed. The integrity of total RNA isolated from each plant was variable from one extraction kit to another. Most of the isolation kits produced total RNA with low quality and that was indicated by the low 28S to18S ratio and low RQI values. Low RQI values indicate degraded RNA. However, the PureLink kit yielded total RNA with good integrity from *A. spinosus* and *C. colocynthis R. eppapsum* and *T. aphylla* in which 28S /18S ratios were 1.17, 1.14 and RQI values were 8.3 and 7.9 for both plants respectively (Figures 3.51A and B).
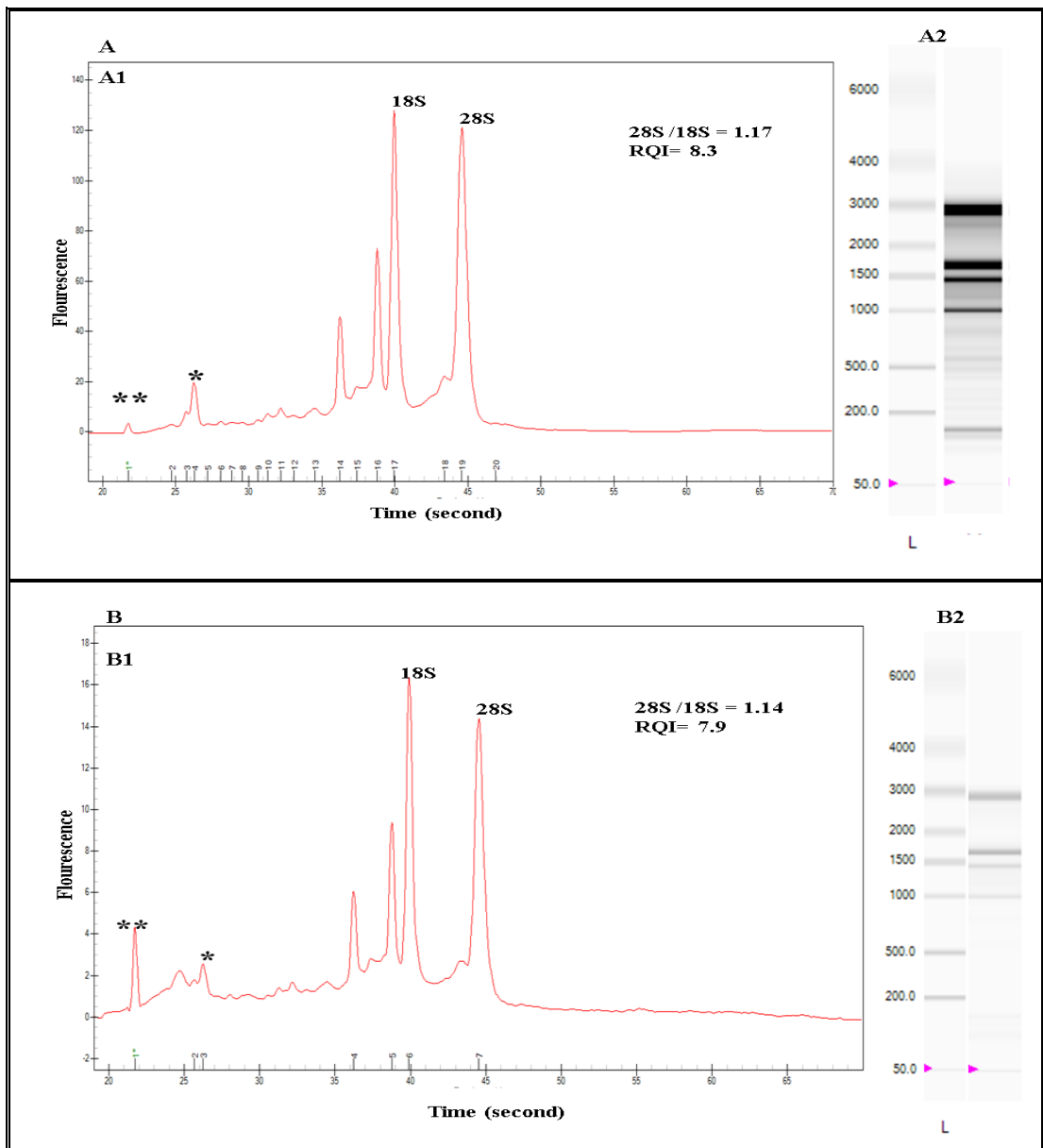
Figure 3.51: Bio-Rad Experion Automated Electrophoresis analysis of plant RNA isolated using PureLink total RNA extraction Kit. A: A1 *R. epappsum* RNA electropherogram; A2 *R. epappsum* virtual gel; and **B**: B1 *T. aphylla* RNA electropherogram; B2 *T. aphylla* virtual gel. * indicates the RNA of small molecular weight, ** indicates the Experion lower RNA size marker.

A RNA integrity analysis was conducted for all of the purified RNA samples from the *A. spinosus* and *C. colocynthis* plants from the in-depth study of the total RNA purification methods. The integrity assessment revealed that the PureLink kit extracted RNA from both plants with better integrity than the other used kits (Table 3.19).

Table 3.19: Comparison of RNA quality from different extraction kits. Higher RQI (RNA quality indicator) values indicate a higher degree of RNA integrity. RQI values range between 10 (intact RNA) and 1 (totally degraded RNA). N/A = not applicable.

Extraction Kit	Plant Name	28S /18S Ratio	RQI
Invitrogen PureLink Total RNA Kit	*A. spinosus*	0.86	7.1
	C. colocynthis	0.84	6.6
Cambio PowerPlant RNA Isolation Kit	*A. spinosus*	0.18	N/A
	C. colocynthis	0.90	2.6
Norgen Total RNA Kit	*A. spinosus*	0.97	3.4
	C. colocynthis	2.39	N/A
Qiagen Plant RNeasy Kit	*A. spinosus*	0.05	5.1
	C. colocynthis	0.71	2.6
Thermo Scientific MagJET Plant RNA Kit	*A. spinosus*	0.75	N/A
	C. colocynthis	0.24	3.3

The quality assessment was also performed on the total RNA purified from the camel milk and urine samples. Low RQIs (1.3, 2.1) and 26S to 18S ratios (0.41, 0.03) of camel milk and urine samples, respectively was observed and was due to the degraded RNA. Further work is needed to optimise effective, collection, preservation

and extraction methods for camel milk and urine samples and to improve the quality of the isolated RNA.

3.6.4 Quantification of miRNA assay

3.6.4.1 Stem-loop reverse transcription reaction

The isolated total RNA from *A. spinosus* and *C. colocynthis* using different extraction kits was converted to cDNA and then assayed for miR-166 TaqMan small RNA assays. As seen in Figure 3.52, real-time amplification plots showed different miR-166 levels of each plant using different kits.
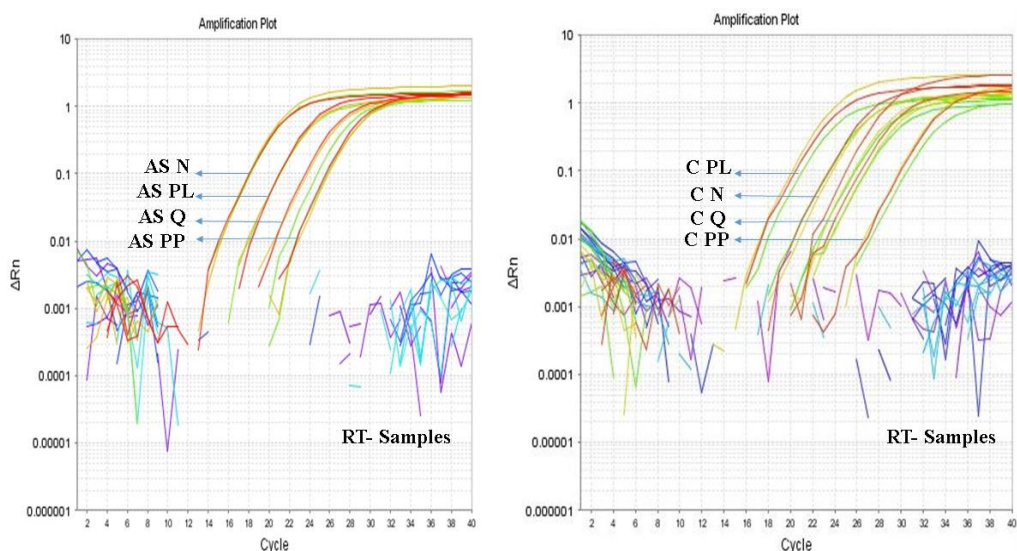
Figure 3.52: TaqMan™ miRNA assay quantitative RT-PCR amplification plots of miR-166 miRNA isolated from two plants using different extraction kits. Each sample was prepared in triplicate. AS: *A. spinosus*, C: *C. colocynthis*, PL: PureLink kit, PP: PowerPlant kit, N: Norgen kit, Q: Qiagen kit. RT-: Reverse transcriptase-negative controls of AS and C cDNA samples.

C_t value is inversely proportional to the amount of target transcript expressed in a sample. Higher C_t values indicate lower amounts of target nucleic acid while lower C_t values refer to high amounts of target nucleic acid. The comparison between Ct values for both plants revealed that the Norgen kit gave the lowest Ct value

(18.8±0.04) which is indicating to abundant miR-166 in *A. spinosus* while the highest level of the miR-166 was obtained using PureLink kit in *C. colocynthis* (21.14±0.12). Ct values of 24.5±0.08 and 25.6±0.09 were indicative of moderate levels of the miR-166 for both plants using Qiagen kit while the Powerplant kit showed the highest Ct values (26.6±0.10, 30.6±0.05) and minimal amounts of miR-166 level for *A. spinosus* and *C. colocynthis* respectively (Figure 3.53).

The variation of Ct values, from one plant, using different RNA extraction techniques indicates that the RNA isolation method can lead to incorrect quantification of target miRNAs. Different RNA purification methods have been reported to have an influence on the quality and the expression profile of the isolated miRNAs. Wang *et al.* (2008) found that RNA quality affects the result of miRNA expression studies. RNA sample with poor quality that contains contaminants such as traces of cell debris, genomic DNA or other components can potentially inhibit PCR reactions and compromise the Ct values. Hammerle-Fickinger *et al.* (2010) also showed that the RNA purification methods have an impact on the RNA quality and integrity, consequently affecting the quantitative gene expression analysis. In which degraded RNA interferes with the measurement of gene expression, and can lead to an incorrect estimation.

miR-166

Astragalus spinosus
Citrallus colocynthis
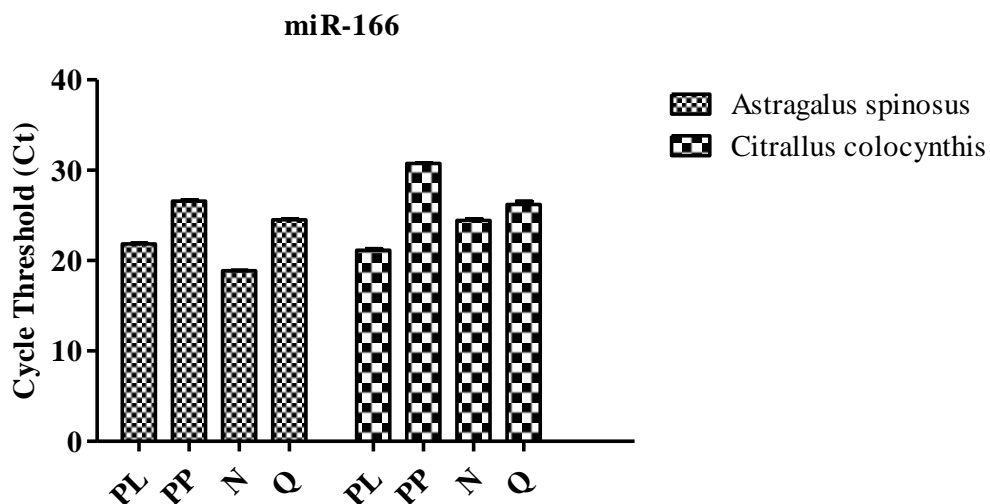
Figure 3.53: The levels of plant miR-166 miRNA in *A. spinosus* **and** *C. colocynthis* **detected by qRT-PCR using various total RNA extraction kits**. **PL**: Purelink kit; **PP**: Power Plant kit; **N**: Norgen kit; **Q**: Qiagen kit. Data are the average ± SEM of triplicate reactions. The lower Ct values indicate the higher miRNA levels.

As seen in Figure 3.54, agarose gel electrophoresis of the TaqMan miR-166 miRNA assay confirmed the presence of a single miR-166-derived amplicon in RNA samples of both plants that extracted with different kits. Lanes 2–10 include RNA samples of *A. spinosus*, *C. colocynthis,* and positive control (Soybean). Lanes 11-15 are RT-samples and a no template negative control and did not display any miR-166 amplicons as one would expect from such controls.
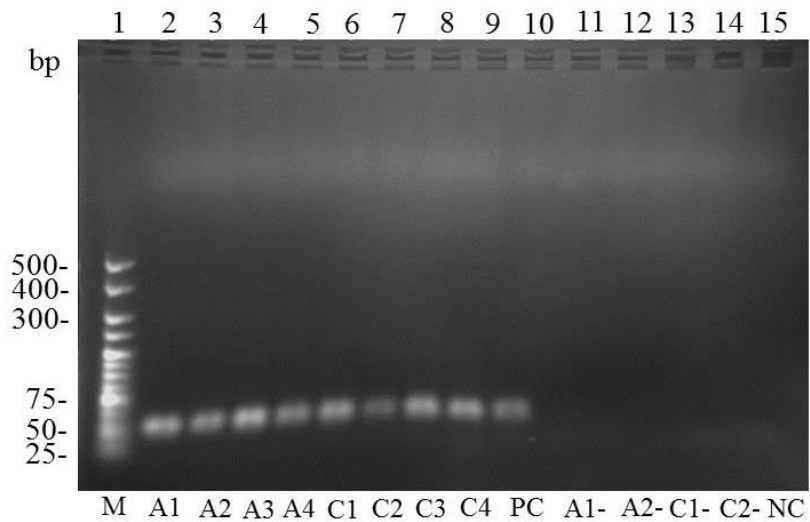
Figure 3.54: Agarose gel image showing amplicons from the qRT-PCR results of the miR-166a assay. Lanes: 1: HyperLadder V DNA marker (Bioline); 2–5 − four RNA samples of *A. spinosus* extracted with different extraction kits; 6-9: three RNA samples of *C. colocynthis* extracted with different extraction kits; 10: positive control (Soybean; PC); 11-13: RT- negative controls of *A. spinosus* and *C. colocynthis*, and 14: H_2O blank negative control (NC). The amplicons were resolved on a 2% (w/v) agarose gel and visualised by ethidium bromide staining.

3.6.4.2 TaqMan-based qRT-PCR

Based on the spectrophotometric and Experion analysis, total RNA extracted from both plants using the Norgen kit were selected to evaluate the presence of miR-167 and miR-168 in a pilot quantitative real-time PCR study with the TaqMan small RNA assays. As seen in Figure 3.55, abundant miR-167 and miR-168 (Ct =23±0.22 and 25±0.01) were detected in *C. colocynthis*. While a moderate quantity (Ct =34.6±0.20 and 31.3±0.21) of both genes were measured in *A. spinosus*. Reaction negative controls such as water blank reactions and RT$^-$ reactions gave "undetermined Ct" values as expected, i.e. no Ct value was returned for these samples over 40 cycles of amplification.

.
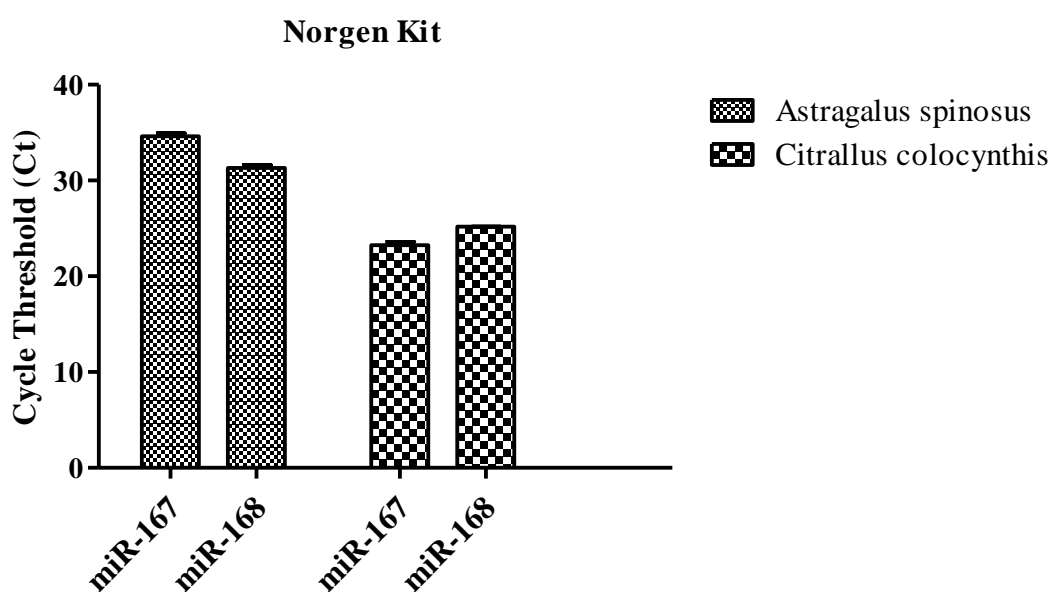
Figure 3.55: The levels of plant miRNAs (miR-167 and miR-168) in *A. spinosus* and *C. colocynthis* samples detected by qRT-PCR following isolation using a Norgen Biotek total RNA extraction kit. The experiment was carried out three independent times (*n* = 3), and the error bars on each column reflect SEM. The lower Ct values indicate the higher miRNA levels.

3.6.4.3 cDNA synthesis and qRT-PCR of biological fluids

The isolated RNA from camel milk and urine were converted to cDNA and then examined using the TaqMan^{TM} miRNA assays to look for the presence of plant miRNAs (miR-166, miR-167, and miR-168). In addition, bovine milk was also analysed to compare it with the camel samples. Ct values showed higher amounts of miR-166 in bovine milk and lower levels in camel milk and urine samples. Detectable levels of miR-167 and miR-168 were found in all the samples (Figure 3.56). No miRNAs were detected in the no-template control which confirmed the lack of nonspecific amplification in the samples. The above preliminary study suggests the presence of plant miRNAs in bovine milk, camel milk, and urine samples.
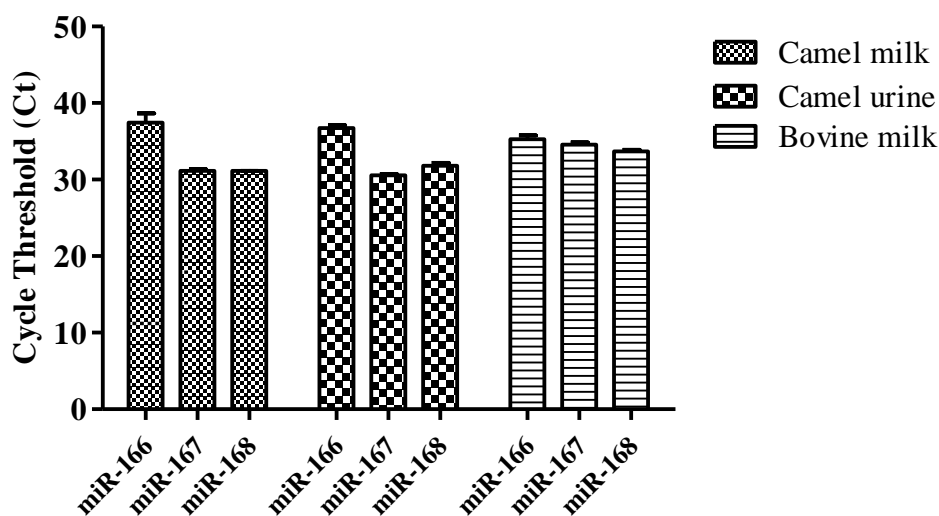
Figure 3.56: The levels of plant miRNAs; miR-166, miR-167 and miR-168 in camel milk, camel urine, and Bovine milk samples detected by TaqMan miRNA qRT-PCR assays. The experiment was carried out three independent times ($n = 3$), and the error bars on each column reflect SEM. The lower Ct values indicate the higher miRNA levels.

3.7 *In vitro* digestion of bovine milk

In vitro digestion of bovine milk was performed to monitor and compare the bioavailability of three plant miRNA in bovine milk following the gastric stage of human digestion. In order to perform this experiment, a drug dissolution tester was used as a simulated digestion system to provide the physical and biochemical conditions similar to that in the human gastric environment to minimise the involvement of human in drug delivery studies (Lee *et al*., 2008).

In the current study, bovine milk samples were tested in the drug dissolution tester to examine the levels of plant-derived miRNAs in these samples after being subjected to the physiological conditions of a human stomach. The bioavailability assessment of plant miRNAs were carried out prior to ingestion and also at a number of time points during the gut stages of digestion. After RNA extraction and stem-loop qRT-PCR, the amplification of qRT-PCR of plant RNA (Figure 3.57) reported that miR-166 levels of bovine milk in the simulated digestion system showed stable levels from 0 min until 19 min and then significant ($p = 0.01$) decrease in their levels after 38 min of digestion suggesting a decrease in their resistance to degradation over time. miR-167 and miR-168 showed constant levels from 0 min until 38 min of early digestion. Their levels during this digestion period suggest a resistance of these miRNAs to degradation unlike miR-166.

The above results demonstrated the survivability and the robustness of some plant-derived miRNAs (miR-167 and miR-168) in a simulated digestion system for 38 min without any significant decrease in their levels. However, a significant ($p = 0.01$) decrease in the levels of the miR-166 was observed during the 38 min incubation in the simulated digestion process.
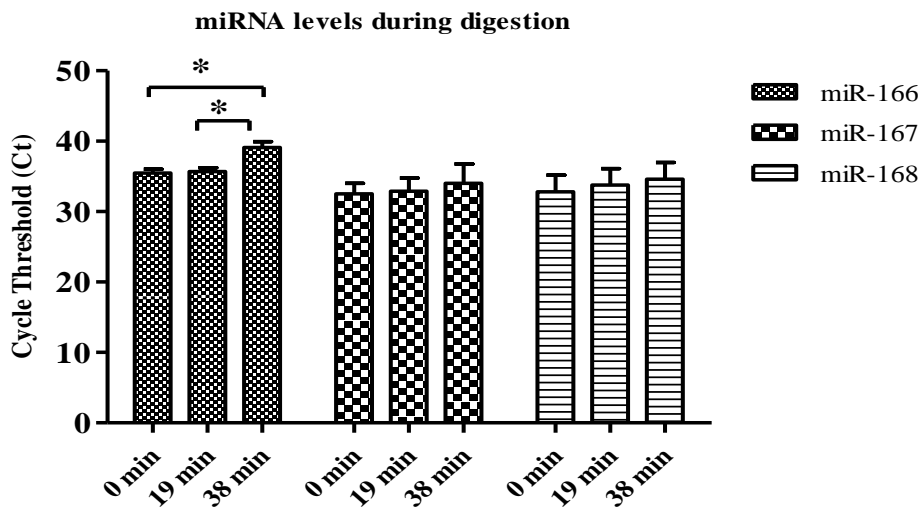
Figure 3.57: qRT-PCR measurement of miRNA levels in bovine milk during digestion in the simulated digestion system (0 min) until 38 min of digestion. Sampling and analysis were carried out three independent times ($n = 3$), and error bars on each column, reflect SEM. The lower the Ct value, the higher the miRNA levels.*The miR-166 levels in the bovine milk sample after 38 min are significantly lower ($p < 0.05$) than the control sample and the incubated sample after 19 min. based on ANOVA and Tukey`s post hoc test. miR-167 and miR-168 show consistent levels from 0 min until 38 min of early digestion and comparable Ct values throughout early digestion for 38 min to the respective values at 0 minute time point.

3.8 Effect of plant miR-167 mimic on *PRLR* expression in cancer cell lines

This assessment was carried out to evaluate the possible regulatory effect miR-167 might have on *PRLR* mRNA expression in several tumour cell lines.

3.8.1 Quantification of human prolactin receptor (*PRLR*) in different human cancer cell lines

3.8.1.1 Total RNA isolation from cancer cell lines and cDNA synthesis

The concentration of isolated total RNA samples was measured using Nanodrop spectrophotometry and showed RNA of high quality and a good yield (Table 3.20). Total RNA isolated from the cancer cells were used as templates for cDNA synthesis.

Table 3.20: RNA yields from several cancer cell lines. LNCap cells showed the highest RNA yield while HeLa cells showed the lowest RNA yield.

Cell line	RNA Yield (µg)	$A_{260/280}$ ratio	$A_{260/230}$ ratio
PANC-1	575.47	2.10	1.96
LNCap	996.14	1.93	2.18
A2780	632.00	2.10	2.02
ZR-75-1	321.76	2.08	1.87
A375	515.20	2.09	2.18
HeLa	175.52	2.07	1.58

3.8.1.2 Quantitative Real-Time Reverse Transcribed Polymerase Chain Reaction (qRT-PCR)

This technique was used to determine relative expression levels of *PRLR* mRNA in six human cancer cell lines: A375, PANC-1, A2780, ZR-75-1, LNCaP, and HeLa cells. As shown in Table 3.21, ZR-75-1 cells express the highest levels of *PRLR* mRNA followed by HeLa cells. The moderate amounts of *PRLR* mRNA were measured in A375 and the levels of *PRLR* mRNA were the lowest in LNCaP cells. While in PANC-1 and A2780 cells, *PRLR* mRNA was not detectable.

Table 3.21: Expression of hPRLR mRNA in several cancer cell lines. Each cell line was placed into 6-well plates and incubated for 24h. Total RNA was prepared from the cells. After reverse transcription, quantitative real-time PCR analysis was performed on the cDNA using selected primers for hPRLR as described in the Methods Section 2.9.7.3. The expression levels of hPRLR mRNA transcripts were normalised to the reference gene *PPIB* using the ΔCt method. Values are the means of $n = 3 \pm$ SEM.

Cancer Cell line	Target Name	Reporter	C_t (Mean±SEM)
ZR-75-1	*PRLR*	SYBR	24.11±0.65
HeLa	*PRLR*	SYBR	29.10±1.21
A375	*PRLR*	SYBR	32.70±0.50
LNCaP	*PRLR*	SYBR	37.00±2.04
PANC-1	*PRLR*	SYBR	ND
A2780	*PRLR*	SYBR	ND

3.8.2 Transfection of several cancer cell lines with plant miR-167

3.8.2.1 Transfection validation

Optimisation of the transfection process is a critical step to ensure successful delivery of small RNAs to studied cell lines.

3.8.2.1.1 Transfection examination by AllStars Hs Cell Death Positive Control siRNA

Successful transfection of the AllStars Cell Death Positive Control siRNA causes a targeted knockdown of genes essential for cell survival. In order to optimise the transfection conditions, the ratio of transfection reagent to siRNA was varied and the viability of each cell line was measured by the MTT cell viability assay. Initially the cells were visualized under microscope at 6h, 12h, 24h, 48h, and 72h post-transfection to observe any changes in the morphology of the transfected cells. The highest level of transfection, as shown by greatest reduction in cell viability, was observed in all cell lines by using a transfection complex of 1μl HiPerFect transfection reagent with 50nM (125ng) siRNA (Figure 3.58). The EC_{50} values of transfected siRNA were calculated in each cell line (Table 3.22). These results suggest that the AllStars Cell Death positive control works as a suitable positive control for transfection and HiPerFect is a suitable transfection reagent for small RNAs for all of the cell lines in this study.
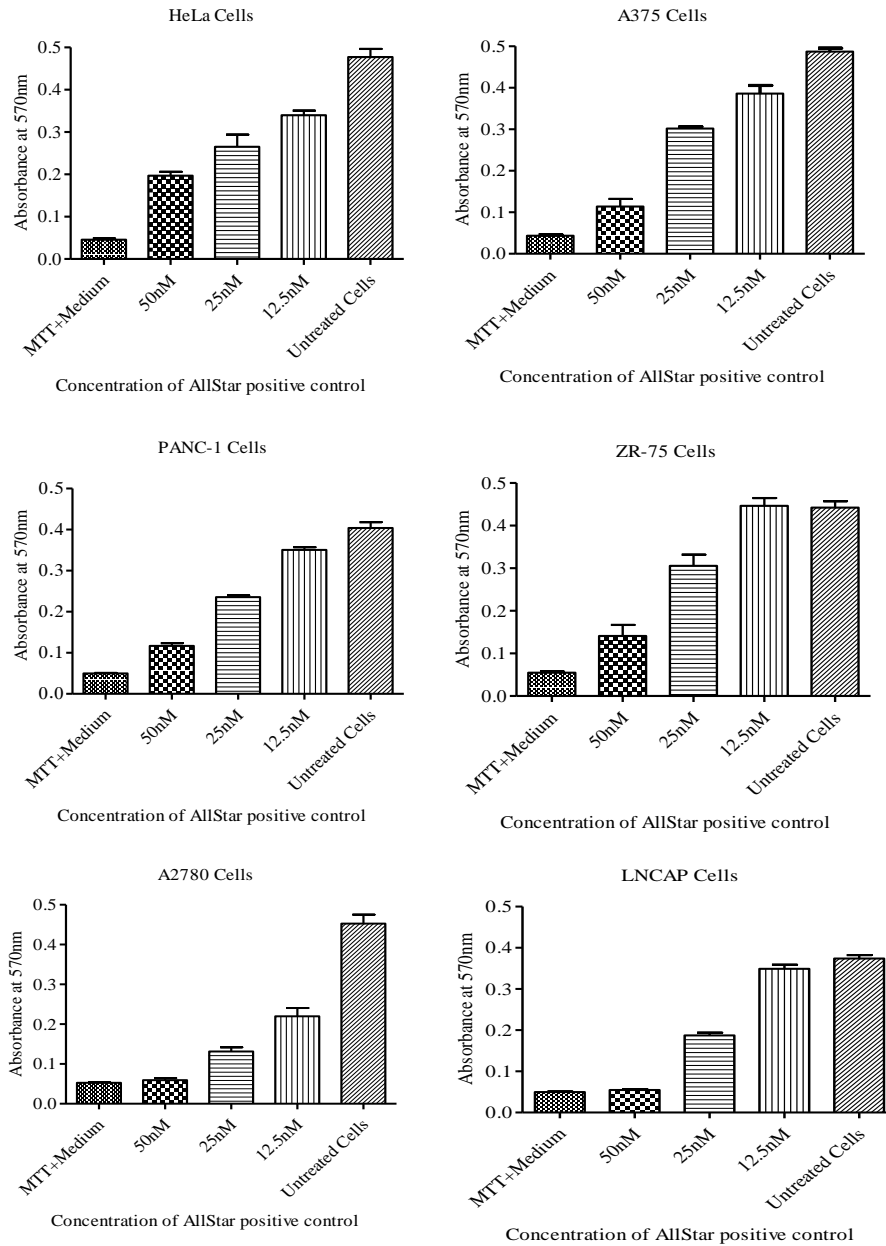
Figure 3.58: The absorbance of the MTT assays of various concentrations of transfected siRNA. Effect of various concentrations of AllStars Cell Death positive control on transfection validation in several cancer cell lines, each cell line was incubated with varying concentrations of AllStars Cell Death positive control (12.5, 25, and 50nM) for 72h at 37°C, 5% CO_2 and 100% humidity, and assayed for cell viability by the MTT assay, Values are the means of $n = 3 \pm SEM$.
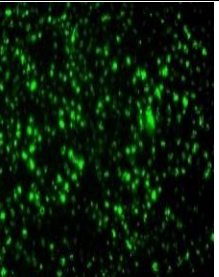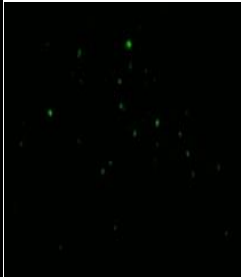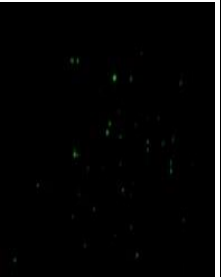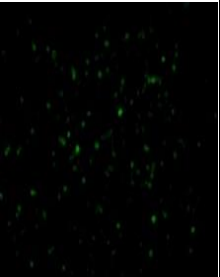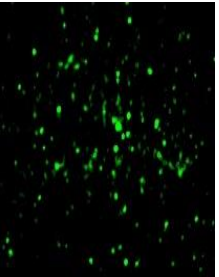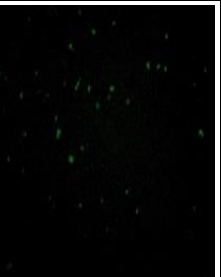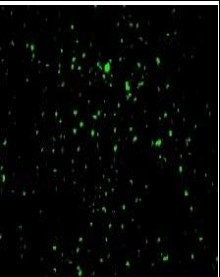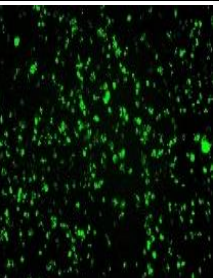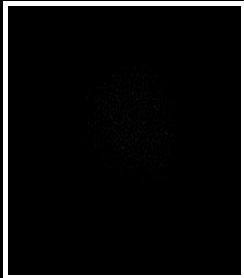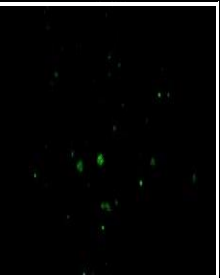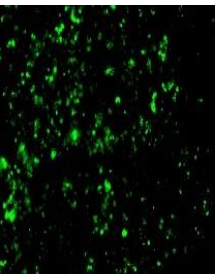
Table 3.22: Effect of AllStars Cell Death positive control on transfection validation in several cancer cell lines. Cells were incubated with 1µl HiPerFect transfection reagent and 50nM (125ng) siRNA for 72h at 37°C, 5% CO2 and 100% humidity, and assayed for cell viability by the MTT assay, EC_{50} values of transfected siRNA were calculated. Values are the means of $n = 3 \pm SEM$.

NO.	Cell line	EC_{50} (nM)±SEM
1	ZR-75-1	38.34±1.76
2	HeLa	36.32±0.69
3	A375	30.66±0.83
4	LNCaP	24.30±0.51
5	A2780	16.61±1.70
6	PANC-1	31.60±0.50

3.8.2.1.2 Transfection examination by AF488-labelled AllStars Negative Control siRNA

AllStars Negative Control siRNA was used for assessment of the transfection method and to determine the optimal conditions for maximum transfection efficiency. The cellular uptake of AF488-labelled AllStars Negative Control siRNA was assessed in each cell line using various concentrations of siRNA and different volumes of transfection reagent at time course study was initially carried out at 6h, 12h, 24h, 48h, and 72h post-transfection. As shown in Table 3.23, the highest level of fluorescence was observed with cells transfected with 150ng AF488-labelled Allstars Negative Control siRNA and 12µl HiPerFect, 72h after transfection. This result suggests that the optimum transfection can be achieved after 72h of transfection with 150ng siRNA and 12µl HiPerFect in all the cell lines.

Table 3.23: Transfection validation using AllStars Cell Death positive control in several cancer cell lines. Fluorescence microscopy of several cancer cells 72h after transfection with Alexa fluorescent AF488-labelled AllStars Negative Control siRNA. The cell lines were treated with the following: 1) 75ng siRNA with 6µl HiPerFect; 2) 75ng siRNA with 12µl HiPerFect; 3) 150ng siRNA with 6µl HiPerFect; 4) 150ng siRNA with 12µl HiPerFect.

Cell line	Treatment 1	Treatment 2	Treatment 3	Treatment4
ZR-75-1				
HeLa				
A375				
LNCaP				

3.8.3 Expression of *PRLR* mRNA after transfection of miR-167 mimic into several human cancer cell lines

To evaluate the possible regulation of *PRLR* expression by miR-167, several cancer cell lines were transfected with miR-167 mimic and processed as described in Methods Section 2.8.8.2.

As shown in Figure 3.59, transfection of ZR-75-1 cells with miR-167 mimic resulted in a significant (p = 0.01) up-regulation of the expression of *PRLR* mRNA by 4.05±0.41 fold compared to non-transfected cells. It has been reported that *PRLR* is involved in breast cancer development and the majority of human breast tumours have higher *PRLR* levels than surrounding normal mammary tissues (Pierce and Chen, 2001). The overexpression of *PRLR* mRNA may induce abnormal proliferation of breast epithelium (Pan *et al*., 2007).

In contrast, transfection of miR-167 mimic into A375 cells induced down-regulation in *PRLR* mRNA expression by 5±0.05 fold, compared with the control (cells only).

The expression levels of *PRLR* mRNA in HeLa and LNCaP cells were similar before and after transfection with miR-167 mimic, suggesting that there was not significant impact of miR-167 mimic on the expression profile of *PRLR* mRNA in both these cancer cell lines (P > 0.05).

The effect of HiPerFect reagent alone on the expression profile of *PRLR* mRNA was assessed in all tested cell lines. It was close to the control in each cell line (fold change from 0.86 to 1.98). This indicated that this transfection reagent did not significantly (P > 0.05) affect the expression level of the target gene (*PRLR*).
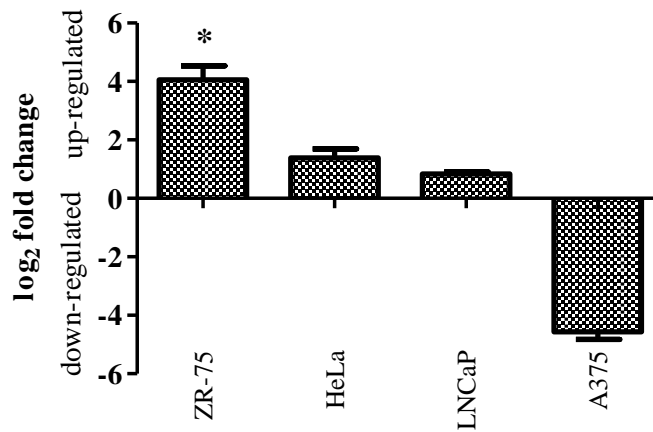
Figure 3.59: The effect of miR-167 mimic on PRLR mRNA expression in several human cancer cells. Each cell line was incubated with a transfection complex of 150ng miR-167 mimic and 12µl HiPerFect for 72h at 37°C, 5% CO_2, and 100% humidity. Total RNA was prepared from the cells. After reverse transcription, quantitative real-time PCR analysis was performed on the cDNA using selected primers for *PRLR*. Relative expression levels of *PRLR* mRNA transcripts were normalised to the reference gene *PPIB* using the ΔΔCt method. All values showed in the histogram represented as log2 fold change compared to the control group average of 1. Values are the means of *n* = 3 ± SEM. *P < 0.05 versus control.

3.8.4 Expression of *PRLR* mRNA after transfection of *C. colocynthis* total RNA sample into several human cancer cell lines

This experiment was performed to assess whether the isolated *C. colocynthis* RNA sample, containing miR-167 amongst others, had a similar effect on PRLR expression as the miR-167 mimic in the tested cancer cell lines. Cancer cells were transfected with plant total RNA sample and processed as described in Methods Section 2.8.8.3.

Figure 3.60 shows a preliminary result of transfection of human cancer cell lines with a *C. colocynthis* total RNA sample. There was a down-regulation of *PRLR* mRNA expression in ZR-75-1 after transfection of 150ng of total RNA showing a 1.31 fold change. While an up-regulation of 0.36 fold of *PRLR* mRNA was observed after transfection of 300ng of plant total RNA compared to the control cells.

After transfection of 150ng of total RNA into HeLa cells, there was an up-regulation of *PRLR* mRNA expression compared to the non-transfected HeLa cells (a 6.06 fold increase in expression). A similar up-regulation effect was observed when the cells were transfected with 300ng of plant total RNA, but with lower fold change of 1.81 when compared to the control cells.

Transfection of LNCaP cells with 150ng of plant total RNA caused a 1.72 fold drop in *PRLR* mRNA expression. In contrast, a 300ng of total RNA up-regulated *PRLR* mRNA expression by 7.31 fold compared to non-transfected LNCaP cells.

A 3.97 fold up-regulation of *PRLR* mRNA expression was observed in A375 cells when transfected with 150ng of total RNA. While transfection of the same cells with higher concentration (300ng) of total RNA resulted in reduction of *PRLR* mRNA expression by 2 fold compared with non-transfected cells.

Compared with the control, there were no noticeable differences observed with the use of HiPerFect reagent alone on the expression profile of *PRLR* mRNA in all tested cell lines.

This initial observation gives an indication that the complex nature of *C. colocynthis* total RNA sample with hundreds of different miRNAs present in the sample, and possible extraction carry-over contaminants could cause cellular responses which could not be attributed to miR-167 alone. The obtained result requires further validation as the data were from an individual experiment. Also, further work is needed to assess if the results are indicating general toxicity.
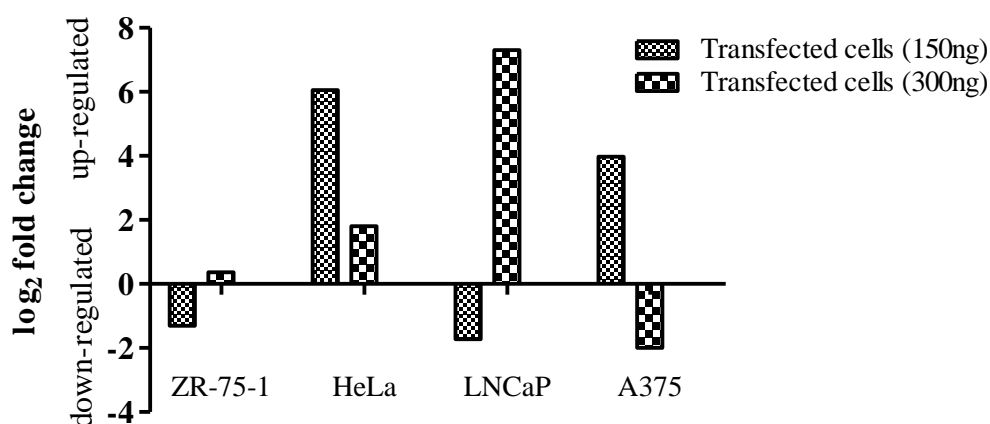
Figure 3.60: The effect of *C. colocynthis* total RNA sample on *PRLR* mRNA expression in several human cancer cells. Each cell line was incubated with two different concentrations (150 and 300ng) of RNA sample for 72h at 37°C, 5% CO_2 and 100% humidity. Total RNA was prepared from the cells. After reverse transcription, quantitative real-time PCR analysis was performed on the cDNA using selected primers for *PRLR*. Relative expression levels of *PRLR* mRNA transcripts were normalised to the reference gene *PPIB* using the ΔΔCt method. All values showed in the histogram represented as log2 fold change compared to the control group average of 1. The figure represents the data from one individual experiment.

3.9 Plant genotyping

3.9.1 Plant genomic DNA isolation

Purified plant genomic DNA samples isolated using the GenElute™ Plant Genomic DNA Miniprep Kit were assessed spectrophotometrically (Table 3.24). Low A260/230 ratios may be due to salt carry-over contamination in the sample.

Table 3.24: DNA yields from plant samples.

Sample Name		DNA Yield (μg)	260/280 ratio	260/230 ratio
T. aphylla	Sample 1	109.60	1.81	1.65
	Sample 2	12.68	0.98	0.25
C. colocynthis	Sample 1	112.84	1.84	1.43
	Sample 2	36.20	1.80	0.64

3.9.2 The Inter-Simple Sequence Repeat-PCR (ISSR-PCR)

As plant samples used in this study were collected from different places, ISSR-PCR was carried out to characterise and evaluate the genetic diversity between two samples of each plant (*T. aphylla* and *C. colocynthis*) to ensure that the plant samples tested were of the same species. Each ISSR marker was repeated twice separately to confirm the result of the ISSR band patterns. The molecular profile generated by each ISSR primer used is presented in Figure 3.61A was different and showed a mixed pattern of variability in both samples of *T. aphylla*. In Figure 3.61B, the primer (A) showed less variation between two samples of *C. colocynthis* comparing with other ISSR markers.

As shown in Figure 3.61 A & B, there was variation of the intensity of the bands that can influence the reproducibility of ISSR reactions. Band variation is attributed to various issues such as integrity, quality and quantity of template DNA (Wolff *et al*., 1995). Working with degraded DNA in ISSR-PCR produced faint or no DNA bands when fractionated by electrophoresis in an agarose gel and affected the results. This concern about ISSR efficacy could be resolved by using fresh plant material to ensure extraction of intact nucleic acid. Also by standardising the quantity of template DNA used in each PCR reaction. For example, using insufficient of DNA quantities across PCR reactions could result in inconsistent concentrations of PCR amplification products, affecting band intensities and compromise the banding pattern in the ISSR experiment.
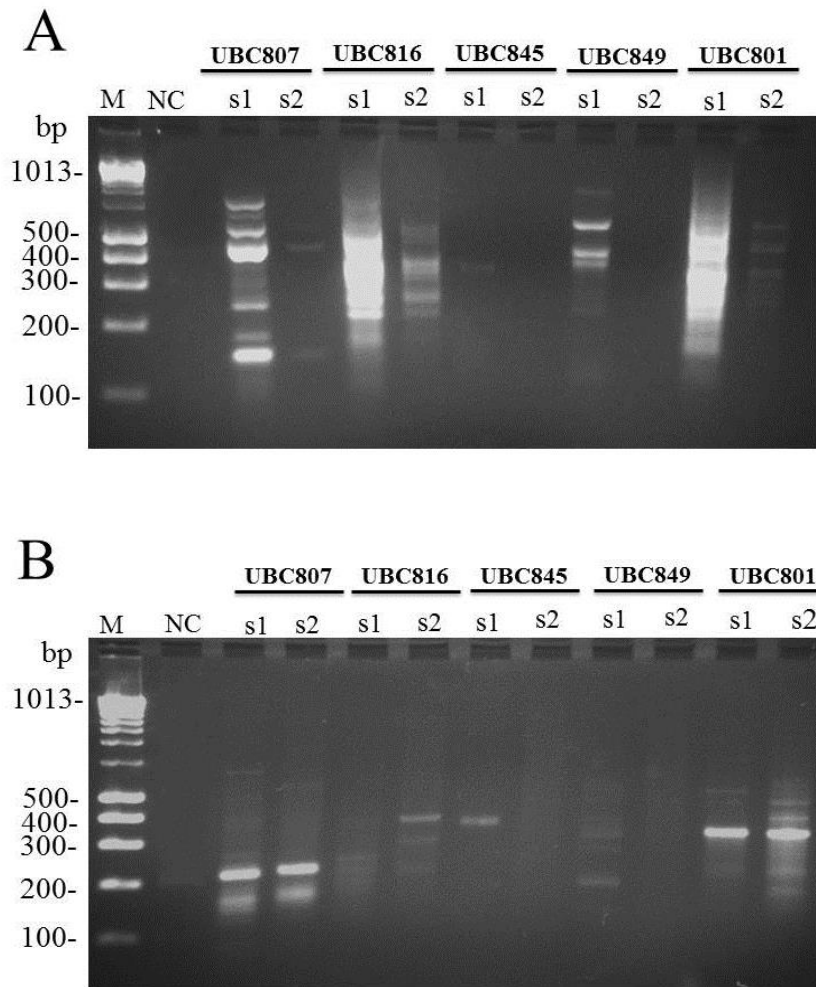
Figure 3.61: **ISSR marker profiles obtained from (A)** *T. aphylla* **and (B)** *C. colocynthis***.** Lane 1 (M): HyperLadder 100bp (Bioline) (100 - 1013 bp); Lane 2 (NC): H$_2$O blank negative control; lane 3,5,7,9 and 11: sample **1**; lane 4, 6,8,10 and 12: sample **2**. ISSR amplification products were produced using primers; UBC(9)807 , UBC(9)816 , UBC(9)845 , UBC(9)849, UBC(9)801 and separated on 0.3% (w/v) agarose gel.

Chapter 4 Discussion

4.1 Phytochemistry and biology

One of the aims of this project was to investigate whether the potential anti-cancer property of camel milk and urine is derived from plants eaten by the camels as fodder, which may be a source of therapeutically active compounds which could transfer to the milk and urine to provide potential medicinal agents. Therefore, isolation and identification of bioactive compounds from the plants was carried out followed by an investigation to see if the presence of any of these compounds or their metabolites could be found in camel milk and urine.

The phytochemical investigation was carried out on *R. epapposum*, *A. spinosus*, *T. aphylla* and *C. colocynthis* as these are commonly found in camel fodder. The isolated compounds in sufficient quantities were then evaluated for potential cytotoxicity against the following cancer cell lines; LNCaP, HeLa, PANC-1, A375, A2780, ZR-75-1 and a normal cell line (PNT2).

Fractionation of the methanol extract of *T. aphylla* led to the isolation of simple phenolic cinnamate compounds; TA-1 which was a mixture of two compounds *trans*-coniferyl alcohol-4-*O*-sulphate and *trans*-coniferyl acetate-4-*O*-sulphate **(TA-1a and TA-1b)** and isoferulic acid-3-*O*-sulphate **(TA-2)**, 3`, 4`, 5, 7-tetrahydroxyflavone **(TA-3)** and the amino acid *N*-methyl-4-hydroxyproline **(TA-4)**. In this study, the cytotoxicity screening of the isolated compounds (Results Section: 3.5.2.1) showed cancer cytotoxicity of the compounds; **TA-1** against A375 (melanoma) cell line (EC_{50}= 25.18±1.5µg/ml) and **TA-3** against HeLa (cervical) cells (EC_{50} =86.50±0.51µM). While the compound **TA-2** did not show any activity against the tested cancer cell lines. The cytotoxicity assessment of **TA-4** was not carried out because of low yield.

Compound **TA-1a** had previously been isolated from the stem bark of *T. gallica*, *T. Africana* and *T. bobeana* (Tomás-Barberán *et al*., 1990) and from the leaves of *T. nilotica* (Abouzid *et al*., 2009). *Trans*-coniferyl alcohol-4-*O*-sulphate was tested by Abouzid *et al*. (2009) for its *in vitro* antioxidant activity using a DPPH radical

scavenging assay and did not show any activity. No other studies have described any bioactivity of this compound, whereas **TA-1b** has not been reported before. This mixture showed cytotoxic activity to the tumour cell line (A375) when compared with the non-tumour cell line (PNT2). Therefore, it was thought that separation of the two compounds could therefore help with development of an anti-cancer therapeutic. Compounds TA-1a and TA-1b are simple phenolic cinnamate compounds and these types of compound are widely reported for many health benefits such as anti-inflammatory, antibacterial, antiproliferative, anticarcinogenic and antioxidative activities (Cheng *et al*. 2007). For example, ferulic acid and its derivatives such as ferulic acid ethyl ester have demonstrated potent antioxidant activity in both *in vitro* and *in vivo* systems. Similarly, caffeic acid and some of its derivatives such as rosmarinic acid and phenethyl ester exhibit antioxidant activity (Kumar and Pruthi, 2014). Therefore, it would be a useful idea to examine TA-1a and TA-1b against the above biological activities.

While different purification methods were applied to attempt to separate this mixture, such as Sephadex column, preparative TLC, Biotage flash system and Reveleris® Prep Purification System, all of these methods failed to separate the mixture. Further work is required to separate the mixture of **TA-1a** and **TA-1b** to isolate the pure compounds in sufficient quantities, using another purification method such as High Performance Liquid Chromatography (HPLC), so that physical data for the pure substances can be obtained (e.g. melting point) and to enable biological tests to be carried out on the pure compounds. In addition, analysis of the milk and/or urine samples using LC-MS to check if any of these compounds or their metabolites exist in the milk or urine would be important. Furthermore, in the case of the presence of these compounds in camel milk, it could be that they work as natural preservatives to the milk thus performing antibacterial and antioxidant tests would be appropriate. Therefore, further investigation needs to be done in this regard to examine the potential biological activity of these compounds. In addition to antibacterial and antioxidant activities, it was reported that *T. aphylla* posesses anti-inflammatory activity (Vadlapudi *et al*., 2009; Yokosuka and Alqasoumi, 2011).

Compound **TA-2** was isolated for the first time from *T. aphylla* leaves and it was isolated previously from the flower of *T. amplexicaulis* (El Moussallami *et al*., 2000). **TA-2** did not exhibit cell toxicity against the cancer cell lines used in the present study. There are no previous reported biological activities of this compound. Thus for future work, screening of this compound for various biological activities needs to be carried out.

TA-3 was previously isolated from *T. aphylla* leaves (Mahfoudhi *et al*., 2014). It showed different biological activities such as antibacterial, antioxidant, hepatoprotective, anti-cancer and anti-inflammatory, anti-allergic, and antiviral activities (Kawai *et al*., 2007; Lopez-Lazaro, 2009; Yadav *et al*., 2013). The flavonoid luteolin has also previously been tested against *Mycobacterium tuberculosis* $H_{37}Rv$ and showed strong activity with a MIC of 25μg/ml (Yadav *et al*., 2013). In addition, the anti-methicillin-resistant *Staphylococcus aureus* (MRSA) activity of luteolin has been previously reported with inhibition against some clinical MRSA strains (MICs= 64μg/ml) (Qiu *et al*., 2011). In this study, **TA-3** exhibited cytotoxic activity against HeLa cells (86.50±0.5μM) compared with the normal cell line (PNT2). Luteolin did not show cell cytotoxicity up to 100μM in PANC-1, A2780, LNCaP and A375 cells. In contrast with this result, Chiu and Lin (2008) demonstrated that luteolin can target the androgen receptor (AR) causing down-regulation of AR expression followed by inhibition of cell proliferation and induction of apoptosis in LNCaP cells and in a xenograft tumour model. Various studies have demonstrated the anti-cancer property of luteolin in several cancer cell lines through different mechanisms including; the induction of apoptosis and cell cycle arrest, and the inhibition of metastasis and angiogenesis, including the A549 non-small lung cancer cell (Cai *et al*., 2011), through a caspase-dependent mechanism in human epitheliod cancer (Attoub *et al*., 2011), human oesophageal adenocarcinoma (Zhang *et al*., 2008) lung cancer cells (NCI-H460) through Sirt1-mediated apoptosis (Ma *et al*., 2015). Moreover, luteolin causes inhibition of the extracellular signal-regulated kinase (ERK) signaling pathway in human mast

cell HMC-1 (Kang *et al.* 2010), prostate cancer (Xavier *et al.*, 2009), colorectal cancer (Yamaguchi *et al.*, 2011), lung cancer (Kim *et al.*, 2007) and human hepatoma HepG2 cells (Lee *et al.*, 2006). Xu *et al.* (2016) revealed that the combination of luteolin with the chemotherapeutic drug 5-fluorouracil could synergise the antitumour effects of 5-fluorouracil on hepatocellular carcinoma cells (HepG2 and Bel7402), which improved tumour protein p53 (tumour suppressor) expression and decreased the dihydropyrimidine dehydrogenase which is involved in the degradation of 5-fluorouracil. In contrast with our result, a recent study conducted by Han *et al.* (2016) investigated the effect of luteolin on PC3 and LNCaP prostate cancer cells. The results demonstrated that luteolin inhibited cell proliferation and induced apoptosis through down-regulation of miR-301 by increasing the expression of death effector domain-containing protein 2 (DEDD2), potent inducers of apoptosis in various cell types. This difference in the results could be due to a different assay used by Han and colleques to measure cell viability in which they used a CCK-8 assay rather than the AlamarBlue® assay used in the present study.

TA-4 was identified as *N*-methyl-4-hydroxyproline and this is the first report of this compound from *T. aphylla*. This compound was isolated previously from the dichloromethane extract of *Trichilia lepidota* leaves (Pupo *et al.*, 2002) and the red alga *Chondria coerulescens* (Sciuto *et al.*, 1983). It was not possible to screen this compound for cytotoxicity due to the limited quantity available. Increasing the initial amount of the plant is required to improve the compound yield followed by further work to purify this compound as it has minor impurities which may also be interesting. However, the political unrest in Libya and the limited time prevented this from being carried out in the present work. There are no previous reports demonstrating any biological activity for this compound. However, *N*-methyl amino acids have shown a potential role in prevention or therapy of Alzheimer′s disease or the physiological symptoms of this disease such as neurofibrillary tangles and amyloid plaque by decreasing neuritic plaques composed of fibrillar beta-amyloid (Gordon *et al.*, 2001).

Fractionation of *T. aphylla* hexane and ethyl acetate extracts was performed using column chromatography. The ^{1}H NMR spectra of both extracts showed signals suggesting the presence of mixtures of triglycerides and fats. No literature has reported phytochemicals from the hexane and ethyl acetate extracts of *T. aphylla*.

Chromatographic separation of the methanol extract of *A. spinosus* leaves resulted in the isolation of four compounds; pinitol **(AS-1)**, cycloartane-type triterpenoids; cycloastragenol **(AS-2)** and its glycoside cycloastragenol-6-*O*-glucoside **(AS-3)**, and maackiain **(AS-4)**. This is the first report of **AS-1** and **AS-4** from *A. spinosus* while, **AS-2** and **AS-3** were isolated previously from this plant. The cytotoxicity screening was performed only on **AS-1** due to the inadequate quantities of the other compounds. **AS-1** did not show any cytotoxic activity against tested cells. **AS-1** has been shown to act as a hypoglycemic agent in mice and its ability to treat symptoms associated with diabetes because of its insulin-like property (Mijares *et al*., 2013; Gao *et al*., 2015). It has been shown to possess an insecticidal effect on the larval growth of *Heliotis zea, Aedes aegypti* and *Culex quinquefasciatus* (Chaubal *et al*., 2005). It is also reported to have antiviral (Zhan *et al*., 2006), larvicidal (Chaubal *et al*., 2005), anti-inflammatory (Singh *et al*., 2001), antihyperlipidemic (Geethan *et al*., 2008), cardioprotective activities (Kim *et al*., 2005) and it causes inhibition of the T helper cell-1 response (Lee *et al*., 2007). Additionally, Rengarajan *et al*. (2011) reported a protective role of pinitol against 7, 12 dimethylbenz (a) anthracene (DMBA) induced breast cancer in rats. Existence of such a compound with the above bioactivities in camel feed could be associated with the therapeutic activities of camel milk and urine claimed by the Bedouins.

Compounds **AS-2** and **AS-3** belong to cycloartane-type triterpenoids, the main compounds encountered in the *Astragalus* genus with a characteristic cyclopropane moiety in the ring of C-9, C-10 and C-19 which is absent in most common triterpenoids such as oleanane- or ursane-type triterpenoids (Vincken *et al*., 2007). The cycloartanoid compounds have shown various biological activities such as

hepatoprotective, wound healing, antineoplastic, diuretic, tonic and antiallergic activities (Yeşilada *et al.*, 2005; Boroujerdnia *et al.*, 2011; Sevimli-Gür *et al.*, 2011; Nalbantsoy *et al.*, 2012). These cycloartanoid compounds with a set of biological activities could be directly connected to the therapeutic uses of camel products.

Cycloastragenol (**AS-2)** is the main aglycone of many cycloartane-type glycosides and has been identified from various species of *Astragalus*. Cycloastragenol is a strong antioxidant and was also shown to extend T cell proliferation by increasing telomarase activity *in vivo* and *in vitro* and thus delaying the on-set of cellular aging (Valenzuela *et al.*, 2009; Weiss and Weiss, 2014). Also, Ip *et al.* (2014) revealed the potential role of cycloastragenol as antidepressant treatment. The authors demonstrated that the compound has the ability to stimulate telomerase activity in human neonatal keratinocytes and rat neuronal cells, and induces cAMP response element binding (CREB) activation in neuronal cells followed by telomerase reverse transcriptase (TERT) and B-cell lymphoma 2 (bcl2) expression indicating its role as a potential treatment for depression. In addition, Sevimli-Gür *et al.* (2011) revealed that cycloastragenol possessed *in vivo* wound healing properties and was found to stimulate fibroblast growth *in vitro*. Furthermore, Zhao *et al.* (2015) investigated the role of cycloastragenol in regulation of endothelial homeostasis in the setting of endoplasmic reticulum stress (ER stress). The authors demonstrated that cycloastragenol protected endothelial homeostasis by suppression of ER stress-associated thioredoxin-interacting protein/NOD-like receptor protein 3 (TXNIP/NLRP3) inflammasome activation.

The compound **AS-3** was identified as cycloastragenol-6-*O*-glucoside also called cycloastragenol monoglycoside. The biological activities of this compound have still to be investigated. However, cycloartane glycosides have a wide range of therapeutic activities (mentioned below) and it will be worthwhile evaluating the potential biological activities of this compound. Astragalus species are rich in cycloartane-type triterpene glycosides that possess various biological activities including AIDS antiviral activity in some cycloartane glycosides such as astragaloside II (Abdallah *et*

al., 1993; Gariboldi *et al*., 1995), antioxidant activity (Tsaruk *et al*., 2010; Denizli *et al*., 2014) and astragaloside I which showed immunostimulant effects on macrophage activation and expression of inflammatory cytokines (Bedir *et al*., 2000). Some cycloastragenol glycosides are reported to act as modulators of lymphocyte proliferation (Verotta *et al*., 2002) and a number of cycloartane glycosides, including cyclocanthoside E and astragaloside II are reported to exhibit trypanocidal activity against *Trypanosoma brucei* and leishmanicidal effects against *Leishmania donovani* with IC$_{50}$ values ranging from 13.2 to 21.3µg/ml (Ozipek *et al*., 2005). Cycloartane glycosides are also reported to have cytotoxic effects against many human cancer cell lines including hepatocarcinoma (SMMC-7721), breast cancer (MCF-7), colon adenocarcinoma (SW480), liver carcinoma (HepG2), and gastric cancer cells (SGC-7091) (Yokosuka *et al*., 2010; Wang *et al*., 2015; Zhu *et al*., 2015; Wu *et al*., 2016), that indicates the importance of these compounds as a source of antitumour agents.

Compound **AS-4** was identified as a pterocarpan compound (maackiain) which was isolated from the roots of *Maackia amurensis* (Matsuura, *et al*., 1994) and this is the first report of maackiain from *A. spinosus*. Pterocarpans are isoflavonoid derivatives that mainly exist in leguminous plants and soybean (*Glycine max*) (Vitch, 2007; Shibata and Dastmalchi and Dhaubhadel, 2014). They are reported to have several bioactivities including anti-cancer, antoxidant, antimicrobial and antifungal effects (Honda and Tabata, 1982; Maximo *et al*., 1998; Yuearatanechemuge *et al*., 2004; Jiménez-Gonza´lez *et al*., 2008). Due to the low yield of this compound, the cytotoxicity assessment was not carried out in this work. One study conducted by Yuearatanechemuge *et al*. (2004) examined cytotoxicity of maackiain and showed that it induced apoptosis in human promyelocytic leukemia (HL-60) cells. Another study by Mizuguchi *et al*. (2015) demonstrated strong cell toxicity of maackiain on HeLa cells at a concentration of 30µM whereas no cytotoxicity effect was shown on basophilic leukemia (RBL-2H3) cells at higher concentration of 150µM. A recent study supports the cytotoxicity effect of maackiain against several human reproductive system cancer cell lines (Yoon *et al*., 2016). This study revealed potent cytotoxicity against the following cancer cells; HeLa (21.33±0.04µM), ovarian

carcinoma (OVCAR-3) (36.12±0.43μM), LNCaP (>100), and prostate cancer (PC-3) (>100) (Yoon *et al.*, 2016). In addition, the antioxidant activity of maackiain was evaluated by Jung *et al.* (2005) using the (1, 1-diphenyl-2-picrylhydrazyl) DPPH radical scavenging activity assay and revealed no activity at the highest concentration (100μM). Mizuguchi *et al.* (2015) evaluated the effect of maackiain in toluene 2, 4-diisocyanate (TDI)-sensitised allergy model rats and revealed the anti-allergic property of maackiain for first time. This study suggested that the compound can improve the allergic symptoms through the inhibition of histamine H_1 receptor (H_1R) and interleukin (IL)-4 gene expression. Furthermore, an earlier study demonstrated a strong antifungal effect of maackiain against *Monilinia fructicola* (Winter) Honey (Perrin and Cruickshank, 1969). It also demonstrated an inhibitory effect on the growth of plant pathogens including *Pythium graminicola* which infects cereals (Yagi *et al.*, 1993) and can inhibit *Fusarium oxysporum* growth which infects chickpea (*Cicer arietinum*) one of the main food sources for human and domestic animals (Stevenson *et al.*, 1997). This potent antifungal activity could be attributed to the fact that the lipophilic nature of the compound can allow it to penetrate more easily through the fungus membranes (Harborne, 1978). No compounds were separated from the fractionation of *A. spinosus* hexane extract and the ^{1}H NMR spectrum of this crude extract displayed signals that indicated the existence of the mixture of fats.

Fractionation of the methanol and ethyl acetate extracts of *C. colocynthis* leaves was carried out and led to identification of two compounds; cucurbitacin E **(CC-1)** and cucurbitacin E-2-*O*-β-D-glucoside **(CC-2)** (Results Section 3.3.1 and 3.3.2). Both compounds have previously been reported from *C. colocynthis* fruits and leaves (Lavie *et al.*, 1964; Hatam *et al.*, 1989; Chawech *et al.*, 2015). Cucurbitacins and their glycosides are triterpenoid steroids isolated initially from plants of the Cucurbitaceae family (Tannin-Spitz, 2007; Wakimoto *et al.*, 2008) and also have been reported in other plant families such as Scrophulariaceae and Brassicaceae (Greige- Gerges *et al.*, 2007; Kaya and Melzig, 2008). They are reported to have a wide range of biological activities such as anti-inflammatory, analgesic,

antimicrobial, antihelminthic, antitumour, antioxidant, free radical-scavenging, antiproliferative, hepatoprotective and cardiovascular *in vitro* and *in vivo* (Agil *et al*., 1999; Jayaprakasam *et al*., 2003; Blaskovich *et al*., 2003; Chen *et al*., 2005b). In this study, these compounds were evaluated for *in vitro* cytotoxic activity on several human cancer cell lines and one normal cell line. The results (Section 3.5.2.1) revealed that one of the isolated compounds **(CC-2)** presented specific cytotoxic activity towards A375 ($58.00\pm1.20\mu M$), A2780 ($62.27\pm1.76\mu M$) and ZR-75-1 ($55.25\pm1.15\mu M$) cell lines while **CC-1** showed cytotoxicity against HeLa ($85.11\pm1.20\mu M$) and was also found to be toxic to normal cells (PNT2) ($73.61\pm1.26\mu M$). Although **CC-1** was investigated previously for its antitumour activity, no data were presented for the cell lines used in the present work.

A study by Bartalis and Halaweish (2005) evaluated the cytotoxic effect of **CC-1** and showed that its activity is related to its structure and demonstrated that the cytotoxicity increased linearly with hydrophobicity and proposed that lipophilicity increases the basal toxicity of cucurbitacins on tumour cells. Compound **CC-1** has been reported to possess various bioactivities such as anti-inflammatory (Abdelwahab *et al*., 2011; Qiao *et al*., 2013), immunomodulatory action on peripheral human lymphocytes, and antitumour activity through different mechanisms (Sun *et al*., 2010; Dong *et al*., 2010; Zhang *et al*., 2012b; Qiao *et al*., 2013; Lan *et al*., 2013). Recent studies have demonstrated that **CC-1** has growth-inhibitory effects on the proliferation of many cancer cells such as bladder cancer, hepatocellular carcinoma, pancreatic cancer, breast cancer (Zhang *et al*., 2012b; Lan *et al*., 2013; Kong *et al*., 2014), leukaemia (Sörensen *et al*., 2012), the chondrosarcoma SW 1353 cell line (Abbas *et al*., 2013) and oral squamous cell carcinoma (Hung *et al*., 2013).

Lee *et al*. (2010) have suggested the use of cucurbitacins in combination with known chemotherapeutic agents to obtain the same therapeutic effect with lower chemo doses and less toxicity because of their nonspecific toxicity. An *in vitro* evaluation of cytotoxic activity of compound **CC-2** against human hepatocellular carcinoma

(HepG2) cells revealed that it had cytotoxicity with an IC_{50} of 226.7μM (Bartalis and Halaweish, 2005). Also, this compound was reported to have an insecticidal effect against *Aphis craccivora* (Torkey *et al.*, 2009).

Silica gel CC was applied to fractionate *R. epapposum* hexane extract and led to isolation of eudesmane-type sesquiterpene lactone **(RE-1)**. The ethyl acetate and methanol extract fractionation of the leaves of *R. epapposum* led to the isolation and characterisation of three compounds; chlorogenic acid **(RE-2)**, 3,4 dicaffeoylquinic acid **(RE-3)** from ethyl acetate extract, and a mixture of two flavonoids **(RE-4a& b)** from the methanol extract. All of the isolated compounds in this study were identified for first time from *R. epapposum*.

RE-1 was identified as 2-hydroxyalantolactone, a sesquiterpene lactone and it was previously isolated from the same plant family from the aerial parts of the *Francoeuria crispa* and *Inula helenrum* (Al-Yahya *et al.*, 1984; Vajs *et al.*, 1989). In this work, no cell cytotoxicity was shown up to 100μM of **RE-1** on the other tested cancer cell lines. Al-Yahya *et al.* (1984) revealed borderline cytotoxic activity of this compound against murine P-388 lymphocytic leukemia. In the same study, the antimicrobial activity of **RE-1** was screened against *S. aureus, E. coli*, *Pseudomonas aeruginosa*, *Salmonella* sp, and *C. albicans* and showed slight activity only against *S. aureus*.

RE-2 was identified as chlorogenic acid and has been shown to possess a wide range of biological activities including anti-cancer, anti-inflammatory, antiviral, and antibacterial. Previous *in vitro* experiments showed that the anti-cancer activity of **RE-2** comes through different mechanisms including inhibition of cell growth, regulation of cell cycle, and induction of apoptosis pathways (Xu *et al.*, 2013). Recently, it was reported that **RE-2** had a protective effect on mitochondria *in vitro*: **RE-2** suppressed mitochondrial membrane depolarisation in H_2O_2-treated PC-12 cells (Park *et al.*, 2013). Cha *et al.* reported that pre-treatment with **RE-2** prevented disruption of the mitochondria permeability potential in UVB-irradiated HaCaT cells (Cha *et al.*, 2014). Chiang *et al.* (2002) revealed that **RE-2** has a strong

inhibitory effect on adenoviruses (ADV-3, ADV-11) and herpes simplex viruses (HSV-1, HSV-2). An *In vivo* experiments carried out by Liu *et al*. (2016) has demonstrated the anti-influenza activity of **RE-2** by promoting the survival rates from 40% to 56% in influenza A H1N1 infected mice. In addition, the compound **RE-2** was reported to have antibacterial effect on *E. coli*, *S. aureus* and *Micrococcus luteus* (Lin *et al*., 2004). Furthermore, a study in 2013 by Amin *et al*. revealed that **RE-2** had an inhibitory effect *in vitro* on collagen-induced platelet aggregation with an IC_{50} of 0.2363μg/ml, suggesting that **RE-2** can be developed as a potential antiplatelet agent in the treatment of cardiovascular diseases associated with hypoglycemic activity. Moreover, Shi *et al*. (2013) found that **RE-2** protects against CCl_4-induced liver fibrosis through the suppression of an inflammatory signalling pathway in rats. Another study by Lee *et al.* (2012) examined the protective effect of **RE-2** on the cardiovascular and central nervous system in a rat model of focal cerebral ischemia. The results suggested that **RE-2** reduces brain damage and brain oedema by its inhibition effect on matrix metalloproteinase-2 and 9 (MMP-2 and MMP-9) and radical scavenging activity.

Compound **RE-3** was identified as 3, 4-dicaffeoylquinic acid, this class of natural polyphenolic compound is characterised by two caffeic acid moieties connected to one quinic acid unit by ester bonds. They exist in many plants, such as coffee (Moreira *et al*., 2001), sweetpotato leaf (Yoshimoto *et al*., 2002), *Ilex brevicuspis* Reisseck (Filip and Ferraro, 2003), *Isertia pittieri* (Um *et al*., 2002), and *Eleutherococcus senticosus* (Tolonen *et al*., 2002). Ooi *et al*. (2006) examined the antiviral activity of **RE-3** against respiratory syncytial virus (RSV) cultured in Human epithelial type 2 (HEp-2) cells. The study revealed that the compound possessed potent anti-RSV activity (IC_{50} of 0.5μg/ml) when compared to ribavirin (clinically used antiviral medicine) with an IC_{50} of 2.5μg/ml. In the same study the compound was tested for antibacterial activity against *Vibrio cholerae* and *V. parahaemolyticus* and showed slight antibacterial activity. In addition, Takemura *et al*. (2012) evaluated the anti-influnza A virus activities of 3, 4-dicaffeolquinic acid (**RE-3**). The authors found that the amount of tumour necrosis factor-related

apoptosis-inducing ligand (TRAIL) mRNA in mice that were administered the compound was significantly increased compared to the control group, while H1N1 hemagglutinin (HA) mRNA was slightly decreased. These data indicate that **RE-3** possesses a novel and unique mechanism of anti-influenza viral activity that may be useful as a potent lead compound for an anti-influenza medicine.

Compound **RE-4** was identified as a mixture of two flavonols; 3`,4`,5,7-tetrahydroxy-3,6-dimethoxyflavone (axillarin) (**RE-4a**) was previously isolated from the same plant family from the aerial parts of *Laggera tomentosa* (Gebreheiwot *et al.*, 2010) while 3`,4`,5,6-tetrahydroxy-3,7-dimethoxyflavone (Tomentin) **(RE-4b)** and was previously isolated from *Chrysosplenium tetrandrum* (Saxifragaceae). Beutler *et al.* (1993) carried out *in vitro* cytotoxicity screening of **RE-4a** against HeLa, MCF-7 breast cancer cells and haxiluman epidermoid carcinoma cells (A431). The study revealed that the compound inhibited the proliferation of HeLa cells (IC_{50} $26.91\pm2.70\mu M$) and was found to be inactive against the other tested cell lines. The evaluation of antioxidant activity of axillarin was carried out by Park *et al.* (2000). The compound showed strong antioxidant activity in a DPPH assay (IC_{50} of $10.1\mu g/ml$) and cytochrome-*c* reduction assay (IC_{50} of $10.1\mu g/ml$) using HL-60 cells. In addition, Moscatelli *et al.* (2006) demonstrated slight anti-inflammatory effects of axillarin by studying the potential inhibitory activity of it on the generation of inflammatory mediators in a mouse macrophages (RAW 264.7) cell line stimulated with lipopolysaccharide. Moreover, neuroprotective activities were evaluated by monitoring the viability of primary cultures of rat cortical cells from oxidative stress induced by glutamate in DPPH and MTT assays. The studies demonstrated that axillarin strongly protected the rat cortical cells from oxidative stress induced by glutamate (Park *et al.*, 2000; Kim *et al.*, 2002; Khan *et al.*, 2010). No studies have described any bioactivity for compound **RE-4b**. However, flavonoids have been intensively studied and they reported to have a variety of biological activities such as anti-inflammatory, antimicrobial and antioxidant (Guardiã *et al.*, 2001; Ross and Kasum, 2002; Kitamura, 2006; Hämäläinen *et al.*, 2007).

The results obtained in the present work included successful isolation and identification of bioactive compounds from selected desert plants and a preliminary screening of their cytotoxic activity on tumour and non-tumour cell lines. On the basis of the results discussed above, it can be concluded that the investigated desert plants used in camel fodder are a rich source of valuable bioactive compounds that are well documented to treat a wide range of diseases. Thus grazing camels on such plants could add a therapeutic value to camel milk and urine through the excretion of the plant active compounds or their bioactive metabolites to camel biological fluids followed by producing a positive effect on the consumer's health.

However, knowledge of bioavailability and pharmacokinetics of the isolated compounds is required to assess the potential impact of these compounds and their metabolites in human health and disease. Also, the isolation and characterisation of bioactive metabolites existing in camel milk and urine samples is necessary, but the political situation in Libya for the past few years and inadequate samples of camel milk and urine prevented this from being carried out fully in the current work. This could be carried out using techniques such as NMR, LC-MS and Gas chromatography–mass spectrometry (GC-MS) (Bouatra *et al*., 2013; Sundekilde *et al*., 2013).

In some cases, the biological actions of some metabolites are different from the biological effects of their parent compound. One example is polyphenolic compounds such as chlorogenic acid **(RE-2)** and 3, 4-dicaffeoylquinic acid **(RE-3)**; these two compounds have anti-influenza activity *ex vivo* (Urushisaki *et al*., 2011), but both of them have no anti-influenza activity *in vivo*. This may occur due to differences in the pharmacokinetic properties of these compounds *in vivo* (Takemura *et al*., 2012). Sato *et al*. (2011) found that the protective effect of **RE-2** against ischemia–reperfusion injury was mainly attributed to the effect of its major metabolite (caffeic acid) which has a stronger antioxidant activity than that of **RE-2** itself.

Saade *et al* (2009) studied the metabolism of cucurbitacin E **(CC-1)** *in vitro* and this study revealed rapid hydrolysis of this compound in neutral, basic, and acidic solutions as well as in human plasma associated with the detection of the active metabolite, cucurbitacin I. Several reports have evaluated the therapeutic properties of **CC-1** (Duncan *et al*., 1996; Momma *et al*., 2008; Sörensen *et al*., 2012; Abbas *et al*., 2013; Feng *et al*., 2014) and its deacylated form cucurbitacin I (Blaskovich *et al*., 2003; Kester *et al*., 2008; Su *et al*., 2008). **CC-1** was reported to have a high hydrophobicity and cytotoxicity when compared with its metabolite (Bartalis and Halaweish, 2005). Saade *et al*. (2009) compared cytotoxicity of **CC-1** and cucurbitacin I against a number of tumour cell lines and revealed that IC_{50} values of **CC-1** and cucurbitacin I were, respectively, 0.34 and 2.14 mg/ml in NUGC-3, 0.08 and 0.89mg/ml in HONE-1 (Wu *et al*., 2004), and 15.3 and 15.8 mg/ml in HepG2 cells (Bartalis and Halaweish, 2005). The authors concluded that both compounds showed high cytotoxity and **CC-1** was more potent as it showed lower IC_{50} than its metabolite. Additionally, it was reported that the antiproliferative activity of both compounds on cancer cells comes through different mechanisms; **CC-1** inhibits actin polymerisation causing suppression of cancer cell migration (Duncan *et al*., 1996; Momma *et al*., 2008) while cucurbitacin I strongly suppressed the STAT3 of Janus kinase selective Janus Kinase/Signal Transducer and Activator of Transcription 3 (JAK-STAT3) signalling pathway (Blaskovich *et al*., 2003; Kester *et al*., 2008; Su *et al*., 2008).

The metabolism of triterpenes leads to structural modifications that can cause pharmacological inactivation or cytotoxicity. In a study by Zhang *et al*. (2007), they revealed that metabolites of 20-(S)-protopanaxatriol showed strong *in vitro* cytotoxicity against human cancer cells, suggesting that hydroxylation at C-28 or C-29 may increase cytotoxicity while the introduction of a hydroxyl group to C-11β, C-15α, or the side chain may decrease the antitumour activity of this compound.

Zhu *et al*. (2010) studied the metabolic modifications of cycloastragenol **(AS-2)** in rat and human microsomes and revealed that the main modification as identified as

mono-hydroxylation and hydroxylation after oxidisation although the positions of the modifications were not confirmed because of inadequate structural information obtained from MS fragmentation. The study reported that after incubation of cycloastragenol with rat and human liver microsomes, an extensive hepatic metabolism was observed, suggesting that only a small part of orally administered cycloastragenol may reach the systemic circulation.

4.2 Molecular biology

This study also attempted to examine some of the miRNAs present in these plants, camel urine and camel milk, which might be involved in health-promoting activities. It was also aimed to assess whether these small nucleic acids could pass through the food chain to humans via camel milk and/or urine where they may regulate human gene expression. The latter is known as the dietary xenomiR hypothesis (Witwer, 2012). This hypothesis was assessed by Zhang and colleagues (2012a) in which plant derived miRNAs from dietary sources are transported into blood circulation and then to target tissues. The authors reported identification of plant miRNA in animals and they also revealed that miR-168, an abundant plant xenomiR, regulated the expression of low-density lipoprotein receptor-associated protein 1 (LDLRAP1) in mice. Thus, miRNAs from exogenous origin could exert the same function as endogenous miRNAs in gene regulation (Bartel, 2009; Mendell and Olson, 2012).

After the first study by Zhang and colleagues (2012a) which demonstratd that plant microRNAs are detected in human blood, several researchers tried to further report those discoveries. Several subsequent studies failed to support the above hypothesis. Some of these studies failed in detection of plant microRNAs in plant-fed mammals. For example, Dickinson *et al*. (2013) detected very low amount of plant-derived miRNAs in mice plasma and liver without any gene regulation activity when they repeated the original experiment. Witwer *et al*. (2013) detected variable amount of plant miRNAs in blood of two *Macaca nemestrina* and low amount with two others. Snow *et al*. (2013) conducted experiments on humans, mice, and bees to detect plant microRNAs (miR-156a, miR-159a, and miR-169a) after fruit ingestion. The study

reported low amounts of plant miRNAs in mice plasma and tissues, and was unable to detect the same plant miRNAs in the bees or in blood of human athletes.

Other reports assume that the detection of plant miRNAs in human datasets could be due to contamination with exogenous sequences or cross-contamination between samples from the same mammalian (Tosar *et al*., 2014; Zhang *et al*., 2012c).

However, other publications support the dietary xenomir hypothesis. A study by Liang *et al*. (2014) demonstrated the presence of *Brassica oleracea* miRNAs in the blood of mice and other organs such as stomach, intestine and spleen, indicating the ability of these molecules to survive through the gastrointestinal system, and enter the bloodstream and various organs of mice. Another study conducted by Pastrello *et al*. (2016) detected other miRNAs from the same plant in human blood in large quantities. Yang *et al*. (2015) reported that miR-2911 is detectable in mice serum and urine after ingestion of diet containing this plant miRNA.

It was reported that the food-derived miRNAs are able to survive in difficult conditions such as high RNase activity and in gastrointestinal tract fluids (Shigehara *et al*., 2011; Philip *et al*., 2015). Some studies suggested that these miRNAs exist in a protective form that is packaged with RNA-binding proteins such as Argonaute2 (Arroyo *et al*., 2011; Turchinovich *et al*., 2011), high-density lipoproteins (Vickers *et al*., 2011), or enclosed in small vesicles such as exosomes (Valadi *et al*., 2007; Zhang *et al*., 2010b; Mittelbrunn *et al*., 2011). The bioavailability and robustness of these molecules support their potential role as extracellular regulators.

The scientefic studies were not restricted on the detection of exogenous miRNAs only, but they assessed their potential biological effects in the mammalian system. Zhou *et al*. (2015) examined the antiviral activity of a plant miRNA, miR-2911, enriched in Honeysuckle (*Lonicera japonica*), which has been used for long time in traditional Chinese medicine to treat influenza infections. The authors demonstrated the uptake of miR-2911 by gastrointestinal tract after ingestion of the plant decoction. Also they revealed that this miRNA can transport through bloodstream to the lungs and then target influenza A virus replication. The results showed that miR-

2911 suppressed viral infection and directly target different influenza A subtypes *in vitro* and *in vivo*. Pastrello *et al*. (2016) demonstrated the role of *B. oleracea* miRNAs in the regulation of the expression of human proteins and genes *in vitro*. They also suggested a possible synergistic effect of these miRNAs with other Brassica-specific compounds in a potential anti-cancer action.

Recent reports demonstrated a potential role of miRNAs in early detection, diagnosis and treatment in cancer (Chen *et al*., 2014b; Schwarzenbach *et al*., 2014). Mlotshwa *et al*. (2015) confirmed the uptake and anti-cancer activity of synthetic tumour suppressor miRNAs designed to mimic plant-produced miRNAs. They examined the oral administration of a mixture of three plant-based tumour suppressor miRNAs along with total plant RNA isolated from *Arabidopsis thaliana* (L.). The result demonstrated the uptake of these miRNAs by the digestive tract of mice after ingestion. It also reported a tumour reduction in a mouse model of colon cancer after high exposure to dietary RNAs. A slight decrease in tumour burden in the mice treated with total plant RNA alone compared with control suggested that plant total RNA might have a therapeutic role.

There are a number of articles illustrating the detection of miRNA in medicinal plants and their potential impact on mammal metabolism. For example, *Gmelina arborea* Roxb. is a medicinal plant in India used to treat abdominal pains, increase appetite, and act as an antifungal treatment (Dubey *et al*., 2013). Dubey and colleges (2013), using computational prediction, predicted six miRNAs from *Gmelina arborea* Roxb. could target various mammalian genes that are associated with different diseases such as diabetes, cancer, and other urinary infections. In another study, using bioinformatics, twelve miRNAs of *Curcuma longa* L. were predicted to have an effect on human gene regulation (Rameshwari *et al*., 2013). Curcumin is the active ingredient of this plant and it was reported to show strong anti-inflammatory, antiviral, antioxidant, and anti-cancer properties *in vitro* and *in vivo*. The genes predicted to be targeted with the miRNAs in this study were linked to several human

diseases such as cardiovascular disorders, Alzheimer's disease, cancer, and diabetes mellitus type II

Once inside the mammalian body after oral ingestion of plants, plant miRNAs require a packaging system to survive the extreme conditions inside the body and for communication between cells (Redis *et al*., 2012). It was reported that microvesicles, exosomes, and high density lipoprotein serve as miRNA carriers and protect miRNAs from degradation (Montecalvo *et al*., 2012). A study conducted by Ju *et al*. (2013) identified for first time, the structure and the composition of exosome-like nanoparticles derived from grape. The study also demonstrated the role of these nanoparticles in communication between cells. The authors used grape exosome-like nanoparticles to demonstrate their transport properties and their biological effect on intestinal tissue after ingestion. The study revealed that these nanoparticles induce intestinal stem cell proliferation and prevent dextran sulphate sodium-induced mouse colitis.

The following section will consist of an evaluation of the methodologies used throughout the present research work and will be followed by a discussion of the experimental data obtained in this study and compare it to those from previous studies.

4.2 Evaluation of RNA Extraction

4.2.1 Evaluation of Plant RNA Extraction

Isolation of high quality total RNA from samples is the most important step in various molecular techniques such as quantitative RT-PCR, array analysis, northern analysis, and cDNA library construction (Yockteng *et al*., 2013).

Plants are a challenge to researchers who need to isolate intact nucleic acids for use in molecular studies (Sah *et al*., 2014). Problems encountered include the nature and composition of plant tissue with molecules such as lignin which make their tissues difficult to break up. Sampling techniques can have also an effect on yield and

minimize degradation (MacRae, 2007). Also, the amount of tissue required to achieve adequate yields of RNA varies according to the material. For example, tissues with high water content per weight require large amounts of tissue to be extracted for good yields of RNA. Low concentrations of nucleic acids in the plant sample will also impact on the ability of isolate good yield of high quality RNA. In addition, there may be partial or complete degradation of nucleic acid due to using dried plant material (Garcia-Baldenegro *et al*., 2015). Furthermore, the presence of large quantities of naturally occurring polysaccharides, high levels of RNases, and various phenolics in the plant material can interfere with the isolation process of nucleic acid (Coana *et al*., 2010).

In addition, the plants are collected from arid zones and desert plants have a natural ability to tolerate abiotic stress. This property of desert plants can be attributed to the presence of high levels of polysaccharides, polyphenols, and other secondary metabolites (Wang *et al*., 2011). Therefore, it may be more challenging to obtain high yields and good quality RNA from desert plants. Moreover, the RNA isolation method may result in the presence of carry-over genomic DNA in some plant RNA samples which can lead to an overestimation of RNA quantity. In summary therefore, RNA isolation procedure must include some important steps before, during, and after the RNA purification. These steps include sample collection and appropriate storage; optimal RNA isolation procedures for maximizing the yield and quality of sample RNA; and appropriate storage of purified RNA samples.

The extraction kits investigated in this study applied different strategies to overcome the main challenging issues regarding nucleic acid extraction and to ensure total RNA of adequate quantity and quality. The RNA yield varied noticeably between the different RNA isolation procedures ranging from 4 to 472µg of *A. spinosus* and *C. colocynthis* (Results Section 3.6.1, Table 3.16). The highest total RNA yields were obtained using the following kits; PureLink, PowerPlant, and TRIzol Reagent. While the Qiagen and Norgen kits showed low total RNA yields, with Spectrum and PowerPlant with DNase kits giving the lowest yields. Noticeably, the PowerPlant

with DNase kit showed much lower RNA yield ranged from 5 to 14µg compared with the original PowerPlant method ranged from 283 and 369µg of both plants.

The isolated RNA from the two plants using various extraction methods was assayed spectrophotometrically and most of the RNA samples gave good $A_{260/280}$ and low $A_{260/230}$ values (Results Section 3.6.1, Table 3.16). Only PureLink and Norgen Kits showed close to ideal $A_{260/280}$ and $A_{260/230}$ ratios of 2.0. Although, the RNA sample from Norgen Kit gave $A_{260/230}$ ratio of 1.49 and this could be due to salt contamination carry-over from the isolation method. Both of these extraction procedures are silica-based column for isolating total RNA from various sources without the use of phenol.

Most of the other purification kits isolated total RNA of lower purity especially the $A_{260/230}$ values are significantly low and ranged from 0.07 to 1.49. A low $A_{260/230}$ ratio is indicative of phenol/guanidine contamination due to inadequate washing steps (Vogelstein & Gillespie, 1979). These low values could also be attributed to residual phenol in the final elution from the phenol/chloroform methods. Thus, a further RNA clean-up step or dilution of the RNA is required to overcome this issue (Deng *et al.* 2005). Most of the methods evaluated were shown to be clear of protein contaminants, as the $A_{260/280}$ ratios were high (≥ 1.9) (Results Section 3.6.1, Table 3.16). However, TRIzol Reagent, Spectrum, PowerPlant, PowerPlant with DNase kits isolated RNA of low $A_{260/280}$ values (from 0.60 to 1.72) indicating the contamination of these samples. It was noted that the PowerPlant with DNase showed higher $A_{260/280}$ and $A_{260/230}$ compared with the original PowerPlant kit. This indicated that the extra purification step in PowerPlant with DNase kit extracted RNA from better quality.

According to the spectrophotometric analysis data in this study, the Norgen kit would be recommended for extraction of *A. spinosus* and *C. colocynthis* as it isolated total RNA of reasonable quantity and quality. The Norgen kit had previously been

reported to extract total RNA from reasonable quality and quantity from hard plant tissues such as seeds (Theriault *et al*., 2016) and roots (Karve *et al*., 2016).

Assessment of the extracted RNA integrity revealed that most of the isolation kits produced total RNA with low quality and indicated by their low 28S to 18S ratios and low RQI values. However, the column-based approach (PureLink kit) yielded RNA from *A. spinosus* and *C. colocynthis* with better integrity than the other kits in this study (Results Section: 3.6.3, Table 3.19). The 28S /18S ratios were 0.86, 0.84 and RQI values were 7.1 and 6.6 for both plants respectively. The other isolation kits produced total RNA with low 28S to 18S ratio ranges from 0.05 to 0.97 and low RQI values (from 2.6 to 5.1) which suggests partial degradation of the RNA samples.

4.2.2 Evaluation of Total RNA Extraction from Body Fluids

In the current study, a Norgen Biotek kit was used to extract Total RNA from body fluids. According to the manufacturer, it is designed for total RNA extraction from plant tissues, animal cells and body fluids including milk, urine and blood. The results indicated that the Norgen kit was not effective in purifying RNA from the body fluid samples used in in this study. NanoDrop spectrophotometric assessments of the RNA from the body fluid samples revealed that the purified RNA was of poor quality and quantity (Results Section 3.6.2, Table 3.17) and suggested further extraction work assessing other extraction methods is required.

The maximum starting volume of each body fluid sample, using Norgen Biotek kit, is 200µl to prevent clogging of the column. Other extraction methods with larger starting volume of the samples could improve the yield. Weber *et al*. (2010) isolated RNA samples from 12 body fluid samples including breast milk, colostrum, saliva, seminal fluid, tears, and urine. The purification of total RNA from these samples was carried out using miRNeasy Serum/Plasma Kit from Qiagen using 300µl as a starting volume of each sample. Weber *et al* extracted RNA from a range of different types of body fluids with good quality and quantity. Hanson and Ballantyne (2013) extracted total RNA from blood, semen, saliva, vaginal secretions, and menstrual

blood using organic solvent RNA extraction. They started with a volume of 500μl of each body fluid sample and purified RNA with good quantity and quality.

Several studies demonstrated the existence of miRNAs in exosomes (Zhang *et al*. 2015; Izumi *et al*, 2015; Cheng *et al* 2014; Montecalvo *et al*., 2012). Exosomes are identified in many biological fluids such as urine (Mitchell *et al*., 2009; Nilsson *et al*., 2009), salvia (Palanisamy *et al*., 2010), blood (Jayachandran *et al*., 2012; Kalra *et al*., 2013), and breast milk (Zhou *et al*., 2012; Zonneveld *et al*., 2014). Exosomes can be an enriched source of miRNAs as they work as a protective vesicle against degradation of transport miRNA by RNase (Cheng *et al*., 2014) and they can transfer exosomal RNA between cells (Montecalvo *et al*., 2012). Therefore, in order to improve on the poor recovery of total RNA obtained by using standard total RNA isolation kits on body fluid samples alone, total exosome isolation from body fluids was carried out followed by total RNA extraction from the isolated exosomes. Total exosome isolation from camel milk and urine samples was carried out using commercial kits (Results Section 3.6.2.1.1). Both commercial kits produced a pellet of exosomes from camel milk and urine samples. However, no pellet of exosomes was formed from bovine milk sample. Therefore, an ultracentrifugation method was used for the exosomes purification from bovine milk sample and a pellet of exosomes was obtained.

Body fluids contain various vesicles and particles; therefore, before carrying out any further analysis, it is important to ensure that the purified pellets are exosomes and no other contaminant particles such as microparticles or cell debris. There are common techniques for characterising and assessing the purity of the isolated exosomes such as Western blotting, flow cytometry, or electron microscopy (Thery, 2011). Western blotting is an appropriate way to achieve this (Lässer *et al*., 2012). There are a number of proteins that are enriched in exosomes, regardless of their cellular origins, which are commonly used for exosome detection. These proteins include tetraspanins such as CD9, CD63, and CD81 (Andreu and Yanez-Mo, 2014). Therefore, in order to confirm the identifying of the purified pellet as exosomes,

immunoblotting analysis was conducted using an antibody against CD63. All the samples were shown to be positive for CD63. Western blot results (Results Section 3.6.2.1.2, Figure 3.50) showed the presence of the tetraspanin CD63 protein, commonly enriched in exosomes, in the isolates from all three body fluid samples.

Total RNA was then isolated from the lysed exosomes using the Norgen Biotek Total RNA purification kit. Total RNA isolated from the exosome samples of the the three body fluids was of low yield and poor quality (Results Section 3.6.2.1.3, Table 3.18). The highest yield of RNA was obtainable from exosome sample of bovine milk (18.37μg), while camel milk and urine exosome samples yielded 11.20 and 1.90μg, respectively. The quality assessment was performed on the total RNA purified from the exosome samples (Results Section 3.6.3). It revealed low RQIs (1.3, 2.1) and 26S to 18S ratios (0.41, 0.03) of the RNA from camel milk and urine samples, respectively. This result suggests further extraction work to identify the most effective method of sample preservation and RNA extraction from body fluids that provides an appropriate yield and the lowest level of RNA degradation.

Due to limited availability and amount of camel milk and urine samples, only 500μl of each body fluid samples was used as starting volume in both commercial kits for total exosome extraction. However, Total Exosome Isolation Reagent (from urine) permits starting volume from 0.8–5ml of urine. Also, the Total Exosome Isolation (from other body fluids) allows using starting volume from 0.2–1ml. Thus, increasing the starting volume of body fluid samples could help to maximize recovery of intact exosomes enriched with miRNAs for downstream application. Also, the nature of the exosome membrane could potentially compromise the RNA extraction process. Exosomal membranes have variable lipid content according to its cellular origin. Some exosomes have firm membranes as its lipid composition is rich in sphingomyelin and cholesterol (Mitchell *et al*., 2009). Therefore, using different RNA extraction methods from exosomes is recommended in case of isolating exosomal RNA from different cellular origins (Eldh *et al*., 2012). There are several reports describing RNA extraction from exosomes using different RNA extraction

methods. For example, Kogure *et al*. (2011) used phenol based techniques (Trizol®) to extract exosomal RNA. Valadi *et al*. (2007) combined phenol and column-based methods for co-purification of microRNA and total RNA, where the RNA was extracted using Trizol and followed by ane RNeasy Mini kit.

4.3 Quantitative Real Time PCR of target miRNAs

There are a range of techniques that have been developed to overcome the challenges of miRNA profiling. Molecular experiments dealing with one or two miRNAs with relatively few test groups use qRT-PCR, while studies aiming to discover and quantify novel miRNAs make use of small RNA seqencing. For larger studies investigating multiple miRNAs at the same time, multiplex miRNA assays using microarrays or RNA sequencing (Pritchard *et al*., 2012). qRT-PCR is characterised with high sensitivity, good reproducibility for miRNA detection with a wide dynamic range of quantification (Bar *et al*., 2003; Chen, *et al.* 2005a; Reichenstein, *et al.* 2010). Therefore, qRT-PCR was the technique selected for validating and accurately quantifying miRNAs in this work. In addition to TaqMan small RNA assays which used to permit a specific detection of the mature, biologically active miRNA for each assay by using miRNA target-specific stem-loop reverse transcription primer.

Three plant miRNAs were selected for this initial study based on both their likelihood of expression in the particular plants under study and their potential to regulate human gene expression. The miRNAs chosen were: miR-166a, miR-167a, and miR-168a (Methods Section 2.8.4, Table 2.5) as they are found to be highly conserved across plant species and have had human gene targets identified or predicted (Zhang *et al*., 2010a).

The comparison between Ct values for two plants *A. spinosus* and *C. colocynthis* revealed that the Norgen kit gave the lowest Ct value (18.8) which indicates abundant miR-166 in *A. spinosus* while the highest level of the miR-166 was obtained using the PureLink kit in *C. colocynthis.* Ct values of 24.5 and 25.6

indicated moderate levels of miR-166 for both plants using the Qiagen kit while the Powerplant kit showed the highest Ct values (26.6, 30.6) and minimal amounts of miR-166 level for *A. spinosus* and *C. colocynthis*, respectively (Results Section 3.6.4, Figure 3.53).

The qRT-PCR results suggest variation in Ct values as a result of the methods of RNA isolation used in this study. This variation could be attributed to quality of isolated nucleic acid arising from the RNA extraction method. There are several reports that provide evidence of the effect of RNA quality on the result of microRNA expression studies (Imbeaud *et al.*, 2005; Wang *et al.,* 2008). A study by Hammerle-Fickinger *et al.* (2010) confirmed that the extraction procedure of RNA can influence the RNA quality and integrity, subsequently affecting the quantitative analysis of gene expression. Accerbi *et al.* (2010) reported the impact of extraction procedure on the composition of microRNA species in the final sample can interfere the expression data obtained. For example, isolated RNA samples with genomic DNA may also be detected in qRT-PCR, leading to inaccurate quantification of the target transcript (Fleige and Pfaffl, 2006).

The isolated RNA from camel milk and urine were assayed for the presence of plant miRNAs (miR-166, miR-167, and miR-168). Relative Ct values showed minimal quantity of miR-166 in camel milk and urine samples and moderate quantity of miR-167 and miR-168 were detected in both samples. The above preliminary study suggests a robustness and ability of plant miRNAs to survive ingestion, digestion, and transport to tissues within the camel. It also reveals that they are detectable in the body fluid samples of camels despite, the low quantity and poor quality of the isolated RNA from these samples.

4.4 Assessment of potential bioavailability of target miRNAs

In the current study, bovine milk samples were subjected to incubation in a drug dissolution tester to examine the release of plant-derived miRNAs in these samples

under the physiological conditions of a human stomach. The bioavailability assessment of plant miRNAs was first carried out prior to ingestion and then while they are in the gut. It was shown (Results Section 3.7, Figure 3.57) that miR-166 levels of bovine milk in the simulated digestion system had consistent levels from 0 min until 19 min and then demonstrated a significant ($p = 0.01$) decrease in their levels after 38 min of digestion, suggesting a decrease in their resistance to degradation over time. While consistent survivability of miR-167 and miR-168 were observed during the early stages of digestion for 38 min. This indicates the resistance of miR-167 and miR-168 to degradation suggested by their levels unlike the other miRNA assayed.

The above results suggest a miRNA-specific robustness and resistance to degradation suggested by the degradation profiles of plant-derived miRNAs. This degradation could be attributed to the sequence-specific features differences between miRNAs examined in this study.

Our findings support, an *in silico* study by Lukasik and Zielenkiewicz (2014) which suggested that plant-derived miRNAs survive degradation in the digestive system in quantities sufficient to make it to the serum and to access organs. Another study by Liang *et al*. (2014) examined the survivability of plant miRNA ingested by mammals. They fed mice with plant total RNAs extracted from *Brassica oleracea,* including miR-172. This miRNA was detected in the blood, spleen, liver, and kidney of the mice. This study demonstrated that plant-derived miRNAs ingested by mammals can survive through the gastrointestinal system, and enter the bloodstream and various organs of mice. Baier *et al*. (2014) studied the bioavailability of plant miRNAs after their absorption and transport into the blood circulation in healthy adult human subjects. They reported an increase of miRNA-200c and miRNA-29b in blood serum after consumption of bovine milk. In contrast, Aucherbach *et al*. (2016) analysed the samples provided by the laboratory of Baier and could not achieve the same findings despite the Aucherbach study making use of samples provide by Baier from his original study. However, lengthy storage of the samples and the change in

the temperature during sample transport could compromise the samples and decrease miRNA recovery.

4.5 Quantification of gene expression

MicroRNA target prediction software for cross-species analysis was not available, so the BLAST search tool was conducted using the sequences of a number of miRNAs found in the plants in this study to see if there was any possibility of complementary pairing. A BLAST database search showed a possible targeting of miR-167 to human prolactin receptor mRNA (Methods Section 2.8.7.1). Therefore, the quantification of PRLR mRNA levels of a number of human cancer cell lines was carried out to help in the selection of cell lines for further studies based on PRLR status. That was followed by examination of the potential for plant-derived miR-167 to alter the expression of *PRLR* mRNA.

The wide distribution of *PRLR* in human tissues facilitates its role in various physiological processes, including cellular growth and differentiation, angiogenesis, hematopoiesis, reproduction, and lactation (Bole-Feysot *et al*., 1998). High expression of *PRLR* has been associated with the development of various types of cancer, particularly breast, prostate, colorectal, gynaecological, laryngeal, and hepatocellular (Sethi *et al*., 2012).

There are various techniques that can provide quantitative values reflecting the amounts of measured mRNA in samples. They differ in their accuracy and reproducibility and the selection of the appropriate method can also depend on the design of a particular experiment. These methods include *in situ* hybridization techniques, nuclease protection assays (NPAs), Northern blotting assay, and qRT-PCR (Fryer *et al*., 2002). *In situ* hybridization is used to localise expression of a particular gene within a tissue or cell type, while NPAs are the easiest way to simultaneously examine multiple messages. Northern analysis is the only method that provides information about transcript size. qRT-PCR is the most sensitive and

flexible method for detecting and quantitating the expression of individual or multiple genes (Bustin, 2002; Nolan *et al*., 2006). In the present study, the procedure utilised to detect and determine the abundance of *PRLR* mRNA was qRT-PCR.

The expression of *PRLR* in several human cancer cell lines was measured using qRT-PCR analysis (Results Section 3.8.1, Table 3.20). The finding of high expression levels of *PRLR* mRNA in ZR-75-1 cells is consistent with the findings of Nitze *et al.* (2013) using the same quantification method (qRT-PCR). Several studies have shown that most human breast cancer cells have higher *PRLR* levels when compared with normal breast tissue (Ormandy *et al*., 1997; Touraine *et al*., 1998; Peirce and Chen, 2001; Gill *et al*., 2001; Swaminathan *et al*., 2008). Comparable high expression of *PRLR* mRNA in HeLa cells was also measured in this current study. This data is in agreement with another published study (Lopez-Pulido *et al.*, 2013). Our results are also consistent with other studies, in which low *PRLR* mRNA levels were detected in LNCaP cells using the same quantification strategy (Peirce and Chen, 2001; Xu *et al*., 2001; Van Coppenolle *et al*., 2004). Low *PRLR* mRNA levels were found in A375 cells in this current study. Only one study conducted by Sustarsic *et al*. (2013) reported the expression of *PRLR* mRNA in human melanoma cell lines (MDA-MB-435, UACC-62 and SK-MEL-5). In contrast to Wen *et al*. (2014), our result reported that *PRLR* mRNA was not detectable in A2780 and PANC-1 cell lines. This difference in the results could be influenced by the use of different techniques as Wen and colleagues used immunoblotting for quantification of *PRLR* expression. Quantification of *PRLR* mRNA in A2780 and PANC-1 cell lines was not reported in any other study.

Data normalisation in quantitative RT-PCR is a crucial and fundamental step to ensure accurate measurement of relative mRNA expression levels in the cells (Pfaffl, 2001; Bustin, 2002; Lindqvis, 2013). *PPIB* has been identified as a suitable reference gene in an earlier miRNA transfection study in our research group.

4.6 Modulation of gene expression by plant miRNAs

To examine if the identified plant miRNAs could have an effect on the expression of the prolactin receptor, human cell lines which natively expressed *PRLR* were transfected with a plant miRNA mimic or *C. colocynthis* total RNA and the *PRLR* expression levels were measured. Transfection of cancer cell lines was carried out using synthetic miRNA (miR-167 mimic) and miR-167-enriched fractions obtained from the plants studied in this work.

Small RNAs such as miRNA and siRNA are potent tools for controlling cellular processes of gene silencing leading to the degradation of mRNAs in a sequence-specific manner dependent on complimentary binding of the target mRNA. The target specificity of siRNAs in cell culture and animal studies has led to use them as robust therapeutic and diagnostic tools (Dorsett and Tuschl, 2004). A study conducted by Elbashir *et al.* (2001) demonstrated that synthetic siRNAs could mimic the natural siRNAs product and suppress expression of endogenous and heterologous genes in different mammalian cell lines including human HeLa cells. In 2014, Kavarthapu *et al*. studied the expression of *PRLR* mRNA in T-47D breast cancer cells after transfection of these cells with synthesized siRNA targeting the *PRLR* gene. The study revealed that the synthetic siRNA had a noticeable down-regulation effect on *PRLR* mRNA expression.

To obtain an effective transfection process, there were essential parameters that were taken into consideration. Firstly, a suitable transfection agent is needed to enable effective small RNA uptake and efficient release of the small RNA inside cells (Khvorova *et al.*, 2003). It has been shown that HiPerFect from Qiagen can successfully transfect sufficient levels of small RNAs into cells to modulate gene expression (Pallet *et al.*, 2008; Fischer *et al.*, 2010). Therefore, Qiagen's HiPerFect was chosen in this current study as the transfection reagent. The effect of HiPerFect reagent alone on expression profile of *PRLR* mRNA was assessed in all tested cell lines to avoid the potential toxicity that might be produced by this reagent. The

expression of *PRLR* mRNA was close to control in each cell line and there was no cytotoxic effect on the cells with HiPerFect. Following the procedure recommended by Qiagen, the HiPerFect efficiency was optimised for volume of reagent and to examine the influence of different ratios of transfection reagent to small RNA. The optimum transfection volume of HiPerFect used was found to be 12μl.

Secondly, a negative siRNA transfection control was required. It was reported that this negative control was not similar in structure to any known mammalian gene (Jensen *et al*., 2014). It was used successfully as negative control siRNA and to assess the efficiency of siRNA uptake in different knockdown experiments (Phillips, 2011; Goldgraben *et al.*, 2016). It was therefore expected that the transfection of this small RNA would not affect the *PRLR* mRNA expression. Indeed, the transfection of cells with the fluorescent AF488-labelled AllStars Negative Control had no effect on *PRLR* mRNA expression. The highest level of fluorescence was observed with cells transfected with 150ng of Allstars Negative Control siRNA and 12μl HiPerFect.

Thirdly, a positive siRNA transfection control was required for this study. All the cancer cells were treated with the Qiagen AllStars Hs Cell Death SiRNA. The AllStars Hs Cell Death SiRNA when successfully transfected results in death of the cells and has been reported as a suitable control for use in optimization of gene knockdown in various experiments (Ovaska *et al*., 2010; Venkatadri *et al*., 2016). The highest level of transfection, as shown by greatest reduction in cell viability, was observed in all cell lines by using 50nM (125ng) siRNA and 12μl HiPerFect. These results suggest that the AllStars Cell Death positive control works as a suitable positive control for transfection.

Fourthly, evaluation of the time point at which gene modulation might occur following transfection was conducted. In the present study (Results Section 3.8.2.1), five different time points (6, 12, 24, 48 and 72h) were chosen to determine the best *PRLR* knockdown time. Among these time points, the highest gene silencing was seen at 72h following delivery of siRNA to the cells. That was compatible with the

range (between 24-96h) as previous studies (Chang *et al.*, 2012). The assessment of the time point of 96h was not be possible because most of the studied cell lines appeared over confluent at that time.

4.6.1 Expression of *PRLR* mRNA after transfection of miR-167 mimic into several human cancer cell lines

In this current study, to evaluate the possible regulation of *PRLR* expression by miR-167, several cancer cell lines were transfected with miR-167 mimic and processed as described in Methods Section 2.8.8.2. Quantification of the PCR signals was performed by comparing the cycle threshold value of the gene of interest with the cycle threshold value of the reference gene *PPIB*. Values are expressed as fold increase of mRNA relative to that in not treated cells.

The result data (Results Section 3.8.3, Figure 3.59) showed that 150nM of miR-167 mimic was able to significantly up-regulate (4.05±0.41 fold, P = 0.01) *PRLR* mRNA expression in ZR-75-1 cells compared with control cells. This up-regulation effect of miR-167 mimic could be attributed to the interaction between miR-167 mimic and another gene or pathway that was able to induce an up-regulation effect on the *PRLR* mRNA expression. It has been shown that an individual miRNA is able to control the expression of more than one target mRNAs and that each mRNA may be regulated by multiple miRNAs (Jones-Rhoades and Bartel 2004). Also, it has been reported that the overexpression of *PRLR* mRNA may induce abnormal proliferation of breast epithelium (Pan *et al*., 2007). However, there are several studies reported that the down-regulation of *PRLR* mRNA expression in breast cancer cells causing reduction of proliferation of cancer cells (Tan *et al*., 2011).

In contrast, miR-167 mimic caused down-regulatated (5±0.05 fold) of the *PRLR* mRNA expression in A375 cells compared with their corresponding controls. To date, there have been no studies focusing on the analysis of *PRLR* expression in melonoma. The data presented in this work suggest that further studies are required to determine the potential role of *PRLR* in melanoma.

The expression levels of *PRLR* mRNA remained unchanged in HeLa and LNCaP cells after their transfection with miR-167 mimic. This suggests that there was no interaction between *PRLR* mRNA and the synthetic miRNA to produce down-regulation effect of target gene. There are several studies reported high expression of *PRLR* mRNA in different cervical cancer cells and suggested a potential role for *PRLR* in the progression of cervical cancer, making it a potential target for theraputics (Lopez-Pulido *et al*., 2013; Ascencio-Cedillo *et al*., 2015; Arellano *et al*., 2015). Also, it has been shown that a *PRLR*-specific antagonist, S179D, decreases cell growth and proliferation of prostate cancer cells *in vitro* and *in vivo* (Wu *et al*., 2005; Huang and Walker, 2010).

The results showed that miR-167 mimic did not seem to have a downregultory effect on *PRLR* expression in the studied cancer cells. The major challenge in determining miRNA functions is to identify their regulatory targets. As there is no tools offer the ability to integrate heterogeneous miRNA and mRNA datasets for multiple species within a platform, a BLAST database was used in this study. Therefore, the BLAST database may not be an appropriate tool for predicting cross species targeting of genes by miRNAs. Thus, miR-167 could not target PRLR mRNA effectively to produce silence effect on this gene so using other target prediction software could be successful. There are other microRNA target prediction tools reported to succesfully predict target gene of plant-derived miRNAs. One study by Zhou *et al.* (2015) used RNAhybrid tool (Krüger and Rehmsmeier, 2006) to identify the sequences in influenza virus mRNA that bound to plant miRNA, miR-2911. The study showed that miR-2911 directly interacts with the predicted genes, inhibits their levels, and prevent viral infection *in vivo*. A study by Pastrello *et al*. (2016) demonstrated that Brassica miRNAs regulate expression of human genes and proteins *in vitro*. Targeting of Brassica miRNAs to human genes was predicted using the Probability of Interaction by Target Accessibility (PITA) algorithm version 6 against human 3′ UTR (Kertesz *et al*., 2007).

4.6.2 Expression of *PRLR* mRNA after transfection of plant total RNA sample into several human cancer cell lines

Transfection of cancer cell lines was also carried out using total RNA sample obtained from the plants studied in this work. That was to assess whether the isolated *C. colocynthis* RNA sample (containing miR-167 among others) would have an effect on *PRLR* expression as the miR-167 mimic in the tested cancer cell lines. The initial observation was obtained from a single experiment and gave an indication that the effect of the plant total RNA sample could be a part of what the miR-167 mimic could accomplish.

A preliminary result (Section 3.8.4, Figure 3.60) of transfection of human cancer cell lines with a plant-derived total RNA sample showed an up-regulation effect on the most treated cells and a down-regulation effect was observed at 150ng of total RNA sample on ZR-75-1 and at 300ng on A375 and LNCaP cells.

Depending upon the isolation method used, extracted total plant RNA can contain the high and low molecular weight RNA species present in the plant. These would include all miRNAs, and other small RNAs. As xenomiRs, these molecules could potentially regulate mammalian transcripts and produce effects if they were able to enter cells. However, the level of miR-167, for example, would be too low in the total RNA sample to cause an effect on *PRLR* expression since the miRNAs with low levels have a reduced probability of interacting with the target gene and downregulating it (Brown *et al.*, 2006). It is possible that the presence of salt and solvent carry-over contamination in the extracted RNA from the isolation method could have an effect on other genes and pathways within the cells which in combination might cause an up-regulation effect on the expression of the *PRLR*.

The cell lines used in the current study are widely used in many scientific studies and they are well reported as an important tool in the study of human biology (Ferreira *et al.,* 2013; Hasan *et al.,* 2015).

Further experemint could be done on to identify the endogenous miRNAs existing in camel milk and urine followed by examination of these miRNAs for possible targting of *PRLR*.

4.7 Assessment of genetic variability

As plant samples used in this study were collected from different sites, ISSR-PCR was carried out to to ensure that the plant samples tested were of the same species. There are several DNA-based molecular marker methods available for genetic analysis of plant genomes. Characterisation of plants with such markers is an ideal method for identification of plant species. These techniques include random amplified polymorphic DNA (RAPD; Williams *et al*. 1990), directed amplification of minisatellite DNA regions (DAMD; Heath *et al*. 1993), inter-simple sequence repeats-PCR (ISSR-PCR; Meyer *et al*., 1993; Zietkiewicz *et al*., 1994) and amplified fragment length polymorphism (AFLP; Vos *et al*. 1995). ISSR-PCR method was used extensively and succesuffuly to study genetic diversity between plant species (Tamhankar *et al*. 2009; Al-Turki and Basahi, 2015). Several studies reported that ISSR markers show higher reproducibility than other approaches such as RAPDs (Micheli *et al*., 1994; Fang and Roose 1997; Kojima *et al*. 1998; Semagn *et al*. 2006). Thus, ISSR-PCR was chosen as the most appropriate strategy in the present work.

ISSR-PCR technique was applied for two samples of each plant (*T. aphylla* and *C. colocynthis*), collected from different locations, to ensure that the samples of each plant belong to the same species. It was shown in Figure 3.61 (Results Section 3.9.2) that DNA bands generated for most dominant DNA markers had variable intensities. This variation can produce low reproducibility of ISSR reactions and compromise the banding pattern in ISSR experiment (Ng and Tan, 2015). Based on these results, it was not possible to confirm if the two plant samples are from the same species or not. Bands with weak intensities which are not enough to be properly visualised when fractionated by electrophoresis in an agarose gel could be a result of using template DNA of low integrity (e.g. degraded DNA). To overcome this issue, it is

recommended that fresh material is used to produce intact DNA as most of the reported DNA extraction protocols use fresh leaves. However, in the current project, dried plant samples were used because the samples were collected from a distant place and it was not possible to keep fresh samples until the extraction process was commenced. Also, using unequal starting quantities and qualities of template DNA for the PCR reactions could result in inconsistent concentrations of PCR amplification products and affect band intensities, compromising the banding pattern (Semagn *et al*. 2006). Therefore, adjusting the amount of template DNA used in each PCR reaction is an important factor to ensure reproducible banding pattern (Ng and Tan, 2015).

Chapter 5 Conclusion and Future work

To sum up, the current study provided some promising results with respect to four investigated desert plants from a natural products perspective.

A total of 16 compounds, including two mixtures were isolated from the plants. One compound was identified as novel natural product, namely *trans*-coniferyl acetate-4-*O*-sulphate **(TA-1b)** which was isolated as part of a mixture with *trans*-coniferyl alcohol-4-*O*-sulphate **(TA-1a)**. This fraction was isolated from the leaves of *T. aphylla* along with isoferulic acid-3-*O*-sulphate **(TA-2)**, luteolin **(TA-3)** and *N*-methyl-4-hydroxyproline **(TA-4)**. All compounds, except for TA-3, are reported for the first time from this plant. The cytotoxicity investigation revealed for the first time that fraction **TA-1a** and **TA-1b** presented cytotoxic effects against the A375 cell line, with an EC$_{50}$ of 25.18±1.5μg/ml compared with the normal cell line. While, TA-3 exerted cytotoxic activity against HeLa cells (86.50±0.51μM), compared with the normal cell line.

Fractionation of *R. epapposum* extracts led to isolation and characterisation of four compounds for the first time from this plant, which were identified as 2-hydroxyalantolactone **(RE-1)**, chlorogenic acid **(RE-2)**, 3, 4-dicaffeoylquinic acid **(RE-3)**, and a mixture of 3`,4`,5,7-tetrahydroxy-3,6 dimethoxyflavone **(RE-4a)** and 3`,4`,5,6-tetrahydroxy-3,7-dimethoxyflavone **(RE-4b)**. All these isolated compounds were previously reported to have activities such as antioxidant, anti-cancer, anti-inflammatory, antiviral, and antibacterial activities (Al-Yahya *et al.*, 1984; Xu *et al.*, 2013; Filip and Ferraro, 2003; Kitamura, 2006).

Chromatographic separation of *A. spinosus* leaves resulted in the isolation of four compounds; pinitol **(AS-1)** and maackiain **(AS-4)** that were reported for first time from *A. spinosus* while, cycloastragenol **(AS-2)** and cycloastragenol-6-*O*-glucoside **(AS-3)** were isolated previously from this plant. The above compounds are well documented as antidepressant, antidiabetic, antifungal, antioxidant, hepatoprotective, wound healing, antineoplastic, diuretic, tonic and antiallergic treatments (Nalbantsoy *et al.*, 2012; Zhao *et al.*, 2015; Wu *et al.*, 2016; Yoon *et al.*, 2016)

Phytochemical investigation of *C. colocynthis* resulted in two known compounds; cucurbitacin E **(CC-1)** and its glucoside **(CC-2).** In this study, **CC-2** exhibited specific cytotoxic activity against A375, A2780 and ZR-75-1 cell lines, with EC_{50} values of $58.00\pm1.20\mu M$, $62.27\pm1.76\mu M$, and $55.25\pm1.15\mu M$, respectively. They are reported to have a wide range of biological activities such as anti-inflammatory, analgesic, antimicrobial, antihelminthic, antitumour, antioxidant, free radical-scavenging, antiproliferative, hepatoprotective and cardiovascular *in vitro* and *in vivo* (Blaskovich *et al*., 2003; Chen *et al*., 2005b).

Therefore, the desert plants used in camel fodder can be considered a rich source of valuable bioactive compounds, some of which are well documented to treat a wide range of diseases. Thus grazing of these plants might add therapeutic value to camel milk and urine through the excretion of the plant active compounds or their bioactive metabolites into camel biological fluids followed by potential availability to help improve the health of the consumer.

From a molecular biology aspect, the results confirmed the presence of some plant-derived miRNAs in camel milk and urine samples and demonstrated the robustness of these molecules to the conditions that would be met in the gastrointestinal tract of animals and humans. However, it was not confirmed that the identified miRNAs are at the levels/concentration needed to elicit an effect at the expected consumption volumes. This preliminary result can be useful for future research to further investigate the therapeutic value of camel milk and urine which could be attributed to other plant-derived miRNAs or the endogenous miRNAs in camel body fluids.

Further work is required to analyse the milk and urine samples to check if any of the isolated compounds or their metabolites exist in the camel milk or urine. This could be carried out using techniques such as NMR, LC-MS and Gas chromatography–mass spectrometry (GC‐MS) (Sundekilde *et al*., 2013; Bouatra *et al*., 2013). This step is required to assess the potential effect of these compounds and their metabolites on human health.

The isolated compounds TA-4 (11mg), AS-4 (13mg), and RE-4 (14mg) were low in quantity with some impurities. The purification work on these compounds has not yet been completed because of the limited time and limited quantities of plant materials. Thus, for future work, the same chromatographic procedures could be repeated with larger amounts of the fractions to improve the yields. Also, further separation and subsequent purification have to be continued to purify the isolated compounds.

The purification work on the mixture of TA-1a and TA-1b to isolate the pure compounds in sufficient quantities was not successful. Therefore, for further work on this mixture, alternative separation techniques such as HPLC could be used. With further investigation into TA-1b, the new compound, its presence could prove to be a useful find. Since other properties such as antimicrobial and anti-inflammatory activities are common in this plant (Vadlapudi *et al*., 2009; Yokosuka and Alqasoumi, 2011), tests could be carried out to evaluate these properties as well. This would involve techniques such as both dilution and disc diffusion assay, and carrageenan-induced paw oedema model.

The most significant issue in this study was the impact on the work of limited quantities of camel milk and urine samples, dried plant stocks, and the lack of fresh plant material. Therefore, if further work is to be carried out large quantities of body fluid samples and fresh plant material should be made available for an in-depth study.

The results using total RNA sample to examine its possible effect on *PRLR* mRNA expression were considered to be preliminary experiments because they were only conducted once and need to be further investigated. Mlotshwa and others (2015) synthesized three tumor suppressor miRNAs *(*miR-34a, miR-143, and miR-145*)* that mimic plant miRNAs. They reported that oral administration of the mixture of these synthestic miRNAs reduced tumor burden in mouse model of colon cancer. Therefore, it might be possible in the future to use plants to produce potential therapeutic miRNAs with an inherent robustness and in sufficient quantities to

provide a cost-effective alternative to currently available synthetic RNA production and delivery methods.

Further work in the future is required to identify and profile conserved and potential novel miRNAs that could exist not only in the studied plants, but also those endogenous miRNAs in the camel body fluid samples in order to further develop target gene prediction. This step could be done by qRT-PCR, deep-sequencing, miRNA microarray assays, and computational methods (Mackowiak, 2011; Liu *et al*., 2014).There was not any study describing the effect of the plant-derived miRNAs on the camel physiology. Therefore, further study in this regard is important and required to be carried out.

References

Abbas, B., Al-Qarawi, AA., & Al-Hawas, A. (2002). The ethnoveterinary knowledge and practice of traditional healers in Qassim Region, Saudi Arabia. *Journal of Arid Environments, 50*(3), 367-379.

Delazar, A., Gibbons, S., Hossein, AR., Nazemiyeh, H., Modarresi, M., Nahar, L and Sarker, SD. (2006). Flavone C-glycoside and cucurbitacin glycoside from *Citrullus colocynthis*. *DARA, 14*(3), 109-114.

Abbas, S., Vincourt, JB., Habib, L., Netter, P., Greige-Gerges, H., & Magdalou, J. (2013). The cucurbitacins E, D and I: investigation of their cytotoxicity toward human chondrosarcoma SW 1353 cell line and their biotransformation in man liver. *Toxicol Lett, 216*(2-3), 189-199.

Abdallah, RM., Ghazy, NM., El-Sebakhy, NA., Pirillo, A., & Verotta, L. (1993). Astragalosides from Egyptian Astragalus spinosus Vahl. *Die Pharmazie, 48*(6), 452-454.

Abdel Gader, AM., & Alhaider, AA. (2016). The unique medicinal properties of camel products: A review of the scientific evidence. *Journal of Taibah University Medical Sciences, 11*(2), 98-103.

Abdelwahab, SI., Hassan, LE., Sirat, HM., Yagi, SM., Koko, WS., Mohan, S., Hadi, AH. (2011). Anti-inflammatory activities of cucurbitacin E isolated from Citrullus lanatus var. citroides: role of reactive nitrogen species and cyclooxygenase enzyme inhibition. *Fitoterapia, 82*(8), 1190-1197.

Abouzid, SF., Ali, SA., & Choudhary, MI. (2009). A new ferulic acid ester and other constituents from Tamarix nilotica leaves. *Chem Pharm Bull (Tokyo), 57*(7), 740-742.

Accerbi, M., Schmidt, SA., De Paoli, E., Park, S., Jeong, DH., & Green, PJ. (2010). Methods for isolation of total RNA to recover miRNAs and other small RNAs from diverse species. *Methods Mol Biol, 592*, 31-50.

Ageel, AM., Mossa, JS., Tariq, M., Al-Yahya, MA., Saied, MS. (1987). Plants in Saudi Arabia used for folk medicine. Riyadh: King Saud University Press.

Agil, D., Miró, M., Jimenez, J., Aneiros, J., Caracuel, MD., García-Granados, A., & Navarro, MC. (1999). Isolation of an anti-hepatotoxic principle from the juice of Ecballium elaterium. *Planta medica, 65*(07), 673-675.

Akhlaq, M., & Mohammed, Ali. (2011). New phenolic acids from the galls of *Tamarix aphylla* (L.) Karst. *Int Res J Pharm, 4*, 222-225.

Al-Alawi, AA., & Laleye, LC. (2011). Characterization of camel milk protein isolates as nutraceutical and functional ingredients. Sultan Qaboos University & United Arab Emirates University

Al-Awadi, A., & Al-Judaibi, A. (1999). Effect of camel's urine inhibitory growth of some pathogenic fungi and yeast. *J Union Arab Biol, 8*, 335-363.

Al-Awadi, A., & Al-Judaibi, A. (2015). Effects of Heating and Storage on the Antifungal Activity of Camel Urine. *Clinical Microbiologys, 2014*.

Alghamdi, Z., & Khorshid, F. (2012). Cytotoxicity of the urine of different camel breeds on the proliferation of lung cancer cells, A549. *Journal of Natural Sciences Research, 2*, 9-16.

Alhaidar, A., Abdel Gader, AG., & Mousa, SA. (2011). The antiplatelet activity of camel urine. *J Altern Complement Med, 17*(9), 803-808.

Al-Humaid, AI., Mousa, HM., El-Mergawi, RA., & Abdel-Salam, AM. (2010). Chemical composition and antioxidant activity of dates and dates-camel-milk mixtures as a protective meal against lipid peroxidation in rats. *American Journal of Food Technology, 5*(1), 22-30.

Al-Numair, KS, & Alsaif, MA. (2011). Effect of camel milk on collagen abnormalities in streptozotocin-diabetic rats. *African Journal of Pharmacy and Pharmacology, 5*(2), 238-243.

Alonso-Amelot, Miguel E, Castillo, Uvidelio, Smith, Barry L, & Lauren, Denis R. (1998). Excretion, through milk, of ptaquiloside in bracken-fed cows. A quantitative assessment. *Le Lait, 78*(4), 413-423.

Andah, B., Okpoko, A., Shaw, T., & Sinclair, P. (2014). *The Archaeology of Africa: food, metals and towns*: Routledge.

Alrumman, SA. (2016). Phytochemical and Antimicrobial Properties of *Tamarix aphylla* L. Leaves Growing Naturally in the Abha Region, Saudi Arabia. *Arabian Journal for Science and Engineering, 41*(6), 2123-2129.

Alsaweed, M., Hartmann, PE., Geddes, DT., & Kakulas, F. (2015). MicroRNAs in breastmilk and the lactating breast: potential immunoprotectors and developmental regulators for the infant and the mother. *International journal of environmental research and public health, 12*(11), 13981-14020.

Al-Turki, TA., & Basahi, MA. (2015). Assessment of ISSR based molecular genetic diversity of Hassawi rice in Saudi Arabia. *Saudi J Biol Sci, 22*(5), 591-599.

Al-Yahya, MA. (1990). *Saudi plants: a phytochemical and biological approach*: King Abdulaziz City for Science and Technology.

Al-Yahya, MA., Khafagy, S., Shihata, A., Kozlowski, JF., Antoun, MD., & Cassady, J. M. (1984). Phytochemical and biological screening of Saudi medicinal plants, Part 6. Isolation of 2 alpha-hydroxyalantolactone the antileukemic principle of Francoeuria crispa. *J Nat Prod, 47*(6), 1013-1017.

Al-Yousef, N., Gaafar, A., Al-Otaibi, B., Al-Jammaz, I., Al-Hussein, K., & Aboussekhra, A. (2012). Camel urine components display anti-cancer properties in vitro. *Journal of Ethnopharmacology, 143*(3), 819-825.

Amin, RP., Kunaparaju, N., Kumar, S., Taldone, T., Barletta, MA., & Zito, SW. (2013). Structure elucidation and inhibitory effects on human platelet aggregation of chlorogenic acid from Wrightia tinctoria. *Journal of Complementary and Integrative Medicine, 10*(1), 97-104.

Andreu, Z., & Yanez-Mo, M. (2014). Tetraspanins in extracellular vesicle formation and function. *Front Immunol, 5*, 442.

Arellano, AR., Lopez-Pulido, EI., Martínez-Neri, PA, Chávez, CE., Lucano, RG., Fafutis-Morris, M., Pereira-Suárez, AL. (2015). STAT3 activation is required for the antiapoptotic effects of prolactin in cervical cancer cells. *Cancer cell international, 15*(1), 1.

Arntz, OJ., Pieters, BC., Oliveira, MC., Broeren, MG., Bennink, MB., Vries, M., der Kraan, PM. (2015). Oral administration of bovine milk derived extracellular vesicles attenuates arthritis in two mouse models. *Molecular nutrition & food research, 59*(9), 1701-1712.

Arroyo, JD., Chevillet, JR., Kroh, EM., Ruf, IK., Pritchard, CC., Gibson, DF., Tewari, M. (2011). Argonaute2 complexes carry a population of circulating

microRNAs independent of vesicles in human plasma. *Proc Natl Acad Sci U S A, 108*(12), 5003-5008.

Ascencio-Cedillo, R., López-Pulido, EI., Muñoz-Valle, JF., Villegas-Sepúlveda, N., Del Toro-Arreola, S., Estrada-Chávez, Ciro., García-Carrancá, Alejandro. (2015). Prolactin and Prolactin Receptor Expression in Cervical Intraepithelial Neoplasia and Cancer. *Pathology & Oncology Research, 21*(2), 241-246.

Aslani, MR., Movassaghi, AR., Mohri, M., Abbasian, A., & Zarehpour, M. (2004). Clinical and pathological aspects of experimental oleander (Nerium oleander) toxicosis in sheep. *Veterinary research communications, 28*(7), 609-616.

Aslani, MR., Movassaghi, AR., Janati-Pirouz, H., & Karazma, M. (2007). Experimental oleander (Nerium oleander) poisoning in goats: a clinical and pathological study. *Iranian Journal of Veterinary Research, 8*(1), 58-63.

Attoub, S., Hassan, AH., Vanhoecke, B., Iratni, R., Takahashi, T., Gaben, A., Kamalboor, HA. (2011). Inhibition of cell survival, invasion, tumor growth and histone deacetylase activity by the dietary flavonoid luteolin in human epithelioid cancer cells. *European journal of pharmacology, 651*(1), 18-25.

Auerbach, A., Vyas, G., Li, A., Halushka, M., & Witwer, K. (2016). *Uptake of dietary milk miRNAs by adult humans: a validation study [version 1; referees: 3 approved]* (Vol. 5).

Auribie, MA. (2011). Antioxidant activity of tannin from *Tamarix aphylla* L. leaves. *Basrah J Agric Sci, 24*(1), 406-410.

Azaizeh, H., Saad, B., Khalil, K., & Said, O. (2006). The state of the art of traditional Arab herbal medicine in the Eastern region of the Mediterranean: a review. *Evidence-Based Complementary and Alternative Medicine, 3*(2), 229-235.

Badr, G. (2013). Camel whey protein enhances diabetic wound healing in a streptozotocin-induced diabetic mouse model: the critical role of beta-Defensin-1, -2 and -3. *Lipids Health Dis, 12*, 46.

Baesmel, S. (2004). The milk and urine of the camel between the heritage and science. *Journal of science and technology, 18*(70), 17-23.

Baier, SR., Nguyen, C., Xie, F., Wood, JR., & Zempleni, J. (2014). MicroRNAs are absorbed in biologically meaningful amounts from nutritionally relevant doses of

cow milk and affect gene expression in peripheral blood mononuclear cells, HEK-293 kidney cell cultures, and mouse livers. *J Nutr, 144*(10), 1495-1500.

Bakhsh, AA., El-Deeb, WM., & Al-Judaibi, AA. (2012). *Camel Urine and Milk in the Arab Heritage (Folk Medicine): A Review* (Vol. 451): Verlag der Österreichischen Akademie der Wissenschaften.

Bar, T., Stahlberg, A., Muszta, A., & Kubista, M. (2003). Kinetic Outlier Detection (KOD) in real-time PCR. *Nucleic Acids Res, 31*(17), e105.

Barbosa, JM., Costa, M., Gomes, C., & Trolin, G. (1993). Isolation of onopordopicrin, the oxic constitue of Arctium-lappa L (Vol. 4, pp. 186-187): Soc brasileira quimica caixa postal 26037, 05599-970 Sao Paulo, Brazil.

Barnes, J., Anderson, LA., & Phillipson, JD. (2007). Liquorice. *Herbal medicines, Third edition. Pharmaceutical Press, London*, 411-415.

Bartalis, J., & Halaweish, Fathi T. (2005). Relationship between cucurbitacins reversed-phase high-performance liquid chromatography hydrophobicity index and basal cytotoxicity on HepG2 cells. *Journal of Chromatography B, 818*(2), 159-166.

Bartel, DP. (2009). MicroRNAs: target recognition and regulatory functions. *Cell, 136*(2), 215-233.

Beatty, M., Guduric-Fuchs, J., Brown, E., Bridgett, S., Chakravarthy, U., Hogg, R. E., & Simpson, D. A. (2014). Small RNAs from plants, bacteria and fungi within the order Hypocreales are ubiquitous in human plasma. *BMC Genomics, 15*, 933.

Bedir, E., Calis, I., Aquino, R., Piacente, S., & Pizza, C. (1998). Cycloartane triterpene glycosides from the roots of Astragalus brachypterus and Astragalus microcephalus. *J Nat Prod, 61*(12), 1469-1472.

Bedir, E., Pugh, N., Calis, I., Pasco, DS., & Khan, Ikhlas A. (2000). Immunostimulatory effects of cycloartane-type triterpene glycosides from astragalus species. *Biological and Pharmaceutical Bulletin, 23*(7), 834-837.

Berendzen, K., Searle, I., Ravenscroft, D., Koncz, C., Batschauer, A., Coupland, G., Ulker, B. (2005). A rapid and versatile combined DNA/RNA extraction protocol and its application to the analysis of a novel DNA marker set polymorphic between Arabidopsis thaliana ecotypes Col-0 and Landsberg erecta. *Plant Methods, 1*(1), 4.

Blaskovich, MA., Sun, J., Cantor, A., Turkson, J., Jove, R., & Sebti, SM. (2003). Discovery of JSI-124 (cucurbitacin I), a selective Janus kinase/signal transducer and activator of transcription 3 signaling pathway inhibitor with potent antitumor activity against human and murine cancer cells in mice. *Cancer Res, 63*(6), 1270-1279.

Boersma, MG., van der Woude, H., Bogaards, J., Boeren, S., Vervoort, J., Cnubben, N. H., Rietjens, I. M. (2002). Regioselectivity of phase II metabolism of luteolin and quercetin by UDP-glucuronosyl transferases. *Chem Res Toxicol, 15*(5), 662-670.

Bole-Feysot, C., Goffin, V., Edery, M., Binart, N., & Kelly, PA. (1998). Prolactin (PRL) and its receptor: actions, signal transduction pathways and phenotypes observed in PRL receptor knockout mice. *Endocr Rev, 19*(3), 225-268.

Boroujerdnia, MG., Azemi, ME., Hemmati, AA., Taghian, A., & Azadmehr, A. (2011). Immunomodulatory effects of Astragalus gypsicolus hydroalcoholic extract in ovalbumin-induced allergic mice model. *Iranian Journal of Allergy, Asthma and Immunology, 10*(4), 281-288.

Bouatra, S., Aziat, F., Mandal, R., Guo, AC., Wilson, MR., Knox, C., Liu, P. (2013). The human urine metabolome. *PloS one, 8*(9), e73076.

Boulos, L. (1983). Medicinal Plants of North Africa. *Medicinal plants of North Africa.*

Brennecke, J., Stark, A., Russell, RB., & Cohen, SM. (2005). Principles of microRNA-target recognition. *PLoS Biol, 3*(3), e85.

Brown, B. D., Venneri, MA., Zingale, A., Sergi Sergi, L., & Naldini, L. (2006). Endogenous microRNA regulation suppresses transgene expression in hematopoietic lineages and enables stable gene transfer. *Nat Med, 12*(5), 585-591.

Bustin, SA. (2002). Quantification of mRNA using real-time reverse transcription PCR (RT-PCR): trends and problems. *J Mol Endocrinol, 29*(1), 23-39.

Bustin, SA., & Mueller, R. (2005). Real-time reverse transcription PCR (qRT-PCR) and its potential use in clinical diagnosis. *Clin Sci (Lond), 109*(4), 365-379.

Cai, X., Ye, T., Liu, C., Lu, W., Lu, M., Zhang, J., Cao, P. (2011). Luteolin induced G2 phase cell cycle arrest and apoptosis on non-small cell lung cancer cells. *Toxicology in Vitro, 25*(7), 1385-1391.

Cardenas, ME., Cruz, MC., Del Poeta, M., Chung, N., Perfect, JR., Heitman, J. (1999). Antifungal activities of antineoplastic agents: Saccharomyces cerevisiae as a model system to study drug action. *Clin. Microbiol. Rev.* 12: 583–611.

Cha, J. W., Piao, MJ., Kim, KC., Yao, CW., Zheng, J., Kim, SM., Hyun, JW. (2014). The Polyphenol Chlorogenic Acid Attenuates UVB-mediated Oxidative Stress in Human HaCaT Keratinocytes. *Biomol Ther (Seoul), 22*(2), 136-142.

Chan, W., Durairajan, S., Lu, J., W., Xie, L., Kum, W., Li, M. (2009). Neuroprotective effects of Astragaloside IV in 6-hydroxydopamine-treated primary nigral cell culture. *Neurochemistry International, 55*(6), 414-422.

Chan, Y., Cheng, L., Wu, J., Chan, E., Kwan, Y., Lee, S., Chan, S. (2011). A review of the pharmacological effects of Arctium lappa (burdock). *Inflammopharmacology, 19*(5), 245-254.

Chang, K., Marran, K., Valentine, A., & Hannon, GJ. (2012). RNAi in cultured mammalian cells using synthetic siRNAs. *Cold Spring Harbor Protocols, 2012*(9), pdb. prot071076.

Chang, S., Puryear, J., & Cairney, J. (1993). A simple and efficient method for isolating RNA from pine trees. *Plant Molecular Biology Reporter, 11*(2), 113-116.

Charters, YM, Robertson, A, Wilkinson, MJ, & Ramsay, G. (1996). PCR analysis of oilseed rape cultivars (Brassica napus L. ssp. oleifera) using 5′-anchored simple sequence repeat (SSR) primers. *Theoretical and Applied Genetics, 92*(3-4), 442-447.

Chaubal, R., Pawar, PV., Hebbalkar, GD., Tungikar, VB., Puranik, VG., Deshpande, VH., & Deshpande, NR. (2005). Larvicidal Activity of Acacia nilotica Extracts and Isolation of D-Pinitol–A Bioactive Carbohydrate. *Chemistry & biodiversity, 2*(5), 684-688.

Chawech, R., Jarraya, R., Girardi, C., Vansteelandt, M., Marti, G., Nasri, I., Fabre, N. (2015). Cucurbitacins from the Leaves of *Citrullus colocynthis* (L.) Schrad. *Molecules, 20*(10), 18001-18015.

Chen, C., Ridzon, DA., Broomer, AJ., Zhou, Z., Lee, DH., Nguyen, JT., Guegler, KJ. (2005a). Real-time quantification of microRNAs by stem-loop RT-PCR. *Nucleic Acids Res, 33*(20), e179.

Chen, F., Wu, A., & Chen, C. (2004). The influence of different treatments on the free radical scavenging activity of burdock and variations of its active components. *Food chemistry, 86*(4), 479-484.

Chen, JC., Chiu, MH., Nie, RL., Cordell, GA., & Qiu, SX. (2005). Cucurbitacins and cucurbitane glycosides: structures and biological activities. *Natural product reports, 22*(3), 386-399.

Chen, M., Calin, GA., & Meng, QH. (2014b). Chapter Five - Circulating microRNAs as Promising Tumor Biomarkers. In S. M. Gregory (Ed.), *Advances in Clinical Chemistry* (Vol. Volume 67, pp. 189-214): Elsevier.

Chen, T., Xi, QY., Ye, RS., Cheng, X., Qi, QE., Wang, SB., Zhang, YL. (2014). Exploration of microRNAs in porcine milk exosomes. *BMC Genomics, 15*, 100.

Chen, X., Zen, K., & Zhang, C. (2013). Reply to Lack of detectable oral bioavailability of plant microRNAs after feeding in mice. *Nature biotechnology, 31*(11), 967-969.

Cheng, JC., Dai, F., Zhou, B., Yang, L., & Liu, ZL. (2007). Antioxidant activity of hydroxycinnamic acid derivatives in human low density lipoprotein: Mechanism and structure–activity relationship. *Food Chemistry, 104*(1), 132-139.

Cheng, L., Sharples, RA., Scicluna, BJ., & Hill, AF. (2014). Exosomes provide a protective and enriched source of miRNA for biomarker profiling compared to intracellular and cell-free blood. *J Extracell Vesicles, 3*.

Chiang, LC., Chiang, W., Chang, MY., Ng, LT., & Lin, CC. (2002). Antiviral activity of Plantago major extracts and related compounds in vitro. *Antiviral research, 55*(1), 53-62.

Chin, AR., Fong, MY., Somlo, G., Wu, J., Swiderski, P., Wu, X., & Wang, SE. (2016). Cross-kingdom inhibition of breast cancer growth by plant miR159. *Cell Res, 26*(2), 217-228.

Chiu, FL., & Lin, JK. (2008). Downregulation of androgen receptor expression by luteolin causes inhibition of cell proliferation and induction of apoptosis in human prostate cancer cells and xenografts. *Prostate, 68*(1), 61-71.

Chomczynski, P., & Sacchi, N. (2006). The single-step method of RNA isolation by acid guanidinium thiocyanate-phenol-chloroform extraction: twenty-something years on. *Nat Protoc, 1*(2), 581-585.

Coll, JC., & Bowden, BF. (1986). The application of vacuum liquid chromatography to the separation of terpene mixtures. *Journal of Natural Products, 49*(5), 934-936.

Daradka, H., Almasad, MM., Qazan, W., El-Banna, NM., & Samara, O. (2007). Hypolipidaemic effects of *Citrullus colocynthis* L. in rabbits. *Pakistan journal of biological sciences: PJBS, 10*(16), 2768-2771.

Darwish, FA. (2002). Phytochemical Investigation of Biologically Active Fractions of *Astragalus spinosus* Roots Grown in Egypt. *Journal of Medical Sciences, 2*(3), 119-123.

Dastmalchi, M., & Dhaubhadel, S. (2014). Soybean Seed Isoflavonoids: Biosynthesis and Regulation *Phytochemicals–Biosynthesis, Function and Application* (pp. 1-21): Springer.

de Almeida, A., Luiz-Ferreira, A., Cola, M., Di Pietro Magri, L., Batista, LM., de Paiva, JA., Souza-Brito, ARM. (2012). Anti-ulcerogenic mechanisms of the sesquiterpene lactone onopordopicrin-enriched fraction from Arctium lappa L.(Asteraceae): role of somatostatin, gastrin, and endogenous sulfhydryls and nitric oxide. *Journal of medicinal food, 15*(4), 378-383.

De Coaña, YP., Parody, N., Fernández-Caldas, E., & Alonso, C. (2010). A Modified Protocol for RNA Isolation from High Polysaccharide Containing Cupressus arizonica Pollen. Applications for RT–PCR and Phage Display Library Construction. *Molecular biotechnology, 44*(2), 127-132.

Delazar, A., Gibbons, S., Kosari, AR., Nazemiyeh, H., Modarresi, M., Nahar, L., & Sarker, Sd. (2006). Flavone C-glycosides and cucurbitacin glycosides from *Citrullus colocynthis*. *DARU Journal of Pharmaceutical Sciences, 14*(3), 109-114.

Deng, MY., Wang, H., Ward, GB., Beckham, TR., & McKenna, TS. (2005). Comparison of six RNA extraction methods for the detection of classical swine fever virus by real-time and conventional reverse transcription-PCR. *J Vet Diagn Invest, 17*(6), 574-578.

Denisov, V., Strong, W., Walder, M., Gingrich, J., & Wintz, H. (2008). Development and validation of RQI: an RNA quality indicator for the Experion automated electrophoresis system. *Bio-Rad Bulletin, 5761*.

Denizli, N., Horo, I., Gulcemal, D., Masullo, M., Festa, M., Capasso, A., Alankus-Caliskan, O. (2014). Cycloartane glycosides from Astragalus plumosus var. krugianus and evaluation of their antioxidant potential. *Fitoterapia, 92*, 211-218.

Dewick, PM. Medicinal Natural Products. A Biosynthetic Approach. 2009. 3rd ed.; John Wiley & Sons: Chichester, UK, p. 239

Dhanotia, R., Chauhan, NS., Saraf, DK., & Dixit, VK. (2011). Effect of *Citrullus colocynthis* Schrad fruits on testosterone-induced alopecia. *Natural product research, 25*(15), 1432-1443.

Dickinson, B., Zhang, Y., Petrick, JS., Heck, G., Ivashuta, S., & Marshall, WS. (2013). Lack of detectable oral bioavailability of plant microRNAs after feeding in mice. *Nat Biotechnol, 31*(11), 965-967.

Doench, JG., & Sharp, PA. (2004). Specificity of microRNA target selection in translational repression. *Genes Dev, 18*(5), 504-511.

Dong, Y., Lu, B., Zhang, X., Zhang, J., Lai, L., Li, D., Pang, X. (2010). Cucurbitacin E, a tetracyclic triterpenes compound from Chinese medicine, inhibits tumor angiogenesis through VEGFR2-mediated Jak2–STAT3 signaling pathway. *Carcinogenesis, 31*(12), 2097-2104.

Dorsett, Y., & Tuschl, T. (2004). siRNAs: applications in functional genomics and potential as therapeutics. *Nature Reviews Drug Discovery, 3*(4), 318-329.

Dubey, A., Kalra, SS., Trivedi. N. (2013). Computational Prediction of miRNA in Gmelina Arborea and their Role in Human Metabolomics. *American Journal of Bioscience and Bioengineering 1*(5), 62-74.

Duncan, K., Duncan, MD., Alley, MC., & Sausville, EA. (1996). Cucurbitacin E-induced disruption of the actin and vimentin cytoskeleton in prostate carcinoma cells. *Biochemical pharmacology, 52*(10), 1553-1560.

El-Agamy, EI. (2006). Camel milk. *Handbook of milk of non-bovine mammals*, 297-344.

El-Agamy, EI., Nawar, M., Shamsia, SM., Awad, S., & Haenlein, G. (2009). Are camel milk proteins convenient to the nutrition of cow milk allergic children? *Small Ruminant Research, 82*(1), 1-6.

Elbashir, SM., Harborth, J., Lendeckel, W., Yalcin, A., Weber, K., & Tuschl, T. (2001). Duplexes of 21-nucleotide RNAs mediate RNA interference in cultured mammalian cells. *nature, 411*(6836), 494-498.

Eldh, M., Lotvall, J., Malmhall, C., & Ekstrom, K. (2012). Importance of RNA isolation methods for analysis of exosomal RNA: evaluation of different methods. *Mol Immunol, 50*(4), 278-286.

El-Moussallami, A., Hussein, S., & Nawwar, M. (2000). Polyphenolic metabolites of the flower of *Tamarix amplexicaulis*. *Natural Product Sciences*, **6** (193-198).

EL-Elyani, RAA, & Khalifa, SAM. (2006). Histological Studies on the Effect of Camels Urine and Milk on Stomach of Albino Mice.

El-Said, EE., El-Sayed, GR., & Tantawy, E. (2010). *Effect of camel milk on oxidative stresses in experimentally induced diabetic rabbits.* Paper presented at the Veterinary Research Forum.

El-Sebakhy, NA., Harraz, FM., Abdallah, RM., Asaad, AM., Orsini, F., Pelizzoni, F., Verotta, L. (1990). Cycloartane triterpene glycosides from EgyptianAstragalus species. *Phytochemistry, 29*(10), 3271-3274.

El-Sherbini, E., El-Sayed, GR., & Tantawy, E. (2012). *Effect of Camel Milk on Oxidative Stresses in Experimentally Induced Diabetic Rabbits.* Paper presented at the Veterinary Research Forum.

Esterbauer, H. (1993). Cytotoxicity and genotoxicity of lipid-oxidation products. *Am J Clin Nutr, 57*(5 Suppl), 779S-785S; discussion 785S-786S.

Fang, DQ, & Roose, ML. (1997). Identification of closely related citrus cultivars with inter-simple sequence repeat markers. *Theoretical and Applied Genetics, 95*(3), 408-417.

FAO, (2012). *Milk & Dairy Products.* FAO's Animal Production and Health Division.

Farah, Z., Mollet, M., Younan, M., & Dahir, R. (2007). Camel dairy in Somalia: Limiting factors and development potential. *Livestock Science, 110*(1), 187-191.

Farah, Z., Rettenmaier, R., & Atkins, D. (1992). Vitamin content of camel milk. *Int J Vitam Nutr Res, 62*(1), 30-33.

Feng, H., Zang, L., Zhao, Z., & Kan, Q. (2014). Cucurbitacin-E inhibits multiple cancer cells proliferation through attenuation of Wnt/β-catenin signaling. *Cancer Biotherapy and Radiopharmaceuticals, 29*(5), 210-214.

Ferracane, R., Graziani, G., Gallo, M., Fogliano, V., & Ritieni, A. (2010). Metabolic profile of the bioactive compounds of burdock (Arctium lappa) seeds, roots and leaves. *Journal of pharmaceutical and biomedical analysis, 51*(2), 399-404.

Ferreira, D., Adega, F. and Chaves, R. (2013). The Importance of Cancer Cell Lines as in vitro Models in Cancer Methylome Analysis and Anticancer Drugs Testing, Oncogenomics and Cancer Proteomics - Novel Approaches in Biomarkers Discovery and Therapeutic Targets in Cancer. *InTech*, DOI: 10.5772/53110.

Filip, R, & Ferraro, GE. (2003). Researching on new species of "Mate": Ilex brevicuspis. *European journal of nutrition, 42*(1), 50-54.

Fisinin, V. I., Papazyan, T. T., & Surai, P. F. (2009). Producing selenium-enriched eggs and meat to improve the selenium status of the general population. *Crit Rev Biotechnol, 29*(1), 18-28.

FitzGerald, R. J., & Meisel, H. (2000). Milk protein-derived peptide inhibitors of angiotensin-I-converting enzyme. *Br J Nutr, 84 Suppl 1*, S33-37.

Fleige, S., & Pfaffl, M. W. (2006). RNA integrity and the effect on the real-time qRT-PCR performance. *Mol Aspects Med, 27*(2-3), 126-139.

Fleming, A., Sampey, G., Chung, MC., Bailey, C., van Hoek, ML., Kashanchi, F., & Hakami, RM. (2014). The carrying pigeons of the cell: exosomes and their role in infectious diseases caused by human pathogens. *Pathogens and Disease, 71*(2), 109-120.

Fraser, CM., & Nelson, J. (1959). Sweet clover poisoning in newborn calves. *J Am Vet Med Assoc, 135*, 283-286.

Freitas, RN., Brasileiro-Filho, G., Silva, ME., & Pena, SD. (2002). Bracken fern-induced malignant tumors in rats: absence of mutations in p53, H-ras and K-ras and no microsatellite instability. *Mutat Res, 499*(2), 189-196.

Fryer, RM., Randall, J., Yoshida, T., Hsiao, LL., Blumenstock, J., Jensen, KE., Gullans, SR. (2002). Global analysis of gene expression: methods, interpretation, and pitfalls. *Exp Nephrol, 10*(2), 64-74.

Galey, FD., Holstege, DM., Plumlee, KH., Tor, E., Johnson, B., Anderson, ML., Brown, F. (1996). Diagnosis of oleander poisoning in livestock. *J Vet Diagn Invest, 8*(3), 358-364.

Gao, Y., Zhang, M., Wu, T., Xu, M., Cai, H., & Zhang, Z. (2015). Effects of d-Pinitol on Insulin Resistance through the PI3K/Akt Signaling Pathway in Type 2 Diabetes Mellitus Rats. *Journal of agricultural and food chemistry, 63*(26), 6019-6026.

García-Baldenegro, CV., Vargas-Arispuro, I., Islas-Osuna, M., Rivera-Domínguez, M., Aispuro-Hernández, E., & Martínez-Téllez, MÁ. (2015). Total RNA quality of lyophilized and cryopreserved dormant grapevine buds. *Electronic Journal of Biotechnology, 18*(2), 134-137.

Gebreheiwot, K., Amenu, D., & Asfaw, N. (2010). Cuauthemone sesquiterpenes and flavones from Laggera tomentosa endemic to Ethiopia. *Bulletin of the Chemical Society of Ethiopia, 24*(2).

Geethan, P, & Prince, P. (2008). Antihyperlipidemic effect of D-pinitol on streptozotocin-induced diabetic wistar rats. *Journal of biochemical and molecular toxicology, 22*(4), 220-224.

Gehrig, HH., Winter, K., Cushman, J., Borland, A., & Taybi, T. (2000). An improved RNA isolation method for succulent plant species rich in polyphenols and polysaccharides. *Plant Molecular Biology Reporter, 18*(4), 369-376.

Ghawana, S., Paul, A., Kumar, H., Kumar, A., Singh, H., Bhardwaj, PK., Kumar, S. (2011). An RNA isolation system for plant tissues rich in secondary metabolites. *BMC Res Notes, 4*, 85.

Gill, S., Peston, D., Vonderhaar, BK., & Shousha, S. (2001). Expression of prolactin receptors in normal, benign, and malignant breast tissue: an immunohistological study. *Journal of clinical pathology, 54*(12), 956-960.

Gomes, J., Magalhaes, A., Michel, V., Amado, I. F., Aranha, P., Ovesen, RG., Touati, E. (2012). Pteridium aquilinum and its ptaquiloside toxin induce DNA damage response in gastric epithelial cells, a link with gastric carcinogenesis. *Toxicol Sci, 126*(1), 60-71.

Gordon, DJ., Sciarretta, KL., & Meredith, SC. (2001). Inhibition of beta-amyloid (40) fibrillogenesis and disassembly of beta-amyloid (40) fibrils by short beta-amyloid congeners containing *N*-methyl amino acids at alternate residues. *Biochemistry, 40*(28), 8237-8245.

Gray, AI., Igoli, JO., & Edrada-Ebel, R. (2012). Natural products isolation in modern drug discovery programs. *Methods Mol Biol, 864*, 515-534.

Greige-Gerges, H., Khalil, RA., Mansour, EA., Magdalou, J., Chahine, R., & Ouaini, N. (2007). Cucurbitacins from Ecballium elaterium juice increase the binding of bilirubin and ibuprofen to albumin in human plasma. *Chemico-biological interactions, 169*(1), 53-62.

Gross, JC., Chaudhary, V., Bartscherer, K., & Boutros, M. (2012). Active Wnt proteins are secreted on exosomes. *Nature cell biology, 14*(10), 1036-1045.

Guardia, T., Rotelli, AE., Juarez, AO., & Pelzer, LE. (2001). Anti-inflammatory properties of plant flavonoids. Effects of rutin, quercetin and hesperidin on adjuvant arthritis in rat. *Il farmaco, 56*(9), 683-687.

Gurudeeban, S., & Ramanathan, T. (2010). Antidiabetic effect of *Citrullus colocynthis* in alloxon-induced diabetic rats. *Inventi Rapid: Ethno pharmacology, 1*, 112.

Gurudeeban, S., Satyavani, K., & Ramanathan, T. (2010). Bitter apple (*Citrullus colocynthis*): an overview of chemical composition and biomedical potentials. *Asian Journal of Plant Sciences, 9*(7), 394.

Haenszel, W., Kurihara, M., Locke, FB., Shimuzu, K., & Segi, M. (1976). Stomach cancer in Japan. *J Natl Cancer Inst, 56*(2), 265-274.

Hall, P., & Cash, J. (2012). What is the real function of the liver 'function' tests? *Ulster Med J, 81*(1), 30-36.

Hamad, EM., Abdel-Rahim, EA., & Romeih, EA. (2011). Beneficial effect of camel milk on liver and kidneys function in diabetic Sprague-Dawley rats. *Int J Dairy Sci, 6*(3), 190-197.

Hämäläinen, M., Nieminen, R., Vuorela, P., Heinonen, M., & Moilanen, E. (2007). Anti-inflammatory effects of flavonoids: genistein, kaempferol, quercetin, and daidzein inhibit STAT-1 and NF-κB activations, whereas flavone, isorhamnetin, naringenin, and pelargonidin inhibit only NF-κB activation along with their inhibitory effect on iNOS expression and NO production in activated macrophages. *Mediators of inflammation, 2007* (10), 45673.

Hammerle-Fickinger, A., Riedmaier, I., Becker, C., Meyer, HH., Pfaffl, MW., & Ulbrich, SE. (2010). Validation of extraction methods for total RNA and miRNA from bovine blood prior to quantitative gene expression analyses. *Biotechnol Lett, 32*(1), 35-44.

Han, K., Meng, W., Zhang, JJ., Zhou, Y., Wang, YL., Su, Y., Min, DL. (2016). Luteolin inhibited proliferation and induced apoptosis of prostate cancer cells through miR-301. *Onco Targets Ther, 9*, 3085-3094.

Hanson, EK., & Ballantyne, J. (2013). Rapid and inexpensive body fluid identification by RNA profiling-based multiplex High Resolution Melt (HRM) analysis. *F1000Res, 2*, 281.

Harborne, JB., Phytochemical, Society, & Symposium. (1978). *Biochemical aspects of plant and animal coevolution: proceedings of the Phytochemical Society Symposium, Reading, April, 1977*, London.

Harding, C., Heuser, J., Stahl, P. (1984). Endocytosis and intracellular processing of transferrin and colloidal gold transferrin in rat reticulocytes: demonstration of a pathway for receptor shedding. *Eur J Cell Biol 35: 256–263.*

Hasan, H., Ohman, A., & Dinulescu, D. (2015). The promise and challenge of ovarian cancer models. *Transl Cancer Res*. 4(1): 14–28

Hatam, NR., Whiting, DA., & Yousif, NJ. (1989). Cucurbitacin glycosides from *Citrullus colocynthis*. *Phytochemistry, 28*(4), 1268-1271.

Hayashi, T., Okamuka, K., Kawasaki, M., Morita, N. (1993). Production of Diterpenoids by cultured cells from two chemotypes scoparia dulcis. Phytochemistry 35 (2): 353-356.

Heath, D, Lwama, GK, & Devlin, RH. (1993). PCR primed with VNTR core sequences yields species specific patterns and hypervariable probes. *Nucleic Acids Research, 21*(24), 5782-5785.

Hernández-Mijares, A., Bañuls, C., Peris, JE., Monzó, N., Jover, A., Bellod, L., Rocha, M. (2013). A single acute dose of pinitol from a naturally-occurring food ingredient decreases hyperglycaemia and circulating insulin levels in healthy subjects. *Food chemistry, 141*(2), 1267-1272.

Honda, G., & Tabata, M. (1982). Antidermatophytic substance from Sophora angustifolia. *Planta Med, 46*(2), 122-123.

Hu, J., Han, J., Chu, Z., Song, H., Zhang, D., Zhang, Q., & Huang, Y. (2009). Astragaloside IV attenuates hypoxia-induced cardiomyocyte damage in rats by upergulating superoxide dimutase-1 levels. *Clinical and Experimental Pharmacology and Physiology, 36*(4), 351-357.

Huang, D., Guh, J., Chueh, S., & Teng, C. (2004). Modulation of anti-adhesion molecule MUC-1 is associated with arctiin-induced growth inhibition in PC-3 cells. *The Prostate, 59*(3), 260-267.

Huang, K., & Walker, AM. (2010). Long term increased expression of the short form 1b prolactin receptor in PC-3 human prostate cancer cells decreases cell growth and migration, and causes multiple changes in gene expression consistent with reduced invasive capacity. *The Prostate, 70*(1), 37-47.

Hung, C., Chang, C., Lin, C., Ko, S., & Hsu, Y. (2013). Cucurbitacin E as inducer of cell death and apoptosis in human oral squamous cell carcinoma cell line SAS. *International journal of molecular sciences, 14*(8), 17147-17156.

Huseini, HF., Darvishzadeh, F., Heshmat, R., Jafariazar, Z., Raza, Mohsin., & Larijani, B. (2009). The clinical investigation of *Citrullus colocynthis* (L.) schrad fruit in treatment of Type II diabetic patients: a randomized, double blind, placebo-controlled clinical trial. *Phytotherapy Research, 23*(8), 1186-1189.

Hussain, AI., Rathore, HA., Sattar, MZ., Chatha, SA., Sarker, SD., & Gilani, AH. (2014). *Citrullus colocynthis* (L.) Schrad (bitter apple fruit): a review of its

phytochemistry, pharmacology, traditional uses and nutritional potential. *J Ethnopharmacol, 155*(1), 54-66.

Hussain, M. (2012). Micro-RNAs (miRNAs): genomic organisation, biogenesis and mode of action. *Cell and tissue research, 349*(2), 405-413.

Hussein, F. (1985). *Medicinal plants in Libya*: Arab Encyclopedia House.

Imbeaud, S., Graudens, E., Boulanger, V., Barlet, X., Zaborski, P., Eveno, E., Auffray, C. (2005). Towards standardization of RNA quality assessment using user-independent classifiers of microcapillary electrophoresis traces. *Nucleic Acids Res, 33*(6), e56.

Ip, F., Ng, Y., An, H., Dai, Y., Pang, H., Hu, YQ., Ip, NY. (2014). Cycloastragenol is a potent telomerase activator in neuronal cells: implications for depression management. *Neurosignals, 22*(1), 52-63.

Iqbal, A., Din, SU., Khan, I., & Jan, S. 2015. Antimicrobial activities of selected weed plants. *Pak. J. Weed Sci. Res, 21*(2), 229-238.

Iqbal, A, & Khan, BB. (2001). Feeding behaviour of camel. Review. *Pakistan Journal of Agricultural Sciences*, *38*, 58-63.

Izumi, H, Kosaka, N, Shimizu, T, Sekine, K, Ochiya, Takahiro, & Takase, M. (2012). Bovine milk contains microRNA and messenger RNA that are stable under degradative conditions. *Journal of dairy science, 95*(9), 4831-4841.

Jayachandran, M., Miller, VM., Heit, JA., & Owen, WG. (2012). Methodology for isolation, identification and characterization of microvesicles in peripheral blood. *J Immunol Methods, 375*(1-2), 207-214.

Jayaprakasam, B., Seeram, NP., & Nair, MG. (2003). Anticancer and antiinflammatory activities of cucurbitacins from Cucurbitaandreana. *Cancer letters, 189*(1), 11-16.

Jensen, K., Anderson, J. A., & Glass, E. J. (2014). Comparison of small interfering RNA (siRNA) delivery into bovine monocyte-derived macrophages by transfection and electroporation. *Vet Immunol Immunopathol, 158*(3-4), 224-232.

Jiménez-González, L., Álvarez-Corral, M., Muñoz-Dorado, M., & Rodríguez-García, I. (2008). Pterocarpans: interesting natural products with antifungal activity and other biological properties. *Phytochemistry Reviews, 7*(1), 125-154.

Johnson, M., Zaretskaya, I., Raytselis, Y., Merezhuk, Y., McGinnis, S., & Madden, TL. (2008). NCBI BLAST: a better web interface. *Nucleic Acids Research, 36*(Web Server issue), W5-W9.

Jones-Rhoades, M.W., & Bartel, DP. (2004). Computational identification of plant microRNAs and their targets, including a stress-induced miRNA. *Mol Cell, 14*(6), 787-799.

Ju, S., Mu, J., Dokland, T., Zhuang, X., Wang, Q., Jiang, H., Zhang, H.G. (2013). Grape exosome-like nanoparticles induce intestinal stem cells and protect mice from DSS-induced colitis. *Mol Ther, 21*(7), 1345-1357.

Jung, HJ., Kang, SS., Hyun, SK., & Choi, JS. (2005). In vitro free radical and ONOO- scavengers from Sophora flavescens. *Arch Pharm Res, 28*(5), 534-540.

Ju-ping, H., Yong, Z., Xiao-hong, S., Qi-hua, W., & Ying-jie, Pan. (2012). Antibacterial Effects of Burdock (Arctium Lappa L.) Concentrate on Vibrio parahemolyticus. *Natural Product Research & Development, 24*(3).

Kabbashi, MA., & Al Fadhil, AO. (2016) In vitro Antifungal Activity of Camel's Urine against Dermatophytes. *American Journal of Research Communication, 4*(4).

Kalra, H., Adda, CG., Liem, M., Ang, CS., Mechler, A., Simpson, RJ., Mathivanan, S. (2013). Comparative proteomics evaluation of plasma exosome isolation techniques and assessment of the stability of exosomes in normal human blood plasma. *Proteomics, 13*(22), 3354-3364.

Kamboj, A., & Saluja, AK. (2011). Isolation of stigmasterol and β-sitosterol from petroleum ether extract of aerial parts of Ageratum conyzoides (Asteraceae). *Int J Pharm Pharm Sci, 3*(1), 94-96.

Kamkaen, N., Matsuki, Y., Ichino, C., Kiyohara, H., & Yamada, H. (2006). The isolation of the anti-helicobacter pylori compounds in seeds of Arctium lappa Linn. *Thai Pharm Health Sci J, 1*(2), 12-18.

Kang, O., Choi, J., Lee, J., & Kwon, D. (2010). Luteolin isolated from the flowers of Lonicera japonica suppresses inflammatory mediator release by blocking NF-κB and MAPKs activation pathways in HMC-1 cells. *Molecules, 15*(1), 385-398.

Kang'ethe, EK., & Lang'a, KA. (2009). Aflatoxin B1 and M1 contamination of animal feeds and milk from urban centers in Kenya. *Afr Health Sci, 9*(4), 218-226.

Kappeler, SR., Farah, Z., & Puhan, Z. (2003). 5'-flanking regions of camel milk genes are highly similar to homologue regions of other species and can be divided into two distinct groups. *J Dairy Sci, 86*(2), 498-508.

Kappeler, SR., Heuberger, C., Farah, Z., & Puhan, Z. (2004). Expression of the peptidoglycan recognition protein, PGRP, in the lactating mammary gland. *J Dairy Sci, 87*(8), 2660-2668.

Karve, R., Suarez-Roman, F., & Iyer-Pascuzzi, AS. (2016). The Transcription Factor NIN-LIKE PROTEIN7 Controls Border-Like Cell Release. *Plant Physiol, 171*(3), 2101-2111.

Karve, R., Suárez-Román, F., & Iyer-Pascuzzi, AS. (2016). The transcription factor NIN-LIKE PROTEIN 7 (NLP7) controls border-like cell release in Arabidopsis. *Plant Physiology*, pp. 00453.02016.

Kaskous, S. (2016). Importance of camel milk for human health. *Emir. J. Food Agric, 28*(3), 158-163.

Kavarthapu, R., Tsai Morris, CH., & Dufau, ML. (2014). Prolactin induces up-regulation of its cognate receptor in breast cancer cells via transcriptional activation of its generic promoter by cross-talk between ERalpha and STAT5. *Oncotarget, 5*(19), 9079-9091.

Kawai, M., Hirano, T., Higa, S., Arimitsu, J., Maruta, M., Kuwahara, Y., Tanaka, T. (2007). Flavonoids and related compounds as anti-allergic substances. *Allergol Int, 56*(2), 113-123.

Kaya, GI., & Melzig, MF. (2008). Quantitative determination of cucurbitacin E and cucurbitacin I in homoeopathic mother tincture of Gratiola officinalis L. by HPLC. *Die Pharmazie-An International Journal of Pharmaceutical Sciences, 63*(12), 851-853.

Keyhanfar, M., Nazeri, S., & Bayat, M. (2012). Evaluation of antibacterial activities of some medicinal plants, traditionally used in Iran. *Iranian Journal of Pharmaceutical Sciences, 8*(1), 353-358.

Khan, AA., Alzohairy, MA., & Mohieldein, AH. (2013). Antidiabetic effects of camel milk in streptozotocin-induced diabetic rats. *Am J Biochem Mol Biol, 3*(1), 151-158.

Khan, AL., Hussain, J., Hamayun, M., Gilani, SA., Ahmad, S., Rehman, G., Lee, I. (2010). Secondary Metabolites from Inula britannica L. and Their Biological Activities. *Molecules, 15*(3), 1562.

Khanvilkar, AV., Kulkami, MD., Yadav, GB., Samant, SR., & Thorat, VJ. (2009). Desert friendly animal-The Camel. *Veterinary World, 2*(6), 240-241.

Khaskheli, M., Arain, MA., Chaudhry, S., Soomro, AH., & Qureshi, TA. (2005). Physico-chemical quality of camel milk. *Journal of Agriculture and Social Sciences, 2*, 164-166.

Khatibi, R., and Teymorri., J. (2011). Anticandidal screening and antibacterial of *Citrullus colocynthis* in South East of Iran. *Journal of Horticulture and Forestry*, 3(13): 392-398.

Khvorova, A., Reynolds, A., & Jayasena, SD. (2003). Functional siRNAs and miRNAs exhibit strand bias. *Cell, 115*(2), 209-216.

Kim, HJ., Park, J., & Kim, J. (2014). Cucurbitacin-I, a natural cell-permeable triterpenoid isolated from Cucurbitaceae, exerts potent anticancer effect in colon cancer. *Chemico-biological interactions, 219*, 1-8.

Kim, J., Lee, E., Lee, H., Ku, J., Lee, M., Yang, DC., & Kim, SH. (2007). Caspase activation and extracellular signal-regulated kinase/akt inhibition were involved in luteolin-induced apoptosis in lewis lung carcinoma cells. *Annals of the New York Academy of Sciences, 1095*(1), 598-611.

Kim, J., Kim, JC., Kang, M., Lee, M., Kim, J., & Cha, I. (2005). Effects of pinitol isolated from soybeans on glycaemic control and cardiovascular risk factors in Korean patients with type II diabetes mellitus: a randomized controlled study. *European journal of clinical nutrition, 59*(3), 456-458.

Kim, SR., Park, MJ., Lee, MK., Sung, SH., Park, EJ., Kim, J., Kim, YC. (2002). Flavonoids of Inula britannica protect cultured cortical cells from necrotic cell death induced by glutamate. *Free Radic Biol Med, 32*(7), 596-604.

Kitamura, S. (2006). Transport of flavonoids: from cytosolic synthesis to vacuolar accumulation *The Science of Flavonoids* (pp. 123-146): Springer.

Kogure, T., Lin, WL., Yan, IK., Braconi, C., & Patel, T. (2011). Intercellular nanovesicle-mediated microRNA transfer: a mechanism of environmental modulation of hepatocellular cancer cell growth. *Hepatology, 54*(4), 1237-1248.

Kojima, T., Nagaoka, T., Noda, K., & Ogihara, Y. (1998). Genetic linkage map of ISSR and RAPD markers in Einkorn wheat in relation to that of RFLP markers. *Theoretical and Applied Genetics, 96*(1), 37-45.

Kong, Y., Chen, J., Zhou, Z., Xia, H., Qiu, M., & Chen, C. (2014). Cucurbitacin E induces cell cycle G2/M phase arrest and apoptosis in triple negative breast cancer. *PloS one, 9*(7), e103760.

Konuspayeva, G., Faye, B., & Loiseau, G. (2009). The composition of camel milk: A meta-analysis of the literature data. *Journal of Food Composition and Analysis, 22*(2), 95-101.

Koroshi, A. (2007). Microalbuminuria, is it so important? *Hippokratia, 11*(3), 105-107.

Kozomara, A, & Griffiths-Jones, S. (2014). miRBase: annotating high confidence microRNAs using deep sequencing data. *Nucleic acids research, 42*(D1), D68-D73.

Kumar, N., & Pruthi, V. (2014). Potential applications of ferulic acid from natural sources. *Biotechnology Reports, 4*, 86-93.

Laleye, LC., Jobe, B., & Wasesa, AA. (2008). Comparative study on heat stability and functionality of camel and bovine milk whey proteins. *J Dairy Sci, 91*(12), 4527-4534.

Lamare, A., & Rao, SR. (2015). Efficacy of RAPD, ISSR and DAMD markers in assessment of genetic variability and population structure of wild Musa acuminata colla. *Physiol Mol Biol Plants, 21*(3), 349-358.

Lan, T., Wang, L., Xu, Q., Liu, W., Jin, H., Mao, W., Wang, X. (2013). Growth inhibitory effect of Cucurbitacin E on breast cancer cells. *Int J Clin Exp Pathol, 6*(9), 1799-1805.

Langford, SD., & Boor, PJ. (1996). Oleander toxicity: an examination of human and animal toxic exposures. *Toxicology, 109*(1), 1-13.

Lässer, C., Eldh, M., & Lötvall, J. (2012). Isolation and characterization of RNA-containing exosomes. *JoVE (Journal of Visualized Experiments)* (59), e3037-e3037.

Lavie, D., Willner, D., & Merenlender, Z. (1964). Constituents of *Citrullus colocynthis* (L.) Schrad. *Phytochemistry, 3*(1), 51-56.

Lee, DH., Iwanski, GB., & Thoennissen, NH. (2010). Cucurbitacin: ancient compound shedding new light on cancer treatment. *The Scientific World Journal, 10*, 413-418.

Lee, JS., Lee, C., Jeong, Y., Jung, ID., Kim, BH., Seong, E., Park, Y. (2007). d-pinitol regulates Th1/Th2 balance via suppressing Th2 immune response in ovalbumin-induced asthma. *FEBS letters, 581*(1), 57-64.

Lee, K., Lee, J. S., Jang, H. J., Kim, S. M., Chang, M. S., Park, S. H., Bu, Y. (2012). Chlorogenic acid ameliorates brain damage and edema by inhibiting matrix metalloproteinase-2 and 9 in a rat model of focal cerebral ischemia. *Eur J Pharmacol, 689*(1-3), 89-95.

Lee, SL., Raw, AS., & Yu, L. (2008). Dissolution testing *Biopharmaceutics applications in drug development* (pp. 47-74): Springer.

Lee, WJ., Wu, L., Chen, W., Wang, C., & Tseng, T. (2006). Inhibitory effect of luteolin on hepatocyte growth factor/scatter factor-induced HepG2 cell invasion involving both MAPK/ERKs and PI3K–Akt pathways. *Chemico-biological interactions, 160*(2), 123-133.

Lei, S. (2009). A Novel Fructan Possessing DB Value from Roots of Arctium lappa L. *Open Glycoscience, 2*, 25-27.

Lewis, B. P., Shih, I. H., Jones-Rhoades, M. W., Bartel, D. P., & Burge, C. B. (2003). Prediction of mammalian microRNA targets. *Cell, 115*(7), 787-798.

Li, L., Tao, H., & Chen, JB. (2006). Anti-apoptosis effect of astragaloside on adriamycin induced rat's cardiotoxicity. *Chinese journal of integrated traditional and Western medicine, 26*(11), 1011-1014.

Li, Zi-Pu, & Cao, Qian. (2002). Effects of astragaloside IV on myocardial calcium transport and cardiac function in ischemic rats. *Acta Pharmacologica Sinica, 23*(10), 898-904.

Liang, G., Zhu, Y., Sun, B., Shao, Y., Jing, A., Wang, J., & Xiao, Z. (2014). Assessing the survival of exogenous plant microRNA in mice. *Food Sci Nutr, 2*(4), 380-388.

Lima, Júlio César de, Loss-Morais, Guilherme, & Margis, Rogerio. (2012). MicroRNAs play critical roles during plant development and in response to abiotic stresses. *Genetics and molecular biology, 35*(4), 1069-1077.

Lin, Chun-Ching, Lin, Jer-Min, Yang, Jeng-Jer, Chuang, Shu-Chuan, & Ujiie, Takashi. (1996). Anti-inflammatory and radical scavenge effects of Arctium lappa. *The American journal of Chinese medicine, 24*(02), 127-137.

Lin, Xuezheng, Liu, Chunyan, Chen, Kaoshan, & Li, Guangyou. (2003). Extraction and content comparison of chlorogenic acid in Arctium lappa L. leaves collected from different terrain and its restraining bacteria test. *Natural Product Research and Development, 16*(4), 328-330.

Lindqvist, A., Manders, D., & Word, R. A. (2013). The impact of reference gene selection in quantification of gene expression levels in guinea pig cervical tissues and cells. *BMC Res Notes, 6*, 34.

Liu, Hongjun, Qin, Cheng, Chen, Zhe, Zuo, Tao, Yang, Xuerong, Zhou, Huangkai, Lin, Haijian. (2014). Identification of miRNAs and their target genes in developing maize ears by combined small RNA and degradome sequencing. *BMC genomics, 15*(1), 1.

Liu, KY, Zhang, TJ, Gao, WY, Chen, HX, & Zheng, YN. (2006). Phytochemical and pharmacological research progress in Tussilago farfara. *China journal of Chinese materia medica, 31*(22), 1837-1841.

Liu, Z., Zhao, J., Li, W., Shen, L., Huang, S., Tang, J., Zhang, R. (2016). Computational screen and experimental validation of anti-influenza effects of quercetin and chlorogenic acid from traditional Chinese medicine. *Sci Rep, 6*, 19095.

Livak, K. J., & Schmittgen, T. D. (2001). Analysis of relative gene expression data using real-time quantitative PCR and the 2(-Delta Delta C (T)) Method. *Methods, 25*(4), 402-408.

Logozzi M., De Milito A, Lugini L *et al. (2009) High levels of exosomes expressing CD63 and caveolin 1 in plasma of melanoma patients. PLoS ONE 4:* e5219.

Lopez-Lazaro, Miguel. (2009). Distribution and biological activities of the flavonoid luteolin. *Mini reviews in medicinal chemistry, 9*(1), 31-59.

Lopez-Pulido, E. I., Munoz-Valle, J. F., Del Toro-Arreola, S., Jave-Suarez, L. F., Bueno-Topete, M. R., Estrada-Chavez, C., & Pereira-Suarez, A. L. (2013). High expression of prolactin receptor is associated with cell survival in cervical cancer cells. *Cancer Cell Int, 13*(1), 103.

Lukasik, A., & Zielenkiewicz, P. (2014). In silico identification of plant miRNAs in mammalian breast milk exosomes--a small step forward? *PLoS One, 9*(6), e99963.

Lv, Lin, Wu, Shao-Yu, Wang, Guang-Fa, Zhang, Jia-Jie, Pang, Jian-Xin, Liu, Zhong-Qiu, Rao, Jin-Jun. (2010). Effect of astragaloside IV on hepatic glucose-regulating enzymes in diabetic mice induced by a high-fat diet and streptozotocin. *Phytotherapy research, 24*(2), 219-224.

Ma, Liping, Peng, Hongjun, Li, Kunsheng, Zhao, Runrun, Li, Li, Yu, Yilong, Han, Zhifeng. (2015). Luteolin exerts an anticancer effect on NCI-H460 human non-small cell lung cancer cells through the induction of Sirt1-mediated apoptosis. *Molecular medicine reports, 12*(3), 4196-4202.

Maatooq, Galal T., El-Sharkawy, Saleh H., Afifi, M. S., & Rosazza, Jack P. N. (1997). C-p-hydroxybenzoylglycoflavones from *Citrullus colocynthis*. *Phytochemistry, 44*(1), 187-190.

Mackowiak, Sebastian D. (2011). Identification of novel and known miRNAs in deep-sequencing data with miRDeep2. *Current Protocols in Bioinformatics*, 12.10. 11-12.10. 15.

MacRae, E. (2007). Extraction of plant RNA. *Methods Mol Biol, 353*, 15-24.

Mahfoudhi, Adel, Baaka, Noureddine, Haddar, Wafa, Mhenni, Mohamed Farouk, & Mighri, Zine. (2015). Development and optimization of the extraction process of

natural dye from Tamarix aphylla (L.) Karst. Leaves using response surface methodology (RSM). *Fibers and Polymers, 16*(7), 1487-1496.

Mahfoudhi, A., Prencipe, F. P., Mighri, Z., & Pellati, F. (2014). Metabolite profiling of polyphenols in the Tunisian plant *Tamarix aphylla* (L.) Karst. *J Pharm Biomed Anal, 99*, 97-105.

Maruta, Yoshihiko, Kawabata, Jun, & Niki, Ryoya. (1995). Antioxidative caffeoylquinic acid derivatives in the roots of burdock (Arctium lappa L.). *Journal of Agricultural and Food Chemistry, 43*(10), 2592-2595.

Marwat, Sarfaraz Khan. (2008). Salvadora persica, *Tamarix aphylla* and Zizyphus mauritiana: Three Woody Plant Species Mentioned in Holy Quran and Ahadith, and their Ethnobotanical Uses in North Western Part (DI Khan) of Pakistan. *Ethnobotanical Leaflets, 2008*(1), 135.

Marzouk, Belsem, Haloui, Ehsen, Akremi, Najoua, Aouni, Mahjoub, Marzouk, Zohra, & Fenina, Nadia. (2012). Antimicrobial and anticoagulant activities of *Citrullus colocynthis* Schrad. Leaves from Tunisia (Medenine). *African Journal of Pharmacy and Pharmacology, 6*(26), 1982-1988.

Massey, T. E., Stewart, R. K., Daniels, J. M., & Liu, L. (1995). Biochemical and molecular aspects of mammalian susceptibility to aflatoxin B1 carcinogenicity. *Proc Soc Exp Biol Med, 208*(3), 213-227.

Matoba, M., Saito, E., Saito, K., Koyama, K., Natori, S., Matsushima, T., & Takimoto, M. (1987). Assay of ptaquiloside, the carcinogenic principle of bracken, Pteridium aquilinum, by mutagenicity testing in Salmonella typhimurium. *Mutagenesis, 2*(6), 419-423.

Matsumoto, T, Hosono-Nishiyama, K, & Yamada, H. (2006). Antiproliferative and apoptotic effects of butyrolactone lignans from Arctium lappa on leukemic cells. *Planta medica, 72*(03), 276-278.

Matsuura, Nobuyasu, Nakai, Rie, Iinuma, Munekazu, Tanaka, Toshiyuki, & Inoue, Kenichro. (1994). A prenylated flavanone from roots of Maackia amurensis subsp. Buergeri. *Phytochemistry, 36*(1), 255-256.

Matsuzaki, Youichirou, Koyama, Makoto, Hitomi, Toshiaki, Yokota, Tomoya, Kawanaka, Mayumi, Nishikawa, Akiyoshi, Sakai, Toshiyuki. (2008). Arctiin induces

cell growth inhibition through the down-regulation of cyclin D1 expression. *Oncology reports, 19*(3), 721-728.

Máximo, Patrícia, & Lourenço, Ana. (1998). A pterocarpan from Ulex parviflorus. *Phytochemistry, 48*(2), 359-362.

Meena, Mahesh Chand, & Patni, Vidya. (2008). Isolation and identification of flavonoid" quercetin" from *Citrullus colocynthis* (Linn.) Schrad. *Asian J Exp Sci, 22*(1), 137-142.

Melnik, Bodo C, John, Swen Malte, & Schmitz, Gerd. (2013). Milk is not just food but most likely a genetic transfection system activating mTORC1 signaling for postnatal growth. *Nutrition journal, 12*(1), 1.

Melnik, B. C., John, S. M., & Schmitz, G. (2014). Milk: an exosomal microRNA transmitter promoting thymic regulatory T cell maturation preventing the development of atopy? *J Transl Med, 12*, 43.

Mendell, J. T., & Olson, E. N. (2012). MicroRNAs in stress signaling and human disease. *Cell, 148*(6), 1172-1187.

Merfort, I, Buddrus, J, Nawwar, MAM, & Lambert, J. (1992). A triterpene from the bark of *Tamarix aphylla*. *Phytochemistry, 31*(11), 4031-4032.

Merin, U., Bernstein, S., Bloch-Damti, A., Yagil, R., Van Creveld, C., Lindner, P., & Gollop, N. (2001). A comparative study of milk serum proteins in camel (Camelus dromedarius) and bovine colostrum. *Livestock Production Science, 67*(3), 297-301.

Meyer, W., Mitchell, TG., Freedman, EZ., & Vilgalys, R. (1993). Hybridization probes for conventional DNA fingerprinting used as single primers in the polymerase chain reaction to distinguish strains of Cryptococcus neoformans. *Journal of Clinical Microbiology, 31*(9), 2274-2280.

Micheli, Maria Rita, Bova, Rodolfo, Pascale, Esterina, & D'Ambrosio, Ettore. (1994). Reproducible DNA fingerprinting with the random amplified polymorphic DNA (RAPD) method. *Nucleic Acids Research, 22*(10), 1921.

Mitchell, P. J., Welton, J., Staffurth, J., Court, J., Mason, M. D., Tabi, Z., & Clayton, A. (2009). Can urinary exosomes act as treatment response markers in prostate cancer? *J Transl Med, 7*, 4.

Mittelbrunn, M., Gutiérrez-Vázquez, C., Villarroya-Beltri, C., González, S., Sánchez-Cabo, Fátima, González, Manuel Ángel, Sánchez-Madrid, Francisco. (2011). Unidirectional transfer of microRNA-loaded exosomes from T cells to antigen-presenting cells. *Nature communications, 2*, 282.

Mizuguchi, H., Nariai, Y., Kato, S., Nakano, T., Kanayama, T., Kashiwada, Y., Fukui, H. (2015). Maackiain is a novel antiallergic compound that suppresses transcriptional upregulation of the histamine H1 receptor and interleukin-4 genes. *Pharmacol Res Perspect, 3*(5), e00166.

Mlotshwa, S., Pruss, G. J., MacArthur, J. L., Endres, M. W., Davis, C., Hofseth, L. J., Vance, V. (2015). A novel chemopreventive strategy based on therapeutic microRNAs produced in plants. *Cell Res, 25*(4), 521-524.

Mohamad, R. H., Zekry, Z. K., Al-Mehdar, H. A., Salama, O., El-Shaieb, S. E., El-Basmy, A. A., Sharawy, S. M. (2009). Camel milk as an adjuvant therapy for the treatment of type 1 diabetes: verification of a traditional ethnomedical practice. *J Med Food, 12*(2), 461-465.

Momma, Keiko, Masuzawa, Yuko, Nakai, Naomi, Chujo, Moeko, Murakami, Akira, Kioka, Noriyuki, Nagao, Masaya. (2008). Direct interaction of Cucurbitacin E isolated from Alsomitra macrocarpa to actin filament. *Cytotechnology, 56*(1), 33-39.

Mona, EY, Ragia, OM, Abeer, AKH, & Mosa, TE. (2010). Biochemical effects of fermented camel milk on diarrhea in rats. *New York Science Journal, 3*(5), 106-111.

Montecalvo, A., Larregina, A. T., Shufesky, W. J., Stolz, D. B., Sullivan, M. L., Karlsson, J. M., Morelli, A. E. (2012). Mechanism of transfer of functional microRNAs between mouse dendritic cells via exosomes. *Blood, 119*(3), 756-766.

Moreira, RF, Trugo, LC, De Maria, CA, Matos, AG, Santos, SM, & Leite, JM. (2001). Discrimination of Brazilian arabica green coffee samples by chlorogenic acid composition. *Archivos latinoamericanos de nutricion, 51*(1), 95-99.

Moscatelli, V., Hnatyszyn, O., Acevedo, C., Megías, Javier, Alcaraz, María José, & Ferraro, Graciela. (2006). Flavonoids from Artemisia copa with anti-inflammatory activity. *Planta medica, 72*(01), 72-74.

Nalbantsoy, A., Nesil, T., Yılmaz-Dilsiz, Ö., Aksu, G., Khan, S., & Bedir, E. (2012). Evaluation of the immunomodulatory properties in mice and in vitro anti-

inflammatory activity of cycloartane type saponins from Astragalus species. *Journal of ethnopharmacology, 139*(2), 574-581.

Navas-Carretero, S., Cuervo, M., Abete, I., Zulet, M. A., & Martinez, J. A. (2011). Frequent consumption of selenium-enriched chicken meat by adults causes weight loss and maintains their antioxidant status. *Biol Trace Elem Res, 143*(1), 8-19.

Nawwar, M., Hussein, S., Ayoub, NA., Hofmann, K., Linscheid, M., Harms, M., Lindequist, U. (2009). Aphyllin, the first isoferulic acid glycoside and other phenolics from *Tamarix aphylla* flowers. *Die Pharmazie-An International Journal of Pharmaceutical Sciences, 64*(5), 342-347.

Nawwar, M., Hussein, S., Buddrus, J., & Linscheid, M. (1994). Tamarixellagic acid, an ellagitannin from the galls of *Tamarix aphylla*. *Phytochemistry, 35*(5), 1349-1354.

Nawwar, M. A., Swilam, N. F., Hashim, A. N., Al-Abd, A. M., Abdel-Naim, A. B., & Lindequist, U. (2013). Cytotoxic isoferulic acidamide from Myricaria germanica (Tamaricaceae). *Plant Signal Behav, 8*(1), e22642.

Nilsson, J., Skog, J., Nordstrand, A., Baranov, V., Mincheva-Nilsson, L., Breakefield, X. O., & Widmark, A. (2009). Prostate cancer-derived urine exosomes: a novel approach to biomarkers for prostate cancer. *Br J Cancer, 100*(10), 1603-1607.

Niwa, H., Ojika, M., Wakamatsu, K., Yamada, K., Ohba, S., Saito, Y., Matsushita, K. (1983). Stereochemistry of ptaquiloside, a novel norsesquiterpene glucoside from bracken, Pteridium aquilinum var. latiusculum. *Tetrahedron Letters, 24*(48), 5371-5372.

Nolan, T., Hands, R. E., & Bustin, S. A. (2006). Quantification of mRNA using real-time RT-PCR. *Nat Protoc, 1*(3), 1559-1582.

Okunade, Adewole L. (2002). Ageratum conyzoides L.(Asteraceae). *Fitoterapia, 73*(1), 1-16.

Ooi, LS., Wang, H., He, Z., & Ooi, V. E. (2006). Antiviral activities of purified compounds from Youngia japonica (L.) DC (Asteraceae, Compositae). *J Ethnopharmacol, 106*(2), 187-191.

Orabi, MA., Taniguchi, S., Sakagami, H., Yoshimura, M., Yoshida, T., & Hatano, T. (2013). Hydrolyzable tannins of tamaricaceous plants. V. Structures of monomeric-

trimeric tannins and cytotoxicity of macrocyclic-type tannins isolated from Tamarix nilotica (1). *J Nat Prod, 76*(5), 947-956.

Ormandy, J., Camus, A., Barra, J., Damotte, D., Lucas, B., Buteau, H., Binart, N. (1997). Null mutation of the prolactin receptor gene produces multiple reproductive defects in the mouse. *Genes & development, 11*(2), 167-178.

Otaibi, MA., & Demerdash, H. (2008). Improvement of the quality and shelf life of concentrated yoghurt (labneh) by the addition of some essential oils. *African Journal of Microbiology Research, 2*(7), 156-161.

Ovaska, K., Laakso, M., Haapa-Paananen, S., Louhimo, R., Chen, P., Aittomaki, V., Hautaniemi, S. (2010). Large-scale data integration framework provides a comprehensive view on glioblastoma multiforme. *Genome Med, 2*(9), 65.

Ozipek, M., Donmez, AA., Calis, I., Brun, R., Ruedi, P., & Tasdemir, D. (2005). Leishmanicidal cycloartane-type triterpene glycosides from Astragalus oleifolius. *Phytochemistry, 66*(10), 1168-1173.

Pachot, A., Blond, JL., Mougin, B., & Miossec, P. (2004). Peptidylpropyl isomerase B (PPIB): a suitable reference gene for mRNA quantification in peripheral whole blood. *Journal of biotechnology, 114*(1), 121-124.

Palanisamy, V., Sharma, S., Deshpande, A., Zhou, H., Gimzewski, J., & Wong, D. T. (2010). Nanostructural and transcriptomic analyses of human saliva derived exosomes. *PLoS One, 5*(1), e8577.

Pan, Mei, Wei, Qinjun, Cao, Fang, Lu, Yajie, Zhu, Yibao, Shu, Yongqian, & Cao, Xin. (2007). Inhibition of cell proliferation by siRNA targeting hPRLR in breast cancer MCF-7 cell line. *Journal of Nanjing Medical University, 21*(6), 372-376.

Pari, L, & Prasath, A. (2008). Efficacy of caffeic acid in preventing nickel induced oxidative damage in liver of rats. *Chemico-biological interactions, 173*(2), 77-83.

Park, E. J., Kim, Y., & Kim, J. (2000). Acylated flavonol glycosides from the flower of Inula britannica. *J Nat Prod, 63*(1), 34-36.

Park, J. A., Kim, H. J., Jin, C., Lee, K. T., & Lee, Y. S. (2003). A new pterocarpan, (-)-maackiain sulfate, from the roots of Sophora subprostrata. *Arch Pharm Res, 26*(12), 1009-1013.

Park, Jae B. (2013). Isolation and quantification of major chlorogenic acids in three major instant coffee brands and their potential effects on H 2 O 2-induced mitochondrial membrane depolarization and apoptosis in PC-12 cells. *Food & function, 4*(11), 1632-1638.

Pastrello, C., Tsay, M., McQuaid, R., Abovsky, M., Pasini, E., Shirdel, E., Jurisica, I. (2016). Circulating plant miRNAs can regulate human gene expression in vitro. *Sci Rep, 6*, 32773.

Peirce, S. K., Chen, W. Y., & Chen, W. Y. (2001). Quantification of prolactin receptor mRNA in multiple human tissues and cancer cell lines by real time RT-PCR. *J Endocrinol, 171*(1), R1-4.

Pelletier, S William, Chokshi, Hitesh P, & Desai, Haridutt K. (1986). Separation of diterpenoid alkaloid mixtures using vacuum liquid chromatography. *Journal of natural products, 49*(5), 892-900.

Perrin, Dawn R., & Cruickshank, I. A. M. (1969). The antifungal activity of pterocarpans towards Monilinia fructicola. *Phytochemistry, 8*(6), 971-978.

Peters, Joris, & Driesch, Angela von den. (1997). The two-humped camel (Camelus bactrianus): new light on its distribution, management and medical treatment in the past. *Journal of Zoology, 242*(4), 651-679.

Pfaffl, Michael W. (2001). A new mathematical model for relative quantification in real-time RT–PCR. *Nucleic acids research, 29*(9), e45-e45.

Philip, A., Ferro, V. A., & Tate, R. J. (2015). Determination of the potential bioavailability of plant microRNAs using a simulated human digestion process. *Molecular nutrition & food research, 59*(10), 1962-1972.

Phillips, Glyn O, & Williams, Peter A. (2009). *Handbook of hydrocolloids*: Elsevier.

Phillips, I., Casewell, M., Cox, T., De Groot, B., Friis, C., Jones, R., Waddell, J. (2004). Does the use of antibiotics in food animals pose a risk to human health? A critical review of published data. *J Antimicrob Chemother, 53*(1), 28-52.

Pico de Coaña, Yago, Parody, Nuria, Fernández-Caldas, Enrique, & Alonso, Carlos. (2010). A Modified Protocol for RNA Isolation from High Polysaccharide Containing Cupressus arizonica Pollen. Applications for RT–PCR and Phage Display Library Construction. *Molecular Biotechnology, 44*(2), 127-132.

Pieters, Bartijn CH, Arntz, Onno J, Bennink, Miranda B, Broeren, Mathijs GA, van Caam, Arjan PM, Koenders, Marije I, van der Kraan, Peter M. (2015). Commercial cow milk contains physically stable extracellular vesicles expressing immunoregulatory TGF-β. *PLoS One, 10*(3), e0121123.

Ponosyan, A.G.; Nikishchenko, M.N.; Avetisyan, G.M. 1985. Structure of 22-deoxocucurbitacins isolated from *Bryonia alba* and *Ecballium elaterium. Chem. Nat. Compd. 21*, 638–645.

Poongothai, G, & Sripathi, SHUBASHINI K. (2013). A review on insulinomimetic pinitol from plants. *International Journal of Pharma and Bio Sciences, 4*(2), 992-1009.

Pritchard, C. C., Cheng, H. H., & Tewari, M. (2012). MicroRNA profiling: approaches and considerations. *Nat Rev Genet, 13*(5), 358-369.

Pupo, Mônica T., Adorno, M. Angela T., Vieira, Paulo C., Fernandes, João B., Silva, M. Fátima das G. F. da, & Pirani, José R. (2002). Terpenoids and Steroids from Trichilia Species. *Journal of the Brazilian Chemical Society, 13*, 382-388.

Qadir, Muhammad Imran, Abbas, Khizar, Hamayun, Rahma, & Ali, Muhammad. (2014). Analgesic, anti-inflammatory and anti-pyretic activities of aqueous ethanolic extract of *Tamarix aphylla* L. (Saltcedar) in mice. *Pak. J. Pharm. Sci, 27*(6), 1985-1988.

Qazi, Khaleda R, Paredes, Patricia Torregrosa, Dahlberg, Benita, Grunewald, Johan, Eklund, Anders, & Gabrielsson, Susanne. (2010). Proinflammatory exosomes in bronchoalveolar lavage fluid of patients with sarcoidosis. *Thorax, 65*(11), 1016-1024.

Qiao, J., Xu, L. H., He, J., Ouyang, D. Y., & He, X. H. (2013). Cucurbitacin E exhibits anti-inflammatory effect in RAW 264.7 cells via suppression of NF-kappaB nuclear translocation. *Inflamm Res, 62*(5), 461-469.

Qiu, J, Li, H, Meng, H, Hu, C, Li, J, Luo, M, Deng, Y. (2011). Impact of luteolin on the production of alpha-toxin by Staphylococcus aureus. *Letters in applied microbiology, 53*(2), 238-243.

Rahman, AHM Mahbubur, & Parvin, M Ismot Ara. (2014). Study of medicinal uses on Fabaceae family at Rajshahi, Bangladesh. *Research in Plant Sciences, 2*(1), 6-8.

Rahuman, A Abdul, & Venkatesan, P. (2008). Larvicidal efficacy of five cucurbitaceous plant leaf extracts against mosquito species. *Parasitology research, 103*(1), 133-139.

Rajamanickam, E, Gurudeeban, S, Ramanathan, T, & Satyavani, K. (2010). Evaluation of anti inflammatory activity of *Citrullus colocynthis*. *International Journal of Current Research, 2*, 67-69.

Rameshwari, Rashmi, Singhal, Divya, Narang, Rachit, Maheshwari, Apurvi, & Prasad, TV. (2013). In silico prediction of miRNA in Curcuma longa and their role in human metabolomics. *International Journal of Advanced Biotechnology and Research., 1*(4), 253-259.

Rao, E, Jiang, C, Ji, M, Huang, X, Iqbal, Javeed, Lenz, G, McKeithan, TW. (2012). The miRNA-17~ 92 cluster mediates chemoresistance and enhances tumor growth in mantle cell lymphoma via PI3K/AKT pathway activation. *Leukemia, 26*(5), 1064-1072.

Ravn-Haren, G., Bugel, S., Krath, B. N., Hoac, T., Stagsted, J., Jorgensen, K., Dragsted, LO. (2008). A short-term intervention trial with selenate, selenium-enriched yeast and selenium-enriched milk: effects on oxidative defence regulation. *Br J Nutr, 99*(4), 883-892.

Raya-González, D., T. Pamatz-Bolañ os, R. E. del Rio-Torres, R. E. Martínez-Muñ oz, O. Ron- Echeverría and M. M. Martínez-Pacheco. 2008. D-(+)-Pinitol, a component of the heartwood of *Enterolobium cyclocarpum* (Jacq.) Griseb. Zeitschrift fur Naturforsch.63c:922-924.

Raziq, A., Younas, M., & Kakar, MA. (2008). Camel~ A potential dairy animal in difficult environments. *Pak. J. Agri. Sci, 45*(2), 263-267.

Redis, RS., Calin, S., Yang, Y., You, M. J., & Calin, G. A. (2012). Cell-to-cell miRNA transfer: from body homeostasis to therapy. *Pharmacol Ther, 136*(2), 169-174.

Reichenstein, I., Aizenberg, N., Goshen, M., Bentwich, Z., & Avni, Y. S. (2010). A novel qPCR assay for viral encoded microRNAs. *J Virol Methods, 163*(2), 323-328.

Rengarajan, T., Nandakumar, N., & Balasubramanian, MP. (2012). D-Pinitol attenuates 7, 12 dimethylbenz [a] anthracene induced hazards through modulating protein bound carbohydrates, adenosine triphosphatases and lysosomal enzymes

during experimental mammary carcinogenesis. *Journal of experimental therapeutics & oncology, 10*(1).

Rizk, AF. (1990). *Naturally occurring pyrrolizidine alkaloids*: CRC press.

Roeder, E., & Wiedenfeld, H. (2011). Pyrrolizidine alkaloids in plants used in the traditional medicine of Madagascar and the Mascarene islands. *Die Pharmazie-An International Journal of Pharmaceutical Sciences, 66*(9), 637-647.

Roeder, E., Wiedenfeld, H., & Edgar, JA. (2015). Pyrrolizidine alkaloids in medicinal plants from North America. *Die Pharmazie-An International Journal of Pharmaceutical Sciences, 70*(6), 357-367.

Ross, JA., & Kasum, CM. (2002). Dietary flavonoids: bioavailability, metabolic effects, and safety. *Annual review of Nutrition, 22*(1), 19-34.

Saade, M., Magdalou, J., Ouaini, N., & Greige-Gerges, H. (2009). Stability of cucurbitacin E in human plasma: chemical hydrolysis and role of plasma esterases. *Biopharm Drug Dispos, 30*(7), 389-397.

Sah, SK., Kaur, G., & Kaur, A. (2014). Rapid and reliable method of high-quality RNA extraction from diverse plants. *American Journal of Plant Sciences, 5*(21), 3129.

Salter, MG., & Conlon, HE. (2007). Extraction of Plant RNA. In E. Rosato (Ed.), *Circadian Rhythms: Methods and Protocols* (pp. 309-314). Totowa, NJ: Humana Press.

Sato, Y., Itagaki, S., Kurokawa, T., Ogura, Jiro, Kobayashi, Masaki, Hirano, Takeshi, Iseki, Ken. (2011). In vitro and in vivo antioxidant properties of chlorogenic acid and caffeic acid. *International Journal of Pharmaceutics, 403*(1), 136-138.

Schütz, K., Carle, R., & Schieber, A. (2006). Taraxacum—a review on its phytochemical and pharmacological profile. *Journal of ethnopharmacology, 107*(3), 313-323.

Schwarzenbach, H., Nishida, N., Calin, G. A., & Pantel, K. (2014). Clinical relevance of circulating cell-free microRNAs in cancer. *Nat Rev Clin Oncol, 11*(3), 145-156.

Sciuto, S., Chillemi, R., Piattelli, M., & Impellizzeri, G. (1983). The identification of 4-hydroxy-*N*-methylproline in the red alga Chondria coerulescens—spectral information. *Phytochemistry, 22*(10), 2311-2312.

Seaman, J., Holt, J., & Rivers, J. (1978). The effects of drought on human nutrition in an Ethiopian province. *Int J Epidemiol, 7*(1), 31-40.

Sebbagh, N., Cruciani-Guglielmacci, C., Ouali, F., Berthault, MF., Rouch, C., Sari, DC., & Magnan, C. (2009). Comparative effects of *Citrullus colocynthis*, sunflower and olive oil-enriched diet in streptozotocin-induced diabetes in rats. *Diabetes & metabolism, 35*(3), 178-184.

Seger, C., Sturm, S., Mair, M. E., Ellmerer, E. P., & Stuppner, H. (2005). ^{1}H and ^{13}C NMR signal assignment of cucurbitacin derivatives from *Citrullus colocynthis* (L.) Schrader and Ecballium elaterium L. (Cucurbitaceae). *Magn Reson Chem, 43*(6), 489-491.

Semagn, Kassa, Bjørnstad, Å, & Ndjiondjop, MN. (2006). An overview of molecular marker methods for plants. *African journal of biotechnology, 5*(25).

Sethi, B. K., Chanukya, G. V., & Nagesh, V. S. (2012). Prolactin and cancer: Has the orphan finally found a home? *Indian J Endocrinol Metab, 16*(Suppl 2), S195-198.

Sevimli-Gür, Canan, Onbaşılar, İlyas, Atilla, Pergin, Genç, Rükan, Çakar, Nur, Deliloğlu-Gürhan, İsmet, & Bedir, Erdal. (2011). In vitro growth stimulatory and in vivo wound healing studies on cycloartane-type saponins of Astragalus genus. *Journal of ethnopharmacology, 134*(3), 844-850.

Shabo, Y., Barzel, R., Margoulis, M., & Yagil, R. (2005). Camel milk for food allergies in children. *Isr Med Assoc J, 7*(12), 796-798.

Shahin, Mahmood, Smith, Barry L., & Prakash, Arungundrum S. (1999). Bracken carcinogens in the human diet. *Mutation Research/Genetic Toxicology and Environmental Mutagenesis, 443*(1–2), 69-79.

Shaw, D., & Pearn, J. (1979). Oleander poisoning. *Med J Aust, 2*(5), 267-269.

Shi, Haitao, Dong, Lei, Jiang, Jiong, Zhao, Juhui, Zhao, Gang, Dang, Xiaoyan, Jia, Miao. (2013). Chlorogenic acid reduces liver inflammation and fibrosis through inhibition of toll-like receptor 4 signaling pathway. *Toxicology, 303*, 107-114.

Shi, H., Shi, A., Dong, L., Lu, X., Wang, Y., Zhao, J., Guo, X. (2016). Chlorogenic acid protects against liver fibrosis in vivo and in vitro through inhibition of oxidative stress. *Clin Nutr*.

Shigehara, K., Yokomuro, S., Ishibashi, O., Mizuguchi, Y., Arima, Y., Kawahigashi, Y., Uchida, E. (2011). Real-time PCR-based analysis of the human bile microRNAome identifies miR-9 as a potential diagnostic biomarker for biliary tract cancer. *PLoS One, 6*(8), e23584.

Shi-xiong, Chen, Shu-yun, Bao, Tai-li, Shao, & Kao-shan, Chen. (2011). Chemical Constituents of the Root of Arctium lappa L. *Natural Product Research & Development, 23*(6).

Singh, RK, Pandey, BL, Tripathi, M, & Pandey, VB. (2001). Anti-inflammatory effect of (+)-pinitol. *Fitoterapia, 72*(2), 168-170.

Snow, J. W., Hale, A. E., Isaacs, S. K., Baggish, A. L., & Chan, S. Y. (2013). Ineffective delivery of diet-derived microRNAs to recipient animal organisms. *RNA Biol, 10*(7), 1107-1116.

Song, F., Dai, B., Zhang, H. Y., Xie, J. W., Gu, C. Z., & Zhang, J. (2015). Two new cucurbitane-type triterpenoid saponins isolated from ethyl acetate extract of *Citrullus colocynthis* fruit. *J Asian Nat Prod Res, 17*(8), 813-818.

Sörensen, Pia M, Iacob, Roxana E, Fritzsche, Marco, Engen, John R, Brieher, William M, Charras, Guillaume, & Eggert, Ulrike S. (2012). The natural product cucurbitacin E inhibits depolymerization of actin filaments. *ACS chemical biology, 7*(9), 1502-1508.

Soto-Blanco, B., Fontenele-Neto, J. D., Silva, D. M., Reis, P. F., & Nobrega, J. E. (2006). Acute cattle intoxication from Nerium oleander pods. *Trop Anim Health Prod, 38*(6), 451-454.

Souliman, Ahmed MA, Barakat, Heba H, El-Mousallamy, Amani MD, Marzouk, Mohamed SA, & Nawwar, Mahmoud AM. (1991). Phenolics from the bark of*Tamarix aphylla*. *Phytochemistry, 30*(11), 3763-3766.

Sretenović, Lj, Aleksić, S, Petrović, MP, & Miščević, B. (2007). Nutritional factors influencing improvement of milk and meat quality as well as productive and reproductive parameters of cattle. *Biotechnology in Animal Husbandry, 23*(5-6-1), 217-226.

Stahl, Egon, & Mangold, HK. (1975). Techniques of thin layer chromatography. *A Laboratory Handbook of Chromatography and Electrophoretic Methods. Edited by Heftmann, E. 3th Edition. Van Nostrand Reinhold Company*, 164-188.

Stevenson, Philip C, & Haware, Manohar P. (1999). Maackiain in Cicer bijugum Rech. f. associated with resistance to Botrytis grey mould. *Biochemical systematics and ecology, 27*(8), 761-767.

Su, Yuhang, Li, Gang, Zhang, Xulong, Gu, Jinhai, Zhang, Cai, Tian, Zhigang, & Zhang, Jian. (2008). JSI-124 inhibits glioblastoma multiforme cell proliferation through G2/M cell cycle arrest and apoptosis augmentation. *Cancer biology & therapy, 7*(8), 1243-1249.

Suleiman, Majda Khalil, Bhat, Narayana Ramachandra, Abdal, Mehdi Saleh, Zaman, Sameeha, Jacob, Sheena, & Thomas, Rini Rachel. (2009). Germination studies in Rhanterium epapposum Oliv. *World App Sci J, 7*(4), 468-471.

Sun, Chunyan, Zhang, Meixia, Shan, Xiaolei, Zhou, Xueying, Yang, Jiao, Wang, Yanli, Deng, Yihui. (2010). Inhibitory effect of cucurbitacin E on pancreatic cancer cells growth via STAT3 signaling. *Journal of cancer research and clinical oncology, 136*(4), 603-610.

Sundekilde, Ulrik K, Larsen, Lotte B, & Bertram, Hanne C. (2013). NMR-based milk metabolomics. *Metabolites, 3*(2), 204-222.

Surai, P. F., Karadas, F., Pappas, A. C., & Sparks, N. H. (2006). Effect of organic selenium in quail diet on its accumulation in tissues and transfer to the progeny. *Br Poult Sci, 47*(1), 65-72.

Sustarsic, E. G., Junnila, R. K., & Kopchick, J. J. (2013). Human metastatic melanoma cell lines express high levels of growth hormone receptor and respond to GH treatment. *Biochem Biophys Res Commun, 441*(1), 144-150.

Swaminathan, Gayathri, Varghese, Bentley, Thangavel, Chellappagounder, Carbone, Christopher J, Plotnikov, Alexander, Kumar, KG Suresh, Deng, Luqin. (2008). Prolactin stimulates ubiquitination, initial internalization, and degradation of its receptor via catalytic activation of Janus kinase 2. *Journal of Endocrinology, 196*(2), R1-R7.

Takemura, T., Urushisaki, T., Fukuoka, M., Hosokawa-Muto, J., Hata, T., Okuda, Y., Kuwata, K. (2012). 3, 4-Dicaffeoylquinic Acid, a Major Constituent of Brazilian

Propolis, Increases TRAIL Expression and Extends the Lifetimes of Mice Infected with the Influenza A Virus. *Evid Based Complement Alternat Med*, 946867.

Tamhankar, S., Ghate, V., Raut, A., & Rajput, B. (2009). Molecular profiling of "Chirayat" complex using Inter Simple Sequence Repeat (ISSR) markers. *Planta Med, 75*(11), 1266-1270.

Tan, Dunyong, Chen, KuanHui E, Khoo, Teresa, & Walker, Ameae M. (2011). Prolactin increases survival and migration of ovarian cancer cells: importance of prolactin receptor type and therapeutic potential of S179D and G129R receptor antagonists. *Cancer letters, 310*(1), 101-108.

Tannin-Spitz, Tehila, Grossman, Shlomo, Dovrat, Sara, Gottlieb, Hugo E, & Bergman, Margalit. (2007). Growth inhibitory activity of cucurbitacin glucosides isolated from *Citrullus colocynthis* on human breast cancer cells. *Biochemical pharmacology, 73*(1), 56-67.

Theriault, Gabriel, Michael, Paul, & Nkongolo, Kabwe. (2016). Decrypting the regulation and mechanism of nickel resistance in white birch (Betula papyrifera) using cross-species metal-resistance genes. *Genes & Genomics, 38*(4), 341-350.

Thery, C. (2011). Exosomes: secreted vesicles and intercellular communications. *F1000 Biol Rep, 3*, 15.

Thomson, D. W., Bracken, C. P., & Goodall, G. J. (2011). Experimental strategies for microRNA target identification. *Nucleic Acids Res, 39*(16), 6845-6853.

Tian, T., Wang, Y., Wang, H., Zhu, Z. & Xiao, Z. (2010). *Visualizing of the cellular uptake and intracellular trafficking of exosomes by live cell microscopy. J Cell Biochem 111:* 488–496.

Tian, T., Zhu, Y., Zhou, Y., Liang, G., Wang, Y., Hu, F., & Xiao, Z. (2014). Exosome uptake through clathrin-mediated endocytosis and macropinocytosis and mediating miR-21 delivery. *Journal of Biological Chemistry, 289*(32), 22258-22267.

Timms, K., Westwood, M., & Forbes, K. (2014). A potential role for food-derived microRNAs in human placental development.

Todres, E, Nardi, JB, & Robertson, HM. (2000). The tetraspanin superfamily in insects. *Insect molecular biology, 9*(6), 581-590.

Tolonen, A., Joutsamo, T., Mattlla, S., Kämäräinen, T., & Jalonen, J. (2002). Identification of isomeric dicaffeoylquinic acids from Eleutherococcus senticosus using HPLC-ESI/TOF/MS and 1H-NMR methods. *Phytochemical analysis, 13*(6), 316-328.

Tomás-Barberán, FA., Iniesta-Sanmartín, E., Ferreres, F., Tomas-Lorente, F., Trowitzsch-Kienastt, W., & Wray, V. (1990). Trans-coniferyl alcohol 4-o-sulphate and flavonoid sulphates from some Tamarix species. *Phytochemistry, 29*(9), 3050-3051.

Torkey, HM, Abou-Yousef, HM, Abdel Azeiz, AZ, & Hoda, EAF. (2009). Insecticidal effect of cucurbitacin E glycoside isolated from *Citrullus colocynthis* against Aphis craccivora. *Australian Journal of Basic and Applied Sciences, 3*(4), 4060-4066.

Tosar, J. P., Rovira, C., Naya, H., & Cayota, A. (2014). Mining of public sequencing databases supports a non-dietary origin for putative foreign miRNAs: underestimated effects of contamination in NGS. *RNA, 20*(6), 754-757.

Touraine, P., Martini, J, Zafrani, Brigitte, Durand, Jean-Claude, Labaille, Françoise, Malet, Catherine, Kuttenn, Frédérique. (1998). Increased expression of prolactin receptor gene assessed by quantitative polymerase chain reaction in human breast tumors versus normal breast tissues. *The Journal of Clinical Endocrinology & Metabolism, 83*(2), 667-674.

Tsaruk, AV, Iskenderov, DA, Agzamova, MA, Khushbaktova, ZA, Syrov, VN, & Isaev, MI. (2010). Isolation and influence of cycloartane glycosides cycloorbicoside G and cyclosieversioside A on metabolic processes in myocardium. *Pharmaceutical Chemistry Journal, 44*(1), 10-13.

Tsuneki, Hiroshi, Ma, En-Long, Kobayashi, Shinjiro, Sekizaki, Naoto, Maekawa, Kouji, Sasaoka, Toshiyasu, Kimura, Ikuko. (2005). Antiangiogenic activity of β-eudesmol in vitro and in vivo. *European journal of pharmacology, 512*(2), 105-115.

Turchinovich, A., Weiz, L., Langheinz, A., & Burwinkel, B. (2011). Characterization of extracellular circulating microRNA. *Nucleic Acids Res, 39*(16), 7223-7233.

Um, Byung H, Polat, Merve, Lobstein, Annelise, Weniger, Bernard, Aragón, Raul, Declercq, Lieve, & Anton, Robert. (2002). A new dicaffeoylquinic acid butyl ester from Isertia pittieri. *Fitoterapia, 73*(6), 550-552.

Urushisaki, Tomohiko, Takemura, Tomoaki, Tazawa, Shigemi, Fukuoka, Mayuko, Hosokawa-Muto, Junji, Araki, Yoko, & Kuwata, Kazuo. (2011). Caffeoylquinic acids are major constituents with potent anti-influenza effects in Brazilian green propolis water extract. *Evidence-Based Complementary and Alternative Medicine, 2011.*

Vadlapudi, VR., Bobbarala, V., & Naidu, KC. (2009). Comparative screening of selected mangrove plant methanolic extracts against clinical and plant pathogens. *Journal of Pharmacy Research, 2*(6), 1062-1064.

Vajs, V., Jeremić, D., Milosavljević, S., & Macura, S. (1989). Sesquiterpene lactones from Inula helenium. *Phytochemistry, 28*(6), 1763-1764.

Valadi, H., Ekstrom, K., Bossios, A., Sjostrand, M., Lee, JJ., & Lotvall, JO. (2007). Exosome-mediated transfer of mRNAs and microRNAs is a novel mechanism of genetic exchange between cells. *Nat Cell Biol, 9*(6), 654-659.

Valenzuela, HF., Fuller, T., Edwards, J., Finger, D., & Molgora, B. (2009). Cycloastragenol extends T cell proliferation by increasing telomerase activity (90.30). *The Journal of Immunology, 182*(1 Supplement), 90.30-90.30.

Van Coppenolle, F., Skryma, R., Ouadid-Ahidouch, H., Slomianny, C., Roudbaraki, M., Delcourt, P., Gourdou, I. (2004). Prolactin stimulates cell proliferation through a long form of prolactin receptor and K+ channel activation. *Biochemical Journal, 377*(3), 569-578.

Van Kester, MS., Out-Luiting, JJ., von dem B, PA., Rein, T., Cornelis, P., & Vermeer, MH. (2008). Cucurbitacin I inhibits Stat3 and induces apoptosis in Sezary cells. *Journal of Investigative Dermatology, 128*(7), 1691-1695.

Vaucheret, H., & Chupeau, Y. (2012). Ingested plant miRNAs regulate gene expression in animals. *Cell Res, 22*(1), 3-5.

Veitch, NC. (2007). Isoflavonoids of the Leguminosae. *Natural product reports, 24*(2), 417-464.

Venkatadri, R., Muni, T., Iyer, A, Yakisich, JS, & Azad, N. (2016). Role of apoptosis-related miRNAs in resveratrol-induced breast cancer cell death. *Cell death & disease, 7*(2), e2104.

Verotta, L., Guerrini, M., El-Sebakhy, NA., Assad, AM, Toaima, SM., Radwan, Mohamed M,. Pezzuto, John M. (2002). Cycloartane and oleanane saponins from Egyptian Astragalus spp. as modulators of lymphocyte proliferation. *Planta medica, 68*(11), 986-994.

Vetter, J. (2009). A biological hazard of our age: bracken fern [Pteridium aquilinum (L.) Kuhn]--a review. *Acta Vet Hung, 57*(1), 183-196.

Vickers, KC., Palmisano, BT., Shoucri, BM., Shamburek, RD., & Remaley, AT. (2011). MicroRNAs are transported in plasma and delivered to recipient cells by high-density lipoproteins. *Nat Cell Biol, 13*(4), 423-433.

Vincken, J., Heng, L., de Groot, A., & Gruppen, H. (2007). Saponins, classification and occurrence in the plant kingdom. *Phytochemistry, 68*(3), 275-297.

Vogelstein, B., & Gillespie, D. (1979). Preparative and analytical purification of DNA from agarose. *Proc Natl Acad Sci U S A, 76*(2), 615-619.

Vos, P., Hogers, R., Bleeker, M., Reijans, M., Van de Lee, T., Hornes, M., Kuiper, M. (1995). AFLP: a new technique for DNA fingerprinting. *Nucleic acids research, 23*(21), 4407-4414.

Wakimoto, N., Yin, D., O'Kelly, J., Haritunians, T., Karlan, B., Said, J., Koeffler, HP. (2008). Cucurbitacin B has a potent antiproliferative effect on breast cancer cells in vitro and in vivo. *Cancer science, 99*(9), 1793-1797.

Wang, HY, & Yang, JS. (1992). [Studies on the chemical constituents of Arctium lappa L]. *Yao xue xue bao= Acta pharmaceutica Sinica, 28*(12), 911-917.

Wang, K., Li, H., Yuan, Y., Etheridge, A., Zhou, Y., Huang, D., Galas, D. (2012). The complex exogenous RNA spectra in human plasma: an interface with human gut biota? *PLoS One, 7*(12), e51009.

Wang, S., Li, J., Huang, H., Gao, W., Zhuang, C., Li, B., Kong, D. (2009). Anti-hepatitis B virus activities of astragaloside IV isolated from radix Astragali. *Biological and Pharmaceutical Bulletin, 32*(1), 132-135.

Wang, WH., Nian, Y., He, YJ., Wan, LS., Bao, NM., Zhu, GL., Qiu, M. (2015). New cycloartane triterpenes from the aerial parts of Cimicifuga heracleifolia. *Tetrahedron, 71*(42), 8018-8025.

Wang, WX., Wilfred, BR., Baldwin, DA., Isett, RB., Ren, N., Stromberg, A., & Nelson, PT. (2008). Focus on RNA isolation: obtaining RNA for microRNA (miRNA) expression profiling analyses of neural tissue. *Biochim Biophys Acta, 1779*(11), 749-757.

Wang, X., & El Naqa, IM. (2008). Prediction of both conserved and nonconserved microRNA targets in animals. *Bioinformatics, 24*(3), 325-332.

Wang, X., Xiao, H., Chen, G., Zhao, X., Huang, C., Chen, C., & Wang, F. (2011). Isolation of High-Quality RNA from Reaumuria soongorica, a Desert Plant Rich in Secondary Metabolites. *Molecular Biotechnology, 48*(2), 165-172.

Weber, JA., Baxter, DH., Zhang, S., Huang, DY., Huang, KH., Lee, MJ., Wang, K. (2010). The microRNA spectrum in 12 body fluids. *Clin Chem, 56*(11), 1733-1741.

Weiss, R., & Weiss, MA. (2014). Evaluation of a Novel Anti-aging Topical Formulation Containing Cycloastragenol, Growth Factors, Peptides and Antioxidants. *Journal of drugs in dermatology: JDD, 13*(9), 1135-1139.

Wen, Y., Zand, B., Ozpolat, B., Szczepanski, MJ., Lu, C., Yuca, E., Tekedereli, I. (2014). Antagonism of tumoral prolactin receptor promotes autophagy-related cell death. *Cell reports, 7*(2), 488-500.

Williams, JG, Kubelik, AR., Livak, KJ., Rafalski, JA., & Tingey, Scott V. (1990). DNA polymorphisms amplified by arbitrary primers are useful as genetic markers. *Nucleic acids research, 18*(22), 6531-6535.

Witwer, KW. (2012). XenomiRs and miRNA homeostasis in health and disease: evidence that diet and dietary miRNAs directly and indirectly influence circulating miRNA profiles. *RNA biology, 9*(9), 1147-1154.

Witwer, KW., & Hirschi, KD. (2014). Transfer and functional consequences of dietary microRNAs in vertebrates: concepts in search of corroboration: negative results challenge the hypothesis that dietary xenomiRs cross the gut and regulate genes in ingesting vertebrates, but important questions persist. *Bioessays, 36*(4), 394-406.

Witwer, KW., McAlexander, MA., Queen, SE., & Adams, RJ. (2013). Real-time quantitative PCR and droplet digital PCR for plant miRNAs in mammalian blood provide little evidence for general uptake of dietary miRNAs: limited evidence for general uptake of dietary plant xenomiRs. *RNA Biol, 10*(7), 1080-1086.

Wolf, T., Baier, SR., & Zempleni, J. (2015). The intestinal transport of bovine milk exosomes is mediated by endocytosis in human colon carcinoma Caco-2 cells and rat small intestinal IEC-6 cells. *The Journal of nutrition, 145*(10), 2201-2206.

Wolff, K., Zietkiewicz, E., & Hofstra, H. (1995). Identification of chrysanthemum cultivars and stability of DNA fingerprint patterns. *Theoretical and Applied Genetics, 91*(3), 439-447.

Wu, HF., Zhang, G., Wu, MC., Yang, WT., Ma, GX., Chen, DZ., Hu, WC. (2016). A new cycloartane triterpene glycoside from Souliea vaginata. *Nat Prod Res, 30*(20), 2316-2322.

Wu, W., Ginsburg, E., Vonderhaar, BK., & Walker, AM. (2005). S179D prolactin increases vitamin D receptor and p21 through up-regulation of short 1b prolactin receptor in human prostate cancer cells. *Cancer research, 65*(16), 7509-7515.

Wyllie, TD., & Morehouse, LG. (1978). *Mycotoxic Fungi, Mycotoxins, Mycotoxicoses: An Encyclopedic Handbook: Mycotoxic Fungi and Chemistry of Mycotoxins: Mycotoxin Control and Regulatory Aspects*: Dekker.

Xavier, CR., Lima, CF., Preto, A., Seruca, R., Fernandes-Ferreira, M., & Pereira-Wilson, C. (2009). Luteolin, quercetin and ursolic acid are potent inhibitors of proliferation and inducers of apoptosis in both KRAS and BRAF mutated human colorectal cancer cells. *Cancer letters, 281*(2), 162-170.

Xu, H., Yang, T., Liu, X., Tian, Y., Chen, X., Yuan, R., Du, G. (2016). Luteolin synergizes the antitumor effects of 5-fluorouracil against human hepatocellular carcinoma cells through apoptosis induction and metabolism. *Life Sci, 144*, 138-147.

Xu, J., Sun, D., Jiang, J., Deng, L., Zhang, Y., Yu, H., Frank, S. J. (2013). The role of prolactin receptor in GH signaling in breast cancer cells. *Mol Endocrinol, 27*(2), 266-279.

Xu, Ruoshi, Kang, Qiumei, Ren, Jie, Li, Zukun, & Xu, Xiaoping. (2013). Antitumor molecular mechanism of chlorogenic acid on inducting genes GSK-3β and APC and inhibiting gene β-catenin. *Journal of analytical methods in chemistry, 2013*.

Yadav, Alok Kumar, Kumar, Rakesh, Priyadarshini, Lakshmi, & Singh, Jitendra. (2015). Composition and medicinal properties of camel milk: A Review. *Asian Journal of Dairy and Food Research, 34*(2), 83-91.

Yadav, Akhilesh K, Thakur, Jayprakash, Prakash, Om, Khan, Feroz, Saikia, Dharmendra, & Gupta, Madan M. (2013). Screening of flavonoids for antitubercular activity and their structure–activity relationships. *Medicinal Chemistry Research, 22*(6), 2706-2716.

Yagil, R, & Van Creveld, C. (2000). *Medicinal use of camel milk. Fact or Fancy.* Paper presented at the Proceedings of the 2nd International Camelid Conference on Agro-economics of Camelids. Almaty, Kazahstan.

Yamada, K., Ojika, M., & Kigoshi, H. (2007). Ptaquiloside, the major toxin of bracken, and related terpene glycosides: chemistry, biology and ecology. *Nat Prod Rep, 24*(4), 798-813.

Yamaguchi, Takayuki, Kakefuda, Reina, Tajima, Nobuyuki, Sowa, Yoshihiro, & Sakai, Toshiyuki. (2011). Antitumor activities of JTP-74057 (GSK1120212), a novel MEK1/2 inhibitor, on colorectal cancer cell lines in vitro and in vivo. *Cancer Research, 71*(8 Supplement), 3585-3585.

Yesilada, Erdem, Bedir, Erdal, Çalış, İhsan, Takaishi, Yoshihisa, & Ohmoto, Yasukazu. (2005). Effects of triterpene saponins from Astragalus species on in vitro cytokine release. *Journal of ethnopharmacology, 96*(1), 71-77.

Yockteng, R., Almeida, A. M., Yee, S., Andre, T., Hill, C., & Specht, C. D. (2013). A method for extracting high-quality RNA from diverse plants for next-generation sequencing and gene expression analyses. *Appl Plant Sci, 1*(12).

Yokosuka, A., Sato, K., Yamori, T., & Mimaki, Y. (2010). Triterpene glycosides from Curculigo orchioides and their cytotoxic activity. *J Nat Prod, 73*(6), 1102-1106.

Yoon, KH., Park, KJ., Yin, J., Yoon, K., Lee, J., Hwang, YJ., Lee, MW. (2016). Antioxidative and Antitumor Effects of Isoflavones Isolated from the Leaves of Maackia fauriei. *Records of Natural Products, 10*(4), 441-451.

Yoshikawa, M., Morikawa, T., Kobayashi, H., Nakamura, A., Matsuhira, K., Nakamura, S., & Matsuda, H. (2007). Bioactive saponins and glycosides. XXVII. Structures of new cucurbitane-type triterpene glycosides and antiallergic constituents from *Citrullus colocynthis*. *Chem Pharm Bull (Tokyo), 55*(3), 428-434.

Yoshimoto, M., Yahara, S., Okuno, S., Islam, S., Ishiguro, K., & Yamakawa, O. (2002). Antimutagenicity of mono-, di-, and tricaffeoylquinic acid derivatives

isolated from sweetpotato (Ipomoea batatas L.) leaf. *Bioscience, biotechnology, and biochemistry, 66*(11), 2336-2341.

Yuan, G., Yan, S., Xue, H., Zhang, P., Sun, J., & Li, G. (2014). Cucurbitacin I induces protective autophagy in glioblastoma in vitro and in vivo. *Journal of Biological Chemistry, 289*(15), 10607-10619.

Yuearatanechemuge, HH, & Katsuzaki, H. (2004). Induction of apoptosis by maackiain and trifolirhizin (maackiain glycoside) isolated from sanzukon (Sop hora Subpr o stråte Chen et T. Chen) in human promyelotic leukemia HL-60 cells. *Oncology reports, 12*, 1183-1188.

Yusufoglu, H.S., Alam, A., Zaghloul, AM., Al-salkini, M., & Alam, P. (2014). Comparative Anti-Inflammatory and Hepatoprotective Activities of *Astragalus Gummifer* Labill Herb and Roots in Rats. *African Journal of Traditional, Complementary, and Alternative Medicines*, *11*(3), 268–274.

Yusufoglu, HS., & Alqasoumi, SI. (2011). Anti-inflammatory and wound healing activities of herbal gel containing an antioxidant *Tamarix aphylla* leaf extract. *International Journal of Pharmacology, 7*(8), 829-835.

Zhan, T., Ma, Y., Fan, P., Ji, M., & Lou, H. (2006). Synthesis of 4/5-Deoxy-4/5-nucleobase Derivatives of 3-O-Methyl-D-chiro-inositol as Potential Antiviral Agents. *Chemistry & biodiversity, 3*(10), 1126-1137.

Zhang, J., Guo, H., Tian, Y., Liu, P., Li, N., Zhou, J., & Guo, D. (2007). Biotransformation of 20(S)-protopanaxatriol by Mucor spinosus and the cytotoxic structure activity relationships of the transformed products. *Phytochemistry, 68*(20), 2523-2530.

Zhang, J., Li, S., Li, L., Li, M., Guo, C., Yao, J., & Mi, S. (2015). Exosome and Exosomal MicroRNA: Trafficking, Sorting, and Function. *Genomics, Proteomics & Bioinformatics, 13*(1), 17-24.

Zhang, L., Hou, D., Chen, X., Li, D., Zhu, L., Zhang, Y., Zhang, CY. (2012a). Exogenous plant MIR168a specifically targets mammalian LDLRAP1: evidence of cross-kingdom regulation by microRNA. *Cell Res, 22*(1), 107-126.

Zhang, Q., Zhao, X., & Wang, Z. (2008). Flavones and flavonols exert cytotoxic effects on a human oesophageal adenocarcinoma cell line (OE33) by causing G2/M arrest and inducing apoptosis. *Food and chemical toxicology, 46*(6), 2042-2053.

Zhang, T., Li, J., Dong, Y., Zhai, D., Lai, L., Dai, F.,Yi, Z. (2012b). Cucurbitacin E inhibits breast tumor metastasis by suppressing cell migration and invasion. *Breast cancer research and treatment, 135*(2), 445-458.

Zhang, Y., Liu, D., Chen, X., Li, J., Li, L., Bian, Z., Zhang, C. Y. (2010b). Secreted monocytic miR-150 enhances targeted endothelial cell migration. *Mol Cell, 39*(1), 133-144.

Zhang, Y., Wiggins, BE., Lawrence, C., Petrick, J., Ivashuta, S., & Heck, G. (2012c). Analysis of plant-derived miRNAs in animal small RNA datasets. *BMC genomics, 13*(1), 1.

Zhang, Z., Yu, J., Li, D., Zhang, Z., Liu, F., Zhou, X., Su, Z. (2010a). PMRD: plant microRNA database. *Nucleic acids research, 38*(suppl 1), D806-D813.

Zhao, Y., Li, Q., Zhao, W., Li, J., Sun, Y., Liu, K., Zhang, N. (2015). Astragaloside IV and cycloastragenol are equally effective in inhibition of endoplasmic reticulum stress-associated TXNIP/NLRP3 inflammasome activation in the endothelium. *J Ethnopharmacol, 169*, 210-218.

Zhou, Q., Li, M., Wang, X., Li, Q., Wang, T., Zhu, Q., Li, X. (2012). Immune-related microRNAs are abundant in breast milk exosomes. *Int J Biol Sci, 8*(1), 118-123.

Zhou, Z., Li, X., Liu, J., Dong, L., Chen, Q., Liu, J., Zhang, C. (2015). Honeysuckle-encoded atypical microRNA2911 directly targets influenza A viruses. *Cell Res, 25*(1), 39-49.

Zhu, D., Zhu, G., Kong, L., Bao, N., Zhou, L., Nian, Y., & Qiu, M. (2015). Cycloartane glycosides from the roots of Cimicifuga foetida with Wnt signaling pathway inhibitory activity. *Natural products and bioprospecting, 5*(2), 61-67.

Zhu, J., Lee, S., Ho, MK., Hu, Y., Pang, H., Ip, FC., Wong, YH. (2010). In vitro intestinal absorption and first-pass intestinal and hepatic metabolism of cycloastragenol, a potent small molecule telomerase activator. *Drug Metab Pharmacokinet, 25*(5), 477-486.

Ziessman, HA., Chander, A., Clarke, JO., Ramos, A., & Wahl, RL. (2009). The added diagnostic value of liquid gastric emptying compared with solid emptying alone. *J Nucl Med, 50*(5), 726-731.

Zietkiewicz, E., Rafalski, A., & Labuda, D. (1994). Genome fingerprinting by simple sequence repeat (SSR)-anchored polymerase chain reaction amplification. *Genomics, 20*(2), 176-183.

Zonneveld, MI., Brisson, AR., van Herwijnen, MJ., Tan, S., van de Lest, CH., Redegeld, FA., Nolte-'t Hoen, EN. (2014). Recovery of extracellular vesicles from human breast milk is influenced by sample collection and vesicle isolation procedures. *J Extracell Vesicles, 3*.